

**STUDY ON PERSISTENT CELL FORMATION IN A
CLINICAL ISOLATE OF *Klebsiella pneumoniae***

By

SHASHANK PATOLE

LIFE11201404009

National Institute of Science Education and Research, Bhubaneswar

*A thesis submitted to the
Board of Studies in Life Sciences*

*In partial fulfillment of requirements
for the Degree of*

DOCTOR OF PHILOSOPHY

of

HOMI BHABHA NATIONAL INSTITUTE



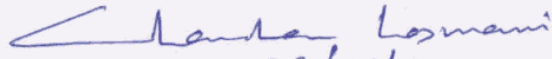
September, 2022

Homi Bhabha National Institute


Recommendations of the Viva Voce Committee

As members of the Viva Voce Committee, we certify that we have read the dissertation prepared by **Mr. Shashank Patole** entitled “**Study on persister cell formation in a clinical isolate of *Klebsiella pneumoniae***” and recommend that it may be accepted as fulfilling the thesis requirement for the award of Degree of Doctor of Philosophy.

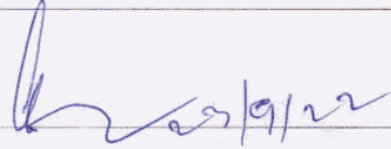
Dr. Chandan Goswami
Chairman


23/09/2022

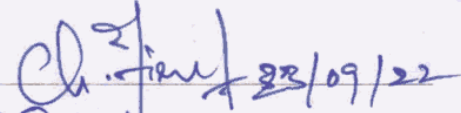
Dr. Harapriya Mohapatra
Guide / Convener


23/09/2022

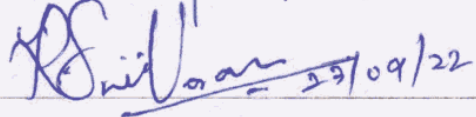
Dr. Hemraj Nandanwar
Examiner


23/09/22

Dr. Tirumala K Chowdary
Member 1


23/09/22

Dr. Ramanujam Srinivasan
Member 2


23/09/22

Dr. D. V. Singh
Member 3



Final approval and acceptance of this thesis is contingent upon the candidate's submission of the final copies of the thesis to HBNI.

I/We hereby certify that I/we have read this thesis prepared under my/our direction and recommend that it may be accepted as fulfilling the thesis requirement.

Date: 23.09.2022

Place: Tatari
NISER

Signature
Co-guide (if any)



Signature
Guide

STATEMENT BY AUTHOR

This dissertation has been submitted in partial fulfillment of requirements for an advanced degree at Homi Bhabha National Institute (HBNI) and is deposited in the Library to be made available to borrowers under rules of the HBNI.

Brief quotations from this dissertation are allowable without special permission, provided that accurate acknowledgement of source is made. Requests for permission for extended quotation from or reproduction of this manuscript in whole or in part may be granted by the Competent Authority of HBNI when in his or her judgment the proposed use of the material is in the interests of scholarship. In all other instances, however, permission must be obtained from the author.



Shashank Patole

DECLARATION

I, hereby declare that the investigation presented in the thesis has been carried out by me.

The work is original and has not been submitted earlier as a whole or in part for a degree

/ diploma at this or any other Institution / University.



Shashank Patole

List of Publications arising from the thesis

Journal

1. “Draft genome sequences of clinical and nonclinical isolates of *Klebsiella* spp. exhibiting nonheritable tolerance toward antimicrobial compounds”, Patole S, Mishra M, Mohapatra H, *Genome Announc*, **2017**, *5(45)*, e01217-17.
2. “Identification and validation of reference genes for reliable analysis of differential gene expression during antibiotic induced persister formation in *Klebsiella pneumoniae* using qPCR”, Patole S, Rout M, Mohapatra H, *J Microbiol Methods*, **2021**, *182*, 106165.
3. “Characterisation of persistence in a clinical isolate of *Klebsiella pneumoniae*”, Patole S, Kumar HS, Mohapatra H (under preparation).

Conferences

1. “Study on persister cell formation in *Klebsiella pneumoniae*”, Patole S, Mohapatra D, Debata NK, Mohapatra H, **The New Microbiology**, 24th August 24 – September 1, 2016, Spetses, Greece (Poster).
2. “Insights into antimicrobial tolerance exhibited by *Klebsiella pneumoniae*”, Patole S, Mohapatra H, **9th Annual Conference of Association of Microbiologists of India and International Symposium on Host Pathogen Interactions**, December 09-12, 2018, University of Hyderabad, Hyderabad (Poster).



Shashank Patole

DEDICATIONS

To Aaji and Aaji

ACKNOWLEDGEMENTS

From the outset, I extend my sincerest gratitude to my supervisor Dr. Harapriya Mohapatra, who has constantly been a guide throughout my journey; buoying me when the circumstances threatened to drown me, anchoring me when situations sought to sweep me up, and guiding me safely to shore. I also thank my doctoral committee members – Dr. Chandan Goswami, Dr. T.K. Chowdary, Dr. R. Srinivasan and Prof. D.V. Singh for their invaluable inputs in streamlining my project and ensuring its scientific rigour. I extend my thanks towards the members of the faculty, scientific- as well as all support-staff for their inestimable support throughout my PhD.

Collaboration is the spirit of research, and I am grateful to have learnt from wonderful teachers and worked with virtuous colleagues during my time at NISER. My sincerest thanks to Dr. Santosh, Dr. Mitali, Dr. Gargi Dr. Charles, Dr. Rakesh, Dr. Moon Moon, Dr. Subhranshu, Dr. Ankit, Dr. Manoj, Dr. Bibek, as well as Sunil, Minu, Sanchari, Jiban, Hitkarsh, Ashish, Matruprasad, Subham, Ananya, Kanishk, Nikhil and Priyobrota. Special thanks are reserved for Tathagata and Ajay whose unwavering helpfulness made this thesis possible.

When the going got tough, the tough got me going and kept me moving. I would be remiss to not proffer my utmost thanks to Manisha, Asmita, Dushali, Kalloly and Sonali. I also thank my family for their continued prayer and support throughout this long and arduous journey; today would not be possible without you. My special thanks are reserved for my precious children – Surma, Prince, Mota, Clingy, Baby, Cadbury, Butterscotch and Cookie. I am here today because you stayed with me during the hardest of times; thank you, wherever you are.

Lastly, I thank my Lord and Saviour Jesus Christ, from whom all things come.

CONTENTS

	Page No.
SUMMARY	I-III
LIST OF ABBREVIATIONS	IV-VIII
LIST OF FIGURES	IX-XIV
LIST OF TABLES	XV-XX
CHAPTER 1 INTRODUCTION	1 – 12
CHAPTER 2 REVIEW OF LITERATURE	13 – 53
CHAPTER 3 MATERIALS AND METHODS	54 – 133
CHAPTER 4 RESULTS AND DISCUSSION	
4.1 Detection and characterization of persister cells in <i>K. pneumoniae</i>	134 – 188
4.2 Elucidation of the genome and transcriptome of persister cells formed by <i>K. pneumoniae</i>	189 – 228
4.3 Investigation of the role of various genes in persister-cell formation in <i>K.</i> <i>pneumoniae</i>	229 – 293
CHAPTER 5 CONCLUSIONS	294 – 297
REFERENCES	298 – 346
APPENDICES	347 – 361

Summary

Certain bacterial populations are known to overcome stress-induced lethality by virtue of entering a non-dividing, non-metabolizing state. While most of the parent population is susceptible to the stress and dies, a small genetically-identical fraction of the population "persists" until the stress is removed. These "persisters" then resuscitate as a normally-growing population of cells. Persister cells are generated stochastically as well as on exposure to certain biotic or abiotic stresses. Studies have inferred a role of toxin-antitoxin systems, alarmone-mediated stringent response, oxidative stress-response, DNA damage-mediated stress response as well as energy production in the formation of persister cells. Understanding the phenomenon of persistence has become crucial given the ever-increasing number of bacterial pathogens that form persister cells as well as the implication of persister cell-forming bacteria in the intractability of chronic clinical infections. *Klebsiella pneumoniae* accounts for one-third of all Gram-negative infections, ranging from pneumonia and urinary-tract infections to liver abscess and septicaemia. The aim of this study was to identify persister cells in clinical isolates of *K. pneumoniae* and decipher the genetic pathways that mediate persistence.

Clinical isolates of *K. pneumoniae* were screened for their sensitivity to various antibiotics, and their survival as a function of time in supra-inhibitory concentrations of specific drugs was observed. Isolates exhibiting a biphasic killing were further characterized. The genome of the selected isolate was sequenced and its gene expression profile under antibiotic treatment was determined. A few candidate genes were chosen and their involvement in persister cell-formation assayed by deletion and overexpression studies.

Results from this study identified a multidrug-resistant isolate of *K. pneumoniae* - KpIMS38 - that forms persister cells in response to treatment with the fluoroquinolone drug levofloxacin. Persister cells were produced at concentrations equivalent to as well as much higher than the minimum inhibitory concentration for levofloxacin, increased in number as the age of the culture increased, and exhibited cross-tolerance to other classes of drugs at inhibitory concentrations. Persistence was observed to not be heritable in nature since successive generations of persister cells did not exhibit any advantage in overcoming the antibiotic. Cell populations treated with levofloxacin exhibited regular-sized and large-sized sub-populations, the latter being enriched on treatment with levofloxacin vis-a-vis untreated populations.

A draft genome of KpIMS38 was generated through this study, as were transcriptomes of untreated and levofloxacin-treated KpIMS38. These datasets aided in the identification of certain components of the DNA-repair pathway as well as toxin-antitoxin systems as being involved in the persistence of KpIMS38. Experimental evidence obtained in the present study also identified the importance of paired reference genes to study gene expression in KpIMS38 persister cells formed by levofloxacin treatment.

This present study sheds light on the relatively-unexplored domain of persistence in *K. pneumoniae* and serves as a starting point for further work on the subject.

*List of
abbreviations*

(p)ppGpp	A collective term representing Guanosine Tetraphosphate and Guanosine Pentaphosphate
°C	Degrees Celsius
ABC	ATP-Binding Cassette
AI-2	Autoinducer 2
ATCC	American Type Culture Collection
ATP	Adenosine Triphosphate
ATP	Adenosine Triphosphate
C/S	Culture-sensitivity
CARD	Comprehensive Antibiotic Resistance Database
CCCP	Carbonyl Cyanide m-Chlorophenylhydrazone
cDNA	Complementary DNA
CFDA	Carboxyfluorescein Diacetate
CGE	Centre for Genomic Epidemiology
CLSI	Clinical and Laboratory Standards Institute
Cq	Quantification cycle
CRISPR	Clustered Regularly Interspaced Short Palindromic Repeat
Csp	Cold Shock Protein
DAP	Diaminopimelic acid
DEPC	Diethyl pyrocarbonate
DMSO	Dimethyl sulfoxide
DNase	Deoxyribonuclease
dNTP	Deoxynucleotide triphosphate
DTT	Dithiothreitol
ED pathway	Entner-Doudoroff pathway
EDTA	Ethylene Diamine Tetraacetic Acid
EF-G	Elongation Factor G
EMB agar	Eosin-Methylene Blue agar
EMBO	European Molecular Biology Organization
ESBL	Extended-Spectrum β -Lactamase

ESKAPE	<i>Enterococcus faecium, Staphylococcus aureus, Klebsiella pneumoniae, Acinetobacter baumannii, Pseudomonas aeruginosa, and Enterobacter sp.</i>
FCS2	Focht Chamber System 2
FRT	Flippase Recognition Target
FSC	Forward Scatter
GDP	Guanosine Diphosphate
GFP	Green Fluorescent Protein
GM	Geometric Mean
GNAT	Gcn5 N-acetyltransferase
GTP	Guanosine Triphosphate
HPF	Hibernation Promoting Factor
IMP	Imipenem
IPTG	Isopropyl β -D-1-thiogalactopyranoside
LB	Luria-Bertani
LB-Lx	Low-salt Luria Bertani
LB-Lx-Hyg ¹⁰⁰	Low-salt Luria Bertani broth with 100 μ g/mL hygromycin
LB-Tet ³	Luria-Bertani broth with 3 μ g/mL tetracycline
LBA-Kan ¹⁵	Luria-Bertani agar with 15 μ g/mL kanamycin
LBA-Lx-Hyg ¹⁰⁰	Low-salt Luria Bertani agar with 100 μ g/mL hygromycin
LBA-Tet ³	Luria-bertani agar with 3 μ g/mL tetracycline
MaC	MacConkey Agar
MAR index	Multiple Antibiotic Resistance index
MBC	Minimum Bactericidal Concentration
MBL	Metallo- β -Lactamases
MCS	Multiple Cloning Sites
MDK	Minimum Duration For Killing
MDR	Multi-Drug Resistant
MFS	Major Facilitator Superfamily
MH	Muller Hinton
MHA-Kan ⁵⁰	MH agar containing 50 μ g/mL kanamycin
MHB-Kan ⁵⁰	MH broth containing 50 μ g/mL kanamycin

MHB-KI	MH broth containing 50 µg/mL kanamycin and 0.1 mM IPTG
MIC	Minimum Inhibitory Concentration
Mins	Minutes
mL	Millilitres
MLST	Multi-Locus Sequence Typing
MR-VP medium	Methyl Red – Voges Prosekauer medium
MRP	Meropenem
ms	Miliseconds
NA	Nutrient agar
NB	Nutrient broth
ng	Nanograms
NGS	Next-Gen Sequencing
NTC	Non-Template Control
OD ₆₀₀	Optical density measured at 600 nm
ORF	Open Reading Frame
PASH	Persistence As Stuff Happens
PBS	Phosphate-buffered Saline
PCR	Polymerase Chain Reaction
TE Buffer	Tris-EDTA Buffer
PFA	Paraformaldehyde
PIPES	Piperazine-N,N-bis(2-ethanesulfonic acid)
ppGpp	Guanosine Tetraphosphate
PPK	Polyphosphate Kinase
pppGpp	Guanosine Pentaphosphate
PPX	Exopolyphosphatase
qPCR	Quantitative Real-time PCR
QRDR	Quinolone Resistance-Determining Region
QRDR	Quinolone Resistance Determining Region
RAST	Rapid Annotations using Subsystems Technology
RGI	Resistance Gene Identifier
RGI	Resistance Gene Identifier
RMF	Ribosome Modulating Factor

RNA-Seq	RNA Sequencing
RNaseA	Ribonuclease
RND	Resistance-Nodulation-Cell Division
ROS	Reactive Oxygen Species
rpm	Revolutions per minute
RQ	Relative Quantity
RSH	RelA-SpoT Homologs
SIM medium	Sulfite Indole Motility medium
SNP	Single-Nucleotide Polymorphism
SOD	Superoxide Dismutase
SSC	Side Scatter
T3SS	Type-3 Secretion System
TA	Toxin-Antitoxin
TA systems	Toxin-Antitoxin systems
TAE	Tris-Acetate EDTA
TCA cycle	Tricarboxylic Acid cycle
TLR	Toll-like Receptor
U/ μ L	Units per microlitre
UV	Ultraviolet
V	Volts
VBNC	Viable but non-culturable
WHO	World Health Organisation
XDR	Extensively-Drug Resistant
μ g	Micrograms
μ L	Microlitres
μ m	Micrometres
μ M	Micromolar

List of figures

- Figure 1.1 Schematic representation of the modes of response – resistance, heteroresistance, persistence and tolerance – exhibited by bacteria that allows them to evade killing by antibiotics.
- Figure 1.2 Schematic representation depicting the response of bacteria exhibiting different responses to antibiotic treatment.
- Figure 2.1 Figure 2.1 Schematic representation of the mode of action of type II toxin-antitoxin systems in bacteria.
- Figure 2.2 Schematic diagram representing the various pathways through which bacteria form persister cells.
- Figure 2.3 Schematic diagram representing the induction of persistence in *E. coli* through the stringent response.
- Figure 3.1.1 Plasmid map of pRedET.
- Figure 3.1.2 Plasmid map of pACBSR-hyg.
- Figure 3.1.3 Plasmid map of pGEX-6P-1^K.
- Figure 3.2.1 Schematic diagram depicting the process of creating deletion mutants in KpIMS38 by Red/ET recombination using the Quick & Easy *E. coli* Gene Deletion Kit (Genebridges, Germany).
- Figure 3.3.1 Schematic representation of the protocol used to a prepare two-fold dilution series for a given antibiotic compound to measure its minimum inhibitory concentration for a particular bacterial isolate.
- Figure 3.3.2 Schematic diagram depicting the protocol used to study persistence by biphasic killing in the present study.
- Figure 3.3.3 Schematic diagram depicting the procedure followed to study the biphasic killing of KpIMS38 across successive generations.
- Figure 3.3.4 Schematic diagram depicting the experimental setup utilized to carry out live-cell microscopy of KpIMS38 exposed to levofloxacin.
- Figure 4.1.1 Comparison of the *gyrA* amino acid sequence of KpIMS38 with that from other *K. pneumoniae* strains.

- Figure 4.1.2 Survival of the isolates of *K. pneumoniae* as a function of time using three different antibiotics.
- Figure 4.1.3 Biphasic killing of KpIMS38 treated with different concentrations of levofloxacin.
- Figure 4.1.4 Growth curve of KpIMS38 in MH broth.
- Figure 4.1.5 Effect of the age of the inoculum on persister cell formation on treatment of KpIMS38 with levofloxacin.
- Figure 4.1.6 Effect of the size of the inoculum on persister cell formation in KpIMS38.
- Figure 4.1.7 Survival of KpIMS38 on treatment with levofloxacin across successive generations.
- Figure 4.1.8 Survival of KpIMS38 persisters, produced by exposure to levofloxacin, in inhibitory concentrations of amikacin and meropenem.
- Figure 4.1.9 Susceptibility of KpIMS38 treated with levofloxacin to varying concentrations of amikacin and meropenem.
- Figure 4.1.10 Dot-plot (with contours) of KpIMS38 culture as visualized through flow cytometry.
- Figure 4.1.11 Proportion of cells in a culture of KpIMS38 stained by varying concentrations of CFDA.
- Figure 4.1.12 Fluorescence of cells in a culture of KpIMS38 stained by varying concentrations of CFDA.
- Figure 4.1.13 Effect treatment of levofloxacin on the size of cells in KpIMS38.
- Figure 4.1.14 Effect of treatment of levofloxacin on the relative proportions of P1 and P2 sub-populations in KpIMS38.
- Figure 4.1.15 Effect of treatment of levofloxacin on the cell-fluorescence observed in sub-populations in KpIMS38.
- Figure 4.1.16 Agarose-gel electrophoresis of products from a PCR for the mCherry gene.
- Figure 4.1.17 Confocal microscopy of KpIMS38 prior to, during and after exposure to levofloxacin.
- Figure 4.2.1 Distribution of genes annotated in the genome of KpIMS38 across categories as performed by the RAST server.

- Figure 4.2.2 Expression of genes in KpIMS38 treated with levofloxacin across all categories.
- Figure 4.3.1 Melt curves of each primer-pair used to amplify *dnaJ*, *groEL*, *kp4432*, *kp751* and *rpoB* from cDNA extracted from KpIMS38.
- Figure 4.3.2 Cq values of five candidate reference genes in levofloxacin-treated and untreated samples of KpIMS38 indicating relative abundance of respective cDNA.
- Figure 4.3.3 Expression of genes in KpIMS38 upon treatment with levofloxacin using individual reference genes.
- Figure 4.3.4 Expression of genes in KpIMS38 upon treatment with levofloxacin using paired reference genes.
- Figure 4.3.5 Expression of toxin-antitoxin genes in KpIMS38 upon treatment with levofloxacin.
- Figure 4.3.6 Expression of stress-response genes in KpIMS38 upon treatment with levofloxacin for 8 hours.
- Figure 4.3.7 Expression of the stress-response genes *recA*, *sulA* and *spoT* in KpIMS38 as a function of time after treatment with levofloxacin.
- Figure 4.3.8 Expression of the genes involved in DNA repair viz. *umuCI* and -2, *umuDI* and -2, *ruvA*, *ruvB* and *ruvC* in KpIMS38 at different points of time after treatment with levofloxacin.
- Figure 4.3.9 Expression of the stress response genes in KpIMS38 persists at different points of time relative to their expression at the 8th hour.
- Figure 4.3.10 Agarose-gel electrophoresis of plasmid DNA extracted from KpIMS38 isolates transformed with pRedET.
- Figure 4.3.11 Agarose-gel electrophoresis of products from a high-fidelity PCR for the deletion-cassettes for *ibrA* (kan-R *ibrA*) and *pspF* (kan-R *pspF*).
- Figure 4.3.12 Agarose-gel electrophoresis of products from a colony PCR for *ibrA* using the qPCR primers.

- Figure 4.3.13 Agarose-gel electrophoresis of products from a PCR for the *ibrA* deletion-cassette using the cassette-synthesis primers for *ibrA*.
- Figure 4.3.14 Agarose-gel electrophoresis of products from a colony PCR for the *ibrA*-deletion cassette using the cassette-synthesis primers for *ibrA*.
- Figure 4.3.15 Agarose-gel electrophoresis of products from a colony PCR for the *ibrA*-deletion cassette using the cassette-synthesis primers for *ibrA*.
- Figure 4.3.16 Agarose-gel electrophoresis of products from a PCR for the *ibrA*-deletion cassette using the cassette-synthesis primers for *ibrA*.
- Figure 4.3.17 Agarose-gel electrophoresis of products from a colony PCR for the *ibrA*-deletion cassette using the new cassette-synthesis primers for *ibrA* (*ibrAn*-D-F and -R) and *pspF* (*pspFn*-D-F and -R).
- Figure 4.3.18 Agarose-gel electrophoresis of products from a colony PCR for *ibrA* and *pspF* using the qPCR and cassette-synthesis primers for the genes respectively.
- Figure 4.3.19 Agarose-gel electrophoresis of products from a PCR for full-length and deletion-cassette sequences of the genes *ibrA* and *pspF*.
- Figure 4.3.20 Agarose-gel electrophoresis of products from a PCR for full-length and deletion-cassette sequences of the gene *pspF*.
- Figure 4.3.21 Persister-cell formation by the putative Δ *ibrA* and Δ *pspF* strains of KpIMS38.
- Figure 4.3.22 Comparison of the *ibrA* sequences obtained from putative Δ *ibrA* strains by multiple sequence alignment.
- Figure 4.3.23 Agarose-gel electrophoresis of products from a PCR for deletion-cassette sequences of the genes *ibrA*, *pspF* and *relE*.
- Figure 4.3.24 Agarose-gel electrophoresis of PCR products for deletion-cassette sequences of the genes *ibrA*, *pspF* and *doc*.
- Figure 4.3.25 Agarose-gel electrophoresis of plasmid DNA extracted from KpIMS38 isolates transformed with pACBSR-hyg.

- Figure 4.3.26 Agarose-gel electrophoresis of products from a PCR for deletion-cassette and full-length sequences of the gene *doc*.
- Figure 4.3.27 Agarose-gel electrophoresis of plasmid DNA extracted from KpIMS38 isolates transformed with pACBSR-hyg and subcultured for three successive generations.
- Figure 4.3.28 Expression of the toxin-antitoxin genes silenced with spacer sequences using CRISPR-based gene silencing.
- Figure 4.3.29 Persister-cell formation in KpIMS38 strains putatively silenced for *relT*, *relAt*, *doc* and *relE*.
- Figure 4.3.30 Agarose-gel electrophoresis of restriction digestion of the plasmids pGEX-6P-1K-*ibrA* and pGEX-6P-1K-*pspF*.
- Figure 4.3.31 Agarose-gel electrophoresis of restriction digestion of the plasmid pGEX-6P-1K-*pspF*.
- Figure 4.3.32 Assessing the expression of *ibrA* in KpIMS38 strains overexpressing *ibrA*.
- Figure 4.3.33 Effect of overexpression of *ibrA* and complementation of Δ *ibrA* on persister-cell formation in KpIMS38.
- Figure 4.3.34 Expression of toxin and antitoxin genes upon overexpression in KpIMS38.
- Figure 4.3.35 Effect of overexpression of the toxin-antitoxin genes *phd-doc* and *relBE* on persister-cell formation in KpIMS38.

List of tables

Table 2.1	Organisms reported to form persister cells, grouped according to taxonomic categories.
Table 2.2	Classification of toxin-antitoxin (TA) systems found in bacteria.
Table 3.1.1	Antibiotics used in the current study.
Table 3.1.2	Composition of Dodeca Enterobacteriaceae discs and their potencies.
Table 3.1.3	EzyMIC™ strips used to determine the response of antibiotics on the bacterial isolates used in this study.
Table 3.1.6	Plasmids used in the current study.
Table 3.2.1	Components used to perform sequencing PCR.
Table 3.2.2	Thermocycler program to perform sequencing PCR.
Table 3.2.3	Composition of the RNA-Primer mix to synthesize cDNA.
Table 3.2.4	Composition of the SuperScript IV master-mix to synthesize cDNA.
Table 3.2.5	Composition of the reaction to synthesize cDNA from RNA.
Table 3.2.6	Thermocycler program to synthesize cDNA from RNA.
Table 3.2.7	Components used to carry out high-fidelity PCR.
Table 3.2.8	Thermocycler program used to perform high-fidelity PCR.
Table 3.2.9	Components used to set up PCR to screen for deletion of the gene-of-interest.
Table 3.2.10	Components used to perform PCR to verify the insertion of the FRT cassette.
Table 3.2.11	Thermocycler program used to perform PCR to amplify the deletion cassette or the full-length sequence of the gene-of-interest.
Table 3.3.1	Primer sequences used to amplify <i>qnrA</i> and <i>qnrB</i> from plasmid DNA extracted from KpIMS38.
Table 3.3.2	Components used to perform PCR to screen for the presence of <i>qnrA</i> and <i>-B</i> genes in KpIMS38.
Table 3.3.3	Thermocycler conditions used to amplify <i>qnrA</i> and <i>qnrB</i> genes.
Table 3.3.4	Primer sequences used to amplify segments of <i>gyrA</i> from genomic DNA extracted from KpIMS38.
Table 3.3.5	Components used to perform PCR to amplify segments of <i>gyrA</i> .

Table 3.3.6	Thermocycler conditions used to amplify the different fragments of the <i>gyrA</i> gene.
Table 3.3.7	Composition of the FACS buffer used to store cell – samples and perform flow cytometry.
Table 3.3.8	Parameters used to gate cell-suspensions of KpIMS38 stained with CFDA.
Table 3.3.9	Components used to perform PCR to amplify the mCherry gene.
Table 3.3.10	Primer sequences used to amplify mCherry for cloning.
Table 3.3.11	Thermocycler conditions used to amplify the mCherry gene.
Table 3.3.12	Protocol for digestion of DNA using type-II restriction enzymes.
Table 3.3.13	Protocol for ligation of insert and vector molecules.
Table 3.3.14	Composition of the Inoue transformation buffer.
Table 3.3.15	Primer sequences of candidates used to identify reference genes to study gene expression in KpIMS38 persister cells.
Table 3.3.16	Components used to perform qPCR to study the expression of the five candidate genes in cDNA samples.
Table 3.3.17	qPCR conditions used to assess the expression of the candidate reference genes in untreated and levofloxacin-treated cells of KpIMS38.
Table 3.3.18	Primer sequences for qPCR to study the expression of phage shock protein (<i>psp</i>) genes as well as <i>ibrA</i> in KpIMS38 treated with levofloxacin.
Table 3.3.19	Primer sequences to assess the expression of various toxin-antitoxin genes in KpIMS38 using qPCR.
Table 3.3.20	Primer sequences to evaluate the expression of stress-response genes in KpIMS38 using qPCR.
Table 3.3.21	Primer sequences to construct deletion cassettes for specific genes from KpIMS38.
Table 3.3.22	Primer sequences to amplify the full-length sequences of specific genes in KpIMS38.
Table 3.3.23	Spacer sequences used to target genes in KpIMS38 for transcriptional silencing.

Table 3.3.24	Components used to perform qPCR to study gene expression in silenced strains of KpIMS38.
Table 3.3.25	qPCR conditions used to assess the gene expression in silenced strains of KpIMS38.
Table 3.3.26	Primer sequences to synthesize gene fragments from KpIMS38 for insertion into pGEX-6P-1 ^K by restriction-enzyme based cloning.
Table 3.3.27	Components used to perform PCR to amplify entire gene sequences using cloning primers.
Table 3.3.28	Thermocycler conditions used to amplify entire gene sequences using cloning primers.
Table 3.3.29	Protocol for digestion of DNA using type-II restriction enzymes (RE).
Table 3.3.30	Protocol for ligation of insert and vector molecules.
Table 4.1.1	Details of the clinical isolates used in this study.
Table 4.1.2	Antibiotic-susceptibility patterns for the isolates KpIMS38 and <i>E. coli</i> ATCC 25922 as tested using the Kirby-Bauer Test.
Table 4.1.3	Multiple antibiotic resistance (MAR) indices of the clinical isolates of <i>Klebsiella pneumoniae</i> used in the study.
Table 4.1.4	MIC of antibiotics from different classes against <i>K. pneumoniae</i> isolates used in the study as determined by the two-fold serial dilution method.
Table 4.1.5	Determination of metallo- β -lactamase (MBL) production among the isolates of <i>K. pneumoniae</i> used in the study.
Table 4.1.6	Minimum inhibitory concentration of amikacin, levofloxacin and meropenem determined using EzyMIC TM strips.
Table 4.1.7	Concentrations of antibiotics used to perform the biphasic killing assay on the clinical isolates of <i>K. pneumoniae</i> .
Table 4.1.8	Survival of <i>K. pneumoniae</i> isolates on treatment with three different antibiotics at suprainhibitory concentrations.
Table 4.1.9	Survival of KpIMS38 on treatment with different concentrations of levofloxacin.
Table 4.1.10	Growth curve of a batch culture of KpIMS38 grown in MH broth.

Table 4.1.11	Effect of the age of the inoculum on persister cell formation in KpIMS38 treated with levofloxacin.
Table 4.1.12	Effect of the size of the inoculum on persister cell formation in KpIMS38 treated with levofloxacin.
Table 4.1.13	Survival of levofloxacin treatment by successive generations of KpIMS38.
Table 4.1.14	Cross-tolerance of levofloxacin-induced KpIMS38 persisters to amikacin and meropenem.
Table 4.1.15	Susceptibility of KpIMS38 to varying concentrations of amikacin and meropenem.
Table 4.1.16	Proportion of stained cells in KpIMS38 stained with varying concentrations of CFDA.
Table 4.1.17	Cell-fluorescence in a culture of KpIMS38 stained with varying concentrations of CFDA.
Table 4.1.18	Effect treatment of levofloxacin on the cell-size of KpIMS38.
Table 4.1.19	Effect of levofloxacin treatment on the abundance of P1 and P2 sub-populations in KpIMS38.
Table 4.1.20	Effect of levofloxacin treatment on the fluorescence observed in cell-sub-populations in KpIMS38.
Table 4.2.1	Sequence type of KpIMS38 obtained through the MLST 2.0 tool.
Table 4.2.2	Antibiotic-resistance genes identified in the genome of KpIMS38 using ResFinder 4.1.
Table 4.2.3	Antibiotic-resistance genes identified in the genome of KpIMS38 using RGI 5.2.0.
Table 4.2.4	Virulence genes identified in the genome of KpIMS38 using the Single genome analysis tool.
Table 4.2.5	Prophage regions located in the genome of KpIMS38 by Phaster.
Table 4.2.6	Statistics of the assembly of the RNA transcripts from untreated as well as levofloxacin-treated KpIMS38 as performed using NGS.
Table 4.2.7	Statistics of differential gene-expression in categories on exposure of KpIMS38 to levofloxacin.

Table 4.3.1	Efficiency of amplification by qPCR for each primer pair corresponding to the candidate reference genes.
Table 4.3.2	Candidate genes ranked according to their stability as obtained from Delta-Ct, BestKeeper, NormFinder and geNorm algorithms using the RefFinder tool.
Table 4.3.3	Candidate genes ranked according to their stability using the RefFinder tool.
Table 4.3.4	Fold-change for each of the genes obtained using <i>kp4432</i> , <i>rpoB</i> , or <i>kp751</i> as reference genes.
Table 4.3.5	Fold-change for each of the genes obtained using combinations of <i>kp4432</i> , <i>rpoB</i> , or <i>kp751</i> as reference genes.
Table 4.3.6	Expression of toxin-antitoxin genes in KpIMS38 on treatment with levofloxacin.
Table 4.3.7	Fold-change for the stress-response genes in KpIMS38 upon treatment with levofloxacin for 8 hours.
Table 4.3.8	Expression of the stress-response genes in KpIMS38 15, 30, 45, 60 and 120 minutes after treatment with levofloxacin.
Table 4.3.9	Survival of putative Δ <i>ibrA</i> and Δ <i>pspF</i> strains of KpIMS38 in levofloxacin compared to the wild type.
Table 4.3.10	Survival of KpIMS38 strains putatively silenced for <i>relT</i> , <i>relAt</i> , <i>doc</i> and <i>relE</i> .
Table 4.3.11	Effect of the overexpression of toxin-antitoxin genes on persister-cell formation in KpIMS38.
Table A1.1.1	Bacteriological growth media used in the study and their composition.
Table A1.2.1	Chemicals used in the present study.
Table A1.2.2	Reagents used in the present study.

Chapter-1
Introduction

1.1 Persistence – A history

Survival under changing environmental conditions require adaptations. Bacterial cells seem to have mastered the art of adaptation. They accomplish this by resorting to changes in the cellular physiology and metabolism, that in turn affects other aspects of the cell structure and function, such as membrane permeability, efflux, sporulation, and dormancy. The environments inhabited by micro-organisms are not only of a complex nature but are subject to constant change. Bacterial cultures are grown in laboratories on bacteriological culture media that is nutritionally abundant, whereas bacteria found in nature inhabit environments that are generally oligotrophic. Microbes have evolved numerous responses to starvation, which include endospore formation, biofilm formation (Willey et al, 2017). A significant stress factor that bacteria encounter includes compounds with antimicrobial properties.

Since the discovery of penicillin by Alexander Fleming as a compound lethal to the bacteria causing diphtheria, meningitis, pneumonia, and scarlet fever (Fleming, 1929), antimicrobial compounds active against bacteria, or antibiotics, have been extensively used to treat a wide variety of conditions caused by bacterial infections (Cossart, 2018). The optimism of antibiotic therapy was, however, short-lived and was soon replaced by scourge of antibiotic resistance. Penicillin, the extract of the fungus *Penicillium notatum*, was first used to treat a gonococcal infection of the eye in a neonate in 1930 (Wainwright and Swan 1986) and by 1945, penicillin was being mass produced at over 646 billion units annually in the USA (Parascandola, 1980). However, an enzyme that degrades penicillin, termed "penicillinase", was found to be naturally produced by bacteria as early as 1938 (Booth and Green, 1938). Also discovered was the innate resistance of certain bacteria to the killing action of penicillin (Hobby et al, 1942a), by no less than Fleming himself at the time its discovery (Fleming, 1929). Newer studies have unearthed the prevalence of resistance to

beta-lactams, glycopeptides and tetracycline in bacteria 30,000 years ago (D'Costa et al, 2011). This is testament to the fact that apart from the classical methods of acquiring antibiotic resistance, i.e., errors in replication and horizontal-gene transfer, bacteria inherently possess mechanisms to overcome the toxic stress imposed by antibiotics. Antibiotic resistance has been implicated as the cause of 700,000 annual deaths globally, a figure that could escalate to 10 million deaths per year three decades from now if the situation were to be left unchecked (Morrison and Zembower, 2020). The concern regarding antibiotic resistance is understandably resolute, although another crisis has been fomenting that could exacerbate the predicament posed by antibiotic-resistance even further.

In 1942, Gladys Hobby was examining the activity of penicillin against various gram-positive bacteria. She observed that, given a constant number of hemolytic streptococci, increasing the concentration of penicillin hastened the rate of killing of the bacteria. This killing however failed to eliminate the entire culture. From the original population, 1% of the cells either multiplied and increased in number or were killed at a much slower rate (Hobby et al, 1942b). Two years later while investigating the bactericidal action of penicillin with *Staphylococcus aureus* – then referred to as *Staphylococcus pyogenes* – Joseph Bigger observed the frequent inability of the antibiotic to completely kill all the bacteria present in the culture. The most he could attain was a reduction in the cell number by six orders of magnitude (Bigger, 1944). He explained this phenomenon as a consequence of the presence of variant cells, randomly distributed among the bacterial population, in minute proportions that allowed the bacteria to "persist" through a lethal dose of the antibiotic penicillin. He discovered that specific cells within the original culture were pre-ordained to form "persisters". Bigger also observed that exposure to new environmental conditions led to the induction of persister cells. His most significant finding, however, was

the discovery that persisters were able to endure the lethal action of penicillin as a result of being in a non-dividing and dormant state. He drew this conclusion on the basis of three observations:

- a) The number of survivors, after treatment with penicillin, in bacterial cultures incubated at 37°C and at room temperature were much lower than that observed in cultures incubated at 4°C.
- b) Bacterial growth was stalled when grown in medium diluted with water (1:800). When treated with penicillin, this culture showed a minimal reduction in cell numbers.
- c) Treatment of bacterial cultures with penicillin in the presence of boric acid, a bacteriostatic compound, resulted in the death of only a fraction of the population, with almost 70% of the culture still surviving.

The comprehensive nature of Bigger's examination of the phenomenon laid the foundation for most of the initial work carried out on persister cells. Key among his inferences was the designation of persister cells as separate from resistant cells, due to the absence of any special properties that set them apart from the normal antibiotic-susceptible cells. Since any property that conferred resistance against an antibiotic upon the persister cells should be passed on to their descendants thereby granting them better fitness against the same antibiotic, the lack of an increase in the number of survivors upon being treated with the same antibiotic indicated the ability of intransigence to be distinct from antibiotic resistance.

While Bigger's findings are revolutionary in hindsight, they were obfuscated at the time by antibiotic resistance and the catastrophic outcomes it spawned for microbiology and healthcare. The phenomenon remained largely unexplored, with a handful of reports

describing the survival of a fraction of a bacterial population on treatment with antibiotics and their subsequent resuscitation to normal growth on removal of the antibiotic (McDermott, 1958; Greenwood, 1972) without any further investigation into the mechanisms that cause and maintain the persister state. The first lead towards any sort of explanation was uncovered by Moyed and Bertrand in 1983, when they reported the presence of an *E. coli* mutant that yielded persisters 3-4 orders of magnitude higher than the wild-type allowing it to better survive exposure to ampicillin (Moyed and Bertrand, 1983). The mutation mapped to a novel locus they termed *hipA*, and the specific mutant that yielded a high proportion of persister cells *hipA7*.

The first genuine findings that can be credited to reviving the sphere of bacterial persistence can be considered in two studies published in subsequent years, both carried out by the research group of Kim Lewis. Brooun et al (2000) unearthed a subpopulation of cells present in *Pseudomonas aeruginosa* biofilms that survived exposure to the fluoroquinolone ofloxacin. A dose-response curve for the biofilm resulted a plateau at high concentrations of the antibiotic, which was a consequence of the "superresistant" cells. A year later, another study was published by the same group where they studied the biofilm-antibiotic interaction further, and found that *P. aeruginosa* cells, when dislodged from the biofilm, exhibited sensitivity to ofloxacin comparable to their free-floating planktonic counterparts. They concluded that the recalcitrance of the biofilm to antibiotics was due the presence of persister cells within the biofilm. They further identified persister cells in stationary-phase cultures of *P. aeruginosa*, that allowed the biofilm to tide over high concentrations of the antibiotic (Spoering and Lewis, 2001). These findings significantly broadened interest in the field over the next 20 years and resulted in a greater understanding of the phenomenon of bacterial persistence.

1.2 Persistence vs Resistance

Bacterial persistence was reported for the first time during the 1940s based on observations of antibiotics being unsuccessful in completely eliminating bacteria in broth cultures. They were therefore perceived as bacteria exhibiting some form of resistance to the antibiotic administered. This is evident from the inferences of Brooun et al (2000) who, upon encountering the same phenomenon while studying *P. aeruginosa* biofilms, referred to the cells as superresisters, implying some manner of resistance.

How then can bacterial persisters be defined? In June 2018, a consensus statement was drafted during the workshop ‘Bacterial Persistence and Antimicrobial Therapy’ organized by the European Molecular Biology Organization (EMBO), the motive of which was to standardize definitions relating to antibiotic persistence (Balaban et al, 2019). Under the aegis of the statement, persistence is defined as the capacity of a fraction of a bacterial population to endure exposure to an antibiotic at a concentration that is lethal to the bacteria. It differs from resistance in that the latter confers upon bacteria the attributes of surviving exposure to an antibiotic as well as replicating in its presence. A property to distinguish bacteria exhibiting the two aspects is the minimum inhibitory concentration (MIC), which corresponds to the minimum amount of a particular antibiotic required to inhibit bacterial replication. Resistant bacteria require a higher concentration of an antibiotic to affect cellular metabolism and replication and consequently exhibit a higher MIC than their susceptible counterparts (Figure 1.1). In contrast, the MIC for the antibiotic remains unchanged in persistent bacteria, meaning they are equally sensitive to the drug as are susceptible bacteria.

Another property that distinguishes persistence from resistance is the inability of persister cells to replicate in presence of the antibiotics, akin to the susceptible bacteria. It is important to point out the similarity to heteroresistance or phenotypic resistance (Gollan et

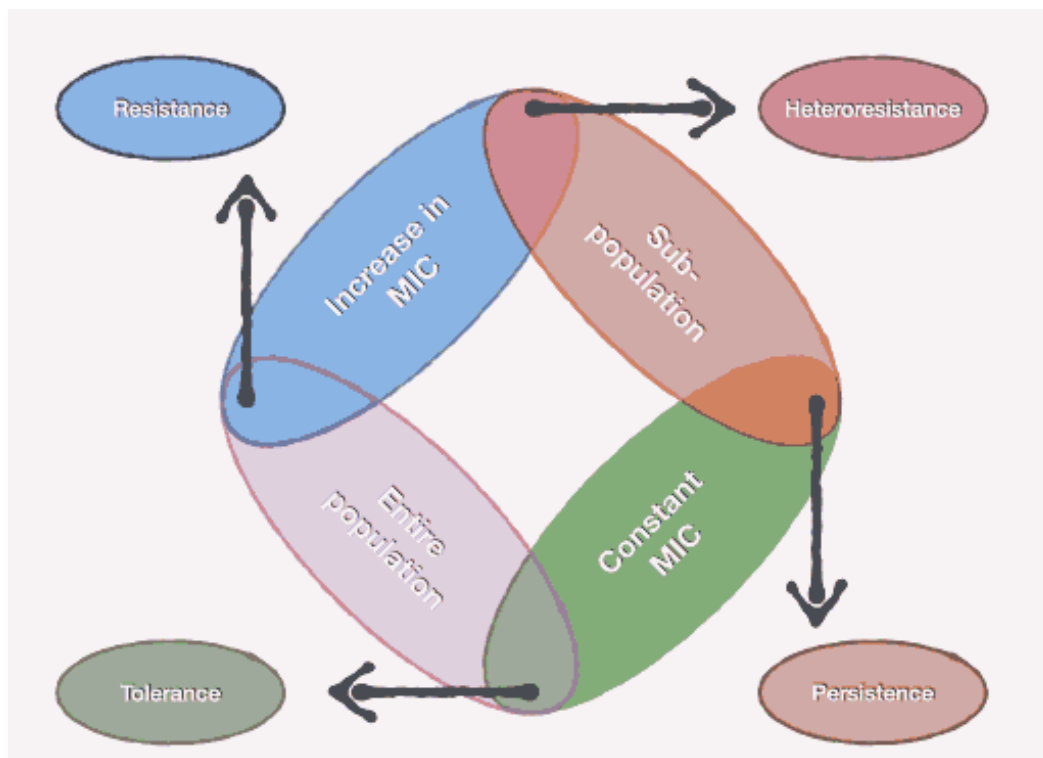
al, 2019), wherein a subset of a susceptible bacterial population becomes transiently resistant to an antibiotic (Figure 1.1). The difference between the two lies in a significant elevation (transient) of the MIC by the cells belonging to the subpopulation, resulting in an increase in population-numbers upon protraction of the antibiotic treatment (Figure 1.2 D).

1.3 Persistence vs Tolerance

Studies of persistence in bacteria tend to use the term interchangeably with tolerance. This tendency seems legitimate considering the similarity between the mechanisms that result in both phenomena; both exhibit reduced levels of ATP as well as cellular metabolism, and appear to be dormant (Lewis, 2007). The difference between the two lies in the fraction of the population that exhibits the phenotype; tolerance allows the entire population to survive exposure to the antibiotic while persistence preserves only a fraction of the original population (Balaban et al, 2019) (Figure 1.1). An effective method of distinguishing persistence from tolerance is by comparing the killing kinetics of a bacterial culture in response to antibiotic-treatment. The cell numbers in a tolerant population reduce at a uniform rate over a much longer period (compared to their susceptible counterparts), whereas the reduction observed in a population containing persisters is discontinuous with an initial rapid reduction followed by an extremely slow decrease in the cell number over time (Figure 1.2 E). This biphasic killing correlates with the death of susceptible cells in the population that leaves behind a small fraction, which represents persisters.

An approach to distinguish between persistence and tolerance was introduced by Fridman et al (2014) that measured the minimum duration for killing (MDK). The cell numbers were represented as the fraction of the original population surviving antibiotic treatment as a function of time and were used to calculate the MDK_{99} and $MDK_{99.99}$, corresponding to the duration required to eliminate 99% and 99.99% of the original population respectively. A

bacterial population exhibiting tolerance had a higher MDK_{99} than its susceptible counterpart; the slow, gradual reduction in the cell numbers indicating the population uniformly tolerating the lethal antibiotic dose. In contrast, a population forming persister cells when treated with a lethal dose of an antibiotic exhibited a MDK_{99} identical to the susceptible population, but a much higher $MDK_{99,99}$. This indicated that persister cells make up only a small fraction of the population (Figure 1.2 D and E).



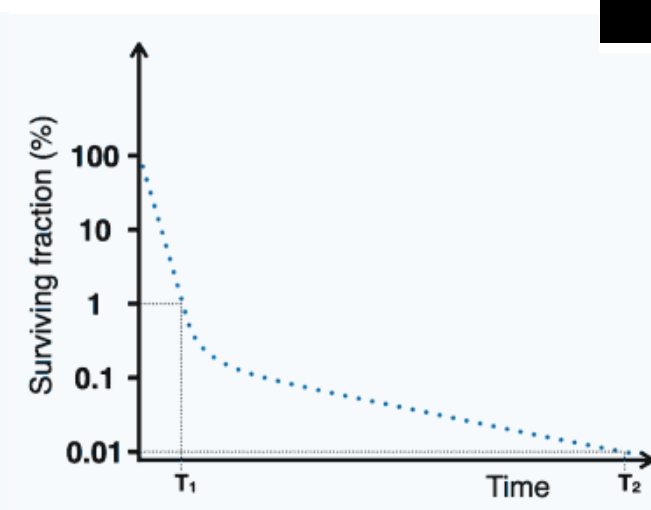
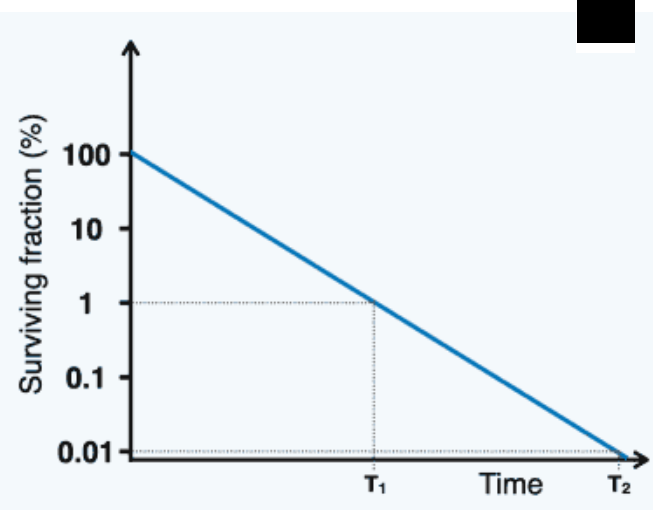
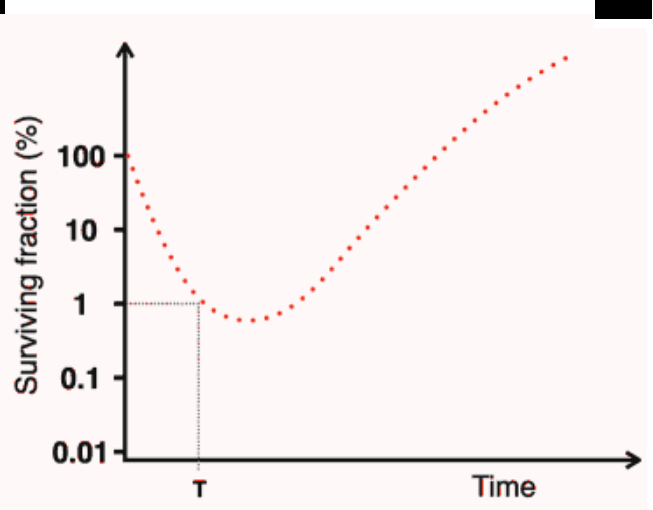
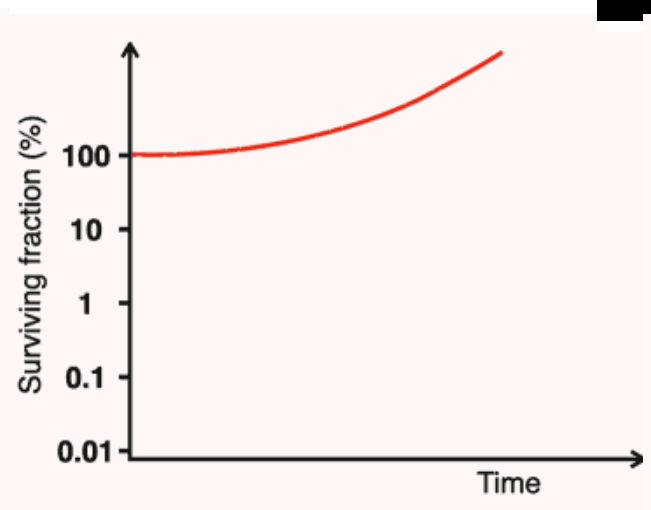
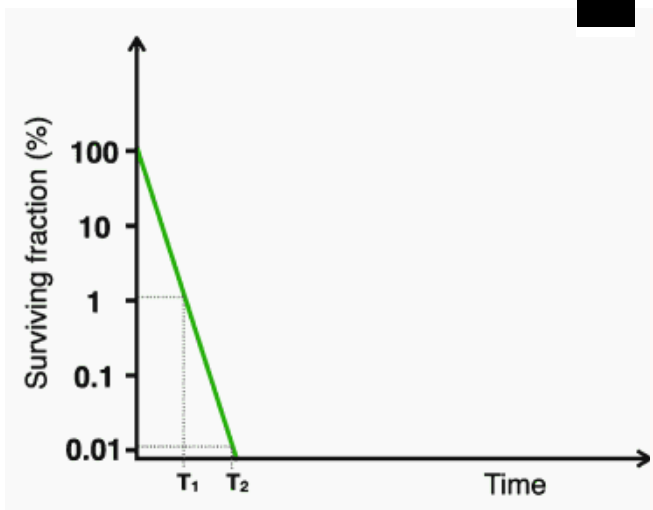


Figure 1.2 (overleaf) Schematic representation depicting the response of bacteria exhibiting different responses to antibiotic treatment. Bacteria demonstrating resistance (red, solid), heteroresistance (red, dotted), tolerance (blue, solid) and persistence (blue, dotted) to an antibiotic are compared to bacteria susceptible (green, solid) to it. Bacterial response is visualised as the proportion of the original culture (%) that survives antibiotic treatment as a function of time. The time required for the cell numbers to reduce to 1% (T1) and 0.01 % (T2) of the original are depicted as an additional means of comparing the different responses to antibiotic exposure.

1.4 Differentiating antibiotic persistence from persistent bacterial infections

It is important, at this juncture, to shed light on two terms that appear to describe the same phenomenon but are actually distinct from each other. As described previously, antibiotic persistence is the presence of a sub-population, which is able to overcome exposure to a lethal dose of an antibiotic compound, in a population predominantly consisting of cells that are killed by the same dose of the antibiotic. In contrast, persistent bacterial infections occur when bacteria that have invaded a host elude its immune system and remain within the host. Some infections remain asymptomatic, all the while retaining the potential to be revived and present as a clinical disease. Some infections do not abate, with the disease-symptoms persisting in spite of standard antibiotic treatment being administered, and become chronic in nature.

Bacterial infections become persistent through a variety of ways. A failure of the immune system to clear the pathogen generally results in a persistent infection when no antibiotic therapy has been administered. This could be a consequence of the immune system being unable to detect the pathogen as observed in *Borrelia* (Norris, 2006). It could also result from the pathogen manipulating the immune response to prevent its clearance, and has been observed in *Listeria monocytogenes* and *Mycobacterium tuberculosis* (Redpath et al, 2001). Additionally, studies have attributed persistence to lysis-avoidance by pathogens on being internalised by host immune-cells – seen in *Legionella pneumophila* and *Salmonella enterica*

var. Typhi (Scott et al, 2003) – as well as to shielding afforded by physical barriers like biofilms in *Pseudomonas aeruginosa* (Jesaitis et al, 2003) or granulomas in *M. tuberculosis* (Lawn et al, 2002) thereby preventing clearance by the immune system.

Persistence within the host by means of evading its immune system is a feature naturally inherent in multiple pathogens, which is either asymptomatic, as seen in infections caused by *Helicobacter pylori* (Monack et al, 2004) and *Mycobacterium tuberculosis* (Gomez and McKinney, 2004), or symptomatic, as observed in infections caused by *Escherichia coli* (Blango and Mulvey, 2010) and *Staphylococcus aureus* (McNamara and Proctor, 2000). Bacterial infections can also become persistent owing to underlying conditions, an example being the chronic infection of *Pseudomonas aeruginosa* in individuals with cystic fibrosis (Gibson et al, 2003).

1.5 Persistence – A clinical perspective

On the face of it, the discovery of persister cells does seem to provide an explanation to the occurrence of chronic or recurring bacterial infections. Persister cells tide over lethal antibiotic treatments and resuscitate to yield a normally growing population, a feature that makes elimination of certain bacterial infections challenging and contributes to their chronicity. There, however, has been no means to evaluate whether the bacteria causing persistent infections actually form persisters, and their prevalence in the host could simply be a consequence of one or more of the factors described in the previous section. In recent years, there has been a growing body of work that has uncovered a link between persister cells and persistent infections. Mutations in the gene *hipA*, including the *hipA7* mutation reported by Moyed and Bertrand, were found to be selected for in urinary-tract infections caused by *E. coli* (Schumacher et al, 2015). Patients with cystic fibrosis suffering from lung infections caused by *P. aeruginosa* were found to contain a high number persister cells with mutations in *hip*,

that rendered the infection recalcitrant to the antibiotic regimens administered (Mulcahy et al, 2010).

Further evidence was acquired by the use of mice as infection models. Ciprofloxacin was able to clear most of the bacterial infection within hours of its administration in mice infected with *Salmonella enterica* var. Typhimurium, though a significant number survived within dendritic cells (Kaiser et al, 2014). Studies have also found the number of persister cells to increase many fold upon internalization within host cells in comparison to that found upon culture in laboratory medium (Helaine et al, 2014; Kaiser et al, 2014).

New evidence is being unearthed pointing to persistence not being limited to bacteria alone. Persister cells have been observed in fungal pathogens like *Candida* (Rosenberg et al, 2018) as well as in viruses like herpes viruses (Speck and Ganem, 2010) and HIV (Sengupta and Siliciano, 2018).

These implications on antimicrobial therapy, healthcare and consequently on human disease make it vital to acquire an in-depth understanding of the phenomenon of persister-cell formation. The present study was undertaken to gain insights into the mechanism of persister cell formation in *Klebsiella* spp., and was carried out through the following objectives:

- a) Detection and characterization of persister cell formation in *K. pneumoniae*
- b) Elucidation of the genome and transcriptome of persister cells formed by *K. pneumoniae*
- c) Investigation of the role of various genes involved in persister-cell formation in *K. pneumoniae*

Chapter-2
Review of Literature

2.1. Diversity of organisms exhibiting persister cell formation

Among the ever-increasing body of work to elucidate the various aspects of persistence are numerous studies that have reported the occurrence of persister cells in a wide variety of organisms. Examples of a few have been collated in table 2.1, and include bacteria (Gram-positive as well as Gram-negative), mycobacteria, archaea, mycoplasma, fungi as well as viruses. Among the findings reported so far, the most striking are persister cell-formation by *Xanthomonas citri* subsp. *citri* – a phytopathogenic bacterium – in response to various chemical cues (Martins et al, 2021), and the discovery of persistence in cancer cells as a waypoint towards the emergence of drug-resistant cancers (Swayden et al, 2020). *Haloferax volcanii*, a haloarcheon formed persisters on encountering starvation or agents which induce oxidative stress or disrupt the membrane through a mechanism involving quorum-sensing (Megaw and Gilmore, 2017). *Mycoplasma mycoides* JCVI-Syn3B, a minimal cell with 1/10th of the total genes and the genome size of *E. coli*, exhibited persistence on exposure of exponential as well as stationary-phase cultures to the bactericidal antibiotics ciprofloxacin and streptomycin. This phenomenon is significant owing to the absence of TA systems and ribosome hibernating genes, which have been demonstrated as key components for persistence (Hossain et al, 2021). Biofilms formed by *Candida* spp. have demonstrated recalcitrance to antibiotic therapy, which has been attributed to the formation of persister cells with a high degree of metabolic dormancy (Li et al, 2015).

2.2 Identification of persister cells

2.2.1 Cultural methods of identifying persisters

The hallmark of a bacterial population containing persister cells is biphasic time-dependent killing. In other words, exposure of the population to a lethal concentration of an antibiotic results in a rapid decrease a large fraction of the population, followed by much slower

reduction of a small fraction of the population. This manner of time-dependent killing of a bacterial culture exhibiting persistence was first demonstrated in 1983 by Moyed and Bertrand (1983). They treated two different strains of *E. coli* K12 viz. HM21 and HM22 – the latter carrying the mutation *hipA7* – with ampicillin, fosfomycin and cycloserine, as well as starved the cultures of diaminopimelic acid (DAP) and observed the cell numbers in all these conditions as a function of time. While HM21 was gradually killed over the duration of the experiment, HM22 cultures exhibited a reduction in the cell numbers by 2 orders of magnitude within 60 minutes of exposure to the stresses. Thereafter, the cell numbers of HM22 did not decline, remaining constant for 4 hours after exposure to the respective stresses.

A similar phenomenon was observed by Keren et al (2004), where the same strains, i.e., HM21 and -22, were treated with lethal concentrations of ampicillin and ofloxacin and the cell numbers monitored over a period of time. While the results obtained with both the strains for ampicillin were similar to those observed by Moyed and Bertrand, treatment with ofloxacin resulted in biphasic killing for both the *E. coli* strains, with the number of survivors in HM22 greater than that in HM21.

This distinct nature of cell death in bacterial populations exhibiting persistence has been attributed to the heterogeneity of the population brought about by the presence of persister cells. The initial rapid killing corresponds to the death of the greater part of the population, which is sensitive to the antibiotic used. After a short period of time, the susceptible cells having been killed off, the bacterial population now consists of cells whose number is either constant or decreases very slowly over a prolonged period of time (Balaban et al., 2004).

Table 2.1 Organisms reported to form persister cells, grouped according to taxonomic categories.

Category	Organism	Reference
Gram-positive bacteria	<i>Bacillus subtilis</i>	(Hahn et al, 2015)
	<i>Enterococcus faecium</i>	(Michiels et al, 2016)
	<i>Listeria monocytogenes</i>	(Knudsen et al, 2013)
	<i>Staphylococcus aureus</i>	(Lechner et al, 2012)
	<i>Staphylococcus epidermidis</i>	(Shapiro et al, 2011)
	<i>Streptococcus mutans</i>	(Leung and Lévesque, 2012)
	<i>Acinetobacter baumannii</i>	(Michiels et al, 2016)
Gram-negative bacteria	<i>Escherichia coli</i>	(Blango and Mulvey, 2010)
	<i>Klebsiella pneumoniae</i>	(Ren et al, 2015)
	<i>Pseudomonas aeruginosa</i>	(Mulcahy et al, 2010)
	<i>Enterobacter aerogenes</i>	(Michiels et al, 2016)
	<i>Salmonella enterica</i> var. Typhimurium	(Helaine et al, 2014)
	<i>Vibrio cholerae</i>	(Jubair et al, 2012)
	<i>Xanthomonas citri</i> subsp. <i>citri</i>	(Martins et al, 2021)
Mycobacteria	<i>Mycobacterium tuberculosis</i>	(Mouton et al, 2016)
	<i>Mycobacterium smegmatis</i>	(Wakamoto et al, 2013)
	<i>Mycobacterium bovis</i>	(Mukherjee et al, 2016)
Archaea	<i>Haloferax volcanii</i>	(Megaw and Gilmore, 2017)
Mycoplasma	<i>Mycoplasma mycoides</i>	(Hossain et al, 2021)
Fungi	<i>Candida albicans</i>	(Lafleur et al, 2010)
	<i>Candida glabrata</i>	(Li et al, 2015)
	<i>Saccharomyces cerevisiae</i>	(Bojsen et al, 2016)
Viruses	Herpesvirus	(Speck and Ganem, 2010)
	HIV-1	(Sengupta and Siliciano, 2018)

Another measure to identify persister cells is the minimum duration for killing or MDK. A detailed explanation of the methodology has been provided in section 1.3 of this document. Briefly, the minimum duration required to kill 99% (MDK₉₉) and 99.99% (MDK_{99.99}) are used to distinguish bacterial persistence from bacterial tolerance. The latter, being a characteristic exhibited by the entire population, features both MDK₉₉ and MDK_{99.99} greater than that of its susceptible counterpart. Persister cells, on the other hand, have a MDK₉₉ identical to but a MDK_{99.99} greater than that of the susceptible cells. This is in direct correlation with persisters cells accounting for a small fraction of the bacterial population, thereby resulting in the death of 99% of the population that is susceptible to the antibiotic. The remaining fraction can withstand the antibiotic pressure, is killed much more slowly and therefore takes a much longer time to be reduced to 99.99% of the original population size. When represented in a cell fraction vs time of antibiotic exposure graph, persister cells show the classic biphasic reduction (Figure 1.2 E) while tolerant populations show continuous but slow reduction (Figure 1.2 D) in cell numbers.

Further explanation of the nature of this bimodal killing was offered by Balaban et al (2019) by examining the relationship between the survival of bacteria (S), the concentration of the antibiotic used (c) and the duration for which the antibiotic is administered (t). The relationship between these variables was described using the killing rate (ψ), which itself is a function of three different parameters:

1. The minimum inhibitory concentration or MIC, which is the minimum amount of an antibiotic required to inhibit growth of a bacterium,
2. The minimum duration required to kill 99% of the population or MDK₉₉, and
3. The Hill coefficient (k) for the steepness of the concentration dependence.

These parameters typify the physicochemical mechanisms that influence the bacterial response to antibiotic-exposure and determine the killing rate. The relationship between the parameters was represented by the equations

$$S(c, t) = e^{\psi \cdot t}$$

$$\psi(c) = \frac{\ln 0.01}{MDK_{99}} \times \frac{1 - \left(\frac{c}{MIC}\right)^k}{\frac{\ln 0.01}{\psi_{max} \times MDK_{99}} - \left(\frac{c}{MIC}\right)^k}$$

A culture exhibiting antibiotic persistence indicates the presence of a subpopulation, within the culture, that possesses a MDK₉₉ greater than the that of the rest of the population. Considering the fraction of persisters formed as α , the survival of the culture can be depicted as the cumulative survival of the two subpopulations with killing rates varying from each other, given as

$$S(c, t) = (1 - \alpha)e^{\psi \cdot t} + \alpha e^{\psi^* \cdot t}$$

where the killing rates of the susceptible population and persister population are ψ and ψ^* respectively.

2.2.2 Novel methods to study persistence

Advances in the field of technology have opened up the field of research to more elaborate analyses than were conceivable previously. Such advances have helped further the understanding of bacterial persistence by enabling detailed studies of bacterial populations as well as individual bacterial cells.

2.2.2.1 Fluorescence

Fluorescent compounds have allowed a vast variety of breakthroughs in the understanding of persister cells in bacteria. Shah and colleagues (2006) utilized unstable variants of the green fluorescent protein (GFP) to isolate persister cells from their normal

counterparts in an unstressed population. The gene coding for the said GFP was fused to the promoter *rrnBP1*, which drives expression of the 16S rRNA gene *rrnB*, and the construct introduced into the genome of the *E. coli* K12 strain MG1665. The population, when grown to the exponential state and sorted using a cell sorter, revealed the presence of two types of cells – brightly-fluorescent cells that accounted for a majority of the population, and dimly-fluorescent cells that made up a small fraction of the original population. The rationale for using the particular variant of the fluorescent protein was that cells with a stalled or low rate of metabolism will not be able to produce GFP in sufficient amounts to offset its degradation and will therefore stain dimly. In comparison, cells undergoing metabolism at normal rates will be able to maintain a much higher concentration of the GFP due to sustained production and will consequently stain brighter than their non-metabolizing counterparts. Both fractions of cells were treated with a lethal concentration of the fluoroquinolone ofloxacin, which killed the bright cells but against which the dim cells survived 20-fold better.

2.2.2.2 Live-cell microscopy

Fluorescent proteins coupled with time-lapse microscopy has proven to be a powerful technique in permitting a refined assessment of the phenomenon of persistence. One of the earlier studies on persister-cell formation in bacteria, carried out by Balaban et al (2004), utilized the technique to effectively dissect the persister state observed in different strains of *E. coli*. A microfluidic device was fabricated to possess a substratum patterned with grooves of dimensions that allowed bacterial cells to orient longitudinally within them. *E. coli* strains transformed to express a yellow fluorescent protein (YFP) were immobilized within the device, allowed to grow in the presence of liquid medium and treated with lethal concentrations of various antibiotics. The *hipA7* strain produced linear microcolonies and upon exposure to ampicillin experienced cell death and lysis. Within

this population was discovered a subpopulation of non-growing cells that were generated during the stationary phase of cell growth. These cells were weakly fluorescent and, upon removal of the antibiotic, were observed to divide like normal cells after a distinct lag phase. These cells were called Type-I persisters.

Another *E. coli* strain called *hipQ*, possessing a mutation in a region different to that of *hipA7* and forming persister cells in the presence of ampicillin, was also used in the same study. The mutation was recently identified to map to *ycdI*, a transcriptional regulator belonging to the LysR family (Hingley-Wilson et al, 2020). The *hipQ* culture contained a sub-population of slow-growing cells that existed prior to exposure to ampicillin but unlike the *hipA7* persisters, continued to grow and divide much slower than the normal cells. The cells continued to grow in the presence of the antibiotic at the same slow rate but switched to normal rates of growth and division upon removal of the antibiotic from the system. These were referred to as Type-II persisters, and it was theorized that a wild-type population consists of both types of persisters in addition to normal cells.

Fluorescent proteins have also played a key role in demonstrating that persister cells formed by *M. tuberculosis* are in a state of dynamic equilibrium where the rate of cell division is balanced by the rate of death. Wakamoto and colleagues (2013) utilized a system where *katG*, the gene coding for the enzyme catalase-peroxidase KatG, was replaced in *M. tuberculosis* with a *katG::dsRed2* fusion, the latter coding for a red-fluorescent protein DsRed. The resultant cells were immobilized in a microfluidic system, exposed to the antimycobacterial compound isoniazid and individual cells observed through time-lapse microscopy. As KatG activates the prodrug isoniazid and renders it toxic to the cell, the fusion protein permitted an assessment of the variation in the levels of KatG in cells exposed to isoniazid. They observed, through time-lapse microscopy, the presence of two different cell-types based on the DsRed fluorescence and by extension

KatG expression. Cells who exhibited frequent pulses of KatG had a low survival and were killed by the drug, while those who exhibited KatG pulses at a low frequency were survived for a much longer duration through isoniazid treatment. This was explained as a consequence of insufficient KatG being present to activate sufficient isoniazid and cause lethality due to infrequent pulsing. The observations demonstrate that rather than being a consequence of stoppage of cellular metabolism, persistence in *M. tuberculosis* was a dynamic phenomenon rooted in stochastic gene expression.

Wakamoto et al (2013) also utilized *M. tuberculosis* cells expressing GFP and observed individual cells through time-lapse microscopy. While the cells divided and formed microcolonies in growth medium, addition of isoniazid slowed their rates of division and growth until eventually the cells began to be lysed. However, a few cells remained intact throughout the treatment, visualized by their dim fluorescence, and once the antibiotic was removed began to rapidly grow and divide to form a microcolony. On a second exposure to isoniazid, the cells in the microcolony underwent replicative cessation and death in a manner similar to those from the first treatment, with a few surviving cells remaining. These observations constituted evidence of the non-genetic basis of persistence since the cells derived from the survivors of the first treatment with the antimycobacterial drug did not have any additional fitness against a second exposure.

2.2.3 Whole transcriptome analysis

The advent of Next-Generation Sequencing (NGS) technology made the sequencing, assembly, and annotation of entire genomes extremely convenient, something that was not possible with the pre-existing Sanger Sequencing technology. NGS orchestrates the enzymatic incorporation of nucleotides in tandem with the acquisition of data in a sequential manner that makes feasible the simultaneous generation of sequence data from thousands to billions of templates (McCombie et al., 2019). A transcriptome can best be

defined as the sum total of RNA transcribed and present within in a cell at a specific physiological state at a given point of time. Studying the transcriptome, also known as transcriptomics, involves characterising all species of RNA transcripts – mRNA, non-coding RNA, small RNA – through sequencing (RNA-Seq) as well as quantifying alterations in the levels of each transcript expressed across various conditions (Wang et al, 2009). RNA-Seq has considerable advantages for examining transcriptome fine structure such as the detection of novel transcripts, allele-specific expression and splice junctions. RNA-Seq does not depend on genome annotation for prior probe selection and avoids the related biases introduced during hybridization of microarrays (Zhao et al, 2014).

Transcriptomics have been used to monitor the transcriptional changes occurring on a global level in persister cells. Persister cells have been observed to exhibit heterogeneity on the basis of the factor inducing persistence as well as the organism being studied, which potentially indicates a distinct expression profile being obtained for each of the distinct persister populations. RNA-Seq has been used to decipher the transcription profile of persisters formed by various bacteria through a multitude of inducing factors. *A. baumannii* persisters, formed by treatment with the cephalosporin ceftazidime, exhibited a diverse expression of genes involved in the metabolism of amino acids, nucleotides, lipids, vitamins and energy, indicating overall a metabolically-dormant state. In addition, an increase in the expression of toxin-antitoxin genes was also observed (Alkasir et al, 2018).

The transcriptomes of *S. Typhimurium* persisters formed within macrophages as well as the macrophages themselves were analysed by Stapels et al (2018) using dual RNA-Seq. While expression patterns were expectantly different between infected and uninfected macrophages, there were differences between those containing bacteria in growing or

non-growing states as compared to those that had lysed bacteria. Genes involved in proinflammatory responses were downregulated while those involved in anti-inflammatory pathways were highly expressed in cells containing live bacteria. Genes associated with infection showed an elevated expression in intracellular bacteria, while both growing and non-growing intracellular bacteria expressed genes coding for the type-3 secretion system (T3SS) apparatus as well as its translocated effectors. This provided evidence which showed that intracellular *Salmonella* persisters are able to deliver pathogenicity factors without growing, unlike persisters grown in vitro, which are metabolically dormant.

Torrey and colleagues (2016) isolated *M. tuberculosis* strains exhibiting a high degree of persistence from clinical samples as well as *M. tuberculosis* mutants with a high-persistence phenotype, and studied their respective transcriptomes. They observed an upregulation in toxin-antitoxin (TA) systems, the greatest being the *higAB1* locus, as well as in the cellular protease *clpC2*, which has been implicated in activation of toxins from TA loci and bringing about a state of persistence. Their findings indicated similarities in the expression profiles of mutants and clinical strains exhibiting the high-persistence phenotype.

More recently, transcriptome analysis was instrumental in imparting novel insights into persister formation and the role of adenine-methylation on DNA in *E. coli*. Strains containing non-functional DNA adenine methylase (Δdam) experienced marked downregulation of various genes, including the TA system *ccdAB*, genes coding for the type II and type VI secretion systems, as well as the ABC transport system. Also observed was upregulation of pathways mediating protein translation and flagella-dependant mobility. Further, repression of pathways involved in DNA repair, and cellular adhesion were also observed. Interestingly, the Δdam strains were also deficient in persister

formation, thereby offering an insight the influence of DAM on persister cell formation in *E. coli* (Xu et al, 2021).

2.3 Mechanisms underlying the formation of persister cells

The first gene to be associated with bacterial persistence was *hipA* (Moyed and Bertrand, 1983). The discovery of a mutant of *E. coli* that was able to tolerate ampicillin many orders of magnitude higher than the wild-type opened the door to the understanding that persistence has a genetic basis. The same study also revealed that persister-cell formation in *E. coli* was not exclusively due to exposure to β -lactam antibiotics but due to any manner of subversion of murein synthesis. This observation pointed towards the possibility that unlike a gain-of-function required to effectuate antibiotic resistance, bacteria already possess the mechanisms necessary to induce persistence. Most, if not all, of the studies describing persistence have identified persisters based on the capability of bacteria to overcome exposure to antibiotics, which in turn suggest the trait originally manifested to permit cells to survive in hostile environments. Exposure to environments containing antibiotics, especially those populated by bacterial communities utilizing antibiotics as means of interspecies communication could have resulted in emergence of persistence (Bakkeren et al, 2020).

Since the discovery of *hipA*, numerous studies dedicated to elucidating the mechanism of persister cell formation have been carried out. These studies have identified two mechanisms whereby persister cells are formed, namely, stochastic generation and responsive generation. As suggested by their names, the latter involves the formation of persisters by bacteria in response to specific stimuli, while the former applies to the formation of persister cells without the presence of any instigating factor (Harms et al, 2016). Certain studies have attempted to ascribe persistence to defects and errors in cellular metabolism that fortuitously result in the formation of persister cells, putting forth the

"persistence as stuff happens" or PASH hypothesis (Johnson and Levin, 2013; Levin et al, 2014). Since its proposition, however, numerous studies have identified concrete molecular pathways that lead to the formation of persister cells. Considering the example of *Pseudomonas aeruginosa*, periodic treatment with the antibiotic ofloxacin was observed to gradually increase the frequency of persister cells formed by selecting for increased persister-formation. In the absence of antibiotic treatment, however, reduced levels of persistence were observed, indicating that persistence has a fitness cost (Stepanyan et al, 2015). This perceptible shift in persistence would not have been feasible if it resulted from chance errors.

2.3.1 Stochasticity and the formation of persister cells

Bacterial cells encounter molecular noise with respect to their gene expression, due to either the biochemistry of the process of expression (intrinsic) or due to fluctuations in other cellular processes that eventually affect expression (extrinsic) (Elowitz et al, 2002). Studies have determined, however, that noise in and of itself is insufficient to generate phenotypic heterogeneity. Amplification of the noise by additional processes, like positive feedback, are vital to bring about variation, which can precipitate the formation of phenotypically distinct subpopulations within a genetically identical or isogenic population that are able to stably coexist (Eldar and Elowitz, 2010). Stochastic persister formation has been described as the generation of phenotypic heterogeneity in an isogenic population of bacteria. It serves as an evolutionary strategy adopted by bacteria with the aim of maximizing its chances of survival and propagation in environments that are diverse and constantly changing (de Jong et al, 2011). Consequently, bacterial populations contain a basal number of persister cells even prior to exposure to antibiotics or other stresses. Populations of *E. coli* growing in a regular exponential manner were observed to contain subpopulations of

metabolically dormant cells (Balaban et al, 2004; Shah et al, 2006; Germain et al, 2015; Maisonneuve et al, 2013; Orman and Brynildsen, 2013).

2.3.2 Persister cell formation as an induced phenomenon

Responsive generation of persister cells involve the formation of persister cells in response to specific stimuli. Multiple studies have demonstrated the same on exposing bacteria to sublethal levels of any stress, including antibiotics.

Gram-positive as well as -negative bacteria were induced to form persisters when exposed to subinhibitory concentrations of ampicillin, gentamicin or ciprofloxacin (Goneau et al, 2014).

In response to starvation, *E. coli* and *P. aeruginosa* form persisters through a pathway under control of a GTPase Obg. The processes result in a reduction of the membrane potential that affects translation and DNA replication (Verstraeten et al, 2015).

Wu and colleagues (2012) observed the fluoroquinolone antibiotic ofloxacin to induce formation of persister cells in *E. coli*. The level of persisters in the treated population was further increased on exposure to paraquat, an oxidative stress inducer but this augmentation was not observed in populations treated with other antibiotics viz. ampicillin, and kanamycin. The increase in persisters was due to efflux of ofloxacin from the cell by the efflux pump AcrAB-TolC, which in turn was induced by paraquat.

The reality of persister cell formation is far from evident, with an explanation that unifies spontaneous persister-formation and induction of persistence still ambiguous. An explication was proposed by Michiels et al (2016) wherein the level of persister proteins expressed in the population on average are regulated by factors in the environment, and individual cells in the population that attained a threshold value for any number of such proteins go on to enter into the state of persistence. It is also possible that several

independent mechanisms rather than a singular mechanism act in conjunction to effect persistence but in the absence of any conclusive proof, it is speculation at best. However, one aspect that is becoming evident about persistence is that it comes under the umbrella of bacterial stress response. Studies on persistence have observed various factors in the environment of the bacteria act as stress signals thereby leading to the formation of persisters, and a majority of the molecular pathways implicated in the generation of persisters are elements of stress responses inherent within bacteria (Gollan et al, 2019).

2.3.2.1 Stress imposed through nutrition

Since the discovery of persistence being induced in *E. coli* by entry into the stationary phase of growth by Keren and colleagues (2004), a multitude of studies have implicated nutritional stress as a key instigator of persister-cell formation. Brown (2019) identified *E. coli* that produced persister cells upon encountering nitrogen starvation. Persistence was modulated by a two-component signaling system *ntrBC*, which functions to allow the cell to tide over conditions of nitrogen deficiency by sensing the deficiency and activating genes that permit scavenging of alternative sources of nitrogen. Brown (2019) also observed NtrC to activate the expression of RelA, a pyrophosphate synthetase, that in turn led to the production of the alarmone (p)ppGpp (a collective symbol representing guanosine tetraphosphate as well as -pentaphosphate). The mechanism by which (p)ppGpp evokes persister-cell formation in bacteria has been well studied and is discussed in detail in further sections, and it was through this mechanism that *E. coli* generated persister cells in the presence of nitrogen stress. Persistence was observed to be moderated in a (p)ppGpp-dependant manner in *Pseudomonas aeruginosa* (Nguyen et al, 2011) too.

A recent report implicated the intracellular concentration of adenosine triphosphate (ATP) as the driving factor in persister-cell formation in *E. coli* (Shan et al, 2017) as well

as *S. aureus* (Conlon et al, 2016). A depletion in the concentration of ATP was observed to restrain cellular metabolism, consequently reducing the activity of components that serve as targets for various antibiotics and resulting in a state of persistence independent of (p)ppGpp.

A study conducted on *E. coli* by Kotte et al (2014) discovered that the organism possesses the ability to control the rate of conversion of normal cells into persister cells in response to specific environmental cues. A change in the substrate, necessitating a shift in the metabolism from glycolysis to gluconeogenesis, resulted in the diversification of the population into two subsets. One subset was able to metabolise the substrate by adopting gluconeogenesis and continuing to grow, another subset of cells entered into a non-growing state. The non-growing cells did not perform gluconeogenesis and resumed normal growth upon the introduction of a glycolytic substrate, and in their state were tolerant to exposure to various antibiotics.

Radzikowski and colleagues (2016), while studying persistence in *E. coli*, observed an increase in the number of persisters on altering the carbon source in the growth medium from glucose to fumarate. The nutritional shift was observed to be the major driving factor in the formation of persisters through a reduction in the rate of cellular metabolism independent of the stringent response, which served to enhance the persistent state rather than induce it.

2.3.2.2 Stress imposed through antibiotics

Formation of persisters by bacteria on treatment with sub-lethal concentrations of an antibiotic has been observed for a large variety of organisms and antibiotics. *E. coli*, when treated with ciprofloxacin, was observed to form persister cells de novo. These persisters varied from those formed on treatment of the same strain with ampicillin and streptomycin - antibiotics belonging to different classes – since strains that did not form

persisters to ciprofloxacin yielded the same number of persisters to the other two antibiotics (Dörr et al, 2009).

Another study carried out by Kwan et al (2013) observed that inhibition of protein synthesis in *E. coli* by chemical treatment produced persister cells. *E. coli* exposed to rifampin, tetracycline and carbonyl cyanide m-chlorophenylhydrazone (CCCP) – that inhibit transcription, translation and ATP synthesis respectively – at concentrations higher than their MIC generated persisters that accounted for 10 to 100% of the total population. Treatment of *S. aureus* cultures with sub-MIC concentrations of various antibiotics viz. ciprofloxacin, gentamicin, oxacillin and vancomycin was seen to result in the formation of persister cells (Johnson and Levin, 2013).

Of greater consequence is the observation made by Ren and colleagues (2015) regarding *Klebsiella pneumoniae* treated with various antibiotics, namely, ciprofloxacin, kanamycin and ceftriaxone, in a gradually increasing manner. This was performed to simulate the gradual build-up of the antibiotic concentration in the human body during antimicrobial therapy, and observations showed the number of persisters formed to increase along with the increase in concentration. The effect was more pronounced for a clinical strain used as against the laboratory type-strain.

2.3.2.3 Stress imposed through acidic, osmotic and oxidative factors

Bacteria possess mechanisms to overcome stresses imposed by adverse conditions of acidity, osmolarity as well as the presence of oxidizing agents. A growing body of work has found persistence to be associated with the bacterial response to these stresses. Vega et al (2012) observed persister cell formation in stationary-phase cultures of *E. coli* exposed to sub-lethal concentrations of hydrogen peroxide (H₂O₂). Persistence was absent on exposure to lethal concentrations of H₂O₂, hinting towards the protection afforded by persistence under nonlethal conditions against future stresses. Another study

conducted by Wang et al (2017) identified persister-cell formation in *E. coli* treated with sodium salicylate. Persistence was established as a consequence of the formation of reactive oxygen species (ROS). A reduction in the membrane potential due to ROS was seen to effect a contraction of the cellular metabolism and an eventual formation of persister cells.

A pioneering study on persistence in *Streptococcus mutans*, carried out by Leung and Levesque (2012), identified various environmental factors to increase the number persister-cells formed. Exposure to acidic conditions (pH 5.0), oxidative stress (0.5M H₂O₂) as well as heat-shock (50°C) increased the number of survivors, after treatment with 20 µg/mL of ofloxacin, by a factor of 10-100 than unstressed cultures.

Conditions of high osmolarity were also observed to induce persister-cell formation. *S. aureus* exposed to 10% (w/v) NaCl formed persister cells 2-5 orders of magnitude higher than in unstressed cells and allowed survival in concentrations of gentamicin and ciprofloxacin 100 times higher than the MIC (Kubistova et al., 2017).

2.3.2.4 Signals from the extracellular environment

Metabolites exuded by bacteria into their extracellular environments have a propensity to induce the formation of persister cells. Vega and colleagues (2012) identified indole to trigger persister-cell formation in *E. coli*. Indole is produced during the stationary phase of growth in bacteria and is known to participate in bacterial responses against oxidative and membrane stress. It is also known to augment resistance to antibiotics by increasing efflux of the drugs. The presence of indole was key in modulating the frequency of persisters produced by *E. coli* during conditions of nutritional stress.

Another study observed indole-mediated persister-cell formation in *Salmonella enterica* var. Typhimurium in a manner similar to that observed in *E. coli*. An extraneous supply

of indole to a culture of *S. Typhimurium* was equally capable of inducing persistence as was indole produced by *E. coli* in a mixed community of both the microorganisms. The latter situation was observed to afford persistence to *S. Typhimurium* when used to simulate gastrointestinal infection in *Caenorhabditis elegans*. The findings are significant considering the inability of *S. Typhimurium* to produce indole by itself, and suggest that indole produced by commensal bacteria can augment the survival of *S. Typhimurium* infecting the intestine of a host through persistence (Vega et al, 2013).

A similar phenomenon was reported by Que and colleagues (2013) where 2'-amino acetophenone produced by *P. aeruginosa* was observed to promote persister-cell formation in a quorum-sensing manner in the same as well as in populations of *Acinetobacter baumannii* as well as *Burkholderia thailandensis*.

Pseudomonas aeruginosa produce much fewer persisters than *E. coli* or *S. aureus*, as observed on comparing the number of survivors after treating logarithmic- and stationary-phase cultures with various antibiotics. The number was observed to increase by 90-fold on exposure to either pyocyanin or the acyl-homoserine lactone 3-OC12-HSL prior to antibiotic treatment. The findings acquire significance due to the detection of both compounds in the sputa of cystic fibrosis patients (Möker et al, 2010), where cases of opportunistic pneumonia were reported to be caused by *P. aeruginosa* producing persister cells (Mulcahy et al, 2010).

2.3.2.5 Stress encountered within a host-system

A majority of the studies carried out to elucidate persister-cell formation in bacteria are *in vitro* procedures performed with bacteria grown in flasks and experiencing a single stressor. In reality, during the course of an infection for instance, bacteria are exposed to a collection of stressors described previously, each at a timing, duration and intensity discrete from one another. This implies that persisters present in an infected host may

very well be different from those formed in flasks using a single stress factor. Internalization within host cells has been observed to be a strong inducer of persistence. The number of persisters formed by *S. Typhimurium* increased 1000-fold on being internalized by bone-marrow-derived macrophages and dendritic cells. The environment within the vacuole, being acidic and nutritionally poor, was seen to induce the formation of persister cells (Helaine et al, 2014). A similar phenomenon was observed in *M. tuberculosis*, with uptake by macrophages dramatically increasing the number of persister cells formed (Mouton et al, 2016).

2.3.3 Toxin-antitoxin systems

Toxin-antitoxin (TA) systems constitute the bacterial framework that regulates cell growth and death in response to stress by effecting a transient arrest in the growth of bacteria (Yamaguchi et al, 2011). TA systems, also known as modules or loci, are essentially bipartite genetic elements consisting of a ‘toxin’ and an ‘antitoxin’. The toxin, usually a protein, hinders metabolic processes essential to bacterial growth whereas the antitoxin impairs the functioning of the toxin until a signalling event supersedes the antitoxin’s inhibition (Gerdes and Maisonneuve, 2012).

An antitoxin forms a tight complex with its cognate toxin, thereby regulating its activity. Additionally, most antitoxins possess a DNA-binding motif through which they autoregulate transcription of the TA module. Cellular proteases degrade the antitoxin, and this interplay controls the activity of the toxin as well as the rate of expression of the TA module. Consequently, antitoxins are synthesized at a higher level than their cognate toxins; a necessity to keep the toxins inactive.

Owing to its binding to the antitoxin, the toxin is considered as a corepressor of TA system. In addition, reports have identified the toxin to function as a derepressor of the transcription of its cognate TA module. This ability of the toxin to inhibit as well as initiate expression

of the TA system was attributed to conditional cooperativity, and the change in its activity was indicated as a function of the ratio of the concentrations of the antitoxin and the toxin (Overgaard et al, 2008; Winther and Gerdes, 2012).

Initial studies on TA modules represented them as “addiction modules” located on plasmid DNA in bacteria wherein the antitoxin was an unstable entity that required continued production. Loss of a plasmid containing a TA module during cell division brought down the concentration of the antitoxin in the progeny. This precipitated in toxin-induced death in or proliferative suppression of the progeny cells, and served as a means of facilitating plasmid maintenance after cell division termed post-segregational killing (Gerdes et al, 1986).

2.3.3.1 TA systems – a classification

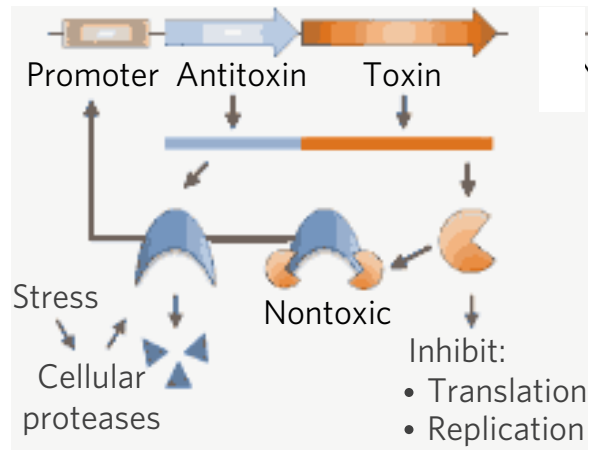
TA systems can be differentiated on the basis of the mechanism by which the antitoxin neutralizes its cognate toxin. To date, seven different categories of TA systems have been described with an eighth being added recently, all of which have been presented in table 2.2. Under the nomenclature scheme followed for TA systems, the name of the system is written first as a three-letter identifier. This is followed by the suffix denoting the antitoxin first, and then by the suffix denoting to toxin. Accordingly, the TA system consisting of HipA and HipB as toxin and antitoxin respectively is denoted as the HipBA TA system. Exceptions to this rule are when both components have different names. There, the name of TA system contains the toxin name followed by the antitoxin name, with a hyphen separating the two. An example is the *hok-sok* TA system consisting of the Hok toxin and the Sok antitoxin.

The most widely studied of the TA systems are those belonging to the type II. The genes in Type II TA loci are structured in an operon, with both toxin and antitoxin genes co-transcribed by a common promoter situated upstream of the pair (Leplae et al, 2011). The

toxin is bound by its cognate antitoxin under unstressed conditions of growth, thereby negating the activity of the toxin (Chan et al, 2016). Studies have identified the antitoxin to be susceptible to proteolytic cleavage due to existing in a partially unfolded state (Cherny and Gazit, 2004), which would result the relatively-stable toxin being free to act on its cellular target and affect cellular metabolism. Successful maintenance of the toxins in an inactive state would therefore require the antitoxin to be constantly replenished. This would explain the arrangement of the genes within the operon, with the antitoxin gene located upstream of the toxin gene, so that the antitoxin is synthesized before the toxin is transcribed and translated (Chan et al, 2016).

Table 2.2 Classification of toxin-antitoxin (TA) systems found in bacteria. The classification is based on the chemical nature of the antitoxin. Cys – Cysteine, sRNA – small RNA.

Type	Chemical nature of		Mode of action of antitoxin	Example	Reference
	Antitoxin	Toxin			
I	Antisense RNA	Protein	Binds to and inhibits translation of toxin mRNA	Hok-Sok	(Pedersen and Gerdes, 1999)
II	Protein	Protein	Binds to toxin	HipBA	(Hansen et al, 2012)
III	RNA	Protein	Binds to toxin	ToxIN	(Fineran et al, 2009)
IV	Protein	Protein	Reduces effect of toxin by performing activity antagonistic to it	YeeUV	(Tan et al, 2011)
V	Protein	Protein	RNase; degrades toxin mRNA	GhoST	(Wang et al, 2012)
VI	Protein	Protein	Stimulates degradation of the toxin	SocAB	(Aakre et al, 2013)
VII	Protein	Protein	Inhibits activity by oxidizing Cys residue	Hha-TomB	(Marimon et al, 2016)
VIII	sRNA	sRNA	Binds to toxin	SdsR-RyeA	(Choi et al, 2018)



The mechanism whereby the genes within the TA system exert their respective activities is explained in a schematic diagram (Figure 3.1) adapted from Page and Peti (2016). Antitoxins ameliorate the activity of their cognate toxins by directly interacting with the toxin and obstructing its active site (Blower et al., 2011; Boggild et al., 2012; Schureck et al., 2014). Antitoxins also possess the ability to bind to the operator of their operon, albeit weakly. This binding is strengthened when the antitoxin is bound to its cognate toxin, with the toxin serving as a co-repressor of its own expression (Bertram and Schuster, 2014; Hayes and Kedzierska, 2014).

Under conditions of normal cellular metabolism, the antitoxin is present in higher amounts than its cognate toxin, whose expression is impeded according to the process described previously. Conditions of stress have been associated with the activation of the cellular proteases Lon and Clp, which degrade the antitoxin and reinitiate expression of

the toxin gene from the TA locus. This process shifts the equilibrium towards a comparative abundance of the toxin, the free toxin then becoming available to act on its designated targets and effect a change in cellular metabolism (Hansen et al, 2012).

2.3.3.2 *The role of TA systems in bacterial persistence*

TA systems generally function as modules that are activated under and respond to conditions of stress experienced by the bacterial cell (Ronneau and Helaine, 2019). The discovery made by Moyed and Bertrand that implicated the toxin HipA – part of the type II TA module *hipBA* – in the formation of persister cells in *E. coli* focussed the investigation of the mechanistic aspect of bacterial persistence on TA systems. Their role in the formation of persister cells has been succinctly explained by Harms et al (2016), who note that TA systems are normally activated in an incremental fashion, which allows the cells to modulate their physiology and withstand the effects of stress without arresting bacterial growth. However, when the concentration of free toxin in the bacteria crosses a pre-defined threshold, the cell enters into a state of metabolic dormancy and growth inhibition. The growth inhibition manifested due to the expression of toxins from various type I and II TA systems have been associated with an increase in the ability of the bacteria to withstand the lethal effects of antibiotics, and have indicated a significant role of TA systems in persistence.

Persister cells exhibit a heightened expression of the TA modules, a phenomenon that has been observed in multiple bacteria. Shah et al (2006) observed an overexpression of genes belonging to TA systems in *E. coli* persisters. Both toxin and antitoxin genes belonging to the *yafQ-dinJ* and *yoeB-yefM* TA modules were overexpressed in persister cells compared to exponentially dividing cells. A total of 10 different TA systems were observed by Keren and colleagues (2011) to be upregulated in *M. tuberculosis* persisters formed on exposure to the drug D-cycloserine. The association between gain-of-function

mutations in TA genes and bacteria producing a higher proportion of persisters has been ratified in several studies carried out on the *hipBA* locus in *E. coli* (Moyed and Bertrand, 1983; Schumacher et al, 2015) as well as *M. tuberculosis* (Torrey et al, 2016), and the *shpBA* locus in *S. Typhimurium* (Slattery et al, 2013).

Interestingly, loss-of-function mutants for TA systems do not concomitantly reduce the frequency of persister-cell formation. Deletion of the *mazEF* and *relBE* TA modules in *S. mutans* did not reduce the number of persisters formed (Leung and Lévesque, 2012). Deletion of individual TA systems did not reduce the survival of *E. coli* persisters when exposed to gentamicin (Shan et al, 2015). The occurrence of this phenomenon is not uniform though, since cases of persistence being negatively affected by perturbations in TA systems have been reported. Deletion of YafQ, the toxin component of the *yafQ-dinJ* TA system, precipitated a 2400-fold reduction in the number of persisters formed by *E. coli* biofilms, and reduced its survival against various classes of antibiotics (Harrison et al, 2009). Single-mutants of *E. coli* deleted for *mqsR* and *relE*, belonging to *mqsAR*- and *relBE* TA systems respectively, observed a significant reduction in the persister-cells formed, increasing their susceptibility to trimethoprim, ampicillin and norfloxacin (Wu et al, 2015).

The elucidation of the mechanistic aspects of persister formation in bacteria have been mostly from studies conducted using *E. coli* (Norton and Mulvey, 2012; Harms et al, 2016). The *hipBA* TA system functions as a master regulator of persister-cell formation induced by starvation. Its role in mediating persistence through the stringent response is explained in further sections, but its importance to the phenomenon has been underscored by augmented persister cell-formation observed in mutants where antitoxin-driven inhibition of the toxin is diminished (Schumacher et al, 2015). The *tisB-istR* system is another example of a type II TA module that causes persister cell formation in *E. coli*.

The gene *tisB* encodes a small hydrophobic protein that binds to the cell membrane and, functioning as an ion channel, disrupts the proton gradient (Unoson and Wagner, 2008). This disruption reduced the ATP production of the cell that concomitantly resulted in metabolic cessation and induced the formation of persister cells (Shan et al, 2017). The role of the *yafQ-dinJ* TA system in persistence in *E. coli* is entwined with cellular signalling mediated by indole. Hu and colleagues (2015) discovered that activation of the toxin YafQ, functioning as an endoribonuclease that recognizes RNA containing 5'-AAA-G/A-3' sites and cleaving the transcripts, was responsible for degradation of mRNA transcribed from *tnaA*. The gene codes for the tryptophanase TnaA that produces indole from the breakdown of tryptophan. A depreciation in the amount of TnaA resulted in a reduction in the levels of indole and consequently an increase in persister cells formed. The significance of the result is in its contradiction to findings that have associated indole with an augmentation of persistence through a quorum-sensing route (Vega et al, 2012). Reports have described the formation of persister cells by *S. Typhimurium* internalized by cellular macrophages where a total of 14 type II TA systems were expressed at levels ranging from 4- to 30-fold greater than uninternalized cells (Helaine et al, 2014). Among the TA systems upregulated were the *relBE*, *shpAB*, *parDE*, *vapBC* and *phd-doc* TA systems, as well as toxins belonging to unrecognized families. One of them was identified as a Gcn5 N-acetyltransferase (GNAT), a superfamily comprised of enzymes catalyzing the transfer of the acetyl group from acetyl-coenzyme A (Ac-CoA). TacT, the toxin component of a type II TA system *tacAT*, was identified as a GNAT: TacT acetylated aminoacyl tRNAs, stalling the process of translation and inducing entry into persistence (Cheverton et al, 2016).

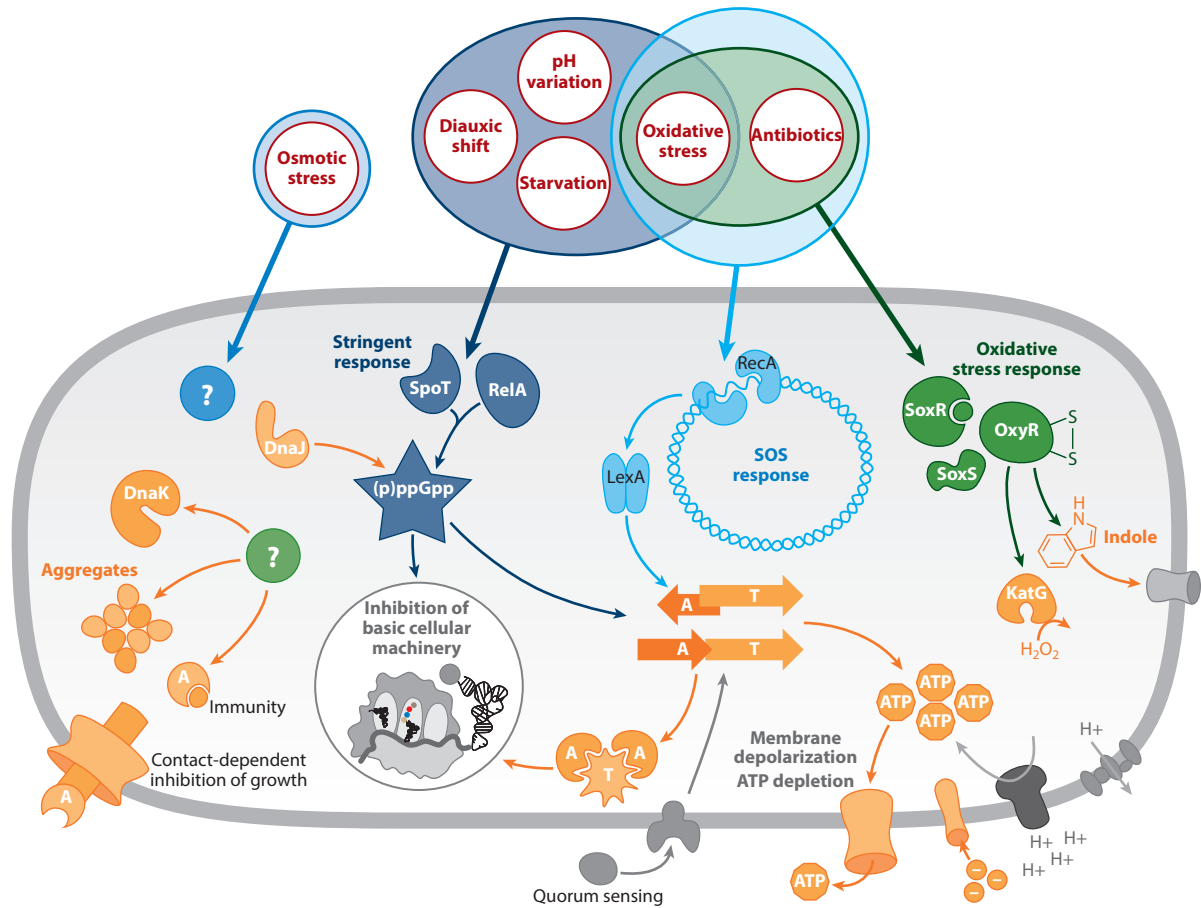
2.3.4 Pathways involved in bacterial persistence

Persister-cell formation may either be stochastic or be triggered by signals from the environment, but in both cases proceeds through the same contingent of signalling pathways (Harms et al, 2016). These pathways are traditionally identified with the response to various stresses, and their implication in persistence serves to further the understanding of persistence as a cellular response to stress (Figure 2.2, adapted from Gollan et al (2019)). A pioneering study carried out by Wu and colleagues illustrated the diversity of persister-forming mechanisms that exist within a single cell (Wu et al, 2015). A total of 21 genes that have been previously implicated in persistence were mutated and their impact on the survival of *E. coli* to varied antibiotic stresses examined. The genes playing a major role in persistence were components of pathways involved in the oxidative-stress, SOS and stringent responses, in energy production, as well as in regulating global metabolic networks. The study pointed towards the dynamic nature of bacterial persistence, influenced by different genes at different times and with varying degrees of significance.

2.3.3.1 (p)ppGpp signalling and the stringent response

The stringent response is a global system of regulation utilized by bacteria to calibrate cellular metabolism in response to conditions of nutrient limitation (Chatnaparat et al, 2015). Key to the response are guanosine tetraphosphate (ppGpp) and guanosine pentaphosphate (pppGpp) – collectively referred to as (p)ppGpp. They are generated in response to conditions of nutrient limitation as well other stresses, and function as the alarmone or a second messenger (Mechold et al, 2013). The (p)ppGpp network influences metabolic processes such as replication, transcription, and translation (Carneiro et al, 2011).

Many organisms have been reported to form persisters through pathways following the stringent response, but it has been best studied in *E. coli*. The cellular homeostasis of



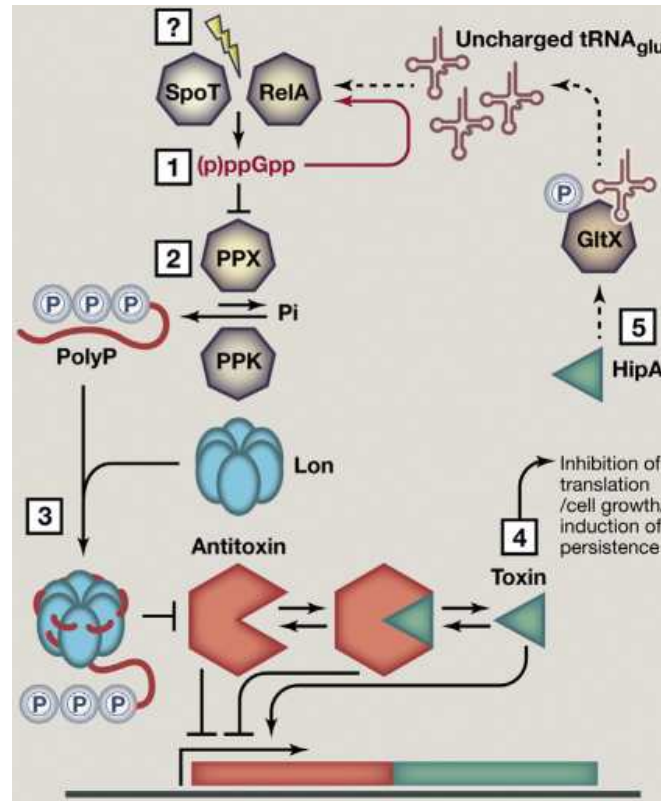
(p)ppGpp in *E. coli* is maintained by a pair of enzymes, namely, RelA and SpoT. RelA functions solely as a (p)ppGpp synthetase, synthesizing (p)ppGpp using adenosine triphosphate (ATP) and either guanosine diphosphate (GDP) or -triphosphate (GTP). SpoT, on the other hand, is a bifunctional enzyme possessing both synthetase as well as

hydrolase activities (Hauryliuk et al, 2015). Apart from the synthesis of (p)ppGpp, SpoT also possesses the ability to break it down to pyrophosphate and GDP/GTP. RelA is activated by conditions of heat shock and amino-acid starvation whereas SpoT is activated by starvation of carbon, fatty acids, iron, nitrogen and phosphate. The metabolic framework utilising (p)ppGpp has also been studied in other bacteria, who possess homologs to the above-mentioned enzymes that are called RelA-SpoT homologs or RSH enzymes. Enzymes that do not belong to the RSH family have also been observed to participate in the turnover of (p)ppGpp. Nudix hydrolases, enzymes widely distributed among bacteria with the ability to breakdown various nucleoside 5'-diphosphate (NDP) compounds, can also hydrolyse (p)ppGpp, while the pppGpp phosphohydrolase GppA and other like the elongation factor G (EF-G) are reported to rapidly convert pppGpp to ppGpp (Hauryliuk et al, 2015).

The current understanding regarding the action of the stringent response that produces persistence in *E. coli* was proposed by Maisonneuve and colleagues; the same is represented here (Figure 2.3) in the form of a schematic adapted from the same article (Maisonneuve et al, 2013). Accordingly, specific signals activate RelA and/or SpoT, which increase the pool of available (p)ppGpp in the bacterial cell. The accumulation of (p)ppGpp, in turn, shifts the flux of polyphosphates in the cell by inhibiting the activity of the enzyme exopolyphosphatase (PPX). As a result, the concentration of polyphosphates within the cell gradually increases through the action of the polyphosphate kinase (PPK). The polyphosphates associate with the cellular protease Lon and direct the degradation of antitoxins from toxin-antitoxin complexes formed by type II TA systems.

The now-free toxins exert their influence of cellular metabolism, culminating in the formation of persister cells. Among the toxins activated is HipA, which acts on the

enzyme glutamyl-tRNA synthetase by phosphorylating it and preventing the charging of glutamyl-tRNA with its cognate amino acid, i.e., glutamine. The concomitant accretion of uncharged glutamyl-tRNA actuates the synthesis of (p)ppGpp in a RelA-dependant



manner, thereby completing a positive-feedback loop and augmenting the phenomenon of persistence (Maisonneuve et al, 2013). (p)ppGpp influences bacterial metabolism in multiple ways to bring about the state of persistence. The binding of (p)ppGpp to the RNA polymerase in *E. coli* was observed to alter transcription of various genes,

accounting for roughly 15% of the genome (Sanchez-Vazquez et al, 2019). (p)ppGpp has also been noted to minimise the synthesis of all forms of RNA during conditions of cytosolic-magnesium deficiency even when the cell is abundant in amino acids and ATP (Pontes et al, 2016). This was demonstrated to reduce the number of ribosomes available and consequently attenuate the rates of both protein synthesis and metabolism, resulting in the induction of persistence (Pontes and Groisman, 2020).

2.3.3.2 *RpoS and the general stress response*

Bacteria encounter a variety of stresses during the course of their growth in natural environments. Certain stressful conditions require the bacteria to divert a significant portion of the available resources towards surviving through it, which is largely mediated by the transcriptional factor σ^S . Coded for by the gene *rpoS*, σ^S is a subunit of the bacterial RNA polymerase, and is involved in the regulatory control of several pathways. The transcription factor has been implicated in the expression of 500 or more different genes, either directly or through indirect means. The genes affected by σ^S are involved in repurposing cellular metabolism, in altering the shape of the cell and the composition of the cell-envelope, forming biofilms, in pathogenesis, and in the increase of mutagenesis induced by the stress (Hengge, 2010). Observations made in *E. coli* have implicated biofilm formation, extremes of pH and temperature, oxidative stress, scarcity of nutrients, and signalling by (p)ppGpp in instigating the general stress response.

The correlation between the general stress response and persistence is not straightforward. Nullifying the general stress response by simultaneously deleting *rpoS*, *gadB*, *gadX*, *osmY* and *mdtF* (downstream targets of σ^S) resulted in a large proportion of the population exhibiting persistence. The same study also showed that the toxin MqsR – part of the *mqsAR* TA module –reduced the RpoS-based stress-response that in turn increased persistence (Hong et al, 2012). Wu et al (2015) observed that in the absence of *rpoS*, *E.*

E. coli persisters survived exposure to ampicillin and norfloxacin better than the wild-type but were killed off in gentamycin. Another study carried out by Murakami et al (2005) observed that *rpoS* was involved in the formation of persisters in stationary- as well as logarithmic-phase cultures of *P. aeruginosa* in response to heat stress, and afforded protection against various antibiotics. Under conditions of osmotic stress however, persister cells were formed in a *rpoS*-independent manner.

2.3.3.3 The SOS response

Bacterial cells tend to accumulate DNA damage by encountering extremes of pH, experiencing oxidative stress or being exposed to antibiotics. Furthermore, interruptions in DNA replication as well as stochastic malfunctions in the cellular metabolism result in DNA damage. Mechanisms of DNA repair generate regions of single-stranded DNA while processing the damage, which induces the SOS response. Autoproteolysis of the repressor LexA – catalysed by RecA – activates the DNA-repair genes present in the SOS regulon, some of which include *dinG*, *recBCD*, *ruvABC*, *sulA*, and *uvrABCD* (Baharoglu and Mazel, 2014).

Evidence for the involvement of the SOS response in bacterial persistence was obtained from observations of upregulation of SOS genes in bacterial cultures containing a high number of persisters (Keren et al, 2004; Orman & Brynildsen, 2013b), and a reduction of the number of persisters upon impairment of DNA repair (de Groote et al, 2009; Dörr et al, 2009; Hansen et al, 2008; Theodore et al, 2013; Völzing & Brynildsen, 2015) or repression of the SOS response (Debbia et al, 2001; Dörr et al, 2009; Fung et al, 2010; Goneau et al, 2014; Völzing & Brynildsen, 2015). Conversely, persistence was increased when the SOS genes were constitutively expressed (Dörr et al, 2009).

Antibiotics that cause DNA-damage, such as fluoroquinolones, and activate the SOS response were observed to act as inducing agents of persistence. Treatment of *E. coli* with

sub-inhibitory concentrations of ciprofloxacin was seen to increase persisters formed against the antibiotic (Dörr et al, 2009), due to the cessation of replication caused by an upregulation of DNA repair pathways (Theodore et al, 2013). Additionally, the SOS response was observed to regulate persister formation through the *tisB-istR-I* TA system. Activation of the SOS response was observed to activate the toxin TisB, which was observed to increase persister-cell formation (Dörr et al, 2009), while *tisB* mutants produced fewer persister cells. Interestingly, persistence was completely eliminated in the mutants on treatment with fluoroquinolones that normally induce it. This could be construed as evidence towards the SOS response being the only mechanism of persister formation against fluoroquinolones, unlike in other modes of persister formation where multiple redundant pathways mediate the process (Dörr et al, 2010). It was hypothesized that TisB acts as an ion channel by inserting in the inner membrane (Unoson and Wagner, 2008) and forming anion-selective pores with a narrow diameter (Gurnev et al, 2012; Steinbrecher et al, 2012). The resulting efflux across TisB is believed to destabilise the proton-motive force across the cell membrane, thereby reducing the synthesis of ATP and disrupting cellular metabolism. One possible explanation for the role of TisB was to maintain the dormancy of the cells while DNA repair is carried out (Theodore et al, 2013).

2.3.3.4 Inactivation of the targets of antibiotics

Studying persister cells that are able to withstand aminoglycoside-exposure has unearthed the role of ribosome hibernation in propagating it. Bacteria possess the property to dimerise their ribosomes as a protective measure during conditions of stress. This leads to the formation of 100S ribosomal particles that are deficient in mRNA and tRNA, and are translationally quiescent (Wada et al, 1995; Kato et al, 2010). The 100S particles immediately dissociate into 70S ribosomes by introduction into fresh medium and can carry out translation (Wada et al, 1990; Wada, 1998). Aminoglycosides associate with

the 30S ribosomal subunit and increase the rate of mismatches between codons in the mRNA and their corresponding aminoacylated tRNAs. Amino acids are misincorporated into the nascent peptide as a consequence and the resulting mistranslated proteins are increasingly liable to misfolding. When the misfolding occurs in membrane proteins that are then inserted into the cell envelope, an increase in the uptake of aminoglycosides has been observed, thereby potentiating the toxicity of the antibiotics and causing cell death (Kohanski et al, 2010). Hibernation promoting factor (HPF), responsible for bringing about ribosome hibernation, was found to be vital to the formation of persister cells that sustain exposure to aminoglycoside antibiotics in *E. coli* and *L. monocytogenes* (McKay and Portnoy, 2015). The ribosome modulating factor (RMF), a protein associated with the 100S dimers and essential for ribosome hibernation (Prossliner et al, 2018), was observed to be overexpressed in stationary-phase persister cells of *E. coli* (Keren et al, 2004).

Fluoroquinolones are bactericidal antibiotics that affect DNA replication. The antibiotics form a ternary complex by binding to DNA topoisomerases already bound to their DNA substrate and immobilising the enzymes. This not only impairs replication and expression of genes in the surrounding region, but also destabilizes the enzyme-DNA complexes, which releases the unwound DNA and eventually results in the fragmentation of the bacterial genome (Pohlhaus and Kreuzer, 2005). Accordingly, mechanisms that inhibit DNA replication have been implicated in persistence. CspD – a protein structurally similar to the cold shock proteins (Csp) – binds to single-stranded DNA in replication forks and inhibits DNA replication (Uppal et al, 2014), and has been implicated in persister cell formation (Kim and Wood, 2010). In addition, DNA replication was observed to be inhibited by the activity of (p)ppGpp on DnaG, the enzyme responsible for the synthesis of RNA primers and thereby initiation of replication (Wang et al., 2007).

A shift in the carbon-source induced the formation of persisters in *E. coli* to withstand exposure to fluoroquinolones in a (p)ppGpp-dependant manner. Higher levels of (p)ppGpp activated DksA, which in turn repressed the activity of RNA polymerase. High concentrations of (p)ppGpp also affected various downstream modulators that inhibited DNA gyrase and reduced negative supercoiling in DNA (Amato et al, 2013).

2.3.3.5 Efflux

An examination of *E. coli* persisters revealed an increase in the expression of the efflux pump TolC, and the cells exhibiting increased efflux activity to maintain a low intracellular concentration of beta-lactam and fluoroquinolone antibiotics (Pu et al, 2016). Evidence in its support was obtained by observations in *E. coli* and *S. aureus* where introduction of specific metabolites along with aminoglycoside antibiotics led to the clearance of persister cells (Allison et al, 2011). A hypothetical scheme was proposed to explain this phenomenon where, upon uptake into the cytoplasm, specific metabolites enter their respective metabolic pathways and lead to the production of NADH. Oxidation of NADH by means of the electron transport chain generates a proton-motive force, which is exploited to bring about influx of the aminoglycosides and act upon their cellular targets, leading to eventual cell death. Efflux was also implicated as the major factor bringing about persistence in *Mycobacterium* growing intracellularly in macrophages. Administration of drugs that inhibit efflux activity greatly reduced the survival of intracellular persisters to the antimycobacterial isoniazid (Adams et al, 2011).

2.3.3.6 The ROS response

Reactive oxygen species (ROS) are produced during the course of normal metabolism in the bacterial cell and are functionally significant with regard to cell signalling and maintaining homeostasis. They are essentially species of oxygen that are chemically reactive, and include molecules such as hydrogen peroxide (H₂O₂) as well as radicals

such as superoxide (O_2^-), and hydroxyl [OH^-] radicals. An increase in the concentration of ROS during conditions of environmental stress – exposure to antibiotics, heat, ultraviolet (UV) radiation – is known to damage cellular components like proteins, lipids and DNA, which in sufficiently high amounts result in cell death (Trastoy et al, 2021). Bacteria possess mechanisms to dispense with ROS in the form of enzymes, such as superoxide dismutase (SOD) or catalase, or antioxidants, like ascorbate or glutathione. Oxidative stress is when the cellular mechanisms cannot keep pace with the generation of ROS, resulting in accumulation of the latter at levels inhibitory to cellular metabolism (Zhao & Drlica, 2014).

The mechanism of persistence induced by exposure to ROS is reliant on the phage-shock protein (*psp*) genes as well as the OxyR and SoxRS systems. The *psp* genes – A, B, C, D, E – were expressed at a higher level as were genes comprising the SoxRS and OxyR regulons in the persisters formed by *E. coli* and *S. Typhimurium* (Vega et al, 2012, 2013).

Various studies have pointed to an inverse relationship between ROS and persistence. Observations on the coexistence of a mixed culture of *P. aeruginosa* and *A. baumannii* in a biofilm that *P. aeruginosa* produced pyocyanin, which induced the production of ROS and consequently led to the formation of *A. baumannii* persisters. Persister cells expressed a high level of catalase and superoxide dismutase, enzymes that detoxify ROS (Bhargava et al, 2014). In contrast, *Mycobacterium smegmatis* cultures treated with thiourea – a scavenger of hydroxyl radicals – survived exposure to a lethal dose of an antibiotic and formed persisters. This indicated persister-cell formation in a ROS-independent manner (Grant et al, 2012). Similarly, hydrogen sulphide (H_2S) was also observed to induce persistence by stimulating the synthesis of catalase and SOD (Shatalin et al, 2011).

2.4 Persistence and evolution

Persisters survive in stressful conditions by existing in a non-growing state, during which the cells encounter multiple stresses that have the propensity to induce mutations. The regrowth of such cells carrying mutations could result in antibiotic resistance (Gollan et al, 2019).

Persisters exhibit a significant degree of metabolic inactivity compared to the regularly-dividing non-persister cells. Hence, the targets of antibiotics, which are components of the metabolic processes, are scarce enough to not corrupt metabolism even if acted upon by antibiotics (Lewis, 2010). However, certain observations have been obtained that are at odds with the features attributed to most persisters. Certain persisters divide slowly, even in presence of antibiotics, and their progeny appear to inherit this property (Balaban et al, 2004; Wakamoto et al, 2013; Goneau et al, 2014), which could possibly be a consequence of epigenetic mechanisms combined with cellular stochasticity (Day, 2016).

E. coli populations exposed to consecutive rounds of antibiotic treatment produced experienced an augmentation in persistence. The number of persister cells formed increased after as little as 2-3 regimens of treatment with aminoglycosides. What is more, the successive antibiotic treatment led to an accumulation of point mutations in various genes previously unrelated to persistence (van den Bergh et al, 2016). In another experiment carried out by Levin-Reisman et al (2017), *E. coli* cells grown in a rich medium were intermittently exposed to ampicillin. They observed that accumulation of mutations that increased persistence was frequently followed by an accumulation of mutations that imparted resistance to ampicillin. Also, while cells required atleast two mutations to develop resistance, persistence could be acquired by as little as a single mutation. In a recent study carried out by Windels et al (2019) in *E. coli*, exposure to bactericidal antibiotics killed all growing cells, with persisters as sole survivors. They also observed high-

persistence populations to have an increased rate of mutation when exposed to low concentrations of the antibiotics. These findings led them to speculate that persistence could lead to the emergence of resistance in the bacterial culture. This observation has translated into real-world scenarios, where strains exhibiting a high degree of persistence have been isolated from cases of recurrent infections involving long-term treatment with antibiotics. Cultures of *E. coli*, *P. aeruginosa* or *S. aureus* isolated from such cases exhibit biphasic killing on treatment with bactericidal antibiotics (McNamara and Proctor, 2000; Mulcahy et al, 2010; Gefen et al, 2017; Windels et al, 2019).

S. Typhimurium was observed to extensively form persister cells in mice, which survive exposure to ceftriaxone or ciprofloxacin by residing intracellularly within the gut tissue. The most striking of the observations was the ability of persisters to serve as a reservoir of plasmids and transmit them to other cells. This ability was recapitulated when persisters acted as plasmid-donors and transformed populations of *E. coli* present in the gut on being seeded into nascent mice (Bakkeren et al, 2019). Taken together, these observations highlight the role of persister cells in promoting horizontal gene transfer, and provide an explanation for the presence of a large number of plasmids and mobile genetic elements that promote resistance and virulence in bacteria causing gut infections (Bakkeren et al, 2020).

2.5 Persistence and *Klebsiella*

In 2017, the World Health Organisation (WHO) stated an urgency of the development of new antimicrobial compounds to combat antimicrobial resistance against a number of pathogenic bacteria. Among those mentioned, six species were grouped together and accorded a priority status on the basis of the frequency of isolation in clinical cases as well as the occurrence of antibiotic resistance. They were collectively referred to as ESKAPE pathogens, and consisted of *Enterococcus faecium*, *Staphylococcus aureus*, *Klebsiella*

pneumoniae, *Acinetobacter baumannii*, *Pseudomonas aeruginosa*, and *Enterobacter* sp. (de Oliveira et al, 2020).

Frequently present in the microflora of the intestines, mouth, skin, *K. pneumoniae* is known to inhabit hospital settings too – especially medical devices. Nosocomial infections caused by the bacteria affect the respiratory and urinary tracts as well as blood (Li et al, 2014). *K. pneumoniae* typically cause opportunistic infections in individuals with a compromised immune system or already suffering from another infection (as secondary infections). The infections frequently develop a chronic nature owing to the formation of biofilms (Jagnow and Clegg, 2003) and/or possession of resistance to multiple classes of antibiotics (Munoz-Price et al, 2013).

The discovery of persister cell-formation on *K. pneumoniae* has severe implications on the management of infections caused by the same. Ren et al (2015) were the first to report the formation of persister cells in non-clinical as well as clinical isolates of *K. pneumoniae*. Persisters were observed as being part of the pre-existing population of exponentially growing cells. They could withstand exposure to various bactericidal antibiotics at concentrations greater than their minimum inhibitory concentration (MIC) and yielded biphasic time-kill curves. An interesting outcome of the study was the observation of an increase in the number of surviving bacteria upon exposure to a gradually-increasing concentration-gradient of an antibiotic.

Michiels and colleagues (2016) studied persister formation in ESKAPE pathogens, including *K. pneumoniae*, against a background of aminoglycosides. Persisters were present in stationary-phase cultures of *K. pneumoniae*, appearing as a biphasic curve when measuring the cell death in amikacin as a function of time. On subjecting cultures to repeated rounds of aminoglycoside exposure, the fraction of the cell-population making up persisters was observed to gradually increase. This high-persistence phenotype was distinct

from resistant cells since the cells exhibiting it did not register elevated MICs with respect to the wild-type. Also, high-persistence populations could survive exposure to other antibiotics significantly better than the wild-type, as evidenced during treatment with amikacin, meropenem and colistin. These observations pointed towards periodic administration of a high dose of antibiotics exerting a selective pressure that directs the evolution of a higher degree of persistence in *K. pneumoniae*.

Li et al (2018) were the first to report the generation of persister cells by *K. pneumoniae* in response to low doses of antibiotics that can then tolerate exposure to much higher concentrations of the same antibiotics. Another key finding from their work was the formation of type I persisters in response to entry into the stationary phase of growth, evidenced by a marked increase in the number of persisters. They also noted a prevalence of type II persisters in cultures during the lag and exponential phases of growth, typified by constant levels of persisters during the time period.

As detailed above, the body of work dealing with persistence in *K. pneumoniae* is sparse when seen in light of the understanding available on the subject for *E. coli*, *P. aeruginosa*, *S. aureus* and even *M. tuberculosis*. While the importance of *K. pneumoniae* from a clinical standpoint is unambivalent, the mechanistic aspects of persister cell formation within the species remains unexplored as of yet. Understanding persistence in *K. pneumoniae* would not only provide novel insights into comprehending its pathophysiology, but would also help fill the gaps in the understanding of persistence as a whole, whose impact on understanding and combating bacterial infections and antimicrobial resistance would be invaluable.

The present study was designed with an aim to investigate the persister-cell formation in a clinical isolate of *K. pneumoniae*, by characterising and deciphering the mechanistic aspects of the same. To carry out the same, the following objectives were proposed:

- a) Detection and characterization of persister cell formation in *K. pneumoniae*
- b) Elucidation of the genome and transcriptome of persister cells formed by *K. pneumoniae*
- c) Investigation of the role of various genes involved in persister-cell formation in *K. pneumoniae*

Chapter-3
Materials and
Methods

3.1 Materials

3.1.1 Chemicals and antibiotics

The antibiotics used in the present study (Table 3.1.1) were available in powdered form and stored at 4°C. For use, stock solutions of appropriate concentrations were prepared in appropriate solvents and sterilised using a 0.22 µm syringe-filter (Jet Biofil, China). The sterile stock-solutions were stored in 1.5 mL microcentrifuge tubes or 15 mL screw-capped tubes at -20°C until required. Containers were covered in aluminium foil to prevent exposure to light wherever required.

Table 3.1.1 Antibiotics used in the current study.

Sr. No.	Antibiotic	Solvent	Concentration (mg/mL)	Make (Catalogue Number)
1	Amikacin	Water	10	Sigma-Aldrich, USA (A2324-5G)
2	Cefepime	Water	10	Lupin Ltd., India
3	Chloramphenicol	70% Ethanol	34	USB, USA (23660)
4	Kanamycin sulphate	Water	50	USB, USA (17924)
5	Levofloxacin	Water	10	Sigma-Aldrich, USA (28266-10G-F)
6	Tetracycline hydrochloride	70% Ethanol	10	USB, USA (22015)
7	Meropenem	Water	10	Macleods Pharmaceuticals Ltd., India

Dodeca Enterobacteriaceae-I (DE053-1PK) and -II (DE054-1PK) (HiMedia, India) discs were used in this study. One dodeca disc contained twelve discs comprised of twelve different antibiotics at unique potencies (Table 3.1.2). The two discs afforded the coverage of 24 different antibiotics simultaneously.

Table 3.1.2 Composition of Dodeca Enterobacteriaceae discs and their potencies

Antibiotic	Symbol	Potency (µg)	Class
Amikacin	AK	30	Aminoglycoside
Gentamicin	GEN	10	
Ciprofloxacin	CIP	5	Fluoroquinolone
Gatifloxacin	GAT	5	
Levofloxacin	LE	5	
Ofloxacin	OF	5	
Cotrimoxazole	COT	25	Sulfonamide + Pyrimidine analog
Ampicillin	AMP	10	β-lactam
Aztreonam	AT	75	
Imipenem	IPM	10	β-lactam (Carbapenem)
Meropenem	MRP	10	
Cefepime	CPM	30	β-lactam (Cephalosporin)
Cefoperazone	CPZ	75	
Cefotaxime	CTX	30	
Cefoxitin	CX	30	
Ceftazidime	CAZ	30	
Ceftizoxime	CZX	30	
Ceftriaxone	CTR	30	
Cefuroxime	CXM	30	
Amoxyclav	AMC	30	
Ampicillin/Sulbactam	A/S	10/10	
Ceftazidime/Clavulanic Acid	CAC	30/10	
Piperacillin/Tazobactam	PIT	100/10	
Ticaricillin/Clavulanic Acid	TCC	75/10	

The minimum inhibitory concentration (MIC) of antibiotics for bacterial isolates was ascertained using Ezy MIC™ strips (HiMedia, India). Each strip contained an antibiotic immobilised in a two-fold concentration gradient for the particular antibiotic. In addition, specialised strips were used to phenotypically assay for the production of metallo-β-lactamases (MBL). The details pertaining to the strips used in this study are organised in table 3.1.3.

Table 3.1.3 EzyMIC™ strips used to determine the response of antibiotics on the bacterial isolates used in this study.

Sr. No.	Antibiotic present	Concentration gradient	Make (Cat.No.)
1	Amikacin	0.016-256 µg/mL	HiMedia, India (EM001-10ST)
2	Levofloxacin	0.002 – 32 µg/mL	HiMedia, India (EM027-10ST)
3	Meropenem	0.002 – 32 µg/mL	HiMedia, India (EM080-10ST)
4	Imipenem	4- 256 µg/mL	HiMedia, India (EM078-10ST)
	Imipenem + EDTA	1-64 µg/mL	
5	Meropenem	4 - 256 µg/mL	HiMedia, India (EM092-30ST)
	Meropenem + EDTA	1 - 64 µg/mL	

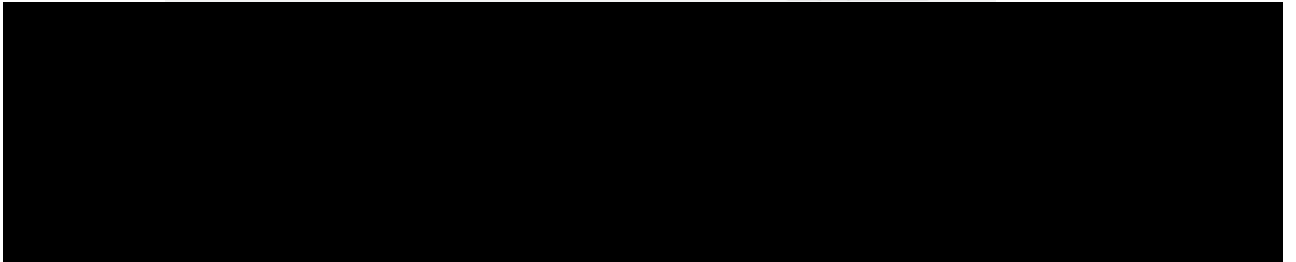
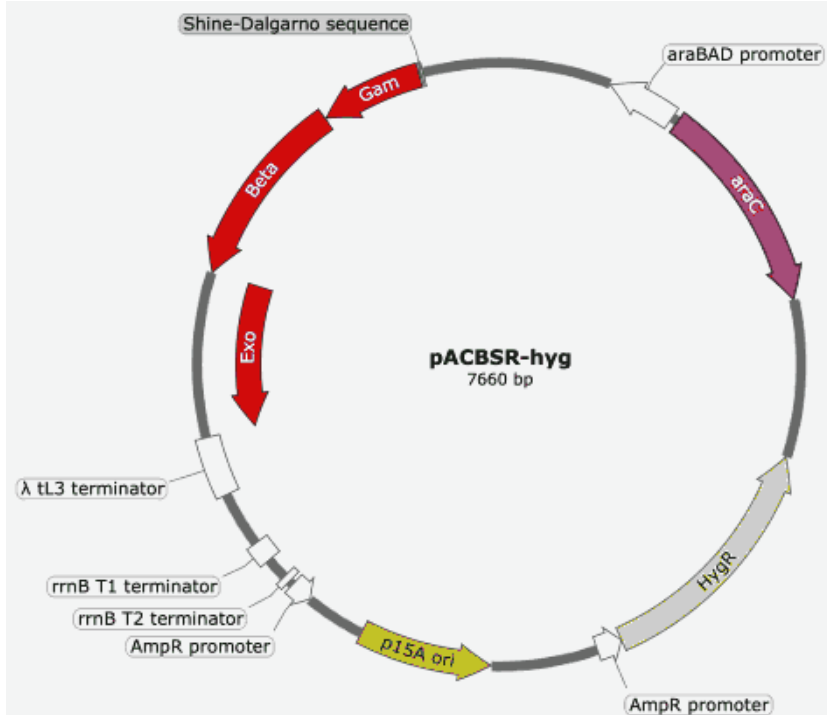
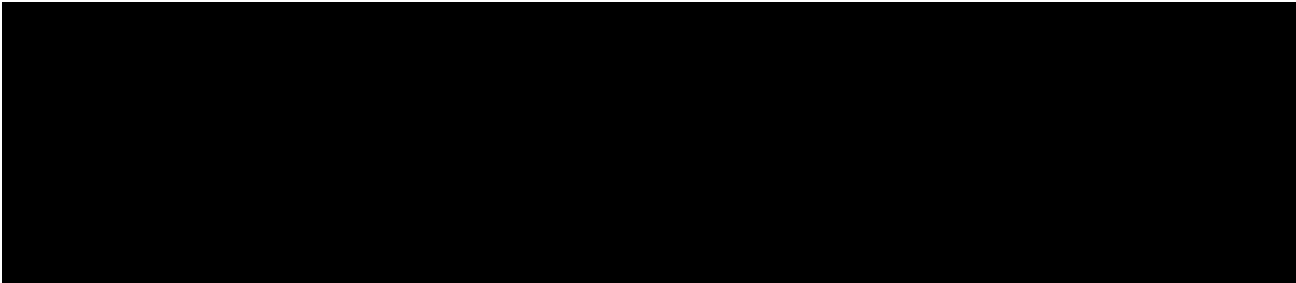
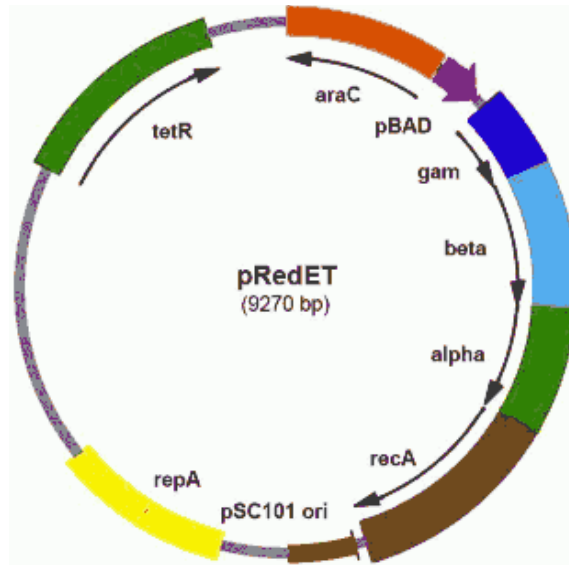
3.1.2 Bacterial strains and plasmid constructs used

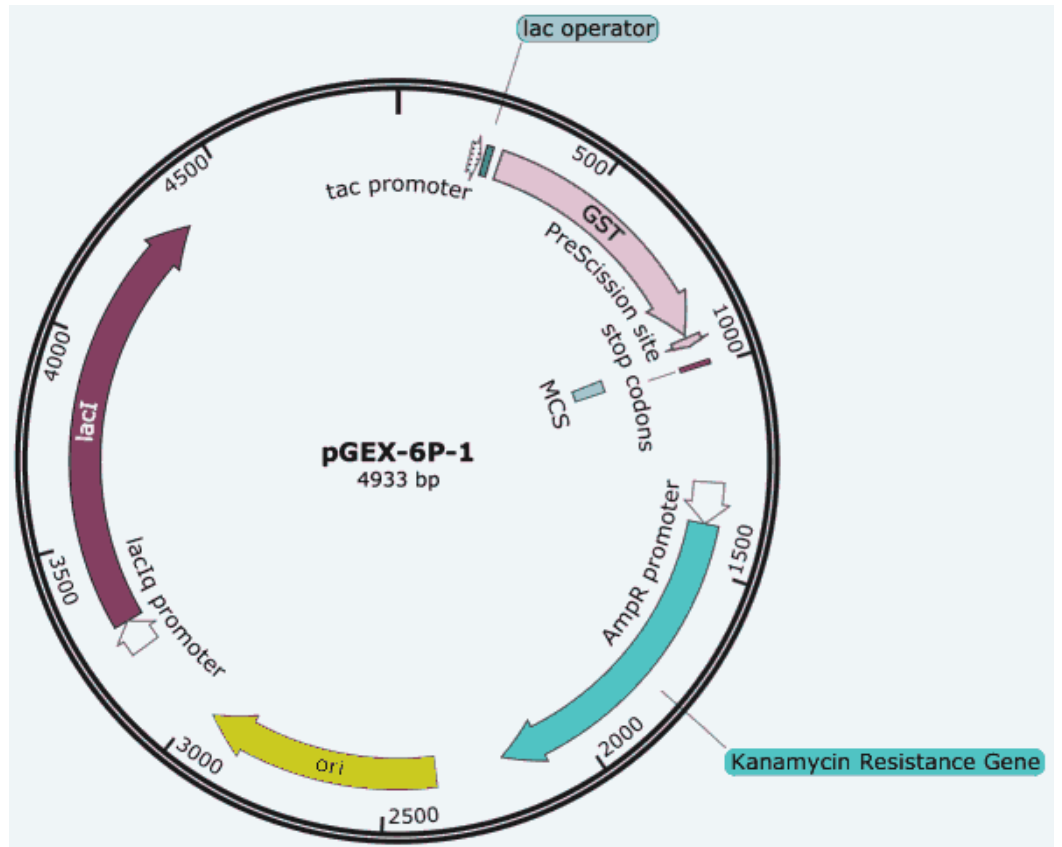
The present study was primarily carried out using clinical isolates of *Klebsiella pneumoniae* that were acquired as pure cultures from a tertiary care centre in Bhubaneswar, Odisha, India. The three isolates used in this study were named according to the nomenclature scheme observed in the lab as KpIMS32, KpIMS34 and KpIMS38. In addition, type strains of *E. coli* and *K. pneumoniae* viz. *E. coli* ATCC 25922 and *K. pneumoniae* ATCC 13883 were also used in the current study.

The present study utilised three different plasmid DNA vectors, the details of which are presented in table 3.1.6. pRedET (Figure 3.1.1) was acquired as a component of the Quick & Easy *E. coli* Gene Deletion Kit while pACBSR-Hyg (Figure 3.1.2), originally constructed by Huang et al (2014), was procured from Addgene. A modified form of pGEX-6P-1 (pGEX-6P-1^K; Figure 3.1.3), with the conventional ampicillin resistance gene replaced by a kanamycin resistance gene, was synthesized by and procured from BiotechDesk.

Table 3.1.6 Plasmids used in the current study. tet^R – tetracycline resistance, hyg – hygromycin resistance, kan^R – kanamycin resistance.

Name	Size (bp)	Selection marker	Purpose	Source
pRedET	9270	tet ^R	Express recombinase genes for lambda recombineering	GeneBridges
pACBSR-Hyg	7660	hyg	Express recombinase genes for lambda recombineering	(Huang et al, 2014)
pGEX-6P-1 ^K	4933	kan ^R	Inducible expression of a gene-of-interest	BiotechDesk





3.2 Protocols – Commercial Kits

3.2.1 Isolation of genomic DNA from a bacterial culture using the Genra Puregene Yeast/Bact Kit B

Genomic DNA was isolated from bacterial cultures according to the manufacturer's instructions. Five hundred μL of an overnight-grown bacterial culture in Luria-Bertani (LB) Broth was harvested by centrifugation at 11,000 rpm for 30 s to obtain a cell pellet. The pellet was resuspended in 300 μL of Cell Lysis Solution by gentle pipetting and incubated at 80°C to allow cell lysis. The mixture was brought to room temperature and added 1.5 μL of RNaseA solution. The contents were mixed by inverting the tube 25 times and incubated at 37°C for 15 mins. The tube was incubated on ice for 1 min, added 100 μL Protein Precipitation Solution and vortex-mixed vigorously for 20 s. The mixture was centrifuged at 16,000 xg for 3 mins to gather the precipitated proteins into a tight pellet.

The supernatant thus obtained was collected in an empty 1.5 mL tube and added 300 μL isopropanol. The contents were mixed by gentle inversion 50 times and centrifuged at 16,000 xg for 3 mins to precipitate the DNA in the form of an opalescent pellet. The supernatant was discarded and the last drops drained out onto a clean adsorbent paper. The tube was added 300 μL of 70% ethanol and inverted 15 times, allowing the pellet to be washed. The ethanol was removed by centrifugation at 16,000 xg for 3 mins, the last drops drained onto a clean adsorbent paper, and the tube allowed to air-dry till all traces of ethanol had evaporated. The tube was added 100 μL of DNA Hydration Solution and incubated at 65°C for 1 h to dissolve the pellet. The tube was then incubated at 37°C overnight to allow further dissolution of the DNA pellet.

The extracted genomic DNA sample was evaluated quantitatively by measuring UV absorption at 260 nm and 280 nm using a nanospectrophotometer, and qualitatively by running a 1 μL aliquot of the sample on a 0.8% TAE-agarose gel (containing 0.5 $\mu\text{g}/\text{mL}$

ethidium bromide) along with a suitable DNA ladder at 50 V and visualized under 302 nm (UV) light in a gel documentation system.

The genomic DNA extracted was stored at -20°C until further use.

3.2.2 Isolation of plasmid DNA from a bacterial culture using the QIAprep Spin Miniprep Kit

Plasmid DNA was isolated from bacterial cultures according to the manufacturer's instructions. Five mL of an overnight bacterial culture in LB Broth was harvested by centrifugation at 11,000 rpm for 30 s. The cell pellet was added 250 µL of Buffer P1 and resuspended by gentle pipetting. The cell suspension was added 250 µL of Buffer P2, mixed by inversion 6 times, and allowed to stand at room temperature for 3 minutes. The mixture was added 350 µL of Buffer N3 and immediately mixed by inversion 8 times. The mixture was allowed to stand for 3 mins, following which it was centrifuged at 17,900 xg for 10 mins.

Without contacting or dislodging the pellet, 750 µL of the supernatant was aspirated into a QIAprep 2.0 spin column (provided in the kit), and the column centrifuged at 17,900 xg for 30s. The flowthrough was discarded, and the column was washed with 500 µL of Buffer PB by centrifugation at 17,900 xg for 30 s. The flowthrough was discarded, and the column washed twice with 700 µL of Buffer PE by allowing the buffer in the column to stand for 2 mins prior to centrifugation. Following the second wash step, the empty column was centrifuged at 17,900 xg for 1 min to remove all traces of ethanol (from the Buffer PE). Discarding the collection tube, the column was placed in a new 1.5 mL tube, added 40 µL Buffer EB at the centre of the membrane in the column, and allowed to stand for 1 min. The setup was centrifuged at 17,900 xg, the column discarded and the eluent collected.

The plasmid DNA was evaluated quantitatively by measuring its UV absorption at 260 nm and 280 nm using a nanospectrophotometer. The DNA was also qualitatively assessed by running a 2 μ L aliquot on a 1% TAE-agarose gel (containing 0.5 μ g/mL ethidium bromide) along with a suitable DNA ladder at 50 V, and visualized under 302 nm (UV) light in a gel documentation system.

The plasmid DNA was stored at -20°C until further use.

3.2.3 Purification of DNA from agarose gels using the QIAquick Gel Extraction Kit

DNA samples such as PCR products, plasmids, restriction-digestion products separated on an agarose gel were purified according to the manufacturer's instructions. DNA samples were run on a TAE-agarose gel at 50 V till adequate separation was achieved. The gel was placed in a UV transilluminator, illuminated with UV (302 nm) light and, using appropriate safety equipment, the band corresponding to the DNA of interest excised using a clean scalpel.

The slice was transferred into a pre-weighed microcentrifuge tube and weighed to obtain its mass in milligrams. Three volumes of Buffer QG were added to the tube containing the gel slice, and the tube incubated at 50°C for 5 minutes in a dry-bath. The gel slurry, when completely dissolved, was added 1 volume isopropanol, mixed by inversion and the mixture transferred to a QIAquick column (provided in the kit).

The column was centrifuged at 17,900 \times g for 1 min, the flowthrough discarded and the column washed with 500 μ L of Buffer QG by centrifugation at 17,900 \times g for 1 min. The flowthrough was discarded, and the column was washed twice with 700 μ L of Buffer PE, by allowing the buffer in the column to stand for 2 mins prior to centrifugation. Following the second wash step, the empty column was centrifuged at 17,900 \times g for 1 min to remove all traces of ethanol (from the Buffer PE). Discarding the collection tube, the column was

placed in a new 1.5 mL tube, added 40 μ L Buffer EB at the centre of the membrane in the column, and allowed to stand for 1 min. The setup was centrifuged at 17,900 xg, the column discarded and the eluent collected.

The eluted DNA was evaluated quantitatively by measuring the UV absorption of the sample at 260 nm and 280 nm using a nanospectrophotometer. The DNA was also qualitatively assessed by running a 2 μ L aliquot on a 1% TAE-agarose gel (containing 0.5 μ g/mL ethidium bromide) along with a suitable DNA ladder at 50 V and visualized under 302 nm (UV) light in a gel documentation system.

The eluted DNA molecule was stored at -20°C until further use.

3.2.4 DNA sequencing by Sanger's dideoxy method using the Big Dye Terminator v3.1 Cycle Sequencing Kit

The nucleotide sequence of DNA molecules was identified by performing Sanger's dideoxy sequencing using the Big Dye Terminator v3.1 cycle sequencing kit according to the manufacturer's instructions. The DNA molecule of interest (in purified form) was amplified by PCR using the protocol outlined in table 3.2.1. The components were added to a PCR tube, mixed well, and incubated in a PCR with the program described in table 3.2.2.

The PCR products were purified using the ethanol/acetate/EDTA method as specified by the kit manufacturer. The entire contents of a PCR reaction were transferred into a 0.6 mL tube, added 12 μ L of Master Mix I, that contained 10 μ L autoclaved Milli-Q water and 2 μ L 125 mM EDTA per reaction, and mixed well. The mixture was further added 52 μ L of Master Mix II, that contained 50 μ L absolute ethanol and 2 μ L 3M sodium acetate (pH 4.6) per reaction, mixed well, and allowed to stand at room temperature for 15 mins. The mixture was centrifuged at 10,000 xg for 20 mins, the supernatant discarded and the DNA pellet washed with 250 μ L 70% ethanol by centrifuging the tube at 10,000 xg for 10 mins. The

supernatant was carefully aspirated and the tubes allowed to air-dry till all traces of ethanol had evaporated. The pellet was resuspended in 12 μ L HiDi Formamide and stored at -20°C until capillary electrophoresis.

Table 3.2.1 Components used to perform sequencing PCR.

Sr. No	Component	Volume per reaction
1	BigDye™ Terminator 3.1 Ready Reaction Mix (2.5x)	0.5 μ L
2	BigDye™ Terminator v3.1 Sequencing Buffer (5X)	1.75 μ L
3	Primer DNA (10 μ M)	2 μ L
4	Template DNA	to 50 ng
5	Deionized water	to 10 μ L

Table 3.2.2 Thermocycler program to perform sequencing PCR.

Stage in the cycle	Conditions
Initial Denaturation	96°C , 1 min
Cycle Denaturation	96°C , 10 s
Cycle Annealing	50°C , 5 s
Cycle Extension	60°C , 4 mins
Hold	4°C , ∞
Number of Cycles	25

The purified sequencing products were loaded into a 96-well plate with one reaction being loaded into one single well. The plate was heated at 95°C for 5 mins, snap-chilled on ice, and allowed to reach room temperature over 10 mins. The plate was then placed within the 3130xl Genetic Analyzer, the appropriate protocol chosen and settings input into the 3130 Data Collection Software 4, and the sequencing allowed to run. Once completed, the output files were assessed for quality (by checking raw data readout) and base-calling performed.

The resultant files were exported and analysed in appropriate software to obtain the sequence of the DNA molecule used.

3.2.5 Extraction total cellular RNA from a bacterial culture using the RNeasy Mini Kit

Total cellular RNA from a bacterial culture was extracted by following protocols 4 and 7 specified in the technical handbook supplied by the manufacturer. The bacterial culture dispensed into a 2 mL RNase-free tube and was added 2 volumes of RNAProtect Bacteria Reagent (Qiagen, Germany) to stabilize the RNA. The mixture was immediately vortex-mixed for 5 s, incubated at room temperature for 5 mins and centrifuged at 5000 xg for 10 mins. The supernatant was discarded and the cell pellet either stored at -20°C until further use or was taken forward for RNA extraction.

The pellet was added 100 µL 15 mg/mL lysozyme (in TE buffer), 10 µL 20 mg/mL proteinase K (in TE buffer) and resuspended using a micropipette. The suspension was vortex-mixed at moderate-speed for 30 mins, added 350 µL Buffer RLT with β-mercaptoethanol (1000:1) and vortex-mixed vigorously for 1 min. The mixture was added 250 µL absolute ethanol, pipette-mixed and the entire content transferred into a new RNeasy mini spin-column.

The column was centrifuged at 8000 xg for 15 s, the flowthrough discarded, and the column added 350 µL Buffer RW1. The column was centrifuged at 8000 xg for 15 s, the flowthrough discarded and the column placed in the same collection tube. The column was added 80 µL of Buffer RDD containing 10 µL RNase-free DNaseI (QIAGEN, Germany) and allowed to stand for 15 mins at room temperature. The column was then added 350 µL of Buffer RW1, allowed to stand for 5 mins and centrifuged at 8000 xg for 15 s. The flowthrough along with the collection tube was discarded and the column placed in a new 2 mL collection tube. The column was then added 500 µL Buffer RPE (containing ethanol), centrifuged at 8000 xg for

15 s, and the flowthrough discarded. The column was washed once more with RPE but the centrifugation time increased to 1 min. The resultant flowthrough was discarded and the empty column centrifuged at 17,900 xg for 1 min to remove traces of ethanol. The column was placed in a new RNase-free 1.5 mL tube (supplied with the kit), added 40 μ L of RNase-free water onto the membrane, centrifuged at 8000 xg for 1 min, and the eluted RNA immediately placed on ice.

The RNA was assessed quantitatively by measuring UV absorption of the sample at 260 nm and 280 nm using a nanospectrophotometer. The RNA was also qualitatively assessed by running a 2 μ L aliquot on a 1.5 % TAE-agarose gel (containing 0.5 μ g/mL ethidium bromide) at 70 V and visualized under 302 nm (UV) light in a gel documentation system.

The extracted RNA molecule was stored at -80°C until further use.

3.2.6 Conversion of total cellular RNA to complementary DNA (cDNA) using the SuperScript™ IV First-Strand Synthesis System

The total cellular RNA extracted from a bacterial culture was converted into cDNA according to the protocols specified by the manufacturer. The first-strand reaction was set up using the scheme described in table 3.2.3. The components were added into a RNase-free PCR tube, and incubated in a thermocycler at 65°C for 5 mins, and shifted to ice for 1 min. To another RNase-free PCR tube were added the following components in the scheme outlined in table 3.2.4. From this mixture, 7 μ L were added to the tube containing RNA, bringing the total reaction volume to 20 μ L. The tube was incubated in a thermocycler at 23°C for 10 mins, 55°C for 10 mins, followed by 80°C for 10 mins. The contents were added 1 μ L RNaseH, incubated at 37°C for 20 mins, and the resultant mixture placed on ice. The cDNA obtained was stored at -20°C until further use.

From this mixture, 7 μL were added to the tube containing RNA, bringing the total reaction volume to 20 μL . The tube was incubated in a thermocycler at 23°C for 10 mins, 55°C for 10 mins, followed by 80°C for 10 mins. The contents were added 1 μL RNaseH, incubated at 37°C for 20 mins, and the resultant mixture placed on ice. The cDNA obtained was stored at -20°C until further use.

Table 3.2.3 Composition of the RNA-Primer mix to synthesize cDNA.

Sr. No.	Component	Volume / Amount per reaction
1	50 ng/ μL Random hexamers	1 μL
2	10 mM dNTP Mix	1 μL
3	RNA template	to 1000 ng
4	DEPC-treated water	to 13 μL

Table 3.2.4 Composition of the SuperScript IV master-mix to synthesize cDNA.

Sr. No.	Component	Volume per reaction
1	5x SS IV Buffer	4 μL
2	100 mM DTT	1 μL
3	RNase inhibitor	1 μL
4	200 U/ μL SuperScript™ IV Reverse Transcriptase	1 μL

3.2.7 Conversion of total cellular RNA to complementary DNA (cDNA) using the iScript™ Reverse Transcription Supermix for RT-qPCR

The total cellular RNA extracted from a bacterial isolate was converted into cDNA according to the protocols specified by the manufacturer. The reaction was set up on ice using the scheme described in table 3.2.5. The components were added into a RNase-free PCR tube and incubated in a thermocycler with a program specified in table 3.2.6. The cDNA obtained was stored at -20°C until further use.

Table 3.2.5 Composition of the reaction to synthesize cDNA from RNA.

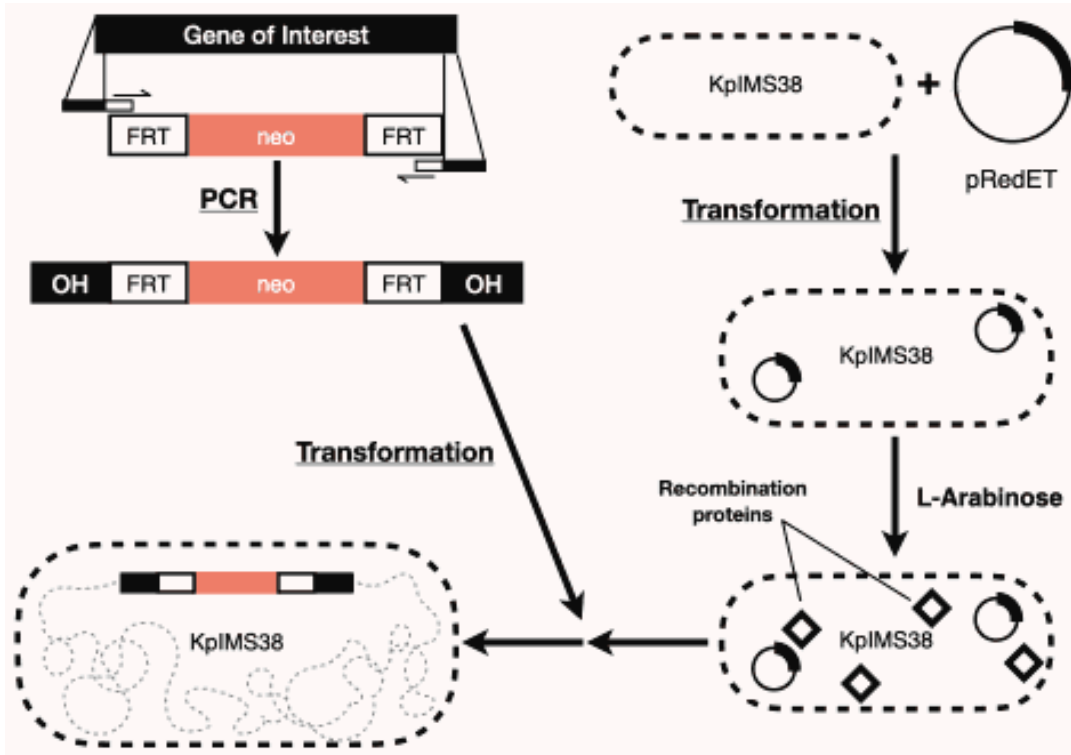
Component	Volume / Amount per reaction
iScript RT Supermix	4 μ L
RNA template	upto 1000 ng
Nuclease-free water	upto 20 μ L

Table 3.2.6 Thermocycler program to synthesize cDNA from RNA.

Stage	Conditions
Priming	25 °C, 300 s
Reverse Transcription	46°C, 1200 s
RT Inactivation	95°C, 60 s

3.2.8 Creation of deletion mutants in a bacterial strain by Red/ET Recombination

The creation of mutants was attempted by introducing gene-deletions into the genome of KpIMS38. In the present study, this was undertaken using the Quick & Easy *E. coli* Gene Deletion Kit, which is based on Red/ET recombination or lambda recombineering. The procedure involves transforming the bacterial strain-of-interest with a plasmid capable of synthesizing the proteins required for Red/ET recombination, synthesizing a deletion cassette targeted to a specific gene present in the strain-of-interest, inducing the expression of the recombination-proteins in the strain and transforming it with the deletion cassette. Successful deletion would warrant insertion of the cassette into the gene-of-interest, the confirmation of which would require PCR and DNA sequencing. The process has been outlined in a schematic presented in figure 3.2.1.



3.2.8.1 Creation of a deletion cassette targeted to the gene-of-interest by PCR using a functional cassette

DNA primers were designed specific to the FRT-pgk-gb2-neo-FRT cassette (provided in the kit), with 60 bp overhangs homologous to the gene-of-interest added to their 5' ends. These primers were used to carry out high-fidelity PCR using the scheme (per reaction) described in table 3.2.7. The components were added to a PCR tube and incubated in a thermocycler with the program delineated in table 3.2.8.

Table 3.2.7 Components used to carry out high-fidelity PCR.

Sr. No.	Component	Volume per reaction
1	Nuclease-free Water	17.5 μ L
2	2X Q5 High-Fidelity Master Mix	25 μ L
3	10 μ M Forward Primer	2.5 μ L
4	10 μ M Reverse Primer	2.5 μ L
5	200 ng/ μ L Template DNA	2.5 μ L

Table 3.2.8 Thermocycler program used to perform high-fidelity PCR.

Stage in the cycle	Conditions
Initial Denaturation	98°C, 30 s
Cycle Denaturation	98°C, 10 s
Cycle Annealing	60°C, 30 s
Cycle Extension	72°C, 60 s
Final Extension	72°C, 120 s
Hold	4°C, ∞
Number of cycles	30

The PCR product was run on a 0.8% TAE-agarose gel (containing 0.5 μ g/mL ethidium bromide), along with a suitable DNA ladder, at 50V till adequate separation was achieved. The gel was placed under a UV-transilluminator, the specific DNA bands corresponding to the homologous DNA cassette were excised and the DNA extracted using a kit following the protocol as mentioned in section 3.2.3. The eluted DNA was qualitatively assessed by measuring its UV absorption at 260 nm and 280 nm using a nanospectrophotometer. The DNA was also qualitatively assessed by running a 2 μ L aliquot on a 1% TAE-agarose gel (containing 0.5 μ g/mL ethidium bromide) along with a

suitable DNA ladder at 50 V and visualized under 302 nm (UV) light in a gel documentation system.

The cassette DNA was stored at -20°C until further use.

3.2.8.2 Transformation of the recombination plasmid pRedET into the host bacterial cell

A single, isolated colony from the strain-of-interest was grown overnight in 3 mL LB broth at 37°C and 220 rpm agitation. Thirty microlitres of the resultant culture were used to sub-culture 1.4 mL of LB broth. This culture was incubated at 37°C and 220 rpm agitation until it reached an optical density (OD₆₀₀) of 0.2. The culture was transferred into chilled 1.5 mL tubes and centrifuged at 11,000 rpm for 30 s in a centrifuge pre-chilled at 2°C, the supernatant decanted and the cell pellet resuspended in 1 mL chilled sterile 10% glycerol by gentle pipetting. The cell suspension was centrifuged using the above-mentioned parameters, the supernatant decanted, and washed with 10% glycerol once again. After the second wash, a minimal volume of supernatant (\approx 50-100 μ L) was left in the tube along and was used to resuspend the cell pellet.

One batch of the cell suspension was added 50 ng of pRedET plasmid, while the other was not and was considered as 'negative control'. Both cell suspensions were transferred to individual pre-chilled 1mm electroporation cuvettes, and successively pulsed in an electroporator set to deliver a 1350 V pulse with a 5 ms time constant. The cuvettes were immediately added 800 μ L LB broth, resuspended, and their entire contents transferred to sterile 1.5 mL tubes. The tubes were incubated at 30°C and 220 rpm agitation for 70 mins, following which both the cultures were concentrated by centrifugation and resuspension in a small-volume supernatant, and spread-plated onto individual LB agar plates containing 3 μ g/mL tetracycline (LBA-Tet³). The plates were covered to protect them from light-exposure and incubated at 30°C overnight.

The colonies obtained in the transformed culture were sub-cultured onto separate LBA-Tet³ plates, isolated colonies grown in broth, and their plasmid DNA extracted. This DNA was run on a 1% TAE-agarose gel, along with the pRedET plasmid DNA and an appropriate DNA ladder at 50V and visualized under 302 nm (UV) light in a gel documentation system. Isolates containing the band for pRedET were marked, preserved and taken ahead for mutant-creation.

3.2.8.3 Transformation of the recombination plasmid pACBSR-Hyg into the host bacterial cell

A single, isolated colony from the strain-of-interest was grown overnight in 3 mL Luria Broth containing low salt (LB-Lx, HiMedia, India) at 37°C and 220 rpm agitation, and 20 µL of it used to sub-culture 2 mL of LB-Lx Broth. This culture was incubated at 37°C and 220 rpm agitation until the it reached an optical density (OD₆₀₀) of 0.2. The culture was divided into multiple 1 mL aliquots and each transferred into chilled 1.5 mL tubes. The culture was centrifuged at 11,000 rpm for 30 s in a centrifuge pre-chilled at 2°C, the supernatant decanted and the cell pellet resuspended in 1 mL chilled sterile 10% glycerol by gentle pipetting. The cell suspension was centrifuged using the above-mentioned parameters, the supernatant decanted, and washed with 10% glycerol once again. After the second wash, a minimal volume of supernatant (≈ 50-100 µL) was left in the tube and was used to resuspend the cell pellet.

One batch of the cell suspension was added 250 ng of pACBSR-Hyg plasmid, while the other was considered as ‘negative control’ and processed as such. Both cell suspensions were transferred to individual pre-chilled 2mm electroporation cuvettes, and successively pulsed in an electroporator set to deliver a 2500 V pulse with a 5 ms time constant. The cuvettes were immediately added 800 µL LB-Lx medium, resuspended, and their entire contents transferred to sterile 1.5 mL tubes. The tubes were incubated at 30°C and 220

rpm agitation for 70 mins, following which both the cultures were concentrated by centrifugation and resuspension in a small-volume supernatant, and spread-plated onto individual LB-Lx Agar plates containing 100 µg/mL hygromycin (MP Bio, USA; LBA-Lx-Hyg¹⁰⁰). The plates were incubated at 30°C overnight.

The colonies obtained in the transformed culture were sub-cultured onto separate LB-Lx-Hyg¹⁰⁰ plates, isolated colonies grown in broth, and their plasmid DNA extracted. This DNA was run on a 1% TAE-agarose gel, along with the pACBSR-Hyg plasmid DNA and an appropriate DNA ladder at 50V and visualized under 302 nm (UV) light in a gel documentation system. Isolates containing the band for pACBSR-Hyg were marked, preserved and taken ahead for mutant-creation.

3.2.8.4 Induction of recombination-genes from pRed/ET and transformation of the deletion cassette into the bacterial cell

A single bacterial colony containing the recombination plasmid pRedET was cultured in 3 mL LB-Tet³ at 30°C and 220 rpm overnight and then sub-cultured in duplicate in 1.4 mL LB-Tet³ using 30 µL of the culture. The cultures were grown till they reached a cell density corresponding to OD₆₀₀ of 0.3. One of the tubes was added 50 µL of 10% L-arabinose and labelled as “induced”, while the other was labelled “uninduced”. Both tubes were incubated at 37°C and 220 rpm for 1 h, following which they were washed with chilled 10% glycerol as described before.

The induced as well as uninduced cell suspensions were added an appropriate amount of the cassette DNA each, transferred to separate chilled 1 mm electroporation cuvettes and pulsed in an electroporator set to deliver a 1350 V pulse with a 5 ms time constant. The cells were immediately added 800 µL LB broth, resuspended, their entire contents transferred to sterile 1.5 mL tubes, and were incubated at 37°C and 220 rpm agitation for 120 mins. The cultures were concentrated by centrifugation and resuspension in a small-

volume supernatant and spread-plated onto individual LB agar plates containing 15 µg/mL kanamycin (LBA-Kan¹⁵).

The colonies obtained on plates spread with induced and uninduced cultures were sub-cultured onto separate LBA-Kan¹⁵ plates, and isolated colonies used to perform a colony PCR, wherein each colony was resuspended in 30 µL of nuclease-free water in a PCR tube, the contents heated at 98°C for 5 mins and the samples immediately chilled on ice. An aliquot of 2 µL from this suspension was used to set up a PCR with the composition as mentioned in table 3.2.9.

Table 3.2.9 Components used to set up PCR to screen for deletion of the gene-of-interest.

Sr. No.	Component	Volume per reaction
1	Nuclease-free Water	17.10
2	5X Green GoTaq® Flexi Buffer	6.00
3	2.5 mM dNTP Mix	2.00
4	25 mM MgCl ₂	1.50
5	10 µM Forward primer	0.60
6	10 µM Reverse primer	0.60
7	5 Units/µL GoTaq® Flexi DNA Polymerase	0.20
8	Template DNA	2.00

3.2.8.5 Induction of recombination-genes from pACBSR-Hyg and transformation of the deletion cassette into the bacterial cell

A single bacterial colony containing the recombination plasmid pACBSR-Hyg was cultured in 2 mL LB-Lx-Hyg¹⁰⁰ at 30°C and 220 rpm overnight. From the resultant culture, 15 µL was used to inoculate single tubes containing 1.5 mL LB-Lx-Hyg¹⁰⁰ containing 0.1M L-arabinose and 1.5 mL LB-Lx-Hyg¹⁰⁰. The cultures were grown at 30°C till they

reached a cell density corresponding to an optical density (OD₆₀₀) of 0.4. The cells from each culture were harvested by centrifugation and washed with chilled 10% glycerol as described previously.

The induced as well as uninduced cell suspensions were added an appropriate amount of the cassette DNA each, transferred to separate chilled 1 mm electroporation cuvettes and pulsed in an electroporator set to deliver a 1350 V pulse with a 5 ms time constant. The cells were immediately added 800 µL LB broth, resuspended, and their entire contents transferred to sterile 1.5 mL tubes. The cell suspensions were incubated at 37°C and 220 rpm for 90 mins. The cultures were concentrated by centrifugation and resuspension in a small-volume supernatant and spread-plated onto individual LBA-Kan¹⁵ plates.

The colonies obtained on plates spread with induced and uninduced cultures were sub-cultured onto separate LBA-Kan¹⁵ plates. Simultaneously, the colonies were also used to prepare a colony lysate as performed in section 3.2.8.4 of this document. An aliquot of 2 µL from each lysate was used to set up a PCR with the composition as mentioned in table 3.2.9.

3.2.8.6 Screening for insertion of the deletion cassette within the gene-of-interest within KpIMS38

Reactions were set up for DNA obtained from colonies from induced as well as uninduced plates, where the colony lysate was utilised as a template to amplify DNA using specific primers. Alternatively, isolated colonies from the patched plates (uninduced and induced) were inoculated into appropriate growth media and their genomic DNA extracted using the Genra Puregene Yeast/Bact Kit B following the protocol outlined in section 3.2.1 of this document. This genomic DNA was further used to set up reactions to amplify DNA using specific primers, according to the protocol described in table 3.2.10.

Table 3.2.10 Components used to perform PCR to verify the insertion of the FRT cassette.

Sr. No.	Component	Volume per reaction (μL)
1	Nuclease-Free Water	17.10
2	5x Green GoTaq® Flexi Buffer	6.00
3	2.5 mM dNTPs	2.00
4	25 mM MgCl_2	1.50
5	10 μM Forward Primer	0.60
6	10 μM Reverse Primer	0.60
7	5 Units/ μL GoTaq® Flexi Polymerase	0.20
8	Template DNA	2.00

Table 3.2.11 Thermocycler program used to perform PCR to amplify the deletion cassette or the full-length sequence of the gene-of-interest.

Stage in the cycle	Conditions
Initial Denaturation	94°C, 2 mins
Cycle Denaturation	94°C, 30 s
Cycle Annealing	variable, 30 s
Cycle Extension	72°C, 30 - 90 s
Final Extension	72°C, 10 mins
Hold	4°C, ∞
Number of cycles	35

Reactions were incubated in a thermocycler using the program outlined in table 3.2.11. A Positive Control – the template DNA used to synthesize the cassette originally – was also used and a reaction set up along with the other templates. Five μL of each PCR product was run on a 1% TAE-agarose gel, along with the cassette DNA previously synthesized,

and an appropriate DNA ladder at 50 V, and visualized under 302 nm (UV) light in a gel documentation system.

Reactions containing the DNA amplicon corresponding to the deletion cassette were noted and their representative isolates marked as 'deletion-positive'.

3.3 Methods

This section elucidates the methods followed to achieve the objectives of the study. Unless mentioned otherwise, (a) all bacterial plates for growth were incubated at 37°C while broth cultures agitated at 220 rpm, and (b) each experiment was performed atleast thrice (three biological replicates) with atleast three technical replicates taken for each.

3.3.1 Culture preservation and storage

3.3.1.1 Preparation of soft agar stabs

Bacterial isolates were inoculated on to appropriate agar medium-plates by streak-planting and incubated to obtain single colonies. To the appropriate culture medium, agar was added to a final concentration of 0.8%, the medium sterilised and poured aseptically into 5 mL cryovials. Each vial was added 3.5 mL of agar medium which was allowed to solidify.

A single isolated colony was picked up using a stab-inoculation wire and used to stab a vial. The vial was closed and incubated at 37°C until visible growth along the line of inoculation appeared. The stabs were stored at room temperature until further use.

3.3.1.2 Preparation of glycerol stocks

Bacterial isolates were inoculated on to appropriate solid media by streak-planting and incubated to obtain single colonies. A single isolated colony was used to inoculate 2 mL of the appropriate broth medium and incubated till the culture reached a cell density corresponding to an OD₆₀₀ of 0.6.

Each culture/strain/mutant was cryopreserved in duplicate. To each 2mL cryovial was added 400 µL of sterile 100% glycerol (Invitrogen, USA) and chilled on ice. Thereafter to each vial 600 µL of the grown broth culture was added, immediately vortex-mixed for a

short duration, and stored in ice. Cryovials containing cultures were stored in a -80°C deep freezer until further use.

3.3.2 Identification of bacterial isolates

3.3.2.1 Identification and confirmation of bacterial isolates using differential media and biochemical tests

The isolates available and used in this study were obtained from a tertiary healthcare centre, where they were already identified using an automated identification system. This information was made available along with the isolates. Nevertheless, the isolates were screened using differential media. For the purpose, two differential bacteriological media were used – MacConkey's Agar and Eosin-Methylene Blue (EMB) Agar.

A single colony of the bacterium was streaked on a Nutrient agar (NA; HiMedia, India) plate, incubated overnight, and a single isolated colony from the plate used to streak a MacConkey agar and an EMB agar plates. The plates were incubated overnight, the characteristics of resulting colonies noted and compared to those expected for standard enteric bacterial genera.

Additionally, biochemical tests were performed to determine the identity of the isolates. SIM medium, MR-VP medium and Simmon's citrate agar were used for the purpose. A single colony of the bacterium was streaked on a NA plate and incubated overnight. A single isolated colony from the plate was inoculated in 2 mL Nutrient Broth (NB; HiMedia, India) and allowed to grow till an optical density (OD_{600}) of 0.6 was attained. The resultant culture was used to inoculate SIM medium by stab-inoculation, Simmon's citrate agar by streaking and MR-VP medium with 10 μ L of the culture. Following overnight incubation, the SIM medium was added 5 drops of Kovac's indole reagent (HiMedia, India) while the MR-VP medium was distributed into two tubes; one was added Methyl Red indicator and the other added 4 drops each of Barritt's reagents A and B. The media, along with the Simmon's citrate agar, were observed for any colour change and the results compared to those expected for standard enteric bacterial genera.

3.3.3 Determination of the antibiotic susceptibility profile of bacterial isolates

3.3.3.1 Determination of antibiotic susceptibility by Kirby-Bauer Method

Bacterial isolates were assessed for their susceptibility to antibiotics from various classes using the disk-diffusion method as specified by Bauer *et al* (1966).

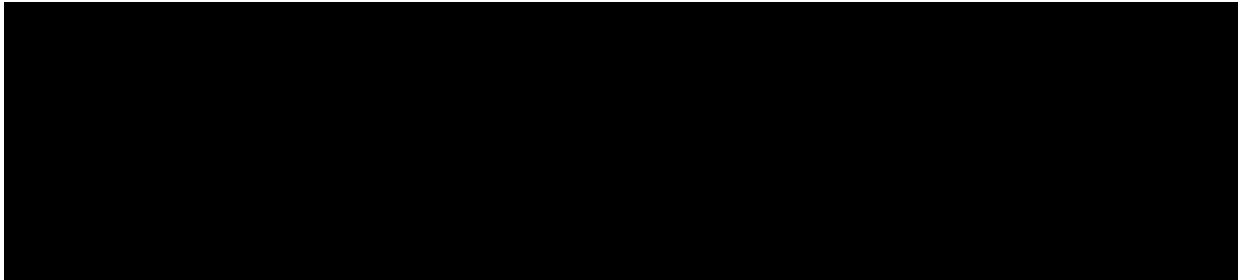
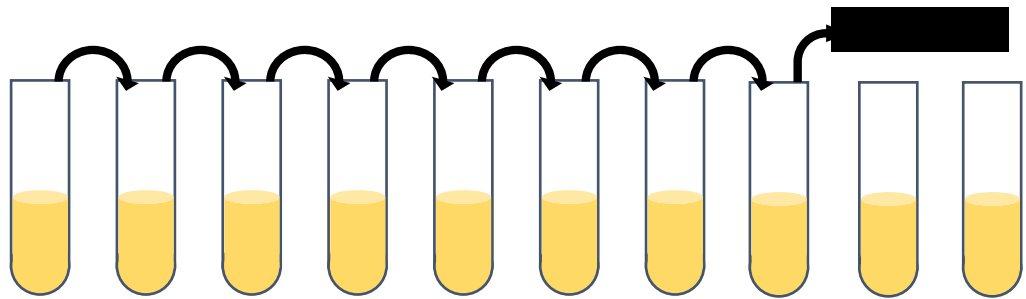
A single colony from a bacterial isolate was streaked on to a Muller-Hinton (MH) agar plate and incubated overnight till isolated colonies were obtained. A single colony from this plate was used to inoculate 2 mL of Muller Hinton (MH) broth, which was then incubated till a culture density corresponding to an optical density (OD₆₀₀) of 0.6 was attained. A sterile cotton swab was used to swab the culture on the surface of two petri dishes (200 mm diameter) containing MH agar and allowed to absorb for 5 minutes. One Dodeca Enterobacteriaceae-I multidisc was placed on the surface of one of the plates using sterile forceps, and one Dodeca Enterobacteriaceae -II disc was similarly placed on the surface of another plate. The plates were placed face up for 2 minutes to allow the discs to adhere to the agar surface, following which they were placed in the incubator face down. Following 12-14 hours of incubation, the plates were removed and the zone of clearance that appeared around discs measured for their diameters. These measurements were compared to standardised breakpoints as stated by the Clinical and Laboratory Standards Institute (CLSI, 2020) and the response to each antibiotic categorised as “Resistant”, “Intermediate” or “Sensitive”.

3.3.3.2 Determination of the minimum inhibitory concentration (MIC) of an antibiotic by two-fold broth-dilution method

The least concentration of a compound that inhibits the growth of bacteria that can be visually identified is called its Minimum Inhibitory Concentration (MIC) (Andrews, 2001). The two-fold broth-dilution method allows the identification of the MIC of an antibiotic towards a specific bacterial isolate. This method can be used to determine the

activity of a particular compound with antimicrobial properties against bacterial isolates, as well as to determine the sensitivity of a specific bacterial isolate to various antimicrobial compounds.

The MIC of a particular antibiotic towards a specific bacterial isolate was determined using the protocol specified for the two-fold broth macrodilution method as outlined by the CLSI (CLSI, 2020) with certain alterations. A single colony of the bacterial isolate grown on agar medium was streaked on to a MH agar plate. A single isolated colony obtained after overnight incubation of the plate was used to inoculate 2 mL of MH broth, which was then incubated till a culture density corresponding to an optical density of 0.5 (A_{600}) was obtained.



In 13 mL sterile test tubes (with caps), 2 mL of MH broth was added according to the number of antibiotic concentrations required. One tube was added a specific volume of the antibiotic stock solution, and the volume made up to 4 mL with additional MH broth; this was the highest concentration (x) of the antibiotic in the series. The contents of the tube

were mixed well, 2 mL withdrawn from this tube and transferred to another tube containing 2 mL broth. This tube now contained antibiotic at a concentration half that of the previous tube, i.e., $x/2$. The process was repeated until the entire two-fold dilution series was obtained for the given antibiotic compound (Figure 3.3.1).

Ten μL of the broth culture was added to each of the tubes in the dilution series. In addition, two tubes each containing 2 mL of MH broth were taken; one added 10 μL of the broth culture, the other left uninoculated. These tubes were labelled 'growth positive control' and 'growth negative control' respectively. All the inoculated tubes as well as the growth negative control tube were incubated at an appropriate temperature with shaking for 14 hours.

The tubes were visually assessed for growth by comparing the growth of each of the tubes from the dilution series with the growth controls. The tubes were examined from lowest to highest concentrations, and the tube with the lowest concentration of antibiotic to exhibit no visible growth was considered the minimum inhibitory concentration of that antibiotic for the given bacterial isolate.

3.3.3.3 Determination of the minimum inhibitory concentration (MIC) of an antibiotic by EzyMIC™ strip Method

The E-test was developed as an alternative to the broth microdilution method commonly used to identify the MIC of compounds towards a specific bacterial isolate. The Ezy MIC™ Strip (HiMedia, India) is analogous to the E-test, and consists of a paper strip coated with a predefined, continuous gradient for a particular antibiotic. This method of identifying the MIC of a particular compound is advantageous as compared to the broth dilution methods in being less resource-intensive, allowing assessment of organisms that do not grow in broth media, as well as permitting the testing of antibiotic compounds that are insoluble in water (Nachnani et al, 1992; Chang et al, 2000).

A single colony from the bacterial isolate was streaked on to a MH agar plate and incubated overnight till isolated colonies were obtained. A single colony from this plate was used to inoculate 2 mL of MH broth, which was incubated till the cell number corresponding to an optical density of 0.6 (OD₆₀₀) was attained. A sterile cotton swab was used to swab the culture on the surface of a petri dish (90 mm diameter) containing MH agar and allowed to adsorb for 2 minutes. A single Ezy MIC™ strip for a specific antibiotic was placed in the centre of the plate using a specialised applicator supplied with the strips and the setup left standing for 1 min to allow the strip to adsorb firmly to the surface of the medium. The plate was placed in an incubator – in a face-down orientation – at 37°C overnight.

The plate was examined for the presence of a zone of clearance around the strip, formed by action of the antibiotic having diffused into the medium to form a continuous gradient of antibiotic concentrations. The point on the strip where the edge of the zone intersects it is read as the minimum inhibitory concentration in µg/mL.

3.3.4 Screening for genetic basis of antibiotic resistance inherent in the bacterial isolates under study

3.3.4.1 Screening for quinolone resistance mediated by plasmids

The presence of *qnr* genes in the plasmid DNA of KpIMS38 was assessed. A single isolated colony of the culture growing on LB agar was inoculated into 5 mL of LB broth and incubated at 37°C overnight. Plasmid DNA was extracted from the culture using the QIAprep Spin Miniprep Kit (Qiagen, Germany) according to the protocol enlisted in section 3.2.2 of this document. The plasmid DNA was used as template to screen for the presence of *qnrA* and *qnrB* through PCR using specific primers for the respective genes (Table 3.3.1) and following the protocol described in table 3.3.2. A non-template control (NTC) without any template DNA was also setup. All reactions were placed in a thermocycler and subjected to PCR using the program outlined in table 3.3.3.

Table 3.3.1 Primer sequences used to amplify *qnrA* and *qnrB* from plasmid DNA extracted from KpIMS38.

Gene	Primer	Sequence (5' → 3')	Amplicon Size	Reference
<i>qnrA</i>	qnrA-F	AGAGGATTTCTCACGCCAGG	580 bp	(Singh et al., 2017)
	qnrA-R	TGCCAGGCACAGATCTTGAC		
<i>qnrB</i>	qnrB-F	GGMATHGAAATTCGCCACTG	264 bp	(Singh et al., 2017)
	qnrB-F	TTTGCYGYGCGCCAGTCGAA		

Five microliters of each reaction were loaded onto a 1.2% TAE-agarose gel (containing 0.5 µg/mL ethidium bromide) and run in 1X TAE buffer at 50V. A 100 bp DNA Ladder (Fermentas, USA) was also run on the agarose gel, and visualized under 302 nm (UV) light in a gel documentation system.

Table 3.3.2 Components used to perform PCR to screen for the presence of *qnrA* and *-B* genes in KpIMS38.

Sr. No.	Component	Volume per reaction (μL)
1	Nuclease-Free Water	17.10
2	5x Green GoTaq® Flexi Buffer	6.00
3	2.5 mM dNTPs	2.00
4	25 mM MgCl ₂	1.50
5	10 μM Forward Primer	0.60
6	10 μM Reverse Primer	0.60
7	5 Units/ μL GoTaq® Flexi Polymerase	0.20
8	Template DNA	2.00

Table 3.3.3 Thermocycler conditions used to amplify *qnrA* and *qnrB* genes.

Stage in the cycle	Conditions
Initial Denaturation	94°C, 120 s
Cycle Denaturation	94°C, 30 s
Cycle Annealing	63°C, 30 s
Cycle Extension	72°C, 30 s
Final Extension	72°C, 600 s
Hold	4°C, ∞
Number of cycles	35

3.3.4.2 Screening for mutations in the quinolone resistance-determining region (QRDR) in the *gyrA* gene

Mutation in specific amino acids of DNA Gyrase and Topoisomerase IV results in a weaker interaction between the enzymes and quinolone compounds, resulting in resistance

of the bacterium to quinolones (Pham et al, 2019). Most of the mutations occur near the N-terminal end of the enzyme, particularly at the Serine 83 and Aspartate / Glutamate 87 residues. These sites, together, are referred to as the Quinolone Resistance Determining Region (QRDR), as the affinity of the drug to the DNA – topoisomerase complex is reduced when mutated (Pham et al, 2019). The Serine 83 site accounts for most of the mutations found in *gyrA*, mainly because mutation of the Aspartate /Glutamate 87 residue has a detrimental effect on the catalytic activity of the enzyme, resulting in a fitness cost to carrying the resistance phenotype (Aldred et al, 2014).

A single isolated colony of the culture growing on LB agar was inoculated into 5 mL of LB broth and incubated at 37°C overnight. Genomic DNA was extracted from the culture using the Genra Puregene Yeast/Bact Kit B (Qiagen, Germany) according to the manufacturer’s instructions. The genomic DNA was used as template to amplify the *gyrA* gene, using the primers *gyrAF1* and *gyrAR2* in one reaction and the primers *gyrAF2* and *gyrAR3* in another reaction (Table 3.3.4). The protocol used to set up the aforementioned reactions is described in table 3.3.5. A non-template control (NTC) without any template DNA was also setup. All reactions were placed in a thermocycler and subjected to PCR using the program outlined in table 3.3.6.

Table 3.3.4 Primer sequences used to amplify segments of *gyrA* from genomic DNA extracted from KpIMS38.

Gene	Primer	Sequence (5' → 3')	Amplicon Size	Reference
<i>gyrA</i>	<i>gyrAF1</i>	ATGAGCGACCTTGCGAGAGA	1429 bp	(Singh et al, 2017)
	<i>gyrAR2</i>	CGTCGAGCAGTTTTTCATG		
<i>gyrA</i>	<i>gyrAF2</i>	TAAATACTACCTGACCGAGC	1297 bp	(Singh et al, 2017)
	<i>gyrAR3</i>	TTATTCTTCGTCTTCGGCG		

Table 3.3.5 Components used to perform PCR to amplify segments of *gyrA*.

Sr. No.	Component	Volume per reaction	
		F1R2	F2R3
1	Nuclease-Free Water	16.50 μ L	16.80 μ L
2	5x Green GoTaq® Flexi Buffer	6.00 μ L	6.00 μ L
3	2.5 mM dNTPs	2.00 μ L	2.00 μ L
4	25 mM MgCl ₂	2.10 μ L	1.80 μ L
5	10 μ M Forward Primer	0.60 μ L	0.60 μ L
6	10 μ M Reverse Primer	0.60 μ L	0.60 μ L
7	5 Units/ μ L GoTaq® Flexi DNA Polymerase	0.20 μ L	0.20 μ L
8	Template DNA	2.00 μ L	2.00 μ L

The entire contents of each reaction were loaded onto a 0.8 % TAE-agarose gel (containing 0.5 μ g/mL ethidium bromide) and run in 1X TAE buffer at 50V. A 100 bp DNA Ladder (Fermentas, USA) was also run on the agarose gel, and visualized under 302 nm (UV) light in a gel documentation system. The DNA bands corresponding to amplified *gyrA* were excised from the agarose gel and the DNA eluted from it using the QIAquick Gel Extraction Kit (Qiagen, Germany) according to the manufacturer's instructions.

The purified *gyrA* DNA PCR product was used as template to carry out Sanger Sequencing using the Big Dye Terminator v3.1 Cycle Sequencing Kit (Applied Biosystems, USA) according to the manufacturer's instructions. The primers used for sequencing were the same as the ones used to amplify the fragment viz. *gyrAF1* and *gyrAR3*. The sequences obtained from both the primers were aligned to obtain a complete sequence of the *gyrA* gene present in KpIMS38. The resultant sequence was taken with the *gyrA* sequence from the type strain *K. pneumoniae* ATCC 13883 and compared by performing pairwise alignment using the ClustalW tool, which was present in the MEGA7 program (Kumar et

al., 2016). The polynucleotide alignments were converted into amino acids and the alignment compared for mismatches.

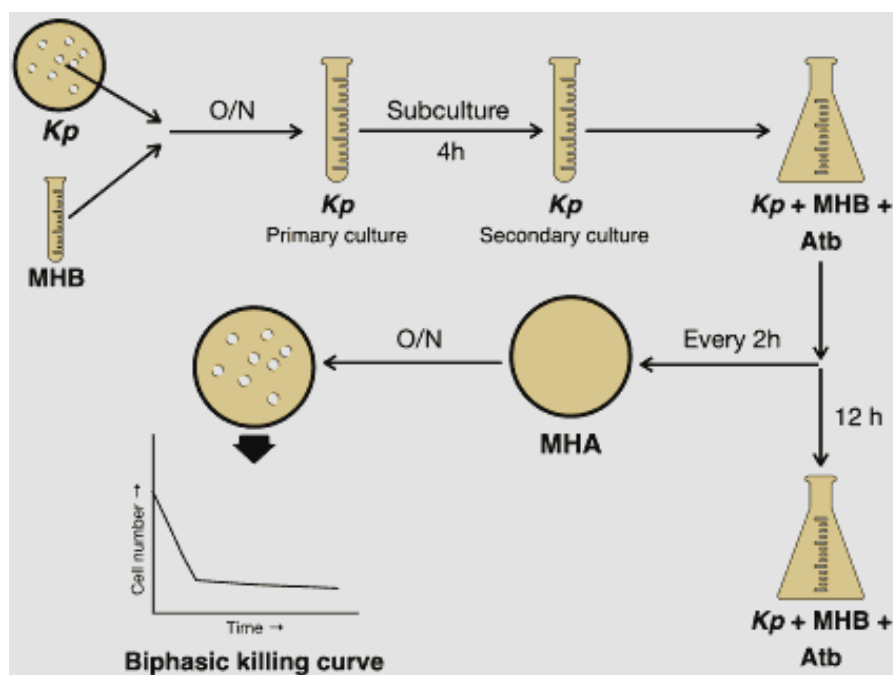
Table 3.3.6 Thermocycler conditions used to amplify the different fragments of the *gyrA* gene.

Stage of the cycle	Cycle conditions	
	F1R2	F2R3
Initial Denaturation	94°C, 120 s	94°C, 120 s
Cycle Denaturation	94°C, 30 s	94°C, 30 s
Cycle Annealing	60°C, 30 s	55°C, 30 s
Cycle Extension	72°C, 90 s	72°C, 90 s
Final Extension	72°C, 600 s	72°C, 600 s
Hold	4°C, ∞	4°C, ∞
Number of cycles	35	35

3.3.5 Identification of biphasic killing of bacterial isolates in response to antibiotic treatment

3.3.5.1 Identification of biphasic killing of isolates of *Klebsiella pneumoniae* in response to treatment with levofloxacin, amikacin and meropenem

The hallmark of a bacterial population that survives antibiotic treatment by forming persister cells is biphasic cell death as a function of time, wherein a rapid killing of most of the susceptible fraction of the population is followed by a much slower killing of the remainder of the population (Balaban et al, 2004). Time-dependant killing of bacterial cultures was assayed using the protocol described by Keren et al (2004) with certain modifications as depicted through a schematic in figure 3.3.2.



To observe the death of KpIMS38 as a function of time, i.e., the time-kill curve, a single, non-duplicate colony of a bacterial isolate grown on nutrient agar was streaked on to a MH agar plate. A single isolated colony obtained after overnight incubation of the plate was used to inoculate 3 mL of MH broth. Following overnight incubation, the culture was sub-cultured in 3 mL of MH broth at a ratio of 1:1000 and grown at 37°C for 4 hours. The resultant culture was used to inoculate 25 mL of MH broth contained in 100 mL conical flasks. Two such flasks were inoculated at a ratio of 1:100. One of the flasks contained either of the three antibiotics at concentrations four times the minimum inhibitory concentration for KpIMS38, the other was maintained without any antibiotic. The flasks were incubated at 37°C and culture aliquots were withdrawn every 2 hours, serially diluted and spread-plated on MH agar. The practice was carried out for 12 hours since the time of inoculation, all plates incubated at 37°C overnight and the resultant colony numbers counted. The colony-forming units per mL of culture were calculated and represented as a function of time. Unless otherwise mentioned, the above-mentioned procedure was used to induce persister cells in subsequent experiments.

3.3.5.2 Effect of different concentrations of Levofloxacin on persister cell formation in KpIMS38

To observe the survival of KpIMS38 in varying concentration of levofloxacin, persister cells were induced as mentioned in section 3.3.5.1 with certain modifications. The 4-hour culture was used to inoculate a total of six flasks, each containing levofloxacin of a concentration among one of the following series: 8, 16, 32, 128, 256, and 512 µg/mL. The flasks were incubated at 37°C and culture aliquots were withdrawn every 2 hours, serially diluted and plated on MH agar. The practice was carried out for 12 hours since the time of inoculation, all plates incubated at 37°C overnight and the resultant colony numbers

counted. The colony-forming units per mL for each of the concentrations used were calculated and represented as a function of time.

3.3.5.3 Effect of different growth phase of inocula on biphasic killing pattern in KpIMS38

To examine persister cell formation in KpIMS38 using inocula of different growth phase, persistence was induced according to the methodology outlined in section 3.3.5.1 with certain modifications. The overnight culture raised in MH broth was subcultured in 3 mL of MH both at a ratio of 1:1000 and grown at 37°C. Three such cultures were maintained; one for 4 hours corresponding to the Early-Log phase of growth, one for 6 hours corresponding to the Mid-Log phase of growth, and one for 10 hours corresponding to the Stationary phase of growth. The cultures, upon reaching their respective ages, were used to inoculate 25 mL of MH broth, contained in 100 mL conical flasks, at a ratio of 1:100. For each inoculum, one flask containing 256 µg/mL of levofloxacin and one flask containing no antibiotic was maintained.

The flasks were incubated at 37°C and culture aliquots were withdrawn every 2 hours, serially diluted and plated on MH agar. The practice was carried out for 12 hours since the time of inoculation, all plates incubated at 37°C overnight and the colony numbers counted. The colony-forming units per mL for each experimental setup were calculated and represented as a function of time.

3.3.5.4 Effect of inoculum size on biphasic killing pattern in KpIMS38

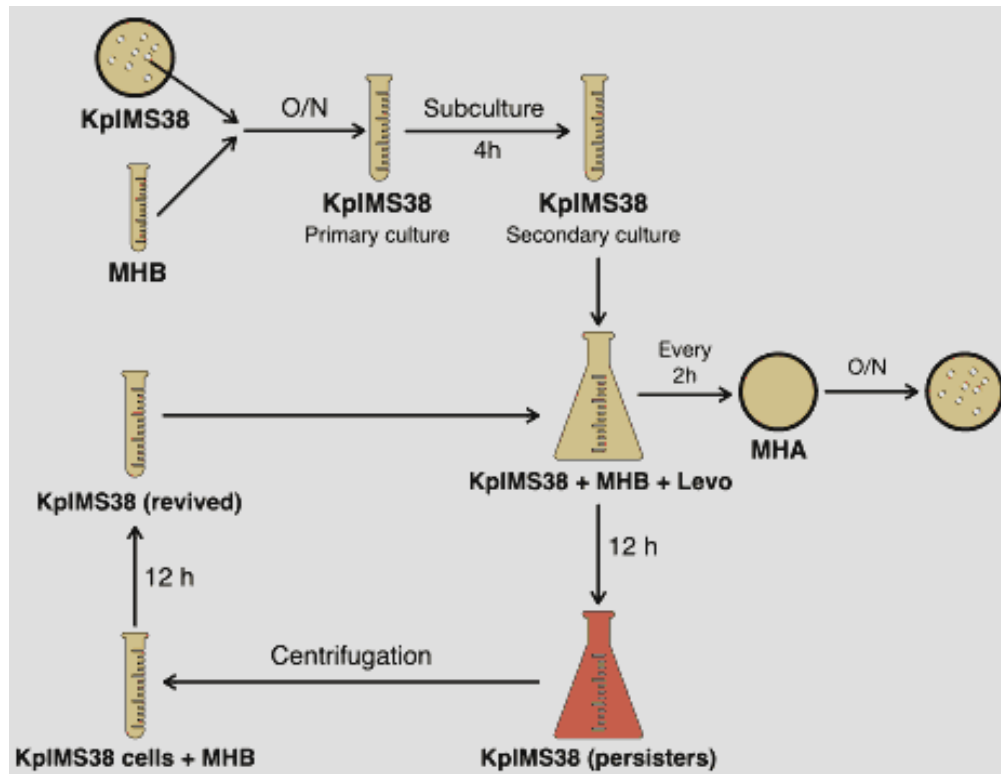
To observe the survival of KpIMS38 on exposure to levofloxacin at different sizes, persistence was induced in KpIMS38 according to the protocol described in section 3.3.5.1 with certain modifications. The 4-hour culture was used to inoculate a total of 3 flasks at ratios of 1:1000, 1:100 and 1:25 individually. All flasks were added levofloxacin at a final concentration of 256 µg/mL and were incubated at 37°C. Culture aliquots were withdrawn

every 2 hours, serially diluted and plated on MH agar for a total of 12 hours since the time of inoculation. All plates were incubated at 37°C overnight, the colony numbers counted and the colony-forming units per mL for each experimental setup were calculated and represented as a function of time.

3.3.5.5 Assessment of the time-kill kinetics in an isolate, exhibiting biphasic killing to levofloxacin, across successive generations

To ascertain whether the formation of persister cells by KpIMS38 is hereditary in nature, persistence was studied in successive generations as detailed in figure 3.3.3. Persister-cell formation was induced as mentioned in section 3.3.5.1 and the procedure carried out for 12 hours. Twelve hours post-inoculation, the contents of the flask were transferred to a sterile 50 mL screw-capped tubes and centrifuged at 3000 xg for 10 minutes at room temperature. The supernatant was discarded and the cell pellet resuspended gently in 1 mL sterile 1X Phosphate-buffered Saline (PBS) pH 7.4. The cell suspension was transferred to a sterile 1.5 mL microcentrifuge tube and centrifuged at 11,000 rpm for 30 seconds. The supernatant was discarded, the cell pellet resuspended in 250 µL of MH broth and the suspension transferred to a 15 mL tube containing 3 mL MH broth without any antibiotic. The tube was incubated at 37°C for 12 hours, following which the resultant culture was used to inoculate a new flask containing 25 mL MH broth with 256 µg/mL levofloxacin at a cell number corresponding to the inoculum used the previous day. The flask was incubated at 37°C and culture aliquots were withdrawn, serially diluted and plated on MH agar every 2 hours. The practice was carried out for 12 hours following which the procedure of harvesting the cells, re-growing them in antibiotic-free medium and using the resultant culture to seed a new flask was repeated.

The process was carried out for a total of 4 days including the first day. The colony numbers were counted, the colony-forming units per mL for each experimental setup were calculated and represented as a function of time.



3.3.5.6 To check cross-tolerance of persister cells to antibiotics against which the non-persister population is sensitive

To examine whether persister cells formed by KpIMS38 in response to levofloxacin were also tolerant to antibiotics that the non-persister populations were susceptible to, persister

cells formed upon levofloxacin-treatment were exposed to amikacin (Sigma-Aldrich, USA) and meropenem (Macleods Pharmaceuticals Ltd, India) at concentrations four times their MIC and the time-kill curve observed. Persistence was induced in KpIMS38 using levofloxacin as mentioned in section 3.3.5.1. Twenty-four hours post-inoculation, the contents of the flask were transferred to sterile 50 mL screw-capped tubes and centrifuged at 3000 xg for 10 minutes at 22°C. The supernatant was discarded and the cell pellet resuspended gently in 250 µL MH broth. The cell suspension was used to inoculate 25 mL of MH broth containing either 6.25 µg/mL of amikacin or 0.25 µg/mL meropenem, and the flasks incubated at 37°C. Culture aliquots were withdrawn, serially diluted and plated on MH agar every 2 hours for a total of 12 hours. The colony numbers were counted, the colony-forming units per mL for each experimental setup were calculated and represented as a function of time.

3.3.5.7 To check the occurrence of spontaneous mutants in the persister cells

To ascertain whether the survival of levofloxacin-treated KpIMS38 cells in supra-inhibitory concentrations of other antibiotics was due to the emergence of any spontaneous mutants against the said antibiotics, the MIC of levofloxacin-treated KpIMS38 cells to amikacin and meropenem was measured.

Persistence was induced as mentioned in section 3.3.5.1, with six flasks of KpIMS38 exposed to levofloxacin for 8 hours. The contents of the flasks containing levofloxacin were transferred to sterile 50 mL screw-capped tubes and centrifuged at 3000 xg for 10 minutes at 22°C. The cell pellet was resuspended gently in 2 mL of the supernatant, while the rest of the supernatant was discarded.

Two-fold dilution series were prepared for amikacin and meropenem in 4 mL MH broth according to the protocol outlined in section 3.3.3.2 of this document. The series for

amikacin and meropenem covered a concentration range of 16 to 0.5 $\mu\text{g}/\text{mL}$ and 1 to 0.03 $\mu\text{g}/\text{mL}$ respectively. Each of the antibiotic series were inoculated with 100 μL of the levofloxacin-treated cells or 10 μL of the untreated culture; a total of four dilution series being therefore generated. Growth-positive (PC) and growth-negative (NC) controls were maintained for both untreated and levofloxacin-treated cultures.

The tubes were incubated at 37°C for 14 hours, following which each culture was used to inoculate MH agar in the form of 10 μL spots in duplicate. Two separate plates were maintained for cultures treated with amikacin and meropenem, and the plates incubated at 37°C. The number of colonies were counted to obtain the number of survivors at each concentration. In addition, tubes were visually assessed for growth by comparing the growth of each of the tubes from the dilution series with the growth controls to determine the MIC.

3.3.6 Quantitative analysis of persister cell populations

3.3.6.1 Analysis of persister cell populations, generated on treatment with Levofloxacin, using fluorescent dyes by flow cytometry

The metabolic state of persister cells formed on treatment with levofloxacin was assessed using the dye carboxyfluorescein diacetate (CFDA; Sigma-Aldrich, USA).

3.3.6.1.1 Optimization of CFDA staining

To determine the appropriate concentration of CFDA to be used to stain KpIMS38 cells, a single colony of KpIMS38 grown on MH agar was inoculated into 3 mL MH broth and incubated at 37°C overnight. The culture was subcultured in 3 mL MH broth in a 1:1000 ratio and incubated at 37°C for 4 hours following which multiple 20 µL aliquots of the culture were withdrawn. Bacterial cells from each aliquot were harvested by centrifugation at 11,000 rpm for 30 seconds, the cell pellet resuspended in 100 µL of 1X PBS pH 7.4 and the suspension centrifuged once more. The cell pellet from each aliquot was resuspended in 1X PBS pH 7.4. Each aliquot was added a different volume of CFDA so that a concentration-series of 25, 50, 75, 100, and 150 µg/mL was obtained. The cell-suspensions were incubated at 37°C at 1200 rpm in a Thermomixer C (Eppendorf, Germany) for 900 seconds in the dark following which, the cells were harvested by centrifugation at 11,000 rpm with gentle acceleration and deceleration for 30 seconds. The cell pellet was resuspended in 100 µL 1X PBS pH 7.4 and the suspension centrifuged once more.

Table 3.3.7 Composition of the FACS buffer used to store cell – samples and perform flow cytometry.

Component	Amount
Bovine Serum Albumen	2 g
10 % Sodium Azide (NaN ₃)	1 mL
1X PBS pH 7.4	199 mL

The cell pellet was resuspended in 100 μ L FACS Buffer, which was prepared according to the composition described in table 3.3.7. To the cell suspension was added 100 μ L of 2% paraformaldehyde (PFA) to bring the final concentration to 1% and the suspension stored at 4°C in the dark. Each cell sample was transferred to an individual RIA vial (TARSONS, India) and the samples analysed in the LSR Fortessa Flow Cytometer (BD Biosciences, USA). Acquisition was performed through the agency of the FACS Diva software (BD Biosciences, USA) using the gating parameters specified in table 3.3.8. A total of 10,000 events were captured for each sample, and the data obtained analysed using FlowJo 10.7.1 (BD Biosciences, USA).

Table 3.3.8 Parameters used to gate cell-suspensions of KpIMS38 stained with CFDA.

Parameter	Voltage
Forward Scatter (FSC)	716
Side Scatter (SSC)	291
Fluorescence Channel (FITC)	430

3.3.6.1.2 Analysis of KpIMS38 persisters using flow cytometry

To analyse the KpIMS38 culture treated with levofloxacin through flow cytometry, persister cells were generated by exposing KpIMS38 according to the protocol outlined in section 3.3.5.1. Culture aliquots were collected at bihourly intervals from untreated as well as levofloxacin-treated cultures, stained with CFDA and fixed with PFA according to the procedure elucidated in section 3.3.6.1.1 of this document; 75 μ g/mL of CFDA being used for the purpose. All samples were analysed in a flow cytometer and results analysed as described in section 3.3.6.1.1 of this document.

3.3.6.2 Analysis of persister cell populations, generated on treatment with Levofloxacin, using fluorescent dyes by confocal microscopy

The response of KpIMS38 cultures to levofloxacin was assayed through live-cell microscopy. For the purpose, a wild-type culture of KpIMS38 was transformed with a plasmid construct containing a red fluorescent protein mCherry under control of the inducible *lac* promoter in the vector pGEX-6P-1^K. The cells were then induced to produce the fluorescent protein, immobilised on pads prepared using MH broth with 1.5% agarose, and placed in a flow-cell chamber. The cells were exposed to levofloxacin and then allowed to revive in levofloxacin-free medium.

3.3.6.2.1 mCherry construct preparation and cloning

The mCherry gene (710 bp) was synthesized by PCR using the protocol outlined in table 3.3.9. The forward and reverse primers used to amplify the mCherry gene (Table 3.3.10) were designed to contain sites for the restriction enzymes BamHI and XhoI (NEB, USA) respectively in regions upstream to the gene-specific sequences. Reactions were set up, placed in a thermocycler and subjected to PCR using the program outlined in table 3.3.11.

Table 3.3.9 Components used to perform PCR to amplify the mCherry gene.

Sr. No.	Component	Volume per reaction
1	Nuclease-Free Water	10.47 μ L
2	5x Green GoTaq® Flexi Buffer	4.00 μ L
3	2.5 mM dNTPs	1.33 μ L
4	25 mM MgCl ₂	1.00 μ L
5	10 μ M Forward Primer	0.50 μ L
6	10 μ M Reverse Primer	0.50 μ L
7	5 Units/ μ L GoTaq® Flexi DNA Polymerase	0.20 μ L
8	Template DNA	2.00 μ L

The reaction was run on a 1% TAE-agarose gel at 60 V for 90 mins. The band corresponding to the size of *mCherry*, i.e., 710 bp, was excised and DNA isolated from it using the QIAquick gel extraction kit according to the instructions outlined in section 3.2.3 of this document.

Table 3.3.10 Primer sequences used to amplify mCherry for cloning.

Gene	Primer	Sequence	Restriction enzyme	Reference
mCherry	gexCher-F	CAGTCGGATCCATGGTGAGC AAGGGCGA	BamHI	This study
	gexCher-R	CAGTCCTCGAGCTACTTGTA CAGCTCGTCCA	XhoI	This study

The amplified gene sequence as well as the plasmid vector pGEX-6P-1^K were digested using the Type-II restriction enzymes BamHI-HF and XhoI. Restriction digestion was performed according to the manufacturer's protocol supplied with the enzymes and is outlined in table 3.3.12.

Table 3.3.11 Thermocycler conditions used to amplify the mCherry gene.

Stage of the cycle	Conditions
Initial Denaturation	94°C, 120 s
Cycle Denaturation	94°C, 45 s
Cycle Annealing	69°C, 30 s
Cycle Extension	72°C, 70 s
Final Extension	72°C, 600 s
Hold	4°C, ∞
Number of cycles	35

The digestion-reactions were incubated in a thermocycler (Bio-Rad, USA) at 37°C for 3 hours to ensure complete digestion of DNA. The products were run on a 0.8% TAE-

agarose gel at 60V for 100 minutes. Fragments of the gel corresponding to the digested DNA were excised and DNA extracted from the gel using the QIAquick gel extraction kit according to the protocol outlined in section 3.2.3 of this document.

Table 3.3.12 Protocol for digestion of DNA using type-II restriction enzymes.

Sr. No.	Component	Volume per reaction
1	Nuclease-free Water	To 50 μ L
2	10X CutSmart® Buffer	5
3	10,000 units BamHI-HF	2 μ L
4	10,000 units XhoI	2 μ L
5	DNA	1000 ng

The digested vector and insert DNA molecules were taken in a molar ratio of 3:1 (Insert: Vector) and ligated using the Quick Ligation™ Kit (NEB, USA) according to the manufacturer's protocol outlined in table 3.3.13.

Table 3.3.13 Protocol for ligation of insert and vector molecules.

Sr. No.	Component	Volume per reaction
1	Nuclease-free Water	To 20 μ L
2	2X Quick Ligase Reaction Buffer	5
3	Vector DNA	To 50 ng
4	Insert DNA	To 3x molar quantity
5	Quick Ligase	1 μ L

The components were mixed together, incubated at room temperature for 15 minutes, following which they were placed on ice and used to transform chemically-competent *E. coli* cells.

3.3.6.2.2 Competent cell preparation

Chemically-competent *E. coli* DH5 α cells were prepared using the method described by Inoue et al (1990). The Inoue Transformation Buffer was prepared using the components detailed in 3.3.14. All the soluble compounds were dissolved in 800 mL distilled water initially. The mixture was added 20 mL of 0.5 M PIPES (pH 6.7) and the volume adjusted with distilled water to 1 L. This buffer was sterilised by filtration through a 0.45 μ m membrane filter (Millipore, USA) using a 90 mm Glass Filter Holder Kit attached to a 2 L vacuum-filtering flask and driven by a vacuum pressure pump (Millipore, USA), and stored at -20°C until use.

To prepare competent cells, a single, non-duplicate colony of *E. coli* DH5 α growing on LB agar was used to inoculate 25 mL SOB medium (HiMedia, India) contained in a 100 mL conical flask, and the culture grown at 37°C, 220 rpm for 8 hours. Two mL of the resultant culture was used to inoculate 125 mL of SOB medium contained in a 500 mL flask. The flask was incubated at 18°C till the culture attained an OD₆₀₀ of 0.55. The flask was placed on an ice-bath for 10 minutes, following which the cultures were centrifuged at 2500 xg for 10 minutes at 4°C. The supernatant was discarded and the cells gently resuspended in 40 mL of chilled Inoue transformation buffer. The suspension was centrifuged at 2500 xg for 10 minutes at 4°C, the supernatant discarded and the cells gently resuspended in 10 mL of chilled Inoue transformation buffer. The suspension was added with 750 μ L of dimethyl sulfoxide (DMSO; MP Biomedicals, USA), the suspension swirled to mix and stored in ice for 10 minutes. Working quickly, the suspension was dispensed into chilled sterile 1.5 mL microcentrifuge tubes on ice as 250 μ L aliquots, the tubes firmly closed and snap-frozen by immersion into liquid nitrogen. The tubes were stored at -80°C until further use.

Table 3.3.14 Composition of the Inoue transformation buffer.

Sr. No.	Component	Amount per litre
1	MnCl ₂ •4H ₂ O	10.88 g
2	CaCl ₂ •2H ₂ O	2.20 g
3	KCl	18.65 g
4	0.5 M PIPES (pH 6.7)	20 ml
5	Distilled Water	to 1 L

3.3.6.2.3 Transformation of pGEX-6P-1^K-mCherry into *E. coli* DH5 α

For transformation of the ligation products, an adequate amount of the competent cell-suspension was thawed on ice and 50 μ L-aliquots transferred into chilled microcentrifuge tubes. Ten μ L of each ligation product was added to an aliquot of competent cells and the mixture allowed to incubate in ice for 30 minutes. A non-transformed control without any DNA was also maintained. The tubes were then placed in a water bath maintained at 42°C for precisely 90 seconds and snap-chilled in ice for 1 minute. The tubes were added 800 μ L of SOC medium (containing 0.4% glucose), incubated at 37°C and 220 rpm for 50 minutes. The cultures were spread-plated onto SOB agar containing 50 μ g/mL kanamycin and incubated overnight at 37°C.

3.3.6.2.4 Screening of transformants to verify cloning of mCherry

Out of the colonies grown on the transformed plates, ten colonies were subcultured from each transformation experiment on LB agar containing 50 μ g/mL kanamycin (LBA-Kan⁵⁰). The colonies were simultaneously used to create a cell lysate as described in section 3.2.7.4 of this document. The resultant suspensions were used as templates to perform a colony PCR to screen for the presence of *mCherry* in the transformants.

Reactions were set up according to the protocol specified in table 3.3.9, using the primers used to synthesize *mCherry* and 2 μ L of each colony lysate as template. The reactions were

incubated in a thermocycler according to the program described in table 3.3.11 and the products run on a 1% TAE-agarose gel at 60 V for 90 mins. The presence of an amplicon of the size corresponding 710 bp in a reaction was considered positive for transformation of mCherry. Any such isolates were stored in the form of 40 % glycerol stocks at -80°C until further use.

3.3.6.2.5 Transformation of mCherry into KpIMS38

KpIMS38 was transformed with pGEX-6P-1^K-mCherry to express the fluorescent protein mCherry under inducible control by isopropyl β-D-1-thiogalactopyranoside (IPTG). To carry out the same, KpIMS38 cells were first made amenable to transformation according to the protocol outlined in section 3.2.7.2 of this document with certain adjustments.

Briefly, a single isolated colony of *E. coli* DH5α growing on LBA-Kan⁵⁰ was inoculated into 2 mL LB-Kan⁵⁰ and allowed to grow overnight at 37°C. The resultant culture was subcultured in 3 mL LB-Kan⁵⁰ at a 1:1000 ratio and incubated at 37°C for 4 hours. The resultant culture was divided into 250 μL aliquots and the cells washed with 10% glycerol and resuspended as 50 μL aliquots according to the conditions specified in section 3.2.7.2.

One cell-suspension was added 200 ng of the pGEX-6P-1^K-mCherry, while another aliquot was maintained as such – hereon referred to as the "non-transformed control" (NTC). Both cell-suspensions were stored on ice for 1 min, transferred to individual 2 mm electroporation cuvettes and stored in ice for 1 min. The cuvettes were placed in an electroporator and pulsed once at 2500 V with a 5 ms time-constant protocol. The cuvettes were immediately added 800 μL LB broth, resuspended, and their entire contents transferred to sterile 1.5 mL tubes. The tubes were incubated at 37°C and 220 rpm agitation for 70 mins, following which the entire contents were spread-plated onto individual LBA-Kan⁵⁰ plates. The plates were incubated at 37°C overnight.

From the plate containing the transformants, four colonies were subcultured on LBA-Kan⁵⁰ as well as screened for the presence of *mCherry* through PCR according to the procedures and protocols detailed in section 3.3.6.2.4 of this document. Isolates seen to possess the *mCherry* gene were stored in the form of 40 % glycerol stocks at -80°C until further use.

3.3.6.2.6 Visualisation of *KpIMS38* treated with levofloxacin through live-cell microscopy

To perform live-cell analysis of the bacterial population, the Focht Chamber System 2 (FCS2; Biopetechs, USA) was used, made available by courtesy of Dr. R. Srinivasan, SBS, NISER. The FCS2 consisted of a white-top (containing perfusion tubes attached), a 0.5 mm silicone ring gasket, a microaqueduct slide to allow for high-volume laminar flow, a 0.75 mm silicone gasket with a rectangular orifice, a 40 mm coverslip, and a self-locking base. Flow through the chamber was achieved using the P720 peristaltic pump (Instech, USA), and conducted using appropriate lengths of Tygon silicone tubing (Sigma-Aldrich, USA) with a 1/16-inch internal diameter. The temperature of the chamber was regulated using an electrical enclosure, containing heater contacts and a temperature sensor, attached to the white-top of the chamber setup and controlled by the FCS2 microenvironment controller.

Each of the components of the FCS2 chamber, except the self-locking base, were wrapped in aluminium foil, sterilised by autoclaving at 121°C for 15 minutes, and allowed to completely dry prior to use. A single colony of *KpIMS38-mCherry* grown on LBA-Kan⁵⁰ was subcultured on MH agar containing 50 µg/mL kanamycin (MHA-Kan⁵⁰) and incubated at 37°C overnight. A single, non-duplicate colony from the resultant culture was used to inoculate 3 mL of MH broth containing 50 µg/mL kanamycin and 0.1 mM IPTG (henceforth known as MHB-KI) and incubated at 37°C and 220 rpm overnight. The

resultant culture was used to inoculate 3 mL MHB-KI in a 1:1000 ratio and incubated at 37°C for 4 hours.

During the interim, suitable lengths of tubing attached to the peristaltic pump and the setup placed in a laminar airflow cabinet. The tubing connected to the input of the pump was placed in a reservoir containing 70% ethanol, while the tubing connected to the output of the pump was placed in an empty reservoir. The pump was connected to power supply and run at full speed to allow ethanol to completely fill the system. The pump was then turned off, UV light turned on in the cabinet and the setup allowed to stand for 30 minutes. The self-locking base of the FCS2 was wiped with ethanol, placed in the cabinet and allowed to sterilize under UV light along with the pump-setup. Following sterilization, the setup was run to allow ethanol to be purged from the system. The inlet was then placed into a reservoir containing sterile distilled water, and 15 mL allowed to run through the system at full speed. The system was then purged of water, and its ends covered with sterile aluminium foil.

To immobilise the bacterial cells, a sterile 22 × 22 mm coverslip was placed on a flat, uniform surface in the laminar airflow cabinet. Sterile MH agar containing 1.5 % agarose was molten and 400 µL pipetted on the surface of the coverslip. Immediately, another sterile coverslip was placed on top of the medium, and the setup allowed to stand for 5 minutes to solidify. The top coverslip was removed and using a sterile scalpel, 5 × 5 mm pads were cut out. The secondary culture of *KpIMS38-mCherry*, grown for 4 hours, was mounted on the pads, with 2 µL of the culture spotted on the surface of each pad, and the cultures allowed to dry.

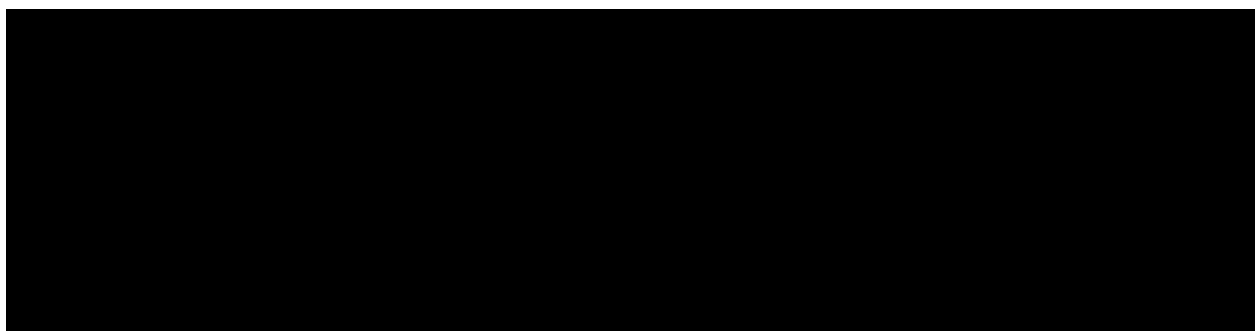
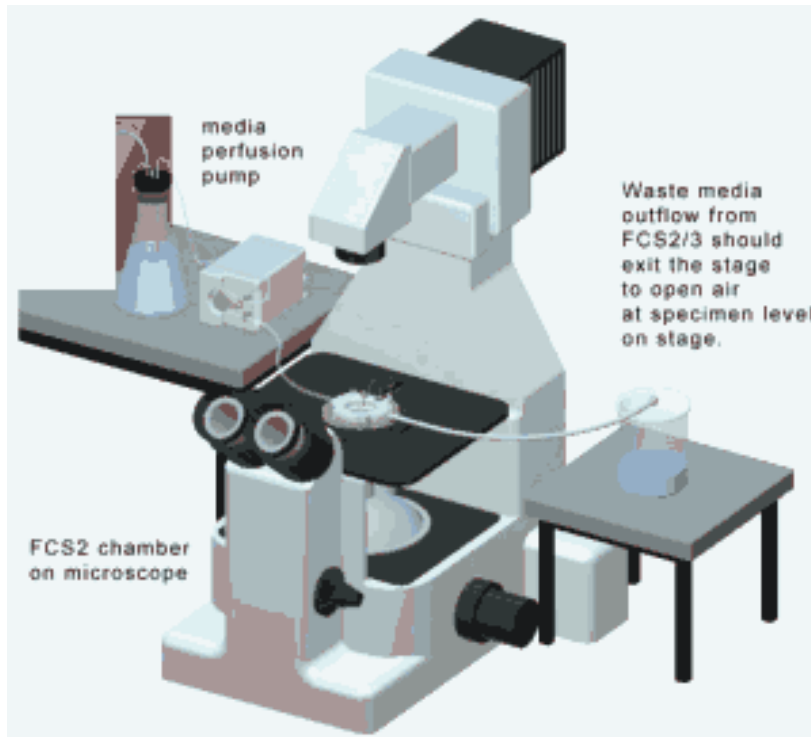
The FCS2 chamber was assembled using the agarose pads mounted with *KpIMS38-mCherry* cells in the following order (bottom to top):

White top → 0.5 mm ring gasket → Microaqueduct slide → 0.75 mm gasket → Agarose pad → 40 mm coverslip → Metal base.

The system was fastened to ensure all components were held in place. The tube from the outlet of the peristaltic pump was attached to one of the perfusion tubes of the white top, while another separate tube was attached to the other perfusion tube. A conical flask containing 50 mL of MHB-KI was covered with sterile aluminium foil at its mouth and the inlet tube from the pump inserted through it into the flask till the opening of the tube was submerged in the medium.

The flow-cell system was set up on the microscope, with the chamber adjusted on the microscope-stage and the medium and waste reservoirs appropriately placed. The FCS2 microenvironment controller was connected to the FCS2 chamber using the electrical enclosure, and the temperature set to 37°C. A schematic diagram representing the setup used to perform live-cell microscopy has been given in Figure 3.3.4. The agarose pad was focussed using a 10x dry objective lens under phase-contrast microscopy first, and then visualised using laser light at a wavelength of 588 nm (excitation). A sequential scan algorithm was set up in the Leica Application Suite X (LASX) software to capture the fluorescent image (detector range = 602 – 618 nm) first followed by the phase-contrast image, with adaptive focus set up to hold the plane of focus steady. A “xyt” mode of acquisition was chosen so as to capture images every 5 minutes for a total of 1 hour (hr). The pump was run at a setting of 25, to allow MHB-KI to flow through the system at a rate of 20 mL/hr. After 30 minutes, the system was run with MHB-KI containing 256 µg/mL levofloxacin at 20 mL/hr, and images captured at a resolution of 2048 × 2048 pixels every 10 minutes for a total of 8 hours. The flow-cell system was then run with

MHB-KI at 20 mL/hr, and images captured every 10 minutes for a total of 6 hours. Images were exported in .tiff format and analysed using ImageJ.



3.3.7 Analysis of gene expression in persister cells by genomic approaches

3.3.7.1 Elucidation of the draft genome of KpIMS38 through Next-Gen DNA Sequencing

Genomic and plasmid DNA were extracted from KpIMS38 cultures according to the protocols elucidated in sections 3.2.1 and 3.2.2 in this document respectively. Sequencing of the DNA was performed at the laboratory facility of ThermoFisher Scientific, Gurgaon, India.

The quality of the DNA samples was assessed using a 2100 Bioanalyzer (Agilent, USA). The samples were used to prepare libraries with the help of the Ion Xpress™ Plus Fragment Library Kit (Thermo Fisher Scientific, USA) using the Ion OneTouch™ 2 Instrument (Thermo Fisher Scientific, USA). The libraries for the genomic and plasmid DNAs were loaded onto individual Ion 520™ chips and sequenced in an Ion S5™ System (Thermo Fisher Scientific, USA) with a coverage of 100x.

Reads obtained for each DNA molecule were assembled into contigs *de novo* using the SPAdes algorithm version 3.1.0 (Bankevich et al, 2012) and the assembly-statistics generated using QUAST (Gurevich et al, 2013). Coding regions were identified within genomic DNA contigs using Prodigal (Hyatt et al, 2010) and within plasmid DNA contigs using Genemark (Besemer and Borodovsky, 1999). The regions thereby identified were annotated using Blast2GO (Conesa et al, 2005) for both the genome as well as the plasmid. In addition, contigs from the genome were also annotated using the Rapid Annotations using Subsystems Technology (RAST) server (Aziz et al, 2008; Overbeek et al, 2014), using *Klebsiella pneumoniae* subsp. *pneumoniae* HS11286 as the reference genome.

The contig-file for KpIMS38 was analysed using the ResFinder 4.1 (Bortolaia et al, 2020) and MLST 2.0 (Larsen et al, 2012) tools available on the Centre for Genomic Epidemiology website. Additional analyses were performed using the Resistance Gene

Identifier (RGI) 5.2.0 tool available on the Comprehensive Antibiotic Resistance Database (CARD) 3.1.4 (McArthur et al, 2013), the Single genome analysis tool available through BacWGSTdb (Feng et al, 2021), and Phaster (Arndt et al, 2016)

3.3.7.2 Determination of the profile of gene expression in bacterial persister cells by Next-Gen RNA Sequencing

Total cellular RNA was extracted from KpIMS38 persister cells formed upon treatment with levofloxacin according to the protocol elucidated in section 3.2.5 in this document. Briefly, a single, non-duplicate colony of a bacterial isolate grown on nutrient agar was streaked on to a MH agar. A single isolated colony obtained after overnight incubation of the plate was used to inoculate 3 mL of MH broth. Following overnight incubation, the culture was subcultured in 3 mL of MH broth at a ratio of 1:1000 and grown at 37°C for 4 hours. The resultant culture was used to inoculate, at a ratio of 1:100, 25mL of MH broth without and with 256 µg/mL levofloxacin individually contained in 100 mL conical flasks. A total of four levofloxacin-treated and one untreated cultures were maintained and incubated at 37°C for 8 hours. The levofloxacin-treated culture was collected by centrifugation at 3000 xg for 10 minutes at room temperature, resuspended in 500 µL of supernatant and then added to two volumes of RNAProtect Bacteria Reagent. On the other hand, 200 µL of the untreated culture was directly added to two volumes of RNAProtect Bacteria Reagent. RNA was extracted from both sets of cultures according to the procedure outlined in section 3.2.5 of this document.

Sequencing of the RNA samples (untreated and levofloxacin-treated) was performed at the laboratory facility of ThermoFisher Scientific, Gurgaon, India. The quality of the RNA samples was assessed using a 2100 Bioanalyzer (Agilent, USA) by determining the RIN value. The samples were depleted of 16S and 23S ribosomal RNA using the MICROBExpress™ Bacterial mRNA Enrichment Kit (Invitrogen, USA). The mRNA

obtained was used to prepare libraries for each of the RNA samples using the Ion Xpress™ Plus Fragment Library Kit (Thermo Fisher Scientific, USA) and the Ion OneTouch™ 2 Instrument (Thermo Fisher Scientific, USA). Libraries were loaded onto Ion 530™ chips and sequenced in an Ion S5™ System (Thermo Fisher Scientific, USA).

Reads obtained for the RNA samples were aligned with the reference draft genome of KpIMS38 using TopHat 2 (Kim et al, 2013). Any unmapped reads were aligned using Bowtie2 (Langmead and Salzberg, 2012) and both alignments were merged using Samtools (Li et al, 2009). Further analysis of the differential expression of genes was performed using Cuffdiff (Trapnell et al, 2010) and aided by gene annotations obtained from analyses using Prodigal and RAST server.

In addition, the reads obtained from sequencing were also assembled *de novo* using rnaSPADES (Nurk et al, 2013) into contigs, the statistics for which were obtained using rnaQUAST (Bushmanova et al, 2016). All contigs were aligned to the NR database using Blast2GO; based on protein ID hits, gene ontology was assigned to each of the genes on the contigs. Based on reads from the samples, counts for each transcript were generated and compared using RSEM (Li and Dewey, 2011).

3.3.8 Investigation of the role of genes in persister cell formation

3.3.8.1 Validation of an appropriate reference gene to study gene expression in persister cells

Following the results of the transcriptome analysis, five genes were selected as candidates for reference genes to study gene expression in KpIMS38 persister cells formed by levofloxacin, on the basis of data obtained from transcriptome of KpIMS38 cells treated with levofloxacin. The genes used were *dnaJ*, *groEL*, *rpoB*, *kp751* (glycerol dehydrogenase) and *kp4432* (phenylacetaldehyde dehydrogenase). Primer pairs were designed for each gene using the coding region of the genes with the PrimerQuest tool available from the IDT website (<https://eu.idtdna.com/Primerquest/Home/Index>). The primer-pairs for each gene were designed with melting temperatures within 1°C of each other and chosen so as to amplify a region between 90 to 120 bp. Additional details of the primer sequences are included in table 3.3.15.

Table 3.3.15 Primer sequences of candidates used to identify reference genes to study gene expression in KpIMS38 persister cells.

Gene	Primer	Sequence (5' → 3')	Amplicon Size	Reference
<i>dnaJ</i>	dnaJ-F	GTTCGGCATCAGTACCAGATAG	114 bp	(Patole et al., 2021)
	dnaJ-R	CGGGAAGGTCAGGAAGTTATC		
<i>groEL</i>	groEL-F	AAGACACCACCACCATCATC	90 bp	(Patole et al., 2021)
	groEL-R	TCGCTTCTTCGATCTGCTTAC		
<i>kp4432</i>	hm4432-F	CGGCATCGTATGGGTCAAT	118 bp	(Patole et al., 2021)
	hm4432-R	CCGACTTCAGCTCCGTATAATC		
<i>kp751</i>	hm751-F	GTGGAAGCCAACACCTATCT	112 bp	(Patole et al., 2021)
	hm751-R	GATAATAGTGATGGGCGTCAGG		
<i>rpoB</i>	KprpoB-F	GATCCGTGGCGTGACTTATT	128 bp	(Patole et al., 2021)
	KprpoB-R	GCCCATGTAGACTTCTTGTTCT		

RNA was extracted from both untreated and levofloxacin-treated cultures of KpIMS38 as described in section 3.3.7.2 of this document. Further, 1000 ng of each RNA sample was converted into cDNA according to the protocols detailed in section 3.2.6 of this document. A 3-point ten-fold dilution series of each of the cDNA samples was prepared and used as templates, namely, 100, 10, and 1 ng of cDNA. A total of three technical and three biological replicates were set up for each cDNA sample according to the protocol outlined in table 3.3.16. The reactions were distributed into individual wells in a 96-well PCR plate (Applied Biosystems, USA) and the plate incubated in a 7500 Fast-Real Time PCR System (ThermoFisher Scientific, USA) using the program outlined in table 3.3.17.

Table 3.3.16 Components used to perform qPCR to study the expression of the five candidate genes in cDNA samples.

Sr. No.	Component	Volume per reaction
1	Nuclease-Free Water	to 20.00 μ L
2	2X FastStart Universal SYBR Green Master Mix with ROX	10.00 μ L
3	10 μ M Forward Primer	0.50 μ L
4	10 μ M Reverse Primer	0.50 μ L
5	Template cDNA	variable

The quantification cycle (C_q) values were obtained for each of the template-gene combinations and plotted as log (template concentration) versus C_q graphs for each of the five genes. Three-point standard curves were obtained for each of the candidate genes for untreated as well as levofloxacin-treated cDNA. The slope of each of the curves was used to deduce the efficiency of amplification of each gene using the formula given by Ramakers et al (2003), where

$$\text{Efficiency} = 10^{-(\text{slope})^{-1}} - 1$$

and $E = 2$ corresponds to 100% amplification efficiency.

Table 3.3.17 qPCR conditions used to assess the expression of the candidate reference genes in untreated and levofloxacin-treated cells of KpIMS38.

Stage of the cycle	Conditions
Initial Denaturation	95°C, 600 s
Cycle Denaturation	95°C, 15 s
Cycle Annealing & Extension	60°C, 60 s
Number of cycles	40
Melt curve	65 - 95°C
Ramp rate	0.5°C / 5 s

The C_q values for each of the genes in untreated and levofloxacin-treated conditions were used to assess expression stability using the BestKeeper (Pfaffl et al, 2004), Delta Ct (Silver et al, 2006), geNorm (Vandesompele et al, 2002) and NormFinder (Andersen et al, 2004) algorithms, which were available in the RefFinder online tool (Xie et al, 2012). For use with the geNorm and NormFinder algorithms, raw C_q values were converted into relative quantity (RQ). The RQ for each reaction was calculated using the equation

$$RQ = E^{\Delta Cq'}$$

where E is the efficiency of amplification and the $\Delta Cq'$ calculated by the formula

$$\Delta Cq' = (\text{minimum } Cq \text{ for the gene}) - (Cq \text{ for the sample}).$$

On the basis on the results obtained from the algorithms, the suggested genes were used as reference genes to examine expression of a selection of genes upon persister cell formation in KpIMS38. The selected genes included phage shock proteins involved in the bacterial membrane-stress response *pspA*, *pspC*, *pspD*, *pspF* and *pspG*, as well as a

coactivator *ibrA*. qPCR reactions were set up using primers for the genes mentioned here (Table 3.3.18) as well as the reference genes according to the protocol described in table 3.3.16.

Table 3.3.18 Primer sequences for qPCR to study the expression of phage shock protein (*psp*) genes as well as *ibrA* in KpIMS38 treated with levofloxacin.

Gene	Primer	Sequence (5'→3')	Amplicon	Source
<i>pspA</i>	pspA-Q-F	GGCGAAGGCATCAACTTCTA	91 bp	This study
	pspA-Q-R	CGCTTTACCCTGACCGATT		
<i>pspC</i>	pspC-Q-F	CTCTCCCAGCCATACCATAGA	120 bp	This study
	pspC-Q-R	CCAGCCAGCAGATAACTACAC		
<i>pspD</i>	pspD-Q-F	TCTGGATGCCATCTGGAAAG	75 bp	This study
	pspD-Q-R	AGCTCGTCGAACAGATTCAG		
<i>pspF</i>	pspF-Q-F	CTCAGGGCTGGGTAAAGTATG	109 bp	This study
	pspF-Q-R	CGTGTCGTATAAGCAGGAGAAA		
<i>pspG</i>	pspG-Q-F	GGTTGAGCTACGTCAGATTGT	149 bp	This study
	pspG-Q-R	GTTGAGGTCGATTCGCTTCT		
<i>ibrA</i>	ibrA-Q-F	GACGATTTCTTCACAGCGTAAAC	103 bp	This study
	ibrA-Q-R	CCAGTCATAGAGCGGGTAGA		

The reactions were run in a 7500 Fast-Real Time PCR System according to the conditions described in table 3.3.17 and the mean Cq values for each gene in both untreated and levofloxacin-treated samples acquired. Gene expression was calculated using the $2^{-\Delta\Delta Cq}$ method outlined by Schmittgen and Livak (2008) according to which

$$\text{Fold change} = 2^{-\Delta\Delta Cq}$$

$$\Delta\Delta Cq = \Delta Cq(\text{Treated}) - \Delta Cq(\text{Untreated})$$

$$\Delta Cq = Cq (\text{Gene} - \text{of} - \text{interest}) - Cq (\text{Reference gene})$$

and whenever more than one reference gene was used to normalise expression, the mean Cq value of the reference genes calculated and considered as the reference-gene Cq. Fold change values using different reference genes or combinations of reference genes were calculated.

3.3.8.2 Assessment of expression profiles of toxin-antitoxin genes found in the bacterial isolate during persistence

The expression of the toxin-antitoxin (TA) loci identified in KpIMS38 was assessed on treatment with levofloxacin. For the purpose, the list of annotated genes available for KpIMS38 was searched for the presence of cognate gene-pairs constituting to TA loci. The sequences of *relTA*, *relBE*, *ficTA* and *phd-doc* were used to construct primers to measure the expression of the genes using qPCR (Table 3.3.19).

RNA was extracted from both untreated and levofloxacin-treated cultures of KpIMS38 as described in section 3.3.7.2 of this document. Further, 1000 ng of each sample was converted into cDNA using the SuperScript™ IV First-Strand Synthesis System (Invitrogen, USA) according to the protocols detailed in section 3.2.6 of this document, which was used as template to assess the expression of the toxin-antitoxin genes. qPCR reactions were set up wherein expression of each of the 8 genes (four toxin-antitoxin pairs) was evaluated in cDNA from untreated and levofloxacin-treated cells. The reference genes used here were *kp4432* and *rpoB*.

Reactions were set up according to the protocol outlined in table 3.3.16. The reactions were distributed into individual wells in a 96-well PCR plate and the plate incubated in a 7500 Fast-Real Time PCR System using the program outlined in table 3.3.17. Fold change values, normalised to the pair of reference genes, were calculated for each gene using the equations described in section 3.3.8.1 of this document.

Table 3.3.19 Primer sequences to assess the expression of various toxin-antitoxin genes in KpIMS38 using qPCR.

Gene	Primer	Sequence (5'→3')	Amplicon	Reference
<i>relT</i>	Xre-RelT-F	CAAAAACGGCAGATAAGC	135 bp	This study
	Xre-RelT-R	AGTGGTTTTTCGGGAGAGG		
<i>relAt</i>	Xre-RelAt-F	GAAGGAAAAGACCAGTATG	96 bp	This study
	Xre-RelAt-R	CCAGTCGCTTTCATCCTC		
<i>relE</i>	relE-Q-F	GCCAGGCTGAGCGATTTA	99 bp	This study
	relE-Q-R	GTAAACCACCACCACACTATCT		
<i>relB</i>	relB-Q-F	CTCAATGTTCTGACTGGACGATAA	79 bp	This study
	relB-Q-R	GCCTCCGTTGGTGT CATATC		
<i>ficT</i>	PHD-FicT-F	CGTGCCGAAGCGATAATG	138 bp	This study
	PHD-FicT-R	TGCCGTACGCTTATTACC		
<i>ficAt</i>	PHD-Fic-ATF	GTCGTGGGCATAAATCTG	102 bp	This study
	PHD-Fic-ATR	CATGAACCGCCATGATAG		
<i>phd</i>	phd-Q-F	CCCGTCGTGGGCATAAAT	107 bp	This study
	phd-Q-R	ACCATGAACCGCCATGATAG		
<i>doc</i>	doc-Q-F	AGCGATAATGTATAGGGTGCTAA	143 bp	This study
	doc-Q-R	GGGTGATAAACAGTGCCGTA		

3.3.8.3 Assessment of the expression profiles of stress-response genes found in the bacterial isolate during persistence

The expression of select stress response genes was studied using qPCR. The genes selected for evaluation were involved in the bacterial response to DNA damage viz. *recA*, *sulA*, *umuC*, *umuD*, *ruvA*, *ruvB*, *ruvC*. In addition, expression of the stringent response gene *spoT* was also studied. Primer sequences for the genes are detailed in table 3.3.20.

Persistence was induced in KpIMS38 as described in section 3.3.5.1 with certain modifications. At designated time-points viz., 0 minutes, 15 minutes, 30 minutes, 45

minutes, 60 minutes, 120 minutes and 480 minutes post-inoculation, cells were harvested from one untreated and two levofloxacin-treated flasks. The total cellular RNA was extracted from the samples of which 500 ng was converted into cDNA according to the protocols detailed in sections 3.2.5 and 3.2.6 respectively of this document.

Table 3.3.20 Primer sequences to evaluate the expression of stress-response genes in KpIMS38 using qPCR.

Gene	Primer	Sequence (5'→3')	Amplicon	Reference
<i>recA</i>	recA-Q-F	GGCGAAGGCATCAACTTCTA	117 bp	This study
	recA-Q-R	CGCTTTACCCTGACCGATTT		
<i>sulA</i>	sulA-Q-F	CTCTCCCAGCCATACCATAGA	77 bp	This study
	sulA-Q-R	CCAGCCAGCAGATAACTACAC		
<i>umuC-1</i>	umuC1-Q-F	TCTGGATGCCATCTGGAAAG	105 bp	This study
	umuC1-Q-R	AGCTCGTCGAACAGATTCAG		
<i>umuC-2</i>	umuC2-Q-F	CTCAGGGCTGGGTAAAGTATG	93 bp	This study
	umuC2-Q-R	CGTGTCGTATAAGCAGGAGAA A		
<i>umuD-1</i>	umuD1-Q-F	GGTTGAGCTACGTCAGATTGT	106 bp	This study
	umuD1-Q-R	GTTGAGGTCGATTCGCTTCT		
<i>umuD-2</i>	umuD2-Q-F	TTACGGTGAAACGGCTTCTG	126 bp	This study
	umuD2-Q-R	GGTGGATGATATGCGTGACAA		
<i>ruvA</i>	ruvA-Q-F	GCAGACTCAGAGGCATCATT	107 bp	This study
	ruvA-Q-R	CAGCTCATAGAAGCAGGTCATT		
<i>ruvB</i>	ruvB-Q-F	CTGCTGGCGGTGATAGATAAG	109 bp	This study
	ruvB-Q-R	AGTAGGGCTCCAGTACATCTT		
<i>ruvC</i>	ruvC-Q-F	GCACCAAAGTGGACGATCT	103 bp	This study
	ruvC-Q-R	ACCTGCTCAATGGCGAAATA		
<i>spoT</i>	spoT-Q-F	ACCGTTTAGGTATCCATCACAT C	120 bp	This study
	spoT-Q-R	CCGCTTTGACCACCTCTTTA		

qPCR reactions were set up wherein expression of each of the 8 genes, along with the reference genes *kp4432* and *rpoB*, was assessed at all the time-points. Reactions were set up according to the protocol outlined in table 3.3.16 and distributed into individual wells in a 96-well PCR plate. The reactions were incubated in a 7500 Fast-Real Time PCR System using the program outlined in table 3.3.17.

The C_q values were obtained for each of the template-gene combinations and further normalised using the pair of *kp4432* and *rpoB*. Gene expression was calculated using the $2^{-\Delta\Delta C_q}$ method (Schmittgen and Livak, 2008) described in section 3.3.8.1 of this document.

3.3.8.4 Creation of gene deletion mutants to study role of specific genes in persistence

Unlike *E. coli*, genetic manipulation systems in multi drug resistant *Klebsiella pneumoniae* have not been robustly established. Therefore, creation of deletion-mutants in KpIMS38 were attempted by using the Red/ET recombination method by means of the Quick & Easy *E. coli* Gene Deletion Kit (Genebridges, Germany) was employed to create gene-deletions. On the basis of data obtained from the transcriptome of KpIMS38 persister cells, four genes were chosen for loss-of-function studies viz., *ibrA*, *pspF*, *doc* and *relE*. To carry out the same, deletion was performed following the protocol described in section 3.2.8 of this document.

Deletion primers were designed that contained 50 - 60 bp overhangs homologous to the gene-of-interest. Based on the sequence data obtained from annotation of the genome of KpIMS38, primers were designed for the same, the sequences for which are given in table 3.3.21.

Deletion cassettes were synthesized for each of the four target genes through high-fidelity PCR using the protocol outlined in section 3.2.8.1 of this document. Either of the plasmids that contained the Red/ET recombination genes viz. pRedET and pACBSR-Hyg were

transformed into KpIMS38 cells following the protocols outlined in sections 3.2.8.2 and 3.2.8.3 respectively of this document. Thereafter, individual cassettes were transformed into these KpIMS38 cells to allow recombination, according to the procedures outlined in sections 3.2.8.4 and 3.2.8.5 of this document.

Table 3.3.21 Primer sequences to construct deletion cassettes for specific genes from KpIMS38. Uppercase segments indicate the sequence homologous to the gene of interest, lowercase segments indicate the sequence identical to and used to amplify the FRT cassette.

Gene	Primer	Sequence (5' → 3')	Reference
<i>ibrA</i>	ibrAn-D-F	GCCTTCCTAT TTATATGACT TTATCTCACC CACTATGCAG CTTCACGCCA TCAACATAGA aattaaccctcactaaagggcgg	This study
	ibrAn-D-R	AGTGGCTGCT TTTGGTTGGG CTAAACGAAA GCTGACGGCA CCAGTAATCG TTATTGAGCA taatacgactcactatagggctcg	
<i>pspF</i>	pspFn-D-F	ACAAATGGCG TGCCAAC TTTT TTATCTTATT GATTTTAAAC AGGGTGGTTG CGAAACGTGC aattaaccctcactaaagggcgg	This study
	pspFn-D-R	ATGATGACCC TCGGCTATCT GGTGACCGTC CTGGCGATGA TCCGGGTCGG CGAGAAGCTG taatacgactcactatagggctcg	
<i>doc</i>	docn-D-F	TGCAGATTAT CTCAGCGGAA GAGATAATAC AGTTTCACGA CAGGCTGCTC CGCGTCACGC aattaaccctcactaaagggcgg	This study
	docn-D-R	AACATGACAT GTTCGAATTA CAGAAAAATA ACTTTTTTTA TTACAAAA taatacgactcactatagggctcg	
<i>relE</i>	relEn-D-F	GGAGTTTGAT CCACGAGCCT GGCGCGAATG GCAGAAGCCT GGCGAGACGG TCAAAAAACA aattaaccctcactaaagggcgg	This study
	relEn-D-R	CAGCAGCAAC CAGGTCGTAC ATCATTGCG ATAGCGTTTA GAGCCGTTTA TTCGCCTGAT taatacgactcactatagggctcg	

The success of the procedure, which would involve insertion of an FRT cassette into the corresponding gene-of-interest, was verified by PCR. The genomic DNA or the colony lysate from the transformants was used as template to set up reactions with primers to amplify the gene-specific deletion cassette (Table 3.3.21) or the full-length gene sequence (Table 3.3.22), according to the protocol described in section 3.2.8.6 of this document.

Table 3.3.22 Primer sequences to amplify the full-length sequences of specific genes in KpIMS38.

Gene	Primer	Sequence (5'→3')	Amplicon Size	Reference
<i>ibrA</i>	ibrA-FL-F	AGCATCGCCTGGCTGAAT	1958 bp	This study
	ibrA-FL-R	GCCTCGTCATCCAGCTTTTG		
<i>pspF</i>	pspF-FL-F	CACGATGTCGGCAAAACGA GA	1917 bp	This study
	pspF-FL-R	GAGCGATTGGCACCATGATG		
<i>doc</i>	doc-FL-F	TCATTAGTGCAGAAGAGTTT GAAC	752 bp	This study
	doc-FL-R	TCATCGGTTATCTCTTTGTT G		
<i>relE</i>	relE-FL-F	GCGAAGCGGCGTTATTAC	454 bp	This study
	relE-FL-R	CGTGCTGGTTGACGGT		

Despite repeated attempts and optimization of various parameters, mutant creation using the commercially available pRedET system or the reported pACBSR-Hyg system was unsuccessful.

3.3.8.5 Assessment of the involvement of genes in persister cell-formation through gene silencing

Owing to the failure of the lambda recombineering approaches to generate gene deletions, the CRISPR-Cas gene silencing system was employed to study the effect of silencing select genes on persistence in KpIMS38.

3.3.8.5.1 Designing of CRISPR and guide RNAs

As an alternative to gene deletion, the effect of loss-of-function of specific genes on the formation of persister cells by KpIMS38 was studied using gene silencing. The method was based on the technique developed by and outlined in Rath et al (2015), which utilises the Cascade complex, formed from the Cas protein associated with a CRISPR (Clustered

Regularly Interspaced Short Palindromic Repeat) RNA (crRNA) containing spacers specific to the gene-of interest, to bind to and prevent transcription of the gene.

For the purpose, CRISPR plasmids were constructed for the genes belonging to the toxin-antitoxin loci *rel*, *relBE* and *phd-doc* in collaboration with Dr. D. Rath, BARC, India. Multiple 19-bp long spacers were selected for each of the six genes, and each were cloned into the plasmid 148cr. The details of the spacers used for each the six genes are mentioned in table 3.3.23.

Each plasmid was transformed into KpIMS38 through electroporation. For the purpose, A single, isolated colony of KpIMS38 was grown overnight in 3 mL LB broth and 20 μ L of it used to sub-culture 1 mL of LB broth. This culture was incubated for 2 h, transferred into chilled 1.5 mL microcentrifuge tubes and centrifuged at 11,000 rpm for 30 s in a centrifuge pre-chilled at 2°C. The supernatant was decanted and the cell pellet resuspended in 1 mL chilled sterile 10% glycerol by gentle pipetting. The cell suspension was centrifuged using the above-mentioned parameters, the supernatant decanted, and washed with 10% glycerol once again. After the second wash, the supernatant was decanted leaving behind a minimal volume (\approx 50 – 100 μ L) in the tube. The cell pellet was resuspended in this supernatant and placed on ice.

One batch of the cell suspension was added 500 ng of a specific CRISPR plasmid, while the other was not and was considered as ‘Negative Control’. Both cell suspensions were transferred to individual pre-chilled 1mm electroporation cuvettes, and successively pulsed in an electroporator set to deliver a single 1350 V pulse with a 5 ms time constant. The cuvettes were immediately added 500 μ L LB medium, resuspended, and their entire contents transferred to sterile 1.5 mL tubes. The tubes were incubated for 70 mins, following which both the cultures were concentrated by centrifugation and resuspension

in a small-volume supernatant, and spread-plated onto individual LBA-Kan⁵⁰ plates. The plates were incubated overnight and colonies obtained in the transformed plates were sub-cultured onto separate LBA-Kan⁵⁰ plates.

Table 3.3.23 Spacer sequences used to target genes in KpIMS38 for transcriptional silencing[#].

Gene	Spacer	Sequence (5' → 3')	Orientation	Position	Reference
<i>relT</i>	RelT-1	AGGTACGGATGAAAATTGT	Sense	-8	This study
	RelT-2	ATAAGAGCCGCATTAAATC	Sense	+58	This study
	RelT-3	CCTCTCCCGAAAACCACTA	Sense	+133	This study
<i>relAt</i>	RelAT As-1	TGTAAGGAATGACGACATA	Antisense	+42	This study
	RelAT As-2	TTTAACCGCCACGACGTAG	Antisense	-44	This study
<i>doc</i>	Doc1	AGATAATACAGTTTCACGA	Sense	+28	This study
	DocAs -1	TCGGGCATACCGGCAACGC	Antisense	+88	This study
<i>phd</i>	Phd1	CGGTAACTATAGCGAAGC	Sense	+7	This study
	Phd2	AGAAGAGTTTGAACGCTAC	Sense	+122	This study
	Phd As-1	TGTACAAAAAAGAGCCA A	Antisense	-42	This study
<i>relE</i>	relE-1	CGGCTGGAAAACCCACGG C	Sense	-40	This study
	relE As-1	TCCAGACTCACCTTAACCC	Antisense	0	This study
	relE As-2	ATCCGGTAAATCGCTCAGC	Antisense	+146	This study
<i>relB</i>	relB-1	CATTACAAAATTCCCCTTT	Sense	-30	This study

The orientation of the spacer specifies the DNA strand it is located on – sense or antisense – while the position specifies the location of the first base (5') from translational start site of the gene. The site being considered as “0”, spacers with their first base located upstream are designated “-” (minus) while those located downstream are designated “+” (plus).

3.3.8.5.2 Confirmation of gene silencing

Silencing of gene expression was examined by evaluating the transcript levels of the genes in silenced strains vis-à-vis wild-type KpIMS38 using qPCR. Isolated colonies on LBA-

Kan⁵⁰ for each strain were streaked on MHA-Kan⁵⁰ and incubated overnight. A single, non-duplicate colony of KpIMS38 with a single gene (among the six candidates chosen) putatively silenced was used to inoculate 3 mL of MHB-Kan⁵⁰.

Following overnight incubation, the culture was subcultured in 3 mL of MHB-Kan⁵⁰ at a ratio of 1:1000 and grown at 37°C and 220 rpm for 5 hours or 8 hours when supplemented with 0.05 µg/mL tetracycline (USB, USA) as inducer for the CRISPR plasmids. The total cellular RNA was extracted from 500 µL of each culture using the RNeasy Mini Kit according to the protocol outlined in section 3.2.5 of this document, of which 1000 ng of total RNA was converted into cDNA with the iScript™ Reverse Transcription Supermix for RT-qPCR (Bio-Rad, USA) using the manufacturer’s instructions as detailed in section 3.2.7 of this document.

Table 3.3.24 Components used to perform qPCR to study gene expression in silenced strains of KpIMS38.

Sr. No.	Component	Volume per reaction
1	Nuclease-Free Water	To 10.00 µL
2	iTaq™ Universal SYBR® Green Supermix	5.00 µL
3	10 µM Forward Primer	0.25 µL
4	10 µM Reverse Primer	0.25 µL
5	Template cDNA	To 10 ng

qPCR reactions were set up wherein the expression of the silenced gene was assessed in the putative silenced strain as well as the wild-type KpIMS38. Reactions were set up according to the protocol outlined in table 3.3.24, and distributed into individual wells in a 96-well PCR plate. The reactions were incubated in a CFX96 Touch Real-Time PCR Detection System (Bio-Rad, USA) using the program outlined in table 3.3.25. The

quantification cycle (Cq) values were obtained for each of the template-gene combinations and compared to examine expression of the gene.

Table 3.3.25 qPCR conditions used to assess the gene expression in silenced strains of KpIMS38.

Stage of the cycle	Conditions
Initial Denaturation	95°C, 30 s
Cycle Denaturation	95°C, 5 s
Cycle Annealing & Extension	60°C, 30 s
Number of cycles	40
Melt curve	65 - 95°C
Ramp rate	0.5°C / 5 s

3.3.8.5.3 Functional analysis of the transformed cells

To study the effect of transcriptional silencing of select genes on persister cell formation in KpIMS38, the time-kill curves of the silencing screens were evaluated. The strains were treated with 256 µg/mL levofloxacin and their survival observed according to the procedure detailed in section 3.3.5.1 of this document.

3.3.8.6 Assessment of overexpression of toxin-antitoxin genes on persister cell-formation

Persister cell formation in KpIMS38 treated with levofloxacin was explored by generating overexpression screens for select genes, to observe the effect of gain-of-function on persister cell-formation. Four genes belonging to TA systems were selected for the purpose, namely *doc*, *phd*, *relE*, and *relB*. Additionally, the genes *ibrA* and *pspF* were also chosen for overexpression, and the vector DNA used was the plasmid pGEX-6P-1^K.

To overexpress each of the target genes, recombinant plasmids were constructed wherein the open reading frame (ORF) of a single gene was inserted into the vector by molecular

cloning. Briefly, the procedure involved synthesizing the gene sequence by PCR, treating the gene sequence as well as the plasmid vector with appropriate restriction endonucleases, purifying the linear DNA molecules, and attaching both using DNA ligase to form a single plasmid containing the gene inserted within.

3.3.8.6.1 Insert synthesis and restriction digestion

To synthesize the gene sequences, specialised 'cloning' primers were designed on the basis of sequence data obtained from the annotated genome sequence of KpIMS38. The primers were designed (Table 3.3.26) to contain sites for specific restriction enzymes upstream to the DNA-binding region as a result of which the amplified polynucleotide molecule contained the gene sequence flanked by restriction enzyme sites at both 5' and 3' ends. Genomic DNA from KpIMS38 was isolated according to the protocol described in section 3.2.1 of this document. The resultant DNA was used as the template to amplify sequences of the four genes of interest using the corresponding cloning primers and performing PCR. The PCR reaction was set up according to the protocol outlined in table 3.3.27. A single non-template control and three template reactions were set up per gene. The reactions were amplified in a thermocycler using the program outlined in table 3.3.28. The entire contents of each reaction were loaded onto a 0.8 % TAE-agarose gel (containing 0.5 µg/mL ethidium bromide) and run in 1X TAE buffer at 50 V. A 100 bp DNA Ladder was also run on the agarose gel and visualized under 302 nm (UV) light in a gel documentation system. DNA bands corresponding to each of the amplified genes were excised from the agarose gel and the DNA eluted from it according to the procedure outlined in section 3.2.3 of this document.

Table 3.3.26 Primer sequences to synthesize gene fragments from KpIMS38 for insertion into pGEX-6P-1^K by restriction-enzyme based cloning. The primers contained sites for one of EcoRI (GAATTC), BamHI (GGATCC) or XhoI (CTCGAG).

Gene	Primer	Sequence (5' → 3')	Amplicon Size	Reference
<i>ibrA</i>	ibrA-clo-F	^{GACG} gaattcCTGATGTCGTTTATTA AATATCCCTTAC	1227 bp	This study
	ibrA-clo-R	^{GCCG} ctcgagCGTCAGTTGTTGTTG CATAATATC		
<i>pspF</i>	pspF-clo-f	^{CTG} ggatccATGGCGAAATTCATC ATGGC	990 bp	This study
	pspF-clo-R	^{CCGG} gaattcCGTCACAGCTGATGC TTTTTCA		
<i>doc</i>	doc-clo-F	^{GACG} ggatccATGACGCTGCAGATT ATCTCAG	391 bp	This study
	doc-clo-R	^{GACG} ctcgagCGTCATCCACGCAAA CGCG		
<i>phd</i>	phd-clo-F	^{GACG} ggatccATGAGAACGGTTAA CTATAGCGAAG	244 bp	This study
	phd-clo-R	^{GACG} ctcgagCGTCATTTATCCGCA AGCTCCC		
<i>relE</i>	relE-clo-F	^{GACG} ggatccATGACCTATGAACTG GAGTTTGAT	307 bp	This study
	relE-clo-R	^{GACG} ctcgagCGTTAGAGCCGTTTA TTCGCCTG		
<i>relB</i>	relB-clo-F	^{GACG} ggatccATGGCCACGCTCAAT GTT	265 bp	This study
	relB-clo-R	^{GACG} ctcgagCGTCATAGGTCATCC AGACTCACC		

Uppercase letters indicate the region identical to the gene to be amplified, lowercase letters indicate the restriction-enzyme recognition sequence, and superscript letters indicate the 5' extension to the restriction site.

Table 3.3.27 Components used to perform PCR to amplify entire gene sequences using cloning primers.

Sr. No.	Component	Volume per reaction
1	Nuclease-Free Water	16.80 μ L
2	5x Green GoTaq® Flexi Buffer	6.00 μ L
3	2.5 mM dNTPs	2.00 μ L
4	25 mM MgCl ₂	1.80 μ L
5	10 μ M Forward Primer	0.60 μ L
6	10 μ M Reverse Primer	0.60 μ L
7	5 Units/ μ L GoTaq® Flexi DNA Polymerase	0.20 μ L
8	Template DNA	2.00 μ L

Table 3.3.28 Thermocycler conditions used to amplify entire gene sequences using cloning primers.

Stage of the cycle	Conditions
Initial Denaturation	94°C, 120 s
Cycle Denaturation	94°C, 30 s
Cycle Annealing	60°C, 30 s
Cycle Extension	72°C, 90 s
Final Extension	72°C, 600 s
Hold	4°C, ∞
Number of cycles	35

Restriction-digestion was set up according to the protocol detailed in table 3.3.28. The appropriate restriction enzymes were used to digest the gene sequences (insert) as well as pGEX-6P-1^K (vector). The digestion-reactions were incubated in a thermocycler at 37°C for 3 hours following which the products were run on 0.8% TAE-agarose at 60 V for 100

minutes. Regions of the gel corresponding to the digested DNA were excised and DNA extracted from the gel according to the protocol outlined in section 3.2.3 of this document.

Table 3.3.29 Protocol for digestion of DNA using type-II restriction enzymes (RE).

Sr. No.	Component	Volume per reaction
1	Nuclease-free Water	To 50 μ L
2	10X CutSmart® Buffer	5
3	10,000 units RE-1	2 μ L
4	10,000 units RE-2	2 μ L
5	DNA	500 to 1000 ng

3.3.8.6.2 Ligation and transformation into DH5 α

The digested insert and vector DNA molecules were and ligated using the Quick Ligation™ Kit (NEB, USA) using a molar ratio of 3:1 (Insert: Vector). Ligation was performed according to the manufacturer's protocol as outlined in table 3.3.30. The components were mixed together, incubated at room temperature for 15 minutes, following which they were placed on ice until further use.

Table 3.3.30 Protocol for ligation of insert and vector molecules.

Sr. No.	Component	Volume per reaction
1	Nuclease-free Water	To 20 μ L
2	2X Quick Ligase Reaction Buffer	5
3	Vector DNA	To 50 ng
4	Insert DNA	To 3x molar quantity
5	Quick Ligase	1 μ L

The ligated DNA was used to transform chemically-competent *E. coli* DH5 α cells, prepared as mentioned in section 3.3.6.2.2 of this document. An adequate amount of competent cell-suspension was thawed on ice from which, 50 μ L aliquots were transferred into chilled microcentrifuge tubes. To an aliquot of competent cells was added 10 μ L of a ligation product and the mixture allowed to incubate in ice for 30 minutes. A non-transformed control consisting of competent cells without any DNA added was also maintained. The tubes were then placed in a water bath (maintained at 42°C for precisely 90 seconds and snap-chilled in ice for 1 minute. The tubes were added 800 μ L of SOC medium containing 0.4% glucose, incubated for 50 minutes. The cultures were spread-plated onto SOB agar containing 50 μ g/mL kanamycin and incubated overnight.

The colonies that grew on the transformed plates were subcultured on LBA-Kan⁵⁰ to obtain isolated colonies. Plasmid DNA was extracted from transformants for each of the four genes according to the protocol outlined in section 3.2.2 of this document. Five hundred μ g of plasmid DNA obtained from the each of the transformants was digested using the appropriate restriction enzymes according to the protocol mentioned in table 3.3.29. The digestion products were run on a 1.2% TAE-agarose gel (containing 0.5 μ g/mL ethidium bromide) along with the corresponding undigested plasmids at 60 V for 100 mins. The gel was visualized under 302 nm (UV) light in a gel documentation system and the DNA bands in digestion products compared with that of the undigested plasmid DNA. Isolates that contained the gene-of-interest inserted within the vector were stored in the form of 40 % glycerol stocks at -80°C until further use.

3.3.8.6.3 Electroporation into KpIMS38

Plasmids containing the gene-of-interest were used to transform KpIMS38 by electroporation using the protocol described in section 3.3.6.2.5 of this document. The

colonies that grew on the transformed plates were subcultured on LBA-Kan⁵⁰ and incubated until isolated colonies appeared.

Plasmid DNA was extracted from KpIMS38 transformants individually containing the four genes according to the protocol outlined in section 3.2.2 of this document. Five hundred micrograms of plasmid DNA obtained from the each of the transformants was digested using the appropriate restriction enzymes according to the protocol mentioned in table 3.3.29. The digestion products were run on 1.2% TAE-agarose (containing 0.5 µg/mL ethidium bromide) along with the corresponding undigested plasmids at 60 V for 100 mins. The gel was visualized under 302 nm (UV) light in a gel documentation system and the DNA bands in digestion products compared with that of the undigested plasmid DNA. Isolates that contained the gene inserted within the vector were stored in the form of 40 % glycerol stocks at -80°C until further use.

Additionally, overexpression of the genes was confirmed by means of qPCR. RNA was extracted from the overexpression strains and converted into cDNA according to the procedures detailed in sections 3.2.5 and 3.2.6 respectively of this document. Using the cDNA as template and, qPCR was set up according to the protocol specified in table 3.3.16 using primers specific to the genes (mentioned in table 3.3.19). The pair of *kp4432* and *rpoB* were used as reference genes and the reactions run according to the program outlined in table 3.3.17. The ΔCq values were calculated for each of the genes according to the procedure delineated in section 3.3.8.1 and compared with those seen in wild-type KpIMS38.

3.3.8.6.4 Examination of persistence in KpIMS38 on overexpressing genes

To study the effect of overexpression of select genes on persister cell formation in KpIMS38, the time-kill curves of the silencing screens were evaluated using 256 µg/mL levofloxacin and compared to that observed for wild-type KpIMS38. For the purpose, a

single colony of a KpIMS38 with an episomal copy of a gene grown on LBA-Kan⁵⁰ was streaked on MHA-Kan⁵⁰. A single isolated colony obtained after overnight incubation of the medium was used to inoculate 3 mL of MHB-Kan⁵⁰ supplemented with 0.1 mM Isopropyl β -D-1-thiogalactopyranoside (IPTG). Following overnight incubation, the culture was subcultured in 3 mL of MHB-Kan⁵⁰, containing 0.1 mM IPTG, at a ratio of 1:1000 and grown under the same conditions for 4 hours. This culture was used to further inoculate 25 mL of MHB-Kan⁵⁰ containing 0.1 mM IPTG, contained in 100 mL conical flasks, at a ratio of 1:100. Two flasks were maintained for each culture: one containing 256 μ g/mL of levofloxacin and one containing no antibiotic. The flasks were incubated, culture aliquots were withdrawn, serially diluted and plated on MHA every 2 hours. The practice was carried out for 12 hours since the time of inoculation, all plates incubated overnight and the number of colonies obtained counted. The colony-forming units per mL for each culture in untreated and levofloxacin-treated conditions were calculated and represented as a function of time.

Chapter-4
Results & Discussion

4.1 Detection and characterization of persister cells in *K. pneumoniae*

4.1.1 Background of the study

The predicament posed by drug resistance is compounded by persistence, a phenomenon whose severity and impact on the development of resistance as well as the progression of infections are being understood only recently (Gollan et al, 2019). Bacteria have been reported to form persister cells in response to a variety of stresses, some of which include entry into the stationary phase of growth (Spoering and Lewis, 2001), treatment with antibiotics (Goneau et al, 2014). This section deals with the identification of a clinical isolate of *K. pneumoniae* that forms persister cells. It also reports the results of the characterization of the persister cells using microbiological assays, flow cytometry and live-cell microscopic analyses.

4.1.2 Detection of persister-cell formation in clinical isolates of *K. pneumoniae*

4.1.2.1 Confirmation of the clinical isolates using differential growth media

The cultures of *K. pneumoniae* used in the present study are from the laboratory culture-collection. The three strains viz. KpIMS32, -34 and -38 were obtained from a tertiary-care centre in Bhubaneswar, Odisha, India. The isolates were obtained as pure cultures, and were originally isolated from patient samples collected from different anatomical sites at the tertiary-care centre. Culture-sensitivity (C/S) reports were also provided along with the isolates. The identity of the isolates was further confirmed using selective and differential media, the results of which are outlined in Table 4.1.1.

Table 4.1.1 Details of the clinical isolates used in this study. EMB – Eosin-Methylene Blue Agar; MaC – MacConkey Agar.

Strain Code	Organism	Specimen	Culture characteristics	
			EMB	MaC
KpIMS32	<i>Klebsiella pneumoniae</i>	Anal Swab	Blue-black colonies	Pink colonies
KpIMS34	<i>Klebsiella pneumoniae</i>	Tracheal aspirate	Blue-black colonies	Pink colonies
KpIMS38	<i>Klebsiella pneumoniae</i>	Pus	Blue-black colonies	Pink colonies

4.1.1.2 Determination of the antibiotic-sensitivity profile of clinical isolates of *K. pneumoniae*

The antibiotic sensitivity-profile of the isolates was determined using the Kirby-Bauer method (Bauer et al, 1966). The response of each of the isolates to 24 different antibiotics was observed, the results for which are compiled in Table 4.1.2. In addition, the strain *E. coli* ATCC 25922 was also used as a control for the assay.

All three clinical isolates were resistant to aminopenicillins (ampicillin), monobactams (aztreonam), and combinations of beta-lactam and beta-lactamase inhibitors (ampicillin-sulbactam, ceftazidime-clavulanic acid, ticarcillin-clavulanic acid). The *K. pneumoniae*

isolates showed sensitivity to the aminoglycosides tested (amikacin, gentamicin), with only KpIMS38 exhibiting resistance to gentamicin. Isolate KpIMS34 was distinct in being resistant to 21 of the 24 antibiotics tested. On the other hand, KpIMS32 was susceptible to 18 of the 24 antibiotics tested. Interestingly, the isolate exhibited susceptibility to all the cephalosporins tested, but was resistant to the ceftazidime-clavulanic acid combination. The control *E. coli* ATCC 25922 was susceptible to all the antibiotics tested. The sensitivity of KpIMS38 lay in between that for the other isolates, exhibiting resistance to 14 antibiotics and intermediate-sensitivity to one antibiotic. The uniqueness of the sensitivity-pattern of KpIMS38 was in its response to the aminoglycosides and carbapenems tested, exhibiting resistance to one member-antibiotic and susceptibility to the other for each of classes.

According to the classification scheme elucidated in Magiorakos et al (2012) any isolate resistant to one or more antibiotics in three or more categories is considered as Multi-Drug Resistant (MDR), whereas an isolate resistant to one or more antibiotics in all but fewer than 2 antibiotic categories is categorized as Extensively Drug Resistant (XDR). Taking into consideration the above and the antibiotic-sensitivity profile obtained herewith, the isolate KpIMS32 were identified as MDR while the isolates KpIMS34 and KpIMS38 were identified as XDR.

The Multiple Antibiotic Resistance (MAR) index of the isolates was also examined as proposed by Krumperman (1983). Here, the ratio of the number of antibiotics resistant to (a) against the number of antibiotics tested against (b) serves to indicate the degree of resistance within each isolate tested, using the formula

$$\text{MAR index} = \frac{a}{b}$$

The MAR indices of the four isolates were compiled in Table 4.1.3 and show a high MAR index exhibited by all three *K. pneumoniae* isolates tested.

Table 4.1.2: Antibiotic-susceptibility patterns for the isolates KpIMS38 and *E. coli* ATCC 25922 as tested using the Kirby-Bauer Test.

Drug	Potency	Kp32	Kp34	Kp38	25922	Drug	Potency	Kp32	Kp34	Kp38	25922
AK	30	S	S	S	S	CTR	30	S	R	R	S
AMC	30	R	R	R	S	CXM	30	S	R	R	S
AMP	10	R	R	R	S	CIP	5	S	R	S	S
A/S	10/10	R	R	S	S	COT	25	S	R	S	S
AT	75	R	R	R	S	GAT	5	S	R	S	S
CPM	30	S	R	I	S	GEN	10	S	S	R	S
CPZ	75	S	R	R	S	IPM	10	S	I	R	S
CTX	30	S	R	R	S	LE	5	S	R	S	S
CX	30	S	R	S	S	MRP	10	S	R	S	S
CAZ	30	S	R	R	S	OF	5	S	R	S	S
CAC	30/10	R	R	R	S	PIT	100/10	S	R	R	S
CZX	30	S	R	R	S	TCC	75/10	R	R	R	S

Note: Kp38 – KpIMS38; 25922 – *E. coli* ATCC 25922; AK – Amikacin; AMC – Amoxicillin-Clavulanic Acid; AMP – Ampicillin; A/S – Ampicillin-Sulbactam; AT – Aztreonam; CPM – Cefepime; CPZ – Cefoperazone; CTX – Cefotaxime; CX – Cefoxitin; CAZ – Ceftazidime; CAC – Ceftazidime-Clavulanic Acid; CZX – Ceftizoxime; CTR – Ceftriaxone; CXM – Cefuroxime; CIP – Ciprofloxacin; COT – Cotrimoxazole; GAT – Gatifloxacin; GEN – Gentamycin; IMP – Imipenem; LE – Levofloxacin; MRP – Meropenem; OF – Ofloxacin; PIT – Piperacillin-Tazobactam; TCC – Ticarcillin-Clavulanic Acid; Potency of each drug is stated in micrograms (μg).

Table 4.1.3 Multiple antibiotic resistance (MAR) indices of the clinical isolates of *Klebsiella pneumoniae* used in the study.

Sr. No.	Isolate	Antibiotics resistant to / Antibiotics tested for	MAR index
1	KpIMS32	6/24	0.25
2	KpIMS34	21/24	0.88
3	KpIMS38	14/24	0.58
4	<i>E coli</i> ATCC 25922	0/24	0

Based on these results, the minimum inhibitory concentration (MIC) of antibiotics belonging to three different classes, i.e., amikacin, levofloxacin and meropenem, was determined for KpIMS32 and -38. The rationale for choosing antibiotics from the aforementioned classes was to identify the MIC for antibiotics the isolates were sensitive to since persistent isolates do not exhibit resistance. KpIMS34 showed extensive resistance to members all three antibiotic-classes and was hence excluded from further investigation. The two-fold serial dilution method was used to carry out this experiment and the MIC values obtained for each antibiotic for both isolates of *K. pneumoniae*. As per the standard cutoff values specified in the CLSI guidelines (CLSI, 2017), both isolates were susceptible to the aminoglycoside and carbapenem antibiotics tested but were resistant to levofloxacin (Table 4.1.4).

Table 4.1.4 MIC of antibiotics from different classes against *K. pneumoniae* isolates used in the study as determined by the two-fold serial dilution method.

Antibiotics	MIC for KpIMS32 (µg/mL)	MIC for KpIMS38 (µg/mL)
Amikacin	0.5	2
Levofloxacin	4	16
Meropenem	<0.06	0.06

The capability of the isolates to produce metallo-β-lactamases (MBL) was assessed through the EzyMIC™ strip method. MBL production was phenotypically examined by comparing

the size of the zone-of-inhibition of an isolate for a carbapenem against the zone-of-inhibition of the carbapenem with EDTA. The concentration at which the zone intersected the strip was considered the MIC, and the ratio of the MIC of carbapenem and carbapenem with EDTA was calculated. EzyMIC™ strips containing imipenem (IPM) and meropenem (MRP) were used for the assay and the MIC values obtained are presented in Table 4.1.5.

Table 4.1.5 Determination of metallo-β-lactamase (MBL) production among the isolates of *K. pneumoniae* used in the study. Enzyme production was assessed using EzyMIC™ strips constituted with imipenem (IPM) or meropenem (MRP) alone as well as with the metallo-β-lactamase inhibitor EDTA. A ratio of the MIC (μg/mL) obtained for each condition for both the antibiotics was represented.

Isolate	MIC (IPM)	MIC (IPM + EDTA)	Ratio	MIC (MRP)	MIC (MRP + EDTA)	Ratio
KpIMS32	4	6	0.67	3	6	0.5
KpIMS38	4	6	0.67	3	6	0.5

Based on the interpretive criteria supplied by the manufacturer, a carbapenem : carbapenem + EDTA ratio of eight or above is indicative of MBL production, while a ratio lower than that number indicates no production of MBLs. Through the results mentioned in table 4.1.5, the isolates KpIMS32 and KpIMS38 were phenotypically MBL-nonproducers.

The Ezy MIC™ strip was also used to determine the MIC of amikacin, levofloxacin and meropenem for the isolates. This was performed since, for reasons unknown, the results of the disc-diffusion and two-fold broth dilution tests for the antibiotic levofloxacin were contradictory. In addition, *E. coli* ATCC 25922 was used as a control. The inhibitory concentrations observed for all the isolates are presented in Table 4.1.6. Both the *K. pneumoniae* isolates were sensitive to all the three antibiotics tested using the EzyMIC™ strip method. The concentrations obtained were similar to those observed using the two-fold broth dilution assay for amikacin and meropenem. The MIC of levofloxacin obtained using

the two-fold broth dilution assay was 16 and 32 times higher than that observed with the EzyMIC™ strip method for KpIMS32 and -38. The sensitivity of the control strain towards the three antibiotics lay in the susceptible range.

Table 4.1.6 Minimum inhibitory concentration (MIC) of amikacin, levofloxacin and meropenem determined using EzyMIC™ strips. The MIC of KpIMS32 and -38, as well as *E. coli* ATCC 25922, were determined by Etest using EzyMIC™ strips for the three antibiotics.

Antibiotic	MIC as determined by EzyMIC™ strips (µg/mL)		
	KpIMS32	KpIMS38	<i>E. coli</i> ATCC 25922
Amikacin	0.38	1.5	0.75
Levofloxacin	0.25	0.5	0.03
Meropenem	0.032	0.064	0.032

4.1.3 Screening for quinolone resistance in KpIMS38

The data from MIC assays indicated KpIMS38 as sensitive to levofloxacin, a third-generation fluoroquinolone antibiotic. To investigate whether this sensitivity extended to other quinolone antibiotics, the presence of quinolone-resistance determinants in the *K. pneumoniae* isolate.

4.1.3.1 Screening for plasmid-mediated quinolone resistance

Quinolone resistance is known to be horizontally transmitted through the plasmid-borne *qnr* genes (*qnrA* and *qnrB*). To screen for their presence in KpIMS38, plasmid DNA was extracted from the isolate and used to perform PCR using primers for *qnrA* and *qnrB* (Table 3.3.1). No amplicons were obtained for both the *qnr* genes in KpIMS38. This indicated the absence of plasmid-mediated quinolone resistance genes and substantiated the observations from phenotypic assays as specified in section 4.1.1.2 of this document.

4.1.3.2 Screening for mutations in the quinolone resistance-determining region (QRDR) in the *gyrA* gene

Mutations in the Serine-83 and Aspartate/Glutamate-87 residues in the DNA gyrase A gene (*gyrA*) weaken the binding of quinolone compounds to the bacterial DNA gyrase. One or both mutations can confer resistance to quinolone antibiotics. The presence of these mutations at both 83 and 87 positions in *gyrA* was assessed by amplifying the entire gene and sequencing it. The sequence obtained was compared with the sequences of a) *K. pneumoniae* ATCC 13883, a type strain susceptible to fluoroquinolones, b) *K. pneumoniae* ATCC 700603, a multi-drug resistant strain susceptible to fluoroquinolones, and c) *K. pneumoniae* ssp. *pneumoniae* HS11286, a multi-drug resistant strain resistant to fluoroquinolones, retrieved from GenBank from the accession numbers KN046818.1, NZ_AOGO00000000.1 and CP003200.1 respectively.

Kp_HS11286	71	G DV I G K Y H P H G I I A V Y D T I V R M A Q P F S L R Y M L V D G Q G N F G S I D G D S A A A M R Y T E I R L A K I A H E L M A D L E K
Kp_13883	71	G DV I G K Y H P H G D S A V Y D T I V R M A Q P F S L R Y M L V D G Q G N F G S I D G D S A A A M R Y T E I R L A K I A H E L M A D L E K
KpIMS38	52	G DV I G K Y H P H G I Y A V Y D T I V R M A Q P F S L R Y M L V D G Q G N F G S I D G D S A A A M R Y T E I R L A K I A H E L M A D L E K
Kp_700603	71	G DV I G K Y H P H G D S A V Y D T I V R M A Q P F S L R Y M L V D G Q G N F G S I D G D S A A A M R Y T E I R L A K I A H E L M A D L E K

The DNA sequences of the *gyrA* genes were aligned using the Clustal W algorithm on MEGA7, and the aligned sequences converted into amino acids, so as to maintain the reading frame. The output was visualized using BoxShade (Duvaud et al, 2021). As depicted in figure 4.1.1, the strains sensitive to fluoroquinolones contained Serine at the amino acid position 83, whereas the resistant strain (*K. pneumoniae* ssp. *pneumoniae* HS11286) possessed Isoleucine at the same position. KpIMS38 was seen to possess Tyrosine at the 83rd position, which is a polar amino acid with a hydroxyl side chain. There was no change at position 87 in *gyrA* for either of the four strains tested. These observations corroborated the phenotypic data that indicated sensitivity to levofloxacin.

The hallmark of bacterial persisters is a biphasic killing curve on exposure to a lethal stress such as an antibiotic. Consequently, further studies were focused on examining this feature in KpIMS38.

4.1.4 Characterization of persister cells formed by KpIMS38 on exposure to levofloxacin

The hallmark of a strain forming persister cells is biphasic killing upon treatment with an antibiotic at a lethal concentration. Hence, the investigation commenced with the assessment of whether the isolates KpIMS32 and -38 formed persister cells in response to the antimicrobial compounds.

4.1.4.1 Biphasic killing assay of *Klebsiella pneumoniae* in response to treatment with antibiotics

Cultures of KpIMS32 and KpIMS38 were exposed to amikacin, levofloxacin and meropenem at concentrations four times their MIC, and their survival measured through counting the viable cells as a function of time. The concentrations used are stated in table 4.1.7. The choice of using supra-inhibitory concentrations of the antibiotic was influenced by findings that indicated a condition of growth-inhibition to be insufficient for inducing persistence (Fung et al, 2010).

Table 4.1.7 Concentrations of antibiotics used to perform the biphasic killing assay on the clinical isolates of *K. pneumoniae*.

Antibiotics	Concentration used ($\mu\text{g}/\text{mL}$)	
	KpIMS32	KpIMS38
Amikacin	2	8
Levofloxacin	16	64
Meropenem	0.25	0.25

Cultures of KpIMS32 exposed to either of the three antibiotics died within 2 hours of exposure, with no survivors obtained thereon (Figure 4.1.2). The same was observed in KpIMS38 treated with Amikacin and Meropenem, with no survivors obtained the second hour onwards. On exposure to levofloxacin however, the cell number of KpIMS38 was reduced by 2 orders of magnitude in the second hour post-antibiotic exposure (Table 4.1.8).

The cell number remained constant for a period of 12 hours, indicating persister cell formation on treatment of KpIMS38 with levofloxacin.

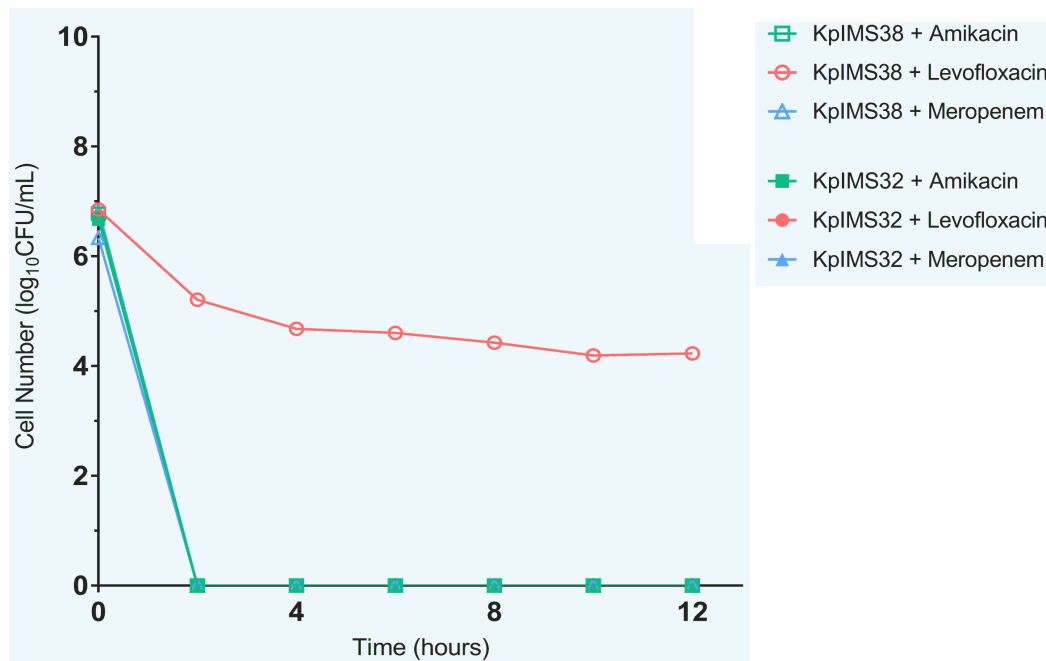
Table 4.1.8 Survival of *K. pneumoniae* isolates on treatment with three different antibiotics at suprainhibitory concentrations. Cell numbers of KpIMS38 treated with amikacin (6.25 µg/mL), levofloxacin (64 µg/mL) or meropenem (0.25 µg/mL) were plotted as a function of time (hours). The cell numbers are reported as log₁₀CFU/mL and represented as averages of biological triplicates (Av) with the standard deviation (SD).

Time (hours)	Cell Number (log ₁₀ CFU/mL; Av. ± SD)					
	Amikacin		Levofloxacin		Meropenem	
	KpIMS32	KpIMS38	KpIMS32	KpIMS38	KpIMS32	KpIMS38
0	6.68 ± 0.09	6.78 ± 0.05	6.73 ± 0.08	6.85 ± 0.05	6.86 ± 0.03	6.33 ± 0.08
2	0.00 ± 0.00	0.00 ± 0.00	0.00 ± 0.00	5.21 ± 0.04	0.00 ± 0.00	0.00 ± 0.00
4	0.00 ± 0.00	0.00 ± 0.00	0.00 ± 0.00	4.68 ± 0.07	0.00 ± 0.00	0.00 ± 0.00
6	0.00 ± 0.00	0.00 ± 0.00	0.00 ± 0.00	4.61 ± 0.05	0.00 ± 0.00	0.00 ± 0.00
8	0.00 ± 0.00	0.00 ± 0.00	0.00 ± 0.00	4.43 ± 0.01	0.00 ± 0.00	0.00 ± 0.00
10	0.00 ± 0.00	0.00 ± 0.00	0.00 ± 0.00	4.19 ± 0.06	0.00 ± 0.00	0.00 ± 0.00
12	0.00 ± 0.00	0.00 ± 0.00	0.00 ± 0.00	4.23 ± 0.05	0.00 ± 0.00	0.00 ± 0.00

4.1.4.2 Effect of different concentrations of levofloxacin on persister cell formation

The survival of KpIMS38 was assessed in different concentrations of levofloxacin to examine whether biphasic killing was recapitulated at inhibitory concentrations as well as sub- and supra-inhibitory concentrations of the antibiotic. The cell numbers were represented as a function of time for each of the concentrations used (Figure 4.1.3). Biphasic killing was observed at all concentrations of levofloxacin used, including at sub-MIC and supra-MIC levels (Table 4.1.9). Biphasic killing was most prominent at the sub-inhibitory concentration of 8 µg/mL, with the cell numbers being reduced by almost four orders of magnitude. In comparison, higher concentrations of levofloxacin resulted in a reduction of the cell number

by three orders of magnitude. An increase in the number of persister cells with an increase in the concentration of levofloxacin was observed. While this applied to cultures treated with 512 µg/mL of levofloxacin too, a reduction in cell number was observed after the sixth hour, reducing the cell density at 12 hours by ≈ 4 (3.70) orders of magnitude as compared to the initial cell number.



4.1.4.3 Effect of age of the inoculum on persister cell formation in KpIMS38

The association between the age of the inoculum and persister cell formation in KpIMS38 treated with levofloxacin was assayed through the biphasic killing assay. The growth curve for KpIMS38 was determined through the viable count and turbidimetric measurement methods. Based on the curve obtained from the OD₆₀₀ vs time plot (Figure 4.1.4, Table 4.1.10), the early log, mid-log and stationary phases of growth were identified as corresponding to cultures 4 hours, 6 hours and 8 hours post-inoculation respectively. Cultures of these three ages were used to carry out further experimentation.

Table 4.1.9 Survival of KpIMS38 on treatment with different concentrations of levofloxacin. Cell numbers derived at each time-point for the culture grown in 8, 16, 32, 128, 256 and 512 $\mu\text{g/mL}$ of levofloxacin were plotted against time (hours). The cell numbers are reported as $\log_{10}\text{CFU/mL}$ and represented as averages of biological triplicates (Av) with the standard deviation (SD).

Concentr ration	8 $\mu\text{g/mL}$	16 $\mu\text{g/mL}$	32 $\mu\text{g/mL}$	128 $\mu\text{g/mL}$	256 $\mu\text{g/mL}$	512 $\mu\text{g/mL}$
Time (hours)	Cell Number ($\log_{10}\text{CFU/mL}$; Av \pm SD)					
0	6.74 \pm 0.18	7.25 \pm 0.06	7.05 \pm 0.15	7.18 \pm 0.07	7.17 \pm 0.21	7.15 \pm 0.15
2	3.53 \pm 0.00	4.20 \pm 0.02	4.54 \pm 0.16	4.85 \pm 0.06	5.31 \pm 0.04	6.02 \pm 0.04
4	3.13 \pm 0.13	4.23 \pm 0.00	4.75 \pm 0.05	4.85 \pm 0.06	5.12 \pm 0.05	5.76 \pm 0.03
6	3.00 \pm 0.00	4.23 \pm 0.03	4.60 \pm 0.00	4.68 \pm 0.02	5.03 \pm 0.03	5.64 \pm 0.04
8	3.12 \pm 0.22	4.21 \pm 0.02	4.51 \pm 0.01	4.59 \pm 0.09	4.63 \pm 0.15	4.78 \pm 0.08
10	2.90 \pm 0.30	4.20 \pm 0.02	4.29 \pm 0.06	4.46 \pm 0.05	4.40 \pm 0.02	4.02 \pm 0.12
12	2.75 \pm 0.15	4.02 \pm 0.07	4.27 \pm 0.02	3.93 \pm 0.15	4.40 \pm 0.02	3.45 \pm 0.15

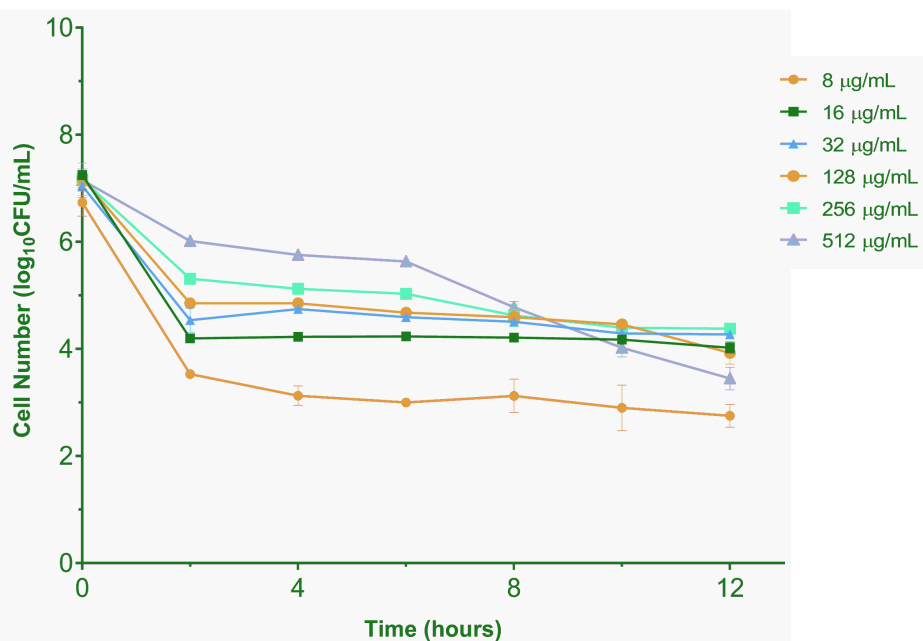
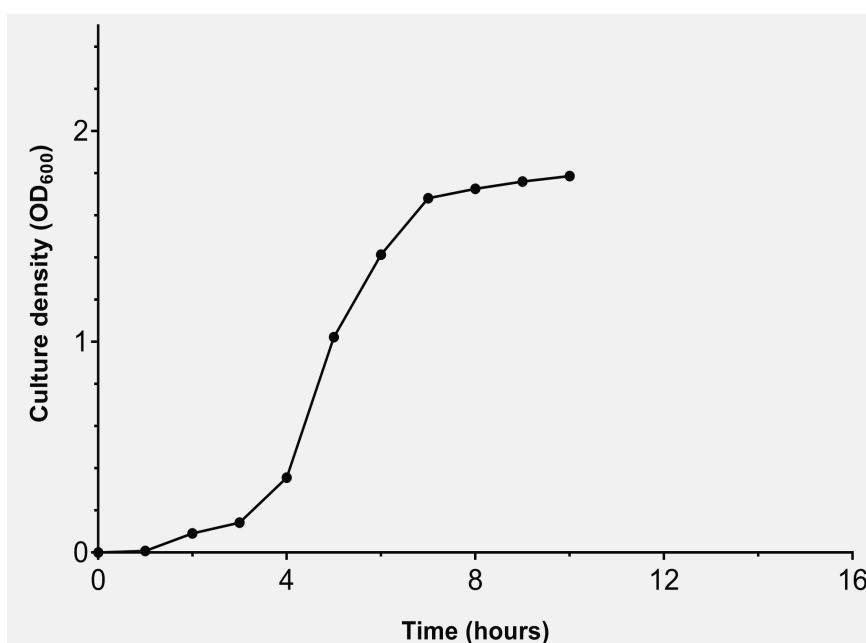


Table 4.1.10 Growth curve of a batch culture of KpIMS38 grown in MH broth. The culture density, given as the optical density measured at 600 nm, was plotted as a function of time.

Time (hours)	Culture density (OD ₆₀₀)	Time (hours)	Culture density (OD ₆₀₀)
0	0.001	6	1.414
1	0.008	7	1.682
2	0.091	8	1.727
3	0.142	9	1.761
4	0.356	10	1.787
5	1.022		



Cultures of each age were used to inoculate medium containing levofloxacin and the cell number measured as a function of time. The number of survivors was much greater in the culture inoculated with stationary phase cells, while the early log phase culture yielded the lowest number of survivors (Figure 4.1.5). Biphasic killing, i.e., an initial quick drop in cell numbers followed by a much slower reduction, was prominently visible in both the early-log

phase and mid-log phase cultures-generated cultures (Table 4.1.11). This trend was missing from the culture seeded with stationary phase cells, where the cell numbers declined steadily from the time of inoculation till 12 hours after exposure to levofloxacin.

4.1.4.4 Effect of the size of the inoculum on persister cell formation in KpIMS38

Persister-cell formation in KpIMS38 in response to levofloxacin was assayed across three different sizes of inocula. The inoculum volume was chosen as a ratio of the volume of the medium being used in the experiment, and consequently culture-to-medium ratios of 1:1000, 1:100 and 1:25 were chosen. The bacterial cell number was plotted against time for each of the three conditions. Biphasic killing was observed for all the three inoculum-sizes (Figure 4.1.6). The number of persister cells formed in the smallest of the inocula, i.e., 1:1000 was the least among the others, and logic would dictate the deficit to be a consequence of the reduced initial inoculum (Table 4.1.12). Also observed was a greater reduction in the cell-number with respect to the initial inoculum, with a 3-fold reduction in the 1:1000 condition as compared to the 1:100 and 1:25 conditions where the cell numbers reduced by 1.9-fold.

4.1.4.5 Studying persister cell formation by KpIMS38 across successive generations

Persistence as a trait is not selectively enriched in its future generations unlike antibiotic resistance. Therefore, persister cells when revived to a normally-metabolizing non-persister state and successively subjected to the persister-producing conditions should technically not result in a heightened number of persister cells.

Table 4.1.11 Effect of the age of the inoculum on persister cell formation in KpIMS38 treated with levofloxacin. Cell numbers obtained from cultures of KpIMS38 inoculated with early log-, mid-log- and stationary phase- cultures, corresponding to 4, 6 and 10 hour-old cultures respectively, were plotted as a function of time (hours). The cell numbers were represented as the average \log_{10} CFU/mL of biological triplicates (Av) with the standard deviation (SD).

Time (hours)	Cell Number (\log_{10} CFU/mL; Av \pm SD)		
	Early log	Mid-log	Stationary
0	7.34 \pm 0.05	7.73 \pm 0.18	7.84 \pm 0.23
2	5.71 \pm 0.02	6.50 \pm 0.01	7.98 \pm 0.06
4	5.63 \pm 0.06	6.46 \pm 0.00	7.61 \pm 0.04
6	5.64 \pm 0.01	6.46 \pm 0.04	7.65 \pm 0.07
8	5.46 \pm 0.09	6.32 \pm 0.08	7.23 \pm 0.04
10	5.04 \pm 0.02	6.36 \pm 0.04	7.18 \pm 0.15
12	5.20 \pm 0.07	6.14 \pm 0.10	6.94 \pm 0.09

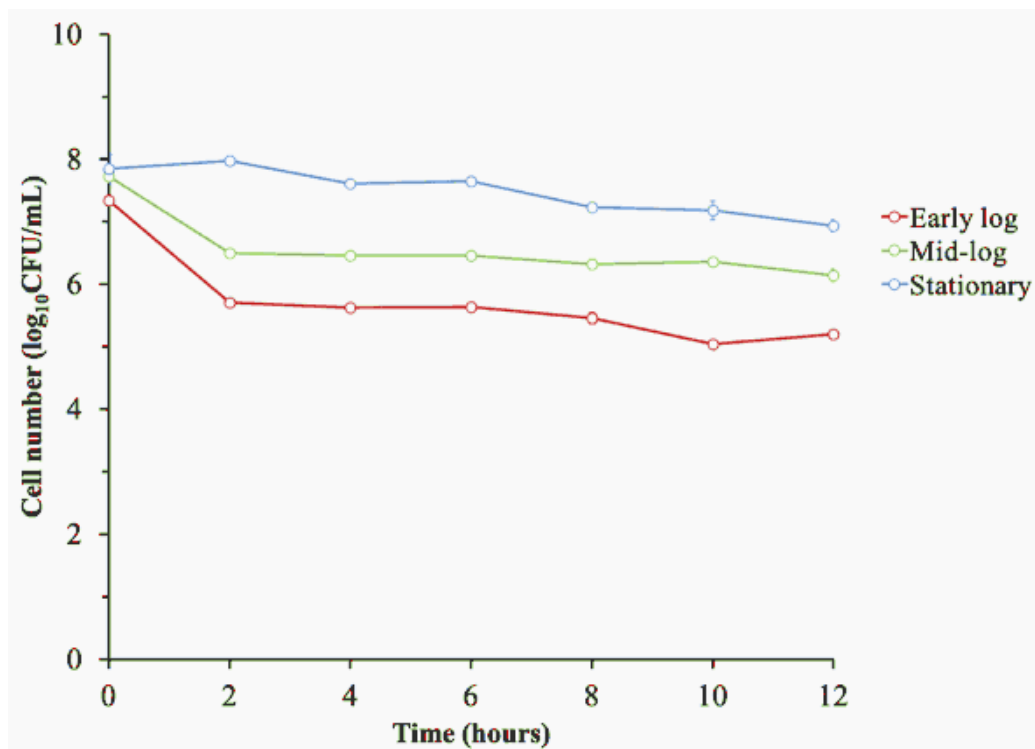
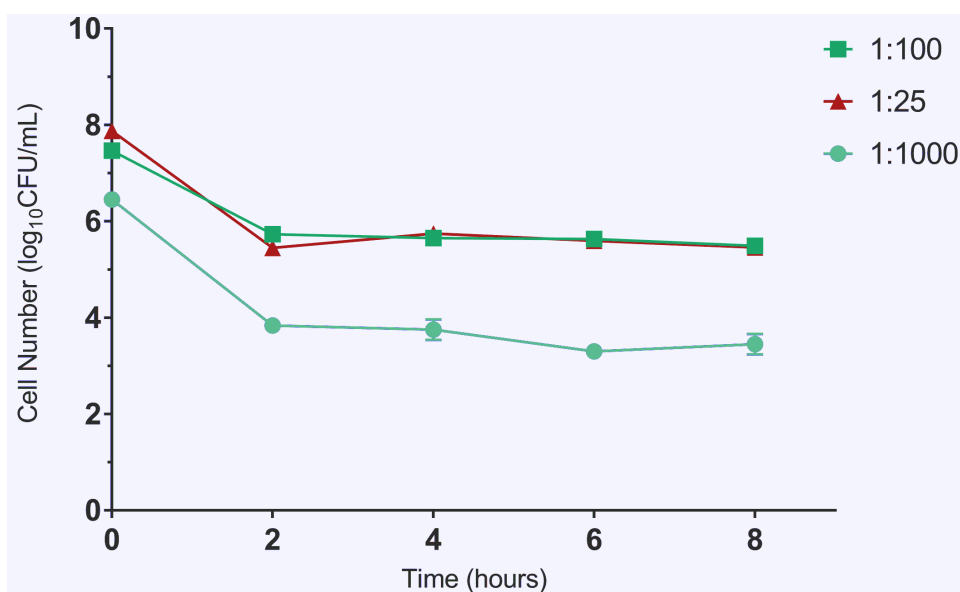


Table 4.1.12 Effect of the size of the inoculum on persister cell formation in KpIMS38 treated with levofloxacin. Cell numbers obtained from cultures of KpIMS38 raised with inocula of 25 μ L (1:1000), 250 μ L (1:100) and 1 mL (1:25), were plotted as a function of time (hours). The cell numbers were represented as the average \log_{10} CFU/mL of biological triplicates (Av) with the standard deviation (SD).

Time (hours)	Cell Number (\log_{10} CFU/mL; Av \pm SD)		
	1:25	1:100	1:1000
0	7.46 \pm 0.13	7.47 \pm 0.20	6.46 \pm 0.08
2	5.73 \pm 0.03	5.73 \pm 0.04	3.84 \pm 0.06
4	5.65 \pm 0.02	5.65 \pm 0.06	3.75 \pm 0.15
6	5.64 \pm 0.00	5.64 \pm 0.02	3.30 \pm 0.00
8	5.49 \pm 0.03	5.49 \pm 0.08	3.45 \pm 0.15



To investigate this hypothesis, persister cells formed by KpIMS38 on treatment with levofloxacin were revived in antibiotic-free medium and the resultant culture used to inoculate medium containing levofloxacin. Through three such rounds of revival and re-exposure, the cell survival was monitored. The result was biphasic killing recapitulated across all successive exposures to levofloxacin (Table 4.1.13), with a rapid reduction in cell numbers followed by a much slower decline for the duration of antibiotic-treatment. This indicated no antibiotic-resistant mutants were formed. A marginal increase in the number of persister cells (from 4.76 to 5.32 orders of magnitude) was observed on the second day (Day 2), i.e., after one round of revival and re-exposure (Figure 4.1.7). This number was seen to gradually reduce with successive re-exposures, going down by an order of magnitude each time.

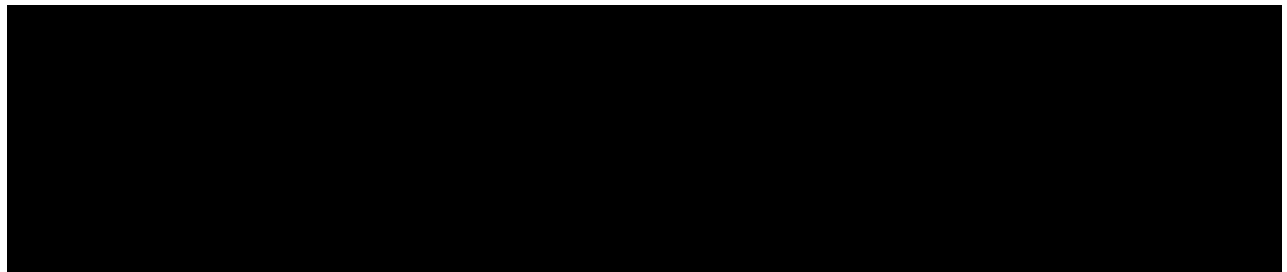
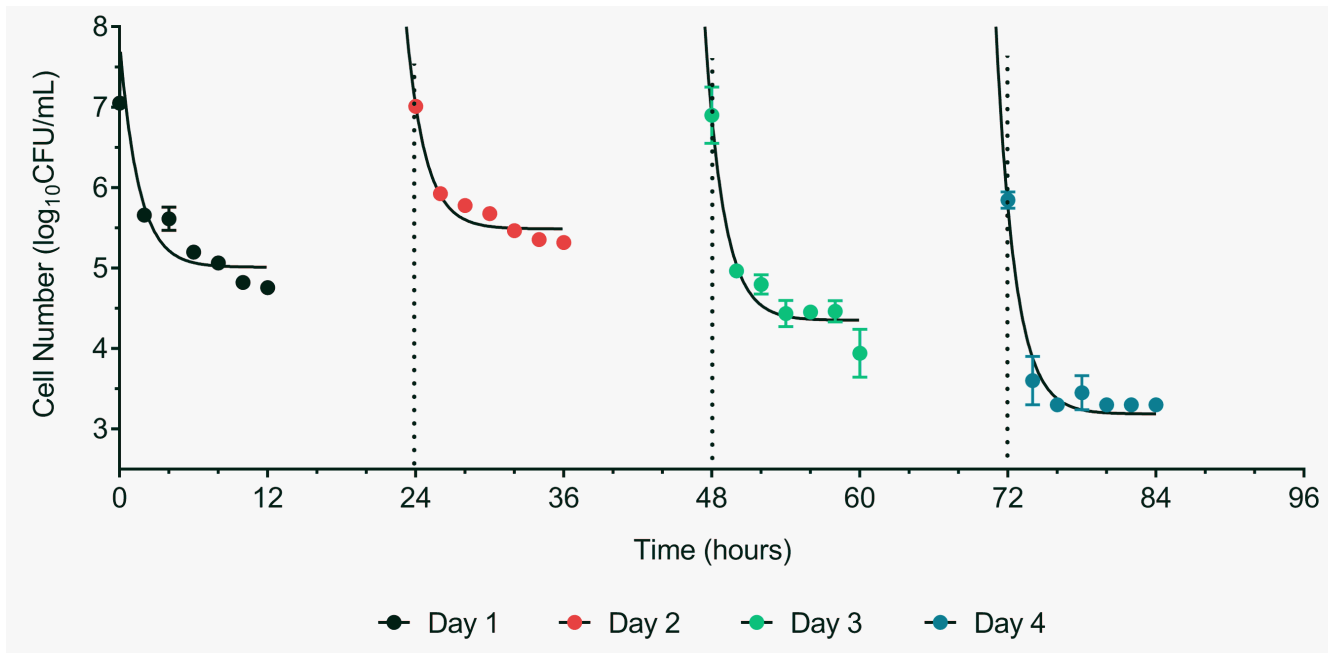
Table 4.1.13 Survival of levofloxacin treatment by successive generations of KpIMS38.

KpIMS38 was subjected to a cyclic regimen consisting of exposure to 256 µg/mL levofloxacin followed by growth in drug-free medium for four successive cycles, named day 1 to day 4. Cell numbers obtained from cultures exposed to levofloxacin for each cycle were plotted as a function of time (hours). The cell numbers were represented as the average \log_{10} CFU/mL of biological triplicates (A_v) with the standard deviation (SD).

Time (hours)	Cell Number (\log_{10} CFU/mL; $A_v \pm SD$)			
	Day 1	Day 2	Day 3	Day 4
0	7.05 ± 0.03	7.01 ± 0.04	6.90 ± 0.28	5.85 ± 0.08
2	5.66 ± 0.05	5.93 ± 0.01	4.97 ± 0.05	3.60 ± 0.25
4	5.61 ± 0.12	5.78 ± 0.04	4.80 ± 0.10	3.30 ± 0.04
6	5.20 ± 0.02	5.68 ± 0.04	4.44 ± 0.13	3.45 ± 0.15
8	5.06 ± 0.02	5.47 ± 0.03	4.45 ± 0.05	3.30 ± 0.00
10	4.82 ± 0.07	5.36 ± 0.03	4.46 ± 0.11	3.30 ± 0.00
12	4.76 ± 0.06	5.32 ± 0.04	3.94 ± 0.24	3.30 ± 0.00

A reduction in the cell number during the latter half of the experiment could be attributed to a loss of fitness of the culture, which in turn could be indicative of a slow growth phenotype

being exhibited by the cells on Day 3 and 4. Evidence for the same can be observed in the density of the culture used as inoculum on each of the days. The OD₆₀₀ of the culture revived from Day 1 cells was 2.16 Abs – greater than that of the culture used on the first day by 0.7 Abs units. The density dropped to 1.33 Abs on Day 3 which was 0.2 times lower than that of the Day 1-culture and fell even further to 0.14 Abs on Day 4.



4.1.4.6 Studying cross-tolerance of persister cells of KpIMS38 to different antibiotics

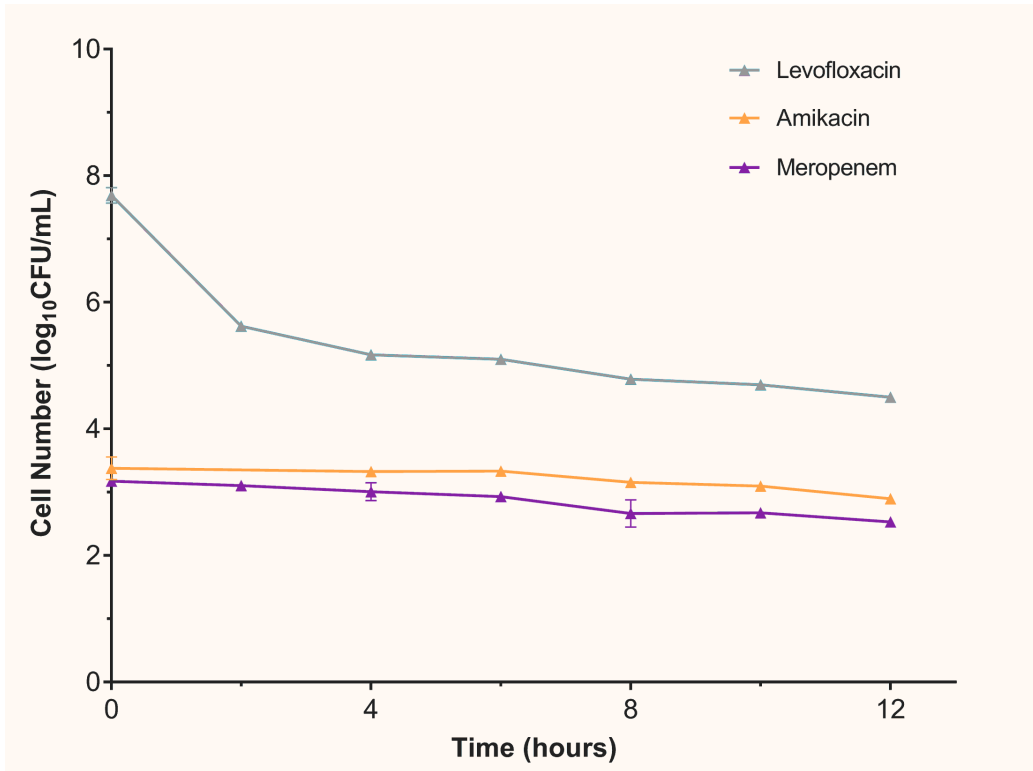
Bacterial persistence is characterized by a ceasure of metabolic processes, eventually culminating in a lack of cell division. This should reduce the available targets for various classes of antibacterial compounds and, in general, confer tolerance to them. To put this to the test, we exposed KpIMS38 to levofloxacin, and treated the resultant persister cells with amikacin and meropenem at concentrations four times their MIC. The levofloxacin-treated cells were able to survive exposure to the antibiotics at concentrations higher than their MIC

without cell death (Figure 4.1.8). It should be noted that the culture of non-persister cells exposed to the same concentration of these drugs rapidly died off and were undetectable even two hours after inoculation, as seen in figure 4.1.2. The cell numbers reduced by only 0.5 orders of magnitude after 12 hours of being incubated with the antibiotics (Table 4.1.14).

Table 4.1.14 Cross-tolerance of levofloxacin-induced KpIMS38 persisters to amikacin and meropenem. Cultures treated with 256 µg/mL levofloxacin were exposed to 8 µg/mL amikacin or 0.25 µg/mL meropenem, and the cell numbers for each of the three treatments were plotted as a function of time (hours). The cell numbers were represented as the average log₁₀CFU/mL of biological triplicates (Av) with the standard deviation (SD).

Time (hours)	Cell Number (log ₁₀ CFU/mL; Av ± SD)		
	Early log	Mid-log	Stationary
0	7.69 ± 0.09	3.38 ± 0.13	3.18 ± 0.03
2	5.63 ± 0.00	-	3.11 ± 0.04
4	5.17 ± 0.00	3.33 ± 0.05	3.01 ± 0.12
6	5.10 ± 0.05	3.33 ± 0.02	2.93 ± 0.05
8	4.79 ± 0.01	3.16 ± 0.02	2.67 ± 0.18
10	4.70 ± 0.02	3.10 ± 0.00	2.68 ± 0.02
12	4.50 ± 0.05	2.90 ± 0.01	2.53 ± 0.04

This ability of KpIMS38 persisters to tolerate lethal concentrations of amikacin and meropenem was further investigated to determine whether the same was a consequence of acquired mutations that impart resistance to the drugs. To carry out the same, the survival of KpIMS38 persisters in various concentrations of amikacin and meropenem was measured. The same was also performed using normally-growing KpIMS38 cultures that were not exposed to levofloxacin (non-persister) and the results of both compared. The MICs of amikacin and meropenem – considered as the lowest concentrations of the antibiotics at which bacterial growth was absent – were 2 and 0.25 µg/mL respectively for both persister and non-persister cultures of KpIMS38.



The cultures were subsequently inoculated on MH agar to determine the lowest concentration of the antibiotic required to kill all bacteria, i.e., the minimum bactericidal concentration (MBC). The MBC of amikacin was determined to be 8 $\mu\text{g}/\text{mL}$ for persister as well as non-persister cultures of KpIMS38. Both sets of cultures survived exposure to lower concentrations of amikacin, i.e., 4 $\mu\text{g}/\text{mL}$ and below. However, the growth of persister cells in amikacin was lower than that of the non-persister cells (Figure 4.1.9A). This disparity was more pronounced below 2 $\mu\text{g}/\text{mL}$ of amikacin, with the persisters being at least 10 orders of magnitude lower than the non-persisters at corresponding concentrations of amikacin (Table 4.1.15 A).

Table 4.1.15 Susceptibility of KpIMS38 to varying concentrations of amikacin and meropenem. (A) Cultures exposed to 256 µg/mL levofloxacin for 8 hours (+L) were used to inoculate two-dilution series of either of the antibiotics. Untreated cultures (-L) were also used, and the cell numbers obtained at each concentration of amikacin or meropenem were represented as the average log₁₀CFU/mL (Av) of biological replicates (n = 3) with the standard deviation (SD). **(B)** KpIMS38 was treated with 0.25 µg/mL of meropenem and the number of survivors evaluated at fixed time-intervals. Cell numbers were represented as the average log₁₀CFU/mL (Av) of biological duplicates (n = 2) with the standard deviation (SD).

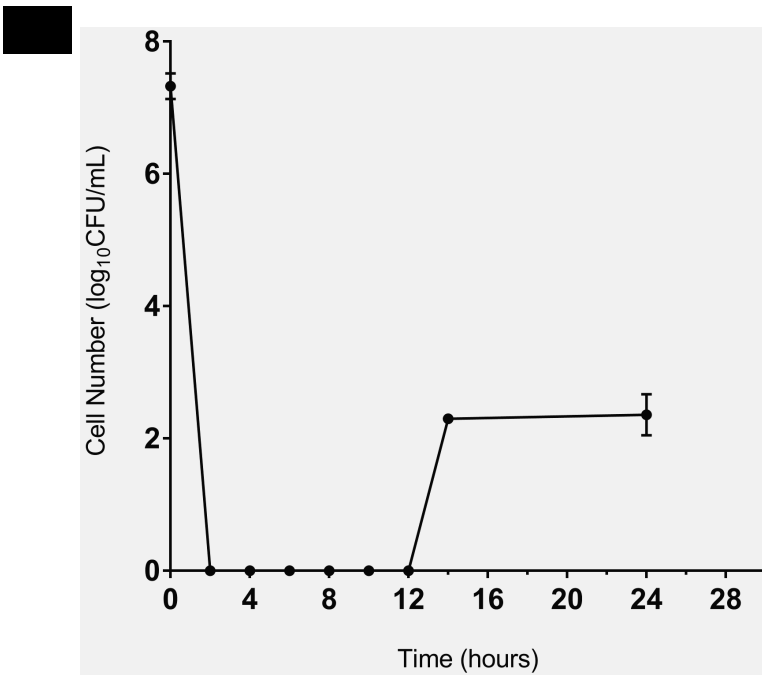
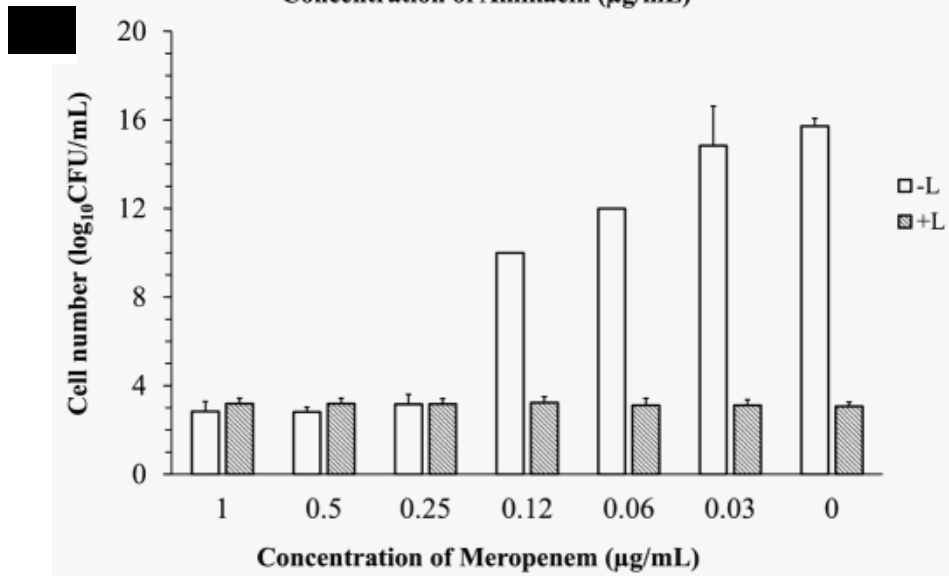
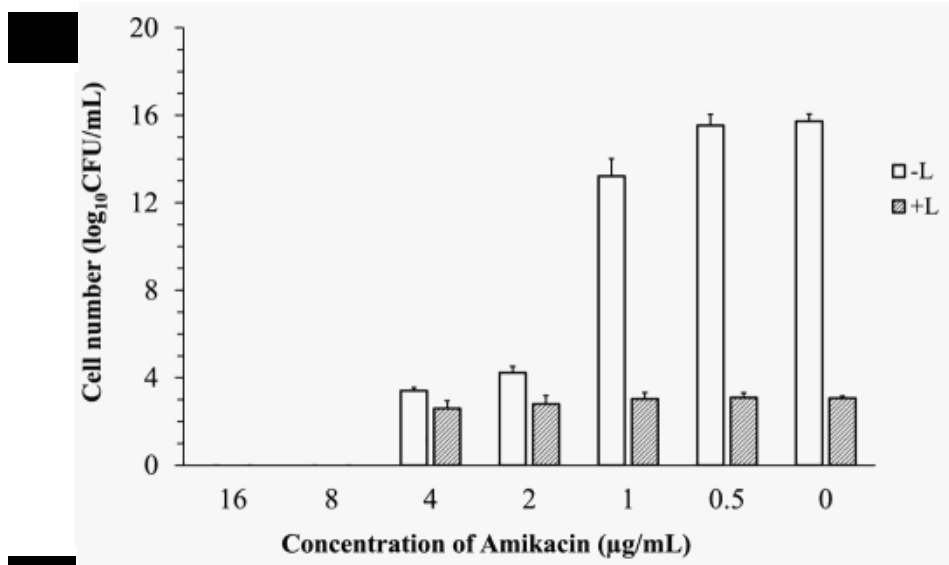
A	Cell Number (log ₁₀ CFU/mL; Av ± SD)			Cell Number (log ₁₀ CFU/mL; Av ± SD)		
	Amikacin (µg/mL)	-L	+L	Meropenem (µg/mL)	-L	+L
	16	0.00 ± 0.00	0.00 ± 0.00	1	2.84 ± 0.45	3.18 ± 0.26
	8	0.00 ± 0.00	0.00 ± 0.00	0.5	2.81 ± 0.22	3.18 ± 0.25
	4	3.40 ± 0.14	2.60 ± 0.35	0.25	3.16 ± 0.45	3.17 ± 0.25
	2	4.22 ± 0.29	2.81 ± 0.38	0.12	10.00 ± 0.00	3.23 ± 0.27
	1	13.22 ± 0.79	3.03 ± 0.30	0.06	12.00 ± 0.00	3.11 ± 31
	0.5	15.53 ± 0.52	3.09 ± 0.23	0.03	14.84 ± 1.79	3.12 ± 0.25
	0	15.73 ± 0.33	3.06 ± 0.10	0	15.72 ± 0.35	3.07 ± 0.20

B	Time (hours)	Cell Number (log ₁₀ CFU/mL; Av. ± SD)
	0	6.97 ± 0.18
	2	0.00 ± 0.00
	4	0.00 ± 0.00
	6	0.00 ± 0.00
	8	0.00 ± 0.00
	10	0.00 ± 0.00
	12	0.00 ± 0.00
	14	2.30 ± 0.22
	24	2.78 ± 0.76

A similar tendency was observed in the survival of persister and non-persister populations of KpIMS38 to various concentrations of meropenem. The number of survivors in both cell-populations were comparable till 0.25 µg/mL of meropenem, and the number of non-persisters surviving lower concentrations of meropenem outweighed the persisters by ≈ 7 to 13 orders of magnitude (Table 4.1.15 A). The major difference that set it apart from the results obtained for amikacin was the inability to obtain an MBC of meropenem for either of the populations of KpIMS38. Cell growth was observed in all concentrations of meropenem for both persister and non-persister cultures (Figure 4.1.9B), indicating the highest concentration used was insufficient to kill all the cells.

The presence of survivors on exposing non-persister KpIMS38 cultures to meropenem was in contrast to the outcome of the same observed previously. As documented in section 4.1.4.1, specifically in figure 4.1.2, KpIMS38 was rapidly killed on exposure to 0.25 µg/mL, whereas treatment with even 1 µg/mL of the same was unsuccessful in eliminating all bacteria. Hence, the survival of KpIMS38 to 0.25 µg/mL of meropenem was re-examined, this time at additional time-intervals of 14 and 24 hours post-antibiotic treatment. The results recapitulated those obtained in the previous experiment, with KpIMS38 rapidly killed after 2 hours of exposure to meropenem and no survivors recovered till 12 hours. After 14 hours of treatment with meropenem, however, the cell number showed an increase to 100 CFU/mL (Table 4.1.15 B) which was sustained till 24 hours (Figure 4.1.9 C).

Figure 4.1.9 (overleaf) Susceptibility of KpIMS38 treated with levofloxacin to varying concentrations of amikacin (A) and meropenem (B). KpIMS38 exposed to 256 µg/mL levofloxacin (+L) was used to inoculate a two-fold dilution series of amikacin (16 to 0.5 µg/mL) and meropenem (1 to 0.5 µg/mL). Cultures not treated with levofloxacin (-L) were also treated similarly with amikacin and meropenem. **Survival of KpIMS38 in meropenem across an extended period of time (C).** Cell numbers obtained for all experiments were represented as the average \log_{10} CFU/mL ($n = 3$) with whiskers representing the standard deviation.

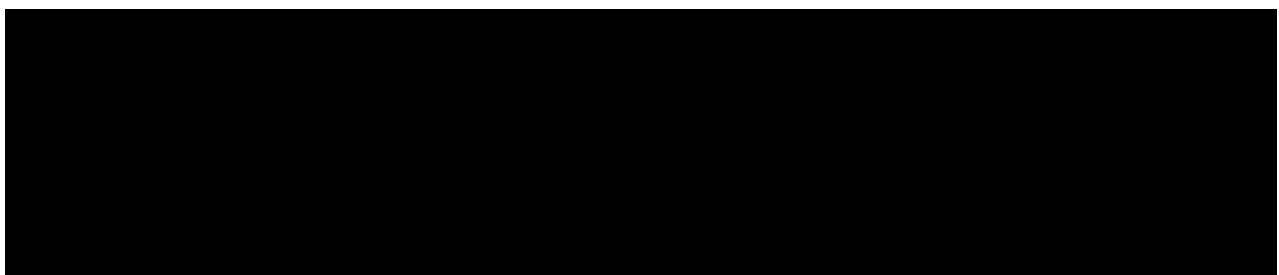
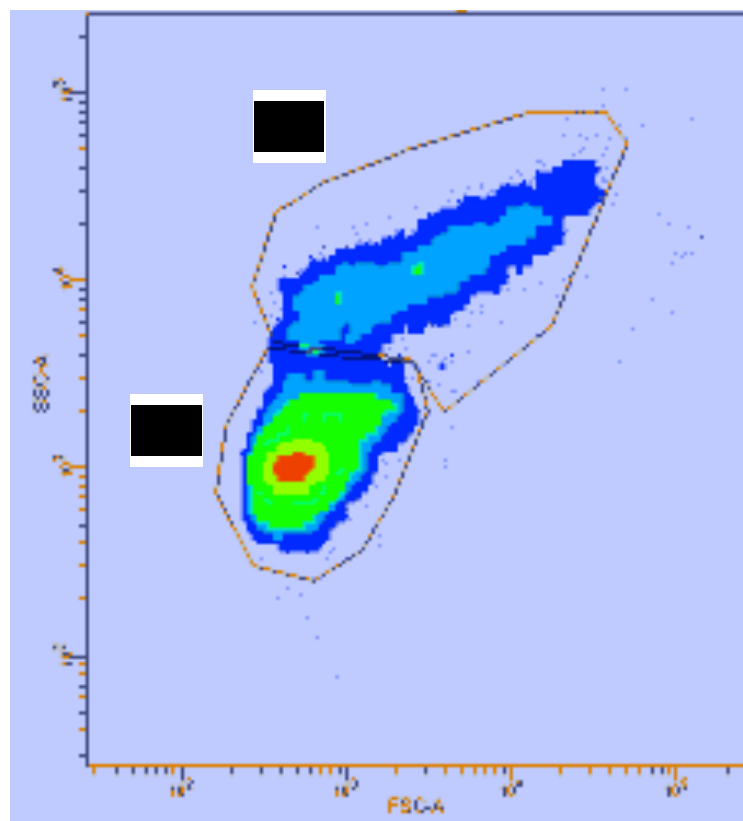


4.1.5 Quantitative analysis of persister-populations of KpIMS38 using fluorescent dyes

4.1.5.1 Analysis of the persister population of KpIMS38 using fluorescent dyes and flow cytometry

Culture-aliquots of KpIMS38 – treated with levofloxacin as well as untreated – were stained with an optimized concentration of 75 μ M CFDA, fixed in 1% PFA and stored at 4°C in the dark. Cell suspensions were analyzed in a flow cytometer, where 10,000 cells were taken for each time-point on the basis of forward scatter (FSC), side scatter (SSC) as well as fluorescence of CFDA.

Each cell-sample was found to contain two different sub-populations – a small sized P1 and larger P2 – based on FSC and SSC data (Figure 4.1.10).



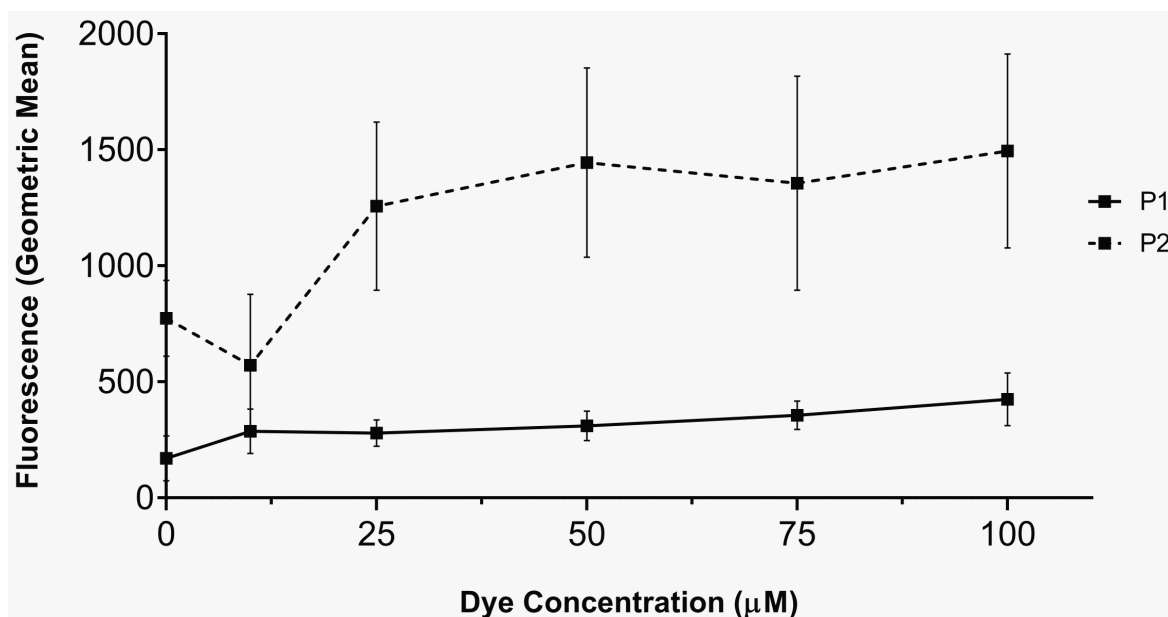
Aliquots of KpIMS38 were stained with varying concentrations of CFDA (as outlined in section 3.3.6.1.1 of this document), and it was observed that an increase in the concentration increased the number of stained cells as well as the staining intensity. A difference was observed for both the parameters between the P1 and P2 sub-populations. The proportion of stained cells was higher in the P2 sub-population compared to the P1 cells (Table 4.1.16), the former being about 1.5 times higher than the latter at all concentrations of CFDA measured (Figure 4.1.11). When comparing the staining intensity (given by the geometric mean of the fluorescence of the cells sampled) of both cell sub-populations, the cells belonging to the P2 sub-population exhibited a higher fluorescence than those from the P1 sub-population (Figure 4.1.12). The difference between both was much greater however, with the fluorescence from the P2 cells almost 4 times higher than that of the P1 cells (Table 4.1.17).

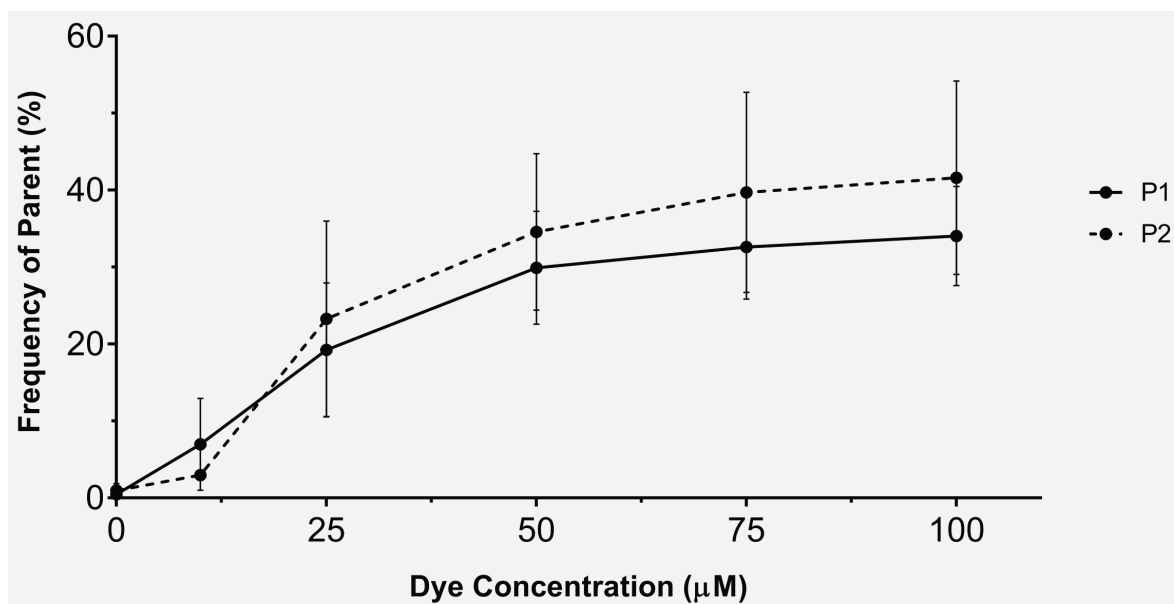
Table 4.1.16 Proportion of stained cells in KpIMS38 stained with varying concentrations of CFDA. The frequency of stained cells stained with different concentrations of CFDA was represented as the mean percentage (n = 2) with the standard deviation (Av. ± SD) of each parent sub-population (P1 or P2).

Concentration of CFDA (µM)	Frequency of stained cells (%)	
	P1	P2
0	0.56 ± 0.30	1.37 ± 0.39
10	7.79 ± 6.81	11.24 ± 11.69
25	21.65 ± 10.39	36.10 ± 5.37
50	33.95 ± 9.26	47.00 ± 7.35
75	36.55 ± 8.56	56.55 ± 10.82
100	38.45 ± 8.13	55.30 ± 6.79

Table 4.1.17 Cell-fluorescence in a culture of KpIMS38 stained with varying concentrations of CFDA. The fluorescent intensity of the stained cells was calculated as the geometric mean of stained cells assessed from the parent sub-population (P1 or P2) and was represented as the mean intensity ($n = 2$) with the standard deviation ($Av \pm SD$).

Concentration of CFDA (μM)	Fluorescent intensity of stained cells (Geometric mean)	
	P1	P2
0	170.50 \pm 96.87	773.50 \pm 163.34
10	287.50 \pm 95.46	571.50 \pm 306.18
25	279.50 \pm 57.28	1257.50 \pm 362.75
50	310.00 \pm 63.64	1445.00 \pm 407.29
75	356.00 \pm 60.81	1356.00 \pm 461.03
100	424.50 \pm 113.84	1494.50 \pm 417.90





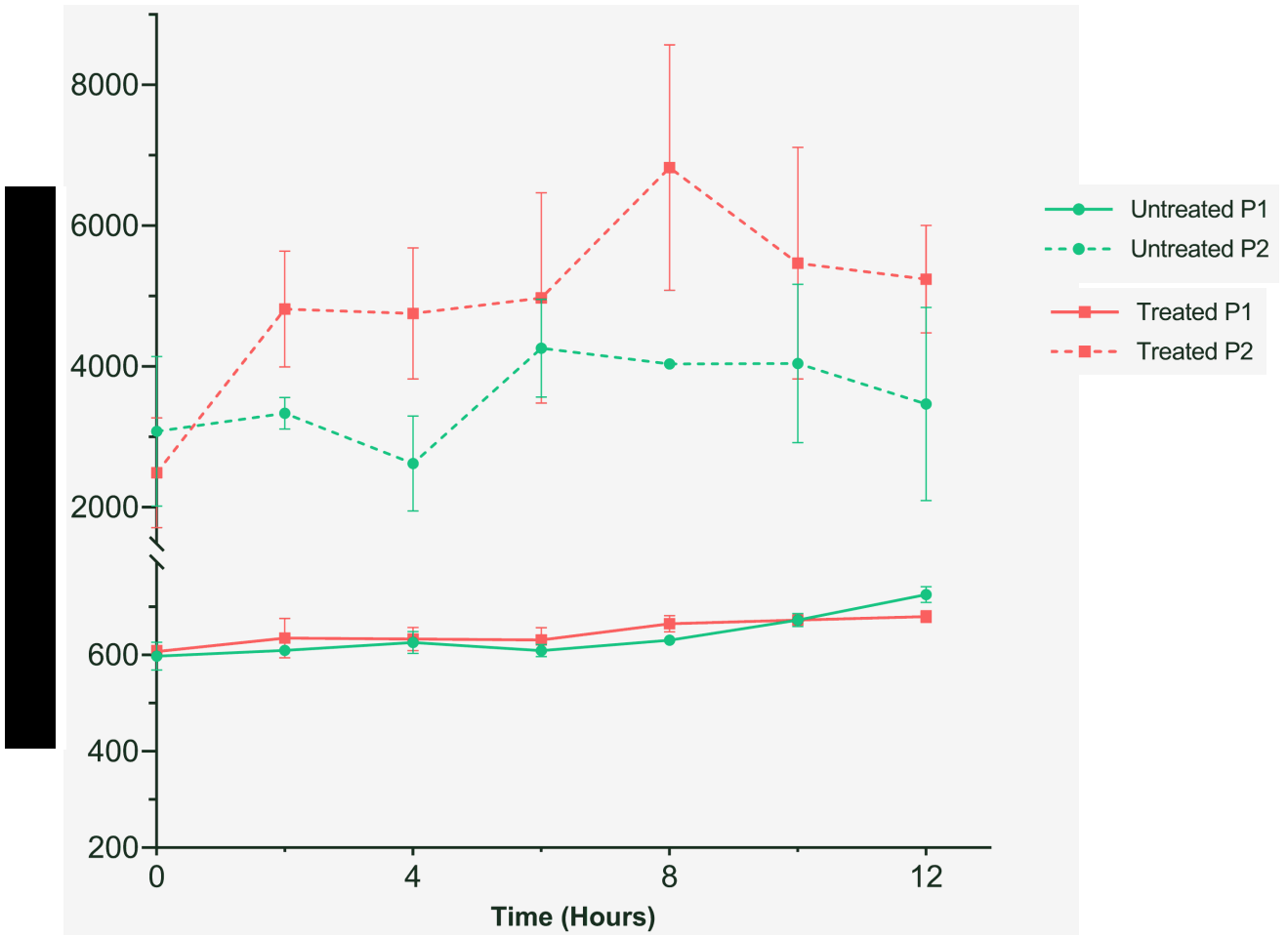
To study the population of KpIMS38 on exposure to levofloxacin, cultures of the same were stained by CFDA and assessed using flow cytometry, using the methods detailed in section 3.3.6.1.2 of this document. Upon plotting the FSC values obtained for each of the cells against time, the size of P1 cells did not change, even upon treatment with levofloxacin (Figure 4.1.13). In addition, there was no variation in the cell sizes at each time-point measured, with all cells sized within the range of 600-700 units (Table 4.1.18). The same could not be said for the P2 subpopulation, the smallest of which was sized at 2500 units. There was an increase in the size of P2 cells with the passage of time in the population treated with levofloxacin. There was a large variation in the cell sizes in both treated and untreated P2 subpopulations as compared to the P1 cells, across the time measured as well as at each time point.

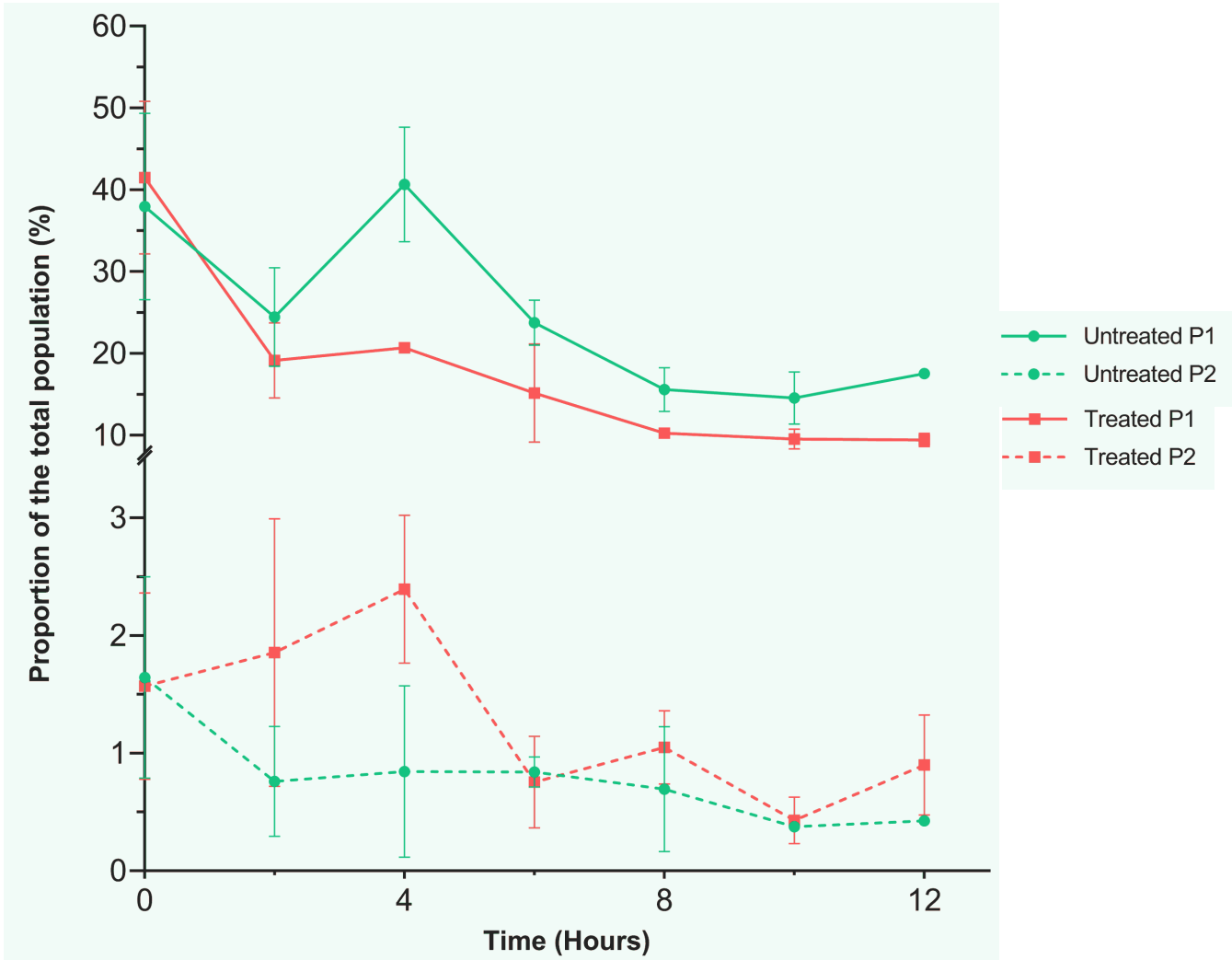
Table 4.1.18 Effect treatment of levofloxacin on the cell-size of KpIMS38. KpIMS38 cultures treated with levofloxacin (+L) as well as untreated (-L) were assessed by flow cytometry, and cell sizes from P1 and P2 sub-populations calculated as the geometric mean of the forward scatter (FSC). The values were represented as the average cell size (n = 2) with the standard deviation (Av. ± SD).

Time (h)	Forward scatter (Av. ± SD)			
	-L P1	-L P2	+L P1	+L P2
0	597.50 ± 28.99	3080.50 ± 1064.20	607.00 ± 12.73	2492.50 ± 781.35
2	609.50 ± 2.12	3338.00 ± 223.45	635.00 ± 41.01	4818.00 ± 823.07
4	626.00 ± 22.63	2622.50 ± 675.29	633.00 ± 24.04	4755.50 ± 929.85
6	609.00 ± 12.73	4262.50 ± 695.09	631.00 ± 25.46	4974.50 ± 1492.70
8	630.50 ± 4.95	4037.00 ± 8.49	665.00 ± 16.97	6828.50 ± 1745.85
10	672.50 ± 13.44	4045.00 ± 1127.13	672.50 ± 2.12	5468.50 ± 1645.44
12	725.50 ± 16.26	3467.50 ± 1372.49	679.50 ± 12.02	5241.50 ± 762.97

Table 4.1.19 Effect of levofloxacin treatment on the abundance of P1 and P2 sub-populations in KpIMS38. KpIMS38 cultures treated with levofloxacin (+L) as well as untreated (-L) were assessed by flow cytometry, and the proportions of stained cells in the P1 and P2 sub-populations calculated as the percent of the total population (%). The values were represented as the average (n = 2) with the standard deviation (Av. ± SD).

Time (h)	Percent of total population (Av. ± SD)			
	-L P1	-L P2	+L P1	+L P2
0	37.95 ± 11.38	1.65 ± 0.86	41.50 ± 9.33	1.57 ± 0.79
2	24.45 ± 6.01	0.76 ± 0.47	19.15 ± 4.60	1.86 ± 1.14
4	40.65 ± 7.00	0.85 ± 0.73	20.70 ± 0.57	2.40 ± 0.63
6	23.75 ± 2.76	0.84 ± 0.13	15.15 ± 6.01	0.76 ± 0.39
8	15.60 ± 2.69	0.70 ± 0.53	10.27 ± 0.62	1.05 ± 0.31
10	14.55 ± 3.18	0.38 ± 0.02	9.54 ± 1.22	0.43 ± 0.20
12	17.55 ± 0.64	0.43 ± 0.02	9.43 ± 0.81	0.90 ± 0.42





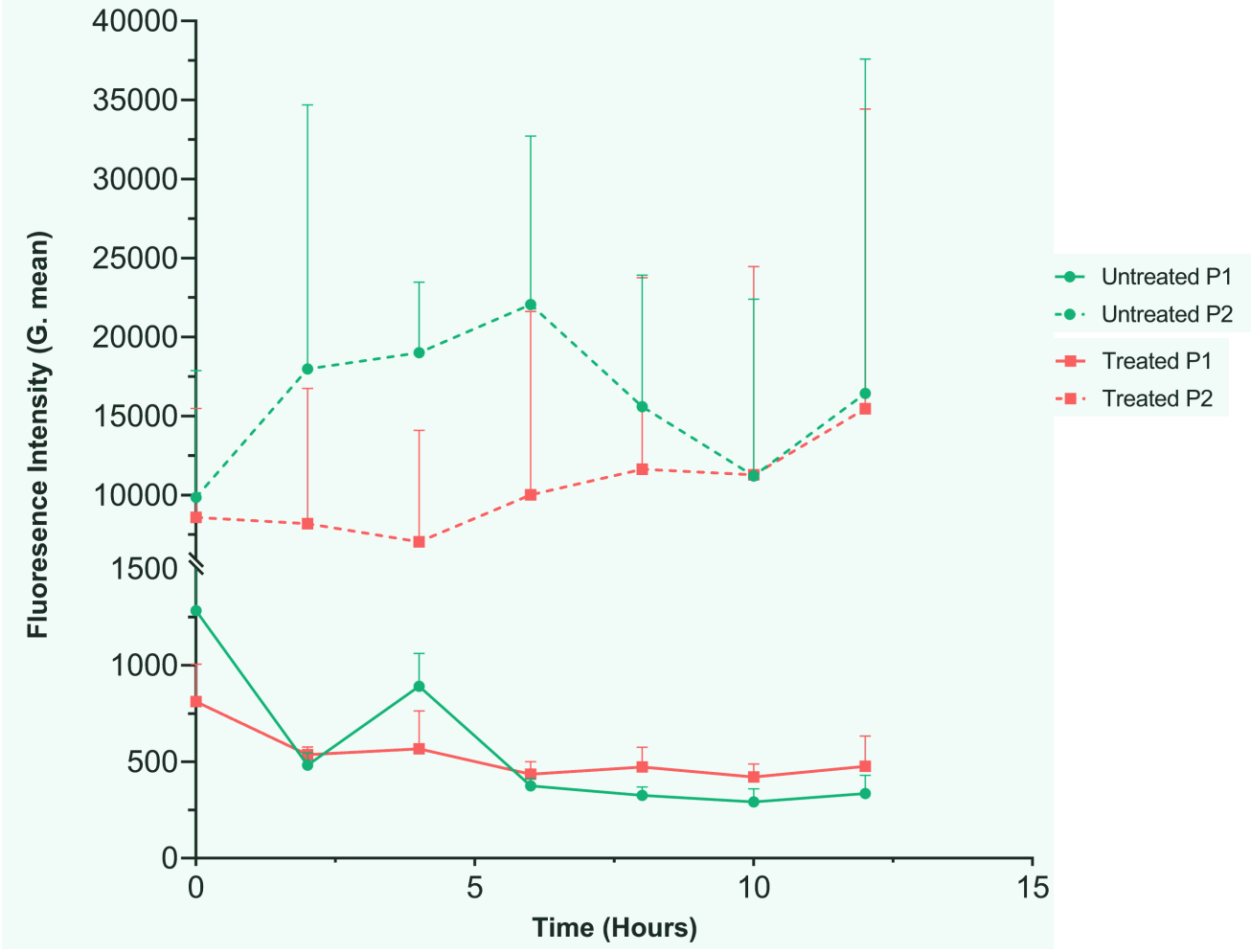


Table 4.1.20 Effect of levofloxacin treatment on the fluorescence observed in cell-sub-populations in KpIMS38. KpIMS38 cultures treated with levofloxacin (+L) as well as untreated (-L) were assessed by flow cytometry, and the fluorescence from CFDA measured in cells from the P1 or P2 sub-populations was calculated as the geometric mean of fluorescence. The values were represented as the average fluorescence (n = 2) with the standard deviation (Av ± SD).

Time (h)	Fluorescence (Av ± SD)			
	-L P1	-L P2	+L P1	+L P2
0	1284.00 ± 494.97	9870.00 ± 8020.01	811.50 ± 194.45	8590.50 ± 6893.58
2	483.50 ± 64.35	17984.50 ± 16711.05	537.00 ± 39.60	8196.50 ± 8552.46
4	891.50 ± 170.41	19018.50 ± 4456.89	567.00 ± 196.58	7059.00 ± 7038.54
6	375.50 ± 38.89	22061.50 ± 10656.81	435.50 ± 65.76	10023.00 ± 11593.72
8	326.00 ± 43.84	15607.00 ± 8324.06	473.50 ± 102.53	11642.50 ± 12109.20
10	292.50 ± 67.18	11220.00 ± 11189.26	422.00 ± 67.88	11285.00 ± 13173.40
12	335.50 ± 94.05	16442.50 ± 21147.44	476.50 ± 157.68	15465.00 ± 18958.95

The P1 cells were found most abundantly throughout the experiment, in untreated as well as levofloxacin-treated cells (Figure 4.1.14). From an initial proportion of 40%, the P1 cell population reduced to 20%, with a further 5% reduction on treatment with levofloxacin (Table 4.1.19). In comparison, the P2 cells constituted only 1.5% of the total population. There was an increase in the number of P2 cells on treatment with levofloxacin until 4 hours, following which it reduced from 2.5% to below 1% of the total cell population.

Each of these populations were further analysed for the CFDA fluorescence of the cells sampled. Cells belonging to the P1 subpopulation stained weaker than the P2 cells, the difference between them, for example, after 8 hours being over 50 times in untreated cell

populations and over 20 times in levofloxacin-treated cell populations (Figure 4.1.15). Treatment with levofloxacin did not affect the fluorescence obtained from the P1 subpopulation of cells, the difference between untreated and treated fractions being around 100 units at most of the time points measured (Table 4.1.20). In comparison, treatment with levofloxacin reduced the CFDA-fluorescence from the P2 subpopulation vis-à-vis the untreated fraction of the same. This reduction, however, was observed till 8 hours of antibiotic treatment following which the fluorescence of P2 cells from both untreated and treated fractions was similar. The variation in the fluorescence was much higher in the P2 subpopulation, with the cells showing much more variation in each time point in untreated as well as levofloxacin-treated cells than their P1 counterparts (Table 4.1.20).

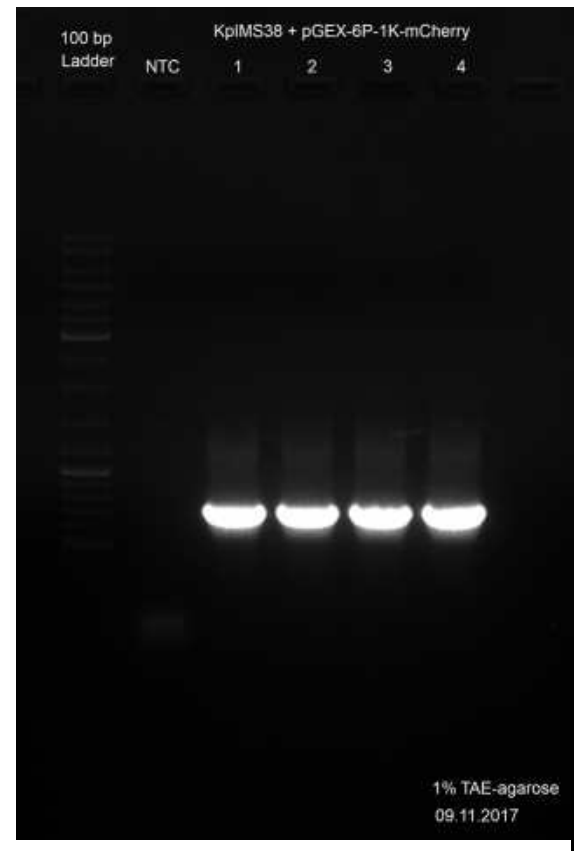
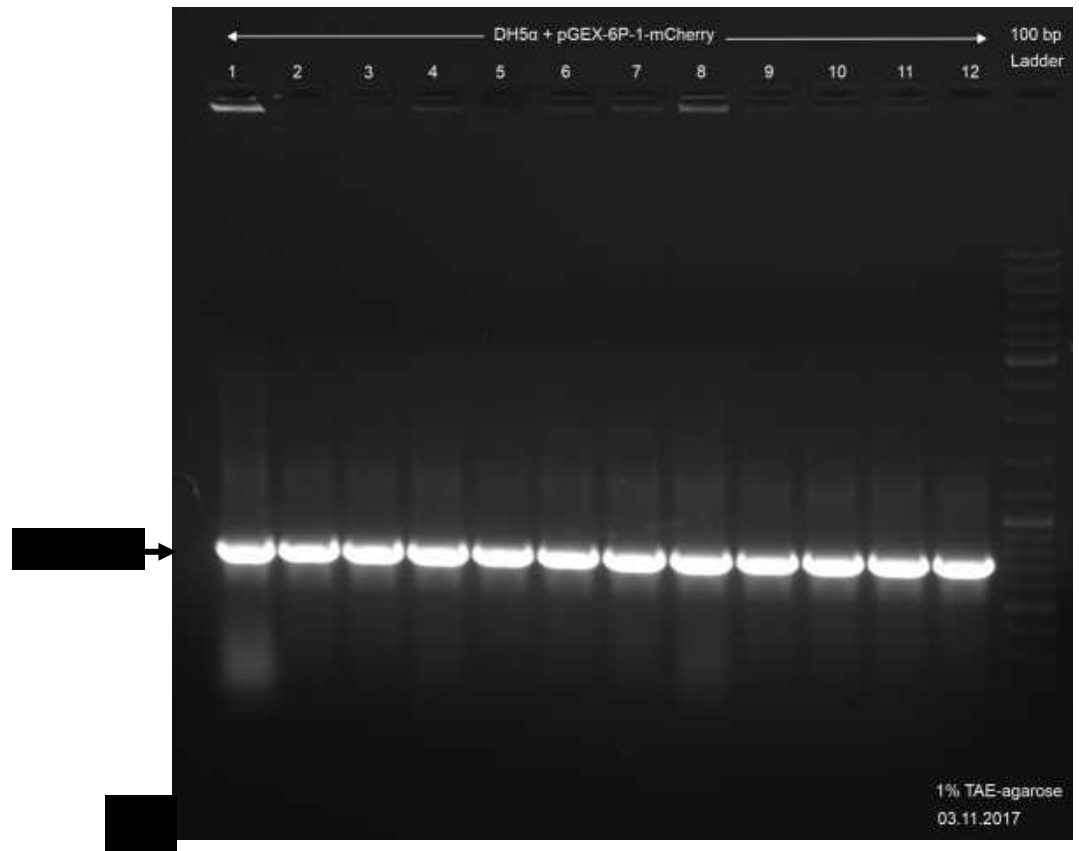
4.1.5.2 Visualizing persister cell formation using a flow-cell system

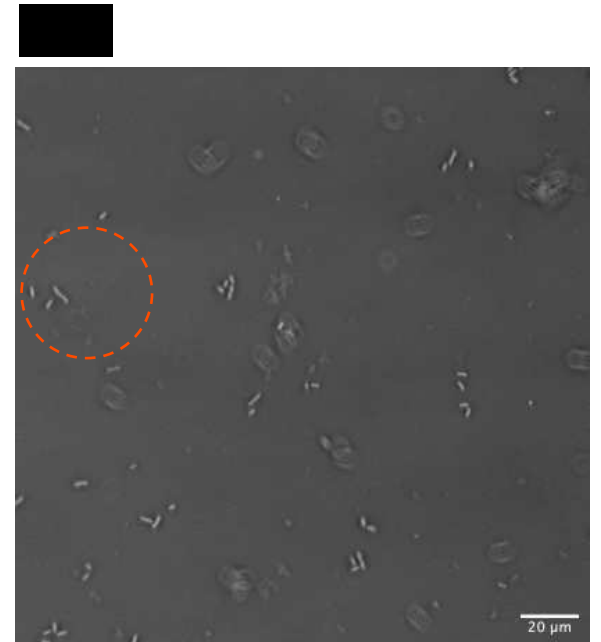
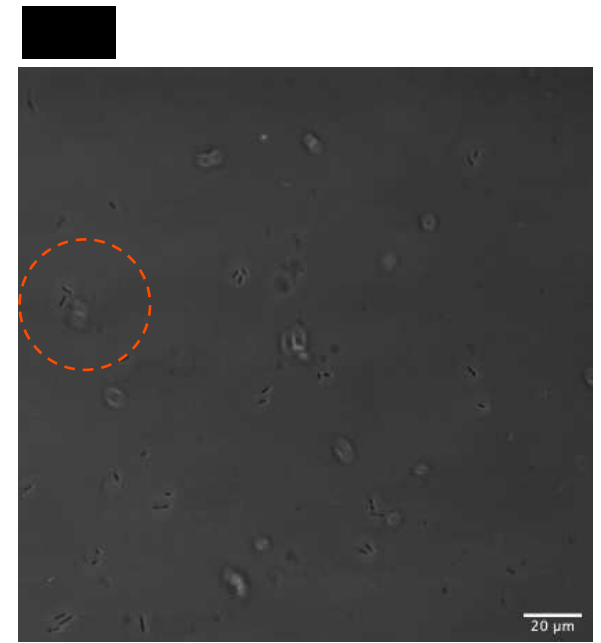
Persister-cell formation of KpIMS38 on treatment with levofloxacin was assessed using live-cell microscopy. A flow-cell system was employed to grow bacterial cells, immobilized on the surface of an agarose pad, and treat them with 256 µg/mL levofloxacin. The flow-cell system was placed in a confocal microscopy system and sequentially imaged using a confocal laser first with an excitation wavelength of 588 nm followed by bright-field microscopy. The entire procedure was performed according to the protocol detailed in section 3.3.6.2.6 of this document. The images (fluorescence and bright-field) obtained at each time-point were merged to form a composite using ImageJ, and individual foci within the field were examined across the three growth conditions viz. untreated, levofloxacin-treated and revival.

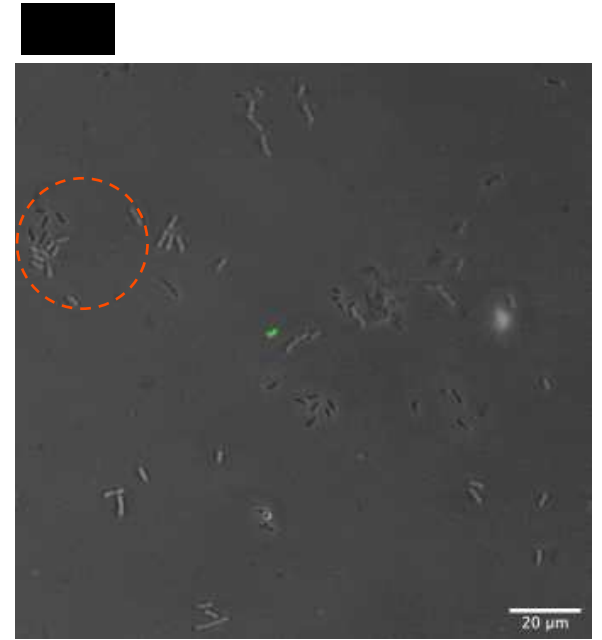
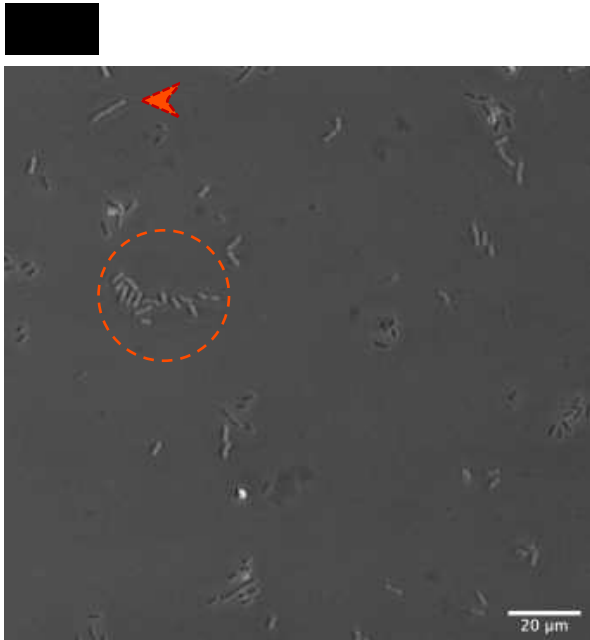
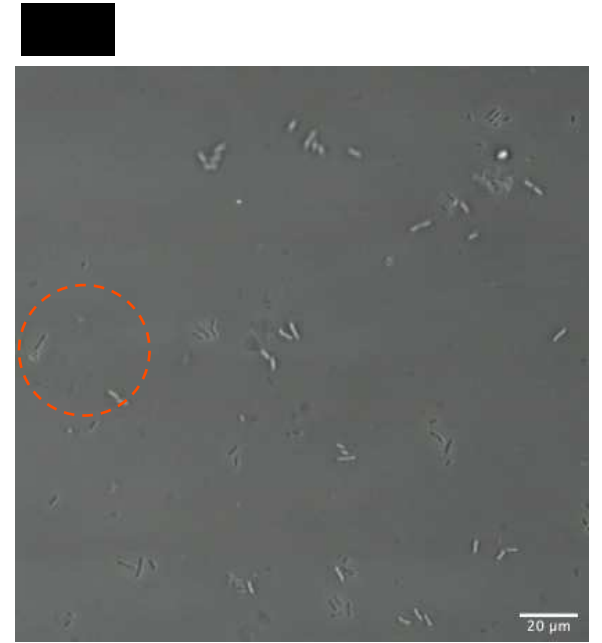
For the purpose, KpIMS38 was transformed to express the fluorescent protein mCherry from the construct pGEX-6P-1^K under inducible control of IPTG. The success of transformation was confirmed by screening for the presence of *mCherry* in putative transformants using colony PCR. The presence of an amplicon approximately 710 bp in size was observed in *E.*

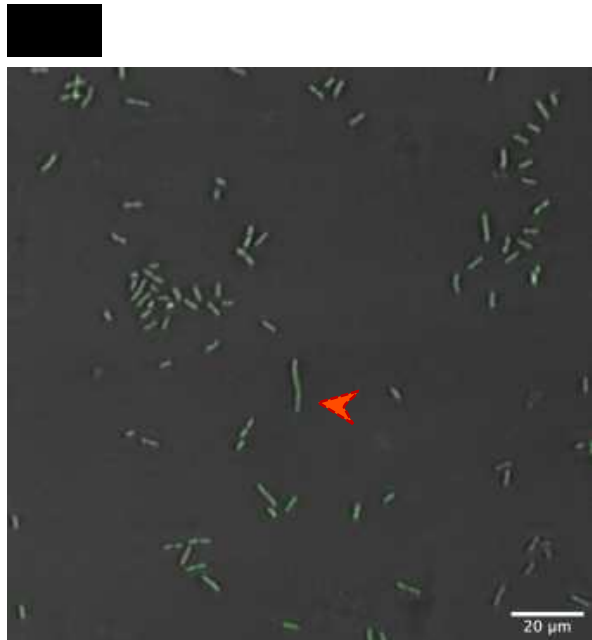
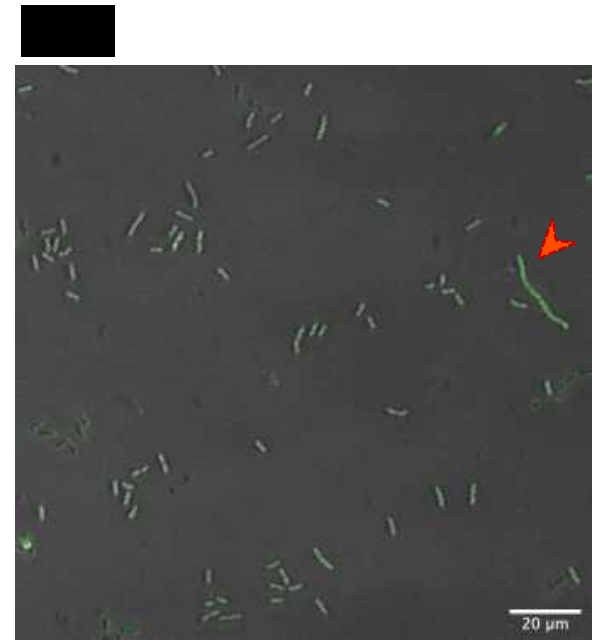
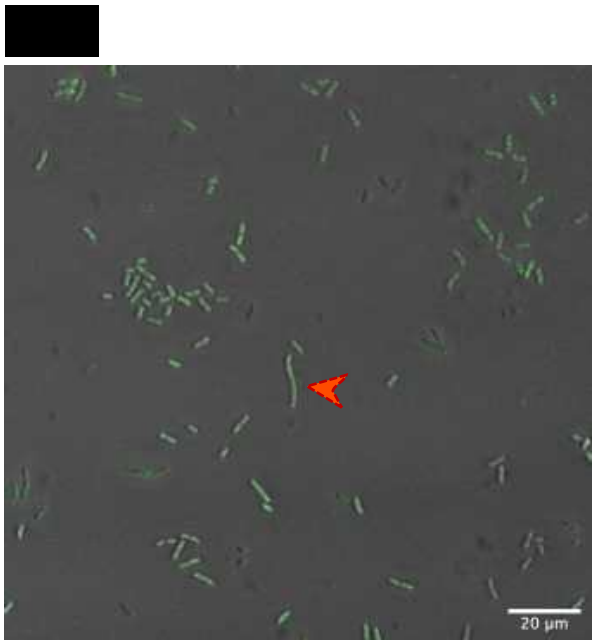
coli DH5 α (Figure 4.1.16 A) as well as KpIMS38 (Figure 4.1.16 B) transformed with pGEX-6P-1^K, thereby confirming successful transformation of the construct.

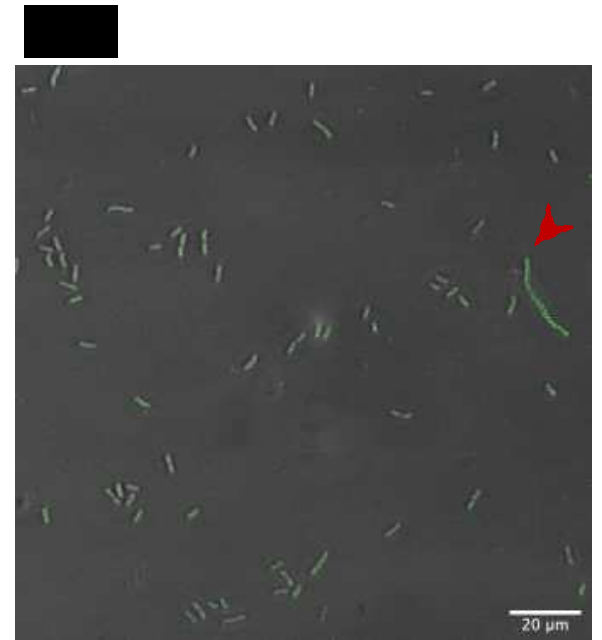
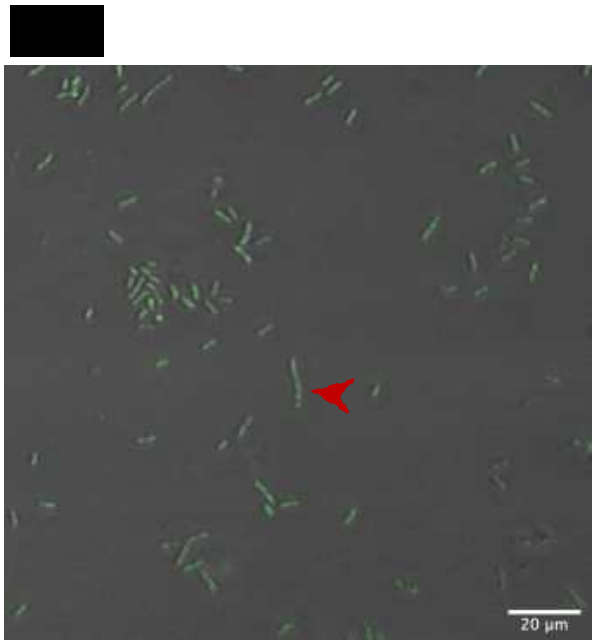
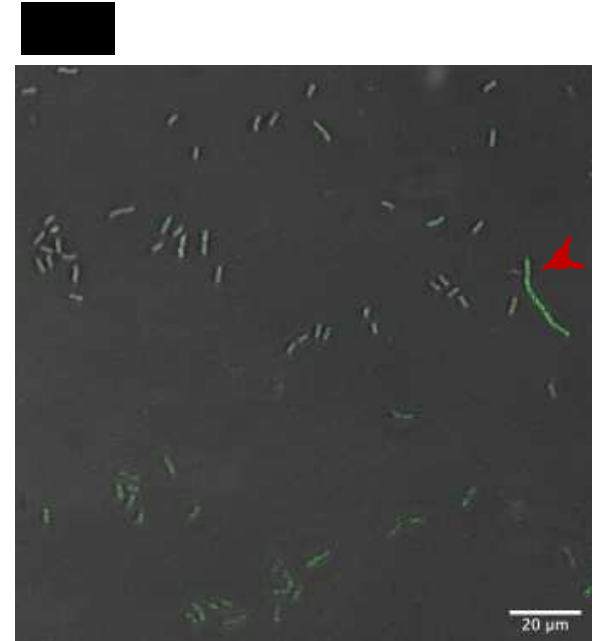
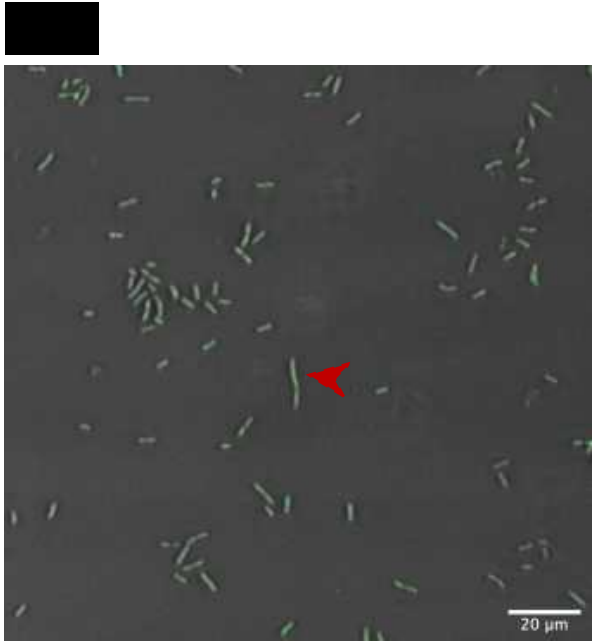
It was observed that the cell number increased during the "untreated" growth-condition, i.e., in the absence of levofloxacin. The number of bacteria present were observed to undergo cell division and produce more cells (Figure 4.1.17 A-C 1, 2, 3, 4). Additionally, specific cells were also observed to undergo cell elongation, with the cell increasing in size without dividing (Figure 4.1.17 A 2, 3, 4). No increase in the cell number was observed during levofloxacin treatment (Figure 4.1.17 A-C 5, 6, 7, 8), with certain cells seen to lose fluorescence and disappear thereby indicating cell death (Figure 4.1.17 B5). Cell elongation was also observed in the cell population, with the number of long cells increasing throughout the period of treatment (indicated by red arrows). On removal of levofloxacin from the population, i.e., during the condition of "revival", the population was administered growth medium without levofloxacin and cell behavior observed. Upon observation, the cell numbers were seen to remain constant. There was no increase in cell numbers, neither was any cell division observed for the 410 minutes that the population was observed (Figure 4.1.17 A-C 9, 10, 11).

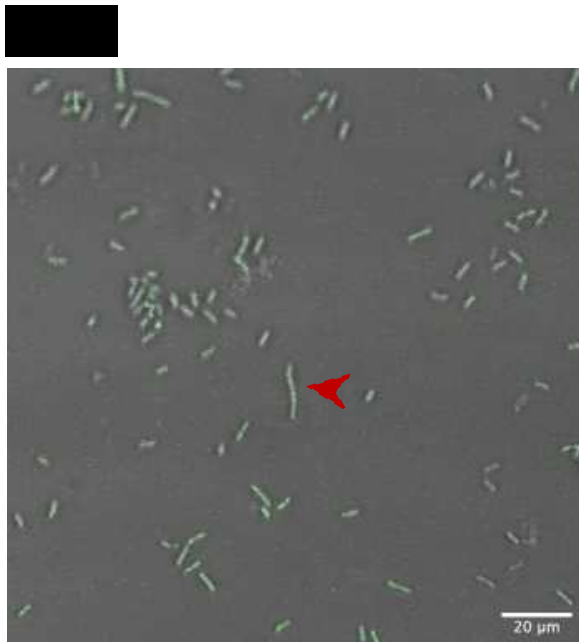
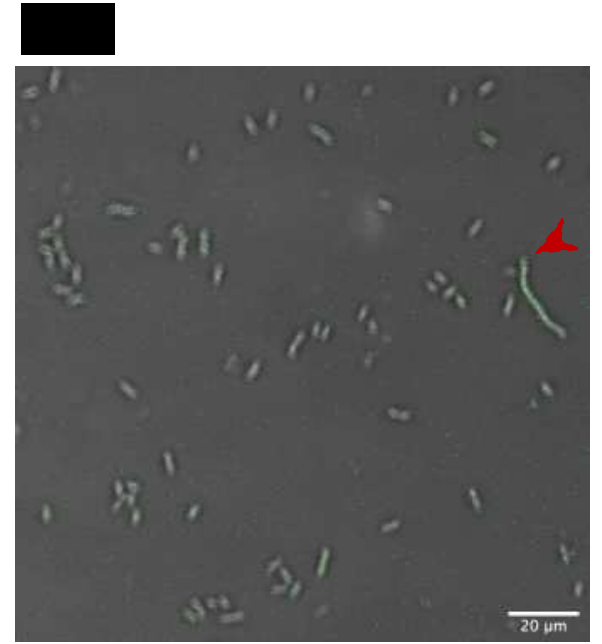
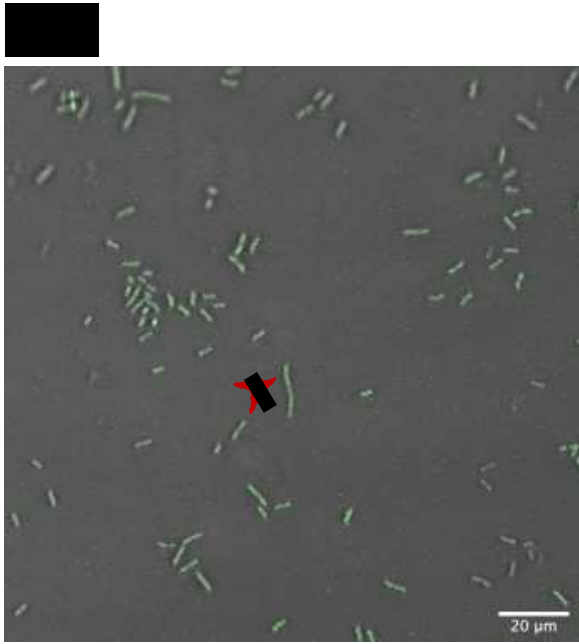


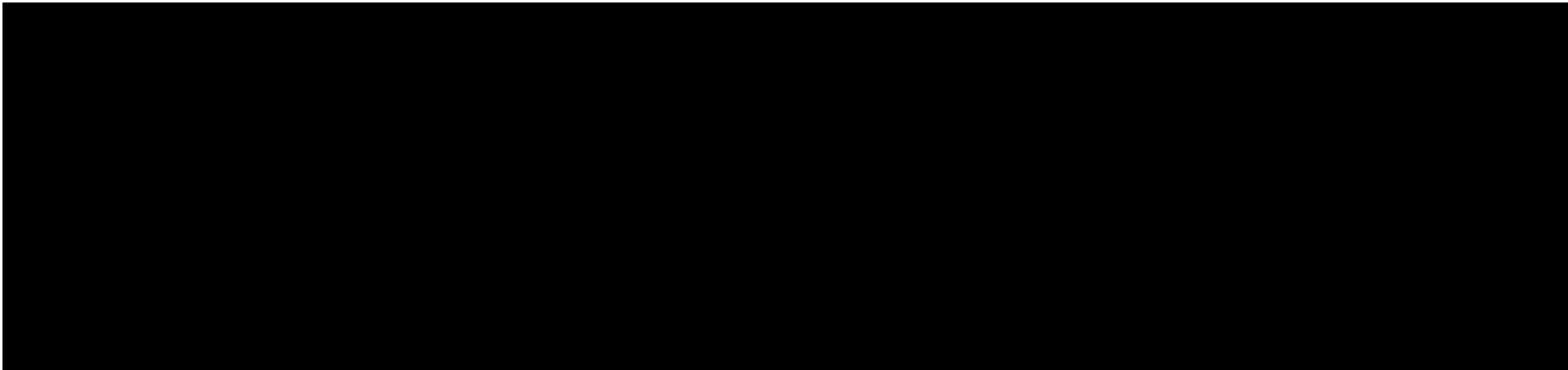
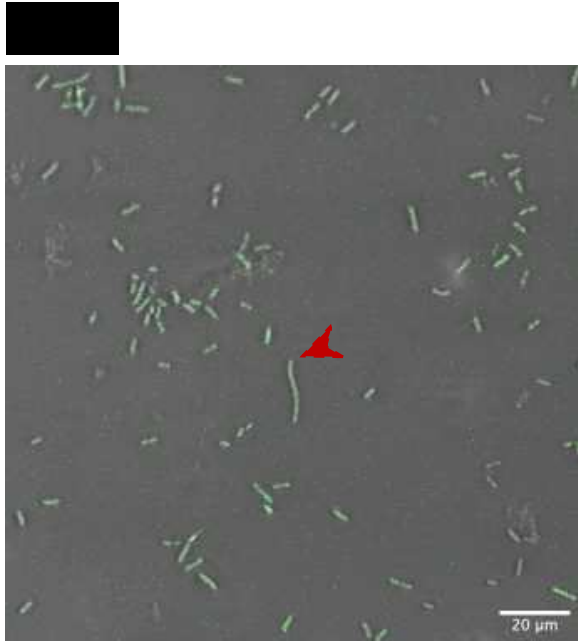












4.1.6 Discussion

The occurrence of bacterial infections that persist within a host for a prolonged period of time despite antibiotic treatment has been realised in the past decade. Bacteria are known to evade the host immune responses through avoiding phagocytosis (Smith and May, 2013), inhibiting recognition of toll-like receptors (TLRs) (Yan et al, 2012), replicating within immune cells and killing them (Mitchell et al, 2016), blocking antigen presentation and inflammatory pathways (Tobar et al, 2004), and inhibiting complement system (Hovingh et al, 2016). The fairly-recent discovery of a mechanism whereby bacteria exhibit heterogeneity in their population to allow the survival of a subpopulation on exposure to antibiotics further compounds the situation. These survivors tide over lethal antibiotic concentrations by virtue of being in a non-dividing, non-metabolising state, and are termed "persisters" (Gollan et al, 2019).

The current study was carried out using three clinical isolates of *Klebsiella pneumoniae* viz. KpIMS32, -34 and -38. Pure cultures of the isolates were obtained from a tertiary-care hospital, and were acquired from independent individuals and different anatomical locations (Table 4.1.1). The isolates were identified as *K. pneumoniae* based on biochemical tests and 16S rRNA sequencing.

K. pneumoniae is one among six bacterial pathogens categorised under the ESKAPE group. The surveillance of as well as development of novel antibiotics for the six pathogens occupies a high priority, primarily based on the frequency at which antibiotic resistance was isolated in clinical cases of infections (Rice, 2008). *K. pneumoniae* infections are conventionally treated using carbapenem and cephalosporin antibiotics, though their efficacy has been compromised of late due to the extensive acquisition of genes for carbapenemases and extended-spectrum beta-lactamases that confer resistance to the corresponding antibiotics (Paterson and Bonomo, 2005). The resistance of the three isolates

to multiple classes of antibiotics indicated the potential they possessed to cause multidrug-resistant bacterial infections. In addition to a lack of susceptibility to early-generation beta-lactam compounds such as monobactams and amino-derivatives of penicillin, all three isolates exhibited a marked resistance to $\geq 80\%$ of the combinations of beta-lactam – beta-lactamase inhibitor used in the present study. The recalcitrance of KpIMS34, an extensively-drug-resistant (XDR) isolate, to fluoroquinolones, metabolic inhibitors, and all beta-lactam formulations tested illuminates the severity of antibiotic resistance that occurs in a community health setting. In comparison, KpIMS38 – also exhibiting the XDR phenotype – was resistant to only gentamicin. Additionally, KpIMS38 showed resistance to all the cephalosporins used except cefoxitin, a second-generation cephalosporin antibiotic. KpIMS38 also did not share the resilience to fluoroquinolone antibiotics and trimethoprim-sulfamethoxazole observed in KpIMS34. The pattern of resistance to beta-lactam-beta-lactamase inhibitor combinations also differed between the three isolates. Among the five different combinations utilised in this study, KpIMS32 was susceptible to only piperacillin-tazobactam and KpIMS38 to ampicillin-sulbactam; KpIMS34 was resistant to all five combinations tested.

The observations from examining the antibiotic sensitivity correlate to the high MAR index of KpIMS34 and -38, and indicate the potential of both isolates to cause severe infections which might become chronic in nature. A cross-sectional study studying the antibiotic sensitivities of isolates cultured from bloodstream infections implicated *K. pneumoniae* in about 7% of total cases. MAR index of the cultures was categorised as moderate and lay between 0.52 and 0.57 (Puspita et al, 2021). A retrospective study examining antibiotic resistance in freshwater isolates observed multiple-antibiotic resistance in *Klebsiella*. The cultures exhibited a MAR index (average) of 0.36, the second-highest among all the isolates assayed (Singh et al, 2017).

Barring the XDR KpIMS34, the two remaining *Klebsiella* isolates in the present study showed susceptibility to aminoglycoside, carbapenem or fluoroquinolone antibiotics. Amikacin, meropenem and levofloxacin were chosen as candidates and the sensitivity of KpIMS32 and -38 to the antibiotics assayed by means of the two-fold serial broth-dilution method. The results obtained corroborated those observed in the antibiotic sensitivity tests for amikacin and meropenem. However, the MIC of levofloxacin was observed to lie in the 'resistant' range for both KpIMS32 and -38. Further scrutiny of the antibiotic-sensitivity using EzyMIC™ strips indicated both isolates to be sensitive to the three drugs. Specifically, the MICs of levofloxacin were 16 and 32 times lower than those observed for KpIMS32 and -38 respectively using the two-fold serial dilution method. Discrepancies in the outcomes from different methods used to assay the MIC have been observed previously in studies using bacteria from the *Lactobacillus acidophilus* group (Mayrhofer et al, 2008; Kulengowski et al, 2019; Gupta et al, 2021). While the same studies reported the MIC values obtained from the E-test to be lower than those observed using broth dilution assays, results obtained from other studies conveyed the opposite (Amsler et al, 2010). Since all further assays were conducted in liquid medium, the values of the broth dilution assay were considered as the MIC.

Assays examining the survival of the two *K. pneumoniae* isolates to various antibiotics indicated the possibility of persister-cell formation being an isolate- or strain-specific trait rather than an attribute of a genus or species. While exposure to levofloxacin reduced the cell number by two orders of magnitude, it did not bring about complete elimination of KpIMS38. An initial decrement followed by a constancy of the cell number on treatment with supra-inhibitory concentrations of antibiotics is the hallmark of bacterial persistence and has been universally utilised to identify the formation of persisters in various bacterial

species (Bigger, 1944; Keren et al, 2004; Que et al, 2013; Liebens et al, 2014; Ren et al, 2015; Michiels et al, 2016).

A distinction between persistence and heteroresistance is vital, the latter involving isogenic cells transiently exhibiting resistance to an antibiotic. Heteroresistant cells are characterised by an increase in the MIC of an antibiotic. Hence, a rise in the killing rate of a culture with an increase in the concentration the antibiotic symbolises heteroresistance. Examining the killing kinetic at higher concentrations of an antibiotic eliminate the role of heteroresistance and ensure no phenotypic mutants arise during the procedure (Balaban et al, 2019). Levofloxacin appeared to promote the formation of persister cells in KpIMS38, evidenced by an increase in the number of KpIMS38 survivors with an increase in the concentration of levofloxacin and thereby ruling out the contribution of heteroresistance to the phenomenon. An increase in the number of survivors with an increase in the concentration of fluoroquinolones used has been known for some time (Crumplin and Smith, 1975; Lewin et al, 1991; Drlica et al, 1996). The contribution of an overactive SOS response (Lewin et al, 1989) and inhibition of quinolone-gyrase complexes (Chen et al, 1996) as causal factors for this phenomenon have been dismissed. Carret et al (1991) observed a biphasic killing-pattern of *E. coli* by various quinolones, where the number of survivors generated in response to 5x MIC was more than those obtained using 3x MIC. Malik et al (2009) came the closest to attributing this paradoxical killing to persistence. According to their observations, the Lon protease was necessary for the paradoxical effect of nalidixic acid on *E. coli*. Lon has been also known to be involved in degrading the antitoxin molecules of TA systems, thus leading to toxin-activity and consequent induction of persistence in bacteria (Maisonneuve et al, 2013). On examining the survival of *K. pneumoniae* treated with various antibiotics including a fluoroquinolone ciprofloxacin, Ren et al (2015) observed the number of persisters reduced with an increase in the drug concentration. This

indicated that the finding obtained in the present study was unique in linking the paradoxical effect of quinolone-mediated killing of bacteria with persister-cell formation.

Keren et al (2004), in their seminal work on bacterial persistence, identified persister-cell formation as being affected by the age of the initial bacterial culture. Stationary-phase cultures of *E. coli*, *P. aeruginosa* and *S. aureus* yielded many more persisters than their counterparts in lag and exponential phases of growth. The observations from the current study too indicate an increase in the number of persister cells with an increase in the age of the culture used. Entry into stationary phase had such a pronounced effect on the survival of KpIMS38 to levofloxacin that the biphasic killing, observed for early-log and mid-log cultures was completely absent. The cell numbers decreased by not even one order of magnitude (Table 4.1.11), the reduction occurring in a linear rather than biphasic fashion (Figure 4.1.5). A study by Dorr et al (2010) identified TisB, a toxin belonging to the *tisAB-istR* toxin-antitoxin system, as the key component in mediating persistence to ofloxacin in exponential-phase *E. coli* cells. The same response did not apply to persisters observed in stationary-phase cultures treated with ofloxacin. Studies have also shown stationary-phase cultures of *P. aeruginosa* to accumulate persisters in numbers comparable to those observed in biofilms (Spoering and Lewis, 2001).

Persister cell formation by KpIMS38 on exposure to levofloxacin was dependant on the size of the inoculum used. The increase in the number of persisters plateaued at a culture-to-medium ratio of 1:100, though biphasic killing was observed for all inocula used. These findings stand out from those observed when assaying persistence using inocula of different ages, indicating there are only a fixed amount of persisters that can be formed when using exponential-phase cultures. Unlike in stationary-phase cultures where multiple factors contribute to the formation of persisters, exposure to levofloxacin was most likely the factor that induced persistence in early-exponential cultures of KpIMS38.

There is a possibility that the survival of a fraction of the KpIMS38 population on exposure to levofloxacin, resulting in a biphasic death, could be a result of spontaneously-arisen resistant mutants. To verify whether this was the case, the KpIMS38 subpopulation obtained at the end of the biphasic-killing curve was grown in antibiotic-free conditions. The resultant culture was re-exposed to the same antibiotic treatment-regimen. If mutants arose in the subpopulation of survivors, they would exhibit diminished killing on retreatment with the antibiotic. Furthermore, subsequent cycles of regrowth and re-exposure would further increase the mutants till a point where antibiotic-induced death would be negligible. If, on the other hand, biphasic reduction of KpIMS38 was a consequence of the formation of persisters, the biphasic-killing curve would not change and be recapitulated in successive cycles of regrowth and re-exposure. The role of mutation in potentiating bacterial persistence is very different from that for antibiotic resistance. Specific mutants like the *E. coli* hipA7 strain, possessing a mutated variant of the toxin *hipA*, increased the frequency of persister formation. While this manifested as an increase in the number of survivors treated with antibiotics that inhibited murein synthesis, it did not increase the fitness of all the cells in the population to the same antibiotics (Moyed and Bertrand, 1983). This differs from mutations that confer antibiotic resistance and consequently increase the ability of all the cells in the population to overcome the inhibitory effect of the antibiotic (Woodford and Ellington, 2007). Biphasic killing of KpIMS38 by levofloxacin across four successive generations was indicative of the non-inheritable nature of survival exhibited by KpIMS38 exposed to levofloxacin. Exposing bacterial cultures to consecutive rounds of bactericidal antibiotics was implicated in increasing persister-cell formation (van den Bergh et al, 2016; Levin-Reisman et al, 2017). The same exercise yielded a different trend in KpIMS38. Persister-cell formation increased in the second generation on treatment with levofloxacin, but fell in the third and fourth generations.

Although biphasic killing was observed, an increase in the amount of time required to reach a particular cell density post-antibiotic exposure indicated a reduction in the fitness of the population emerging from persisters. Windels et al (2019) reported the formation of resistant mutants by *E. coli* on treatment with ciprofloxacin; mutations were accumulated in persister cells when exposed to concentrations close to the MIC. The results obtained in the present study indicate the ability of successive regimens of high concentrations of levofloxacin to reduce the number of persister cells formed by *K. pneumoniae*, thereby offering an avenue to treat persistent infections caused by the same. That being said, the effect of such high concentrations of levofloxacin on the host system remains to be evaluated.

The first plasmid-borne gene discovered that conferred resistance to quinolones in bacteria was *qnrA*, a protein belonging to the pentapeptide repeat family. The gene was identified in a clinical isolate of *K. pneumoniae*, located on the plasmid pMG252, a conjugative plasmid that conferred resistance to a broad class of antibiotics, including fluoroquinolones and nalidixic acid (Martínez-Martínez et al, 1998). The numerous variants of *qnr* genes that have been discovered since are categorised into six families - *qnrA*, *qnrB*, *qnrC*, *qnrD*, *qnrS*, and *qnrVC*, and confer resistance by protecting the DNA Gyrase and Topoisomerase IV enzymes. The proteins encoded by *qnr* genes exist in dimeric forms, forming a structure that mimics that of the β -conformation of DNA (Vetting et al, 2011). The complex competes for binding to the enzymes, thereby inhibiting the quinolones from binding to and inhibiting the activity of the enzymes (Pham et al, 2019). Research has also implicated efflux pumps in conferring plasmid-mediated resistance to quinolones to antibiotics. They however were observed to confer a low-level quinolone resistance, in addition to other antibiotics such as chloramphenicol, tetracycline, trimethoprim, and by themselves were insufficient to raise the resistance past the defined clinical breakpoint (Correia et al, 2017).

The lack of resistance to levofloxacin phenotypically observed by KpIMS38 was confirmed by scrutinising the genetic makeup of the isolate. The absence of *qnr* genes, conventionally located on plasmid DNA and associated with resistance to fluoroquinolones (Tran and Jacoby, 2002; Tran et al, 2005; Xiong et al, 2011), indicated the absence of horizontally-transmitted quinolone resistance in the isolate. Further, analysis of the QRDR in *gyrA* indicated a Ser83Tyr mutation with no mutation observed at the Asp87 site. Quinolone resistance has been linked to mutations at the 83rd amino acid position that generally involve replacements with hydrophobic amino acids such as alanine, isoleucine and leucine (Correia et al, 2017). Minarini and Darini (2012) observed the Ser83Tyr mutation at *gyrA* in *K. pneumoniae*, but did not detect any resistance to the quinolones tested including levofloxacin. Another study carried out by Weigel et al (1998) reported the mutation to be associated with resistance to quinolones, but also highlighted the presence of another mutation Asp87Asn in the same isolate. Alterations at the 83rd amino acid position account for a vast majority of mutations in the QRDR of GyrA, but are not as effective in impacting the activity of the enzyme as are changes to the aspartate residue at the 87th position, which in turn impede the catalytic activity of the enzyme by five- to ten-fold (Correia et al, 2017). The quinolone resistance observed by Weigl and colleagues is likely to be a consequence of the mutation at the 87th amino acid. The absence of this mutation in KpIMS38 can therefore be implicated in the lack of resistance of the isolate to quinolones.

KpIMS38 cultures pre-exposed to levofloxacin resisted the lethal action of amikacin and meropenem. The antibiotics belonged to the aminoglycoside and carbapenem class of drugs respectively, acting on cellular targets different from those affected by the fluoroquinolone levofloxacin. Survival of the cultures at concentrations previously demonstrated to be lethal (Figure 4.1.2) with a reduction by only 0.5 orders of magnitude indicated a degree of protection afforded to the culture by persister-cell formation. Persister cells formed by

strains belonging to the ESKAPE group of bacterial pathogens were able to tolerate exposure to antibiotics much better than their non-persister counterparts. Stationary-phase cultures of *K. pneumoniae* were treated with lethal concentrations of the aminoglycoside amikacin for multiple successive rounds, which resulted in the selection of a subpopulation of cells with increased persister-formation (Michiels et al, 2016). These "high-persistence" clones were able to survive lethal concentrations of amikacin, meropenem and colistin. The number of survivors were at least two orders of magnitude higher than that observed in the wild-type strain of *K. pneumoniae*, although the number of survivors after treatment with the fluoroquinolone ciprofloxacin did not significantly differ between both types of cells. Regardless, the possibility of resistance-causing mutation conferring the ability to survive was ruled out due to the unaltered MICs for the drugs tested (Michiels et al, 2016). The MIC of amikacin and meropenem for KpIMS38 persisters, generated by treating exponential-phase cultures with levofloxacin, was invariant from that for non-persister KpIMS38 cultures, indicating survival to not be a consequence of resistance to both the drugs. When both sets of the cultures – persister and non-persisters – were grown on MH agar, they contained a similar number of survivors. This feature was observed on treatment with amikacin as well as meropenem, but was not observed below the determined MIC; the number of survivors in the non-persisters far exceeded those in the persisters. This could be indicative of a slow-growth phenotype exhibited by the persisters, a phenomenon that has been observed in other studies dealing with bacterial persistence (Bigger, 1944; Balaban et al, 2004; Pontes and Groisman, 2020).

Assessment of KpIMS38 cultures using flow cytometry indicated the presence of two subpopulations - P1 and P2. Cells in the P2 subpopulation were larger, exhibited higher metabolic activity and accounted for a smaller fraction of the overall cell-population when compared to P1. Persistence is reported to have diverse effects on the shape of bacterial

cells. *E. coli* persisters are known to exist as filaments (Sulaiman and Lam, 2020) as well as cells with reduced dimensions (Shah et al, 2006; Uzoechi and Abu-Lail, 2020). Treatment with levofloxacin led to an increase in the number as well as overall size of KpIMS38 cells belonging to the P2 subpopulation, without a concomitant reduction of the same in P1. On exposure to levofloxacin, the number of P2 cells gradually increased for 4 hours. The number sharply declined at the 6th hour, beyond which it was comparable to the number of P2 cells observed at similar time points in the untreated KpIMS38 population. *E. coli* DH5 α treated with ampicillin initially produced small-sized persister cells that gradually increased in size as the treatment prolonged. Adoption of a small cell-size was initially believed to conserve energy and limit exposure to the antibiotic (Power et al, 2021). An explanation for the higher CFDA fluorescence and the considerable variation in the same observed in P2 cells could be acquired from figure 4.1.15. The P2 subpopulation was more heterogenous than the P1 with regard to the FSC and SSC values of cells contained within each; the FSC (and by extension, the size) of P1 cells contained within 1 order of magnitude while the same spanning 3 orders of magnitude for cells belonging to the P2 subpopulation. Larger the cell size, greater the amount of CFDA acquired and consequently higher the fluorescence. This reasoning, taken with the heterogeneity in cell size, would explain the substantial variation in the fluorescence from CFDA observed in the P2 subpopulation of KpIMS38. On the basis of the same reasoning, any cells with reduced metabolism would exhibit weak CFDA fluorescence. Persister cells are known to exhibit reduced metabolism (Shah et al, 2006; Wainwright et al, 2021). However, the presence of weakly fluorescent cells in the P2 subpopulation would be obscured by the presence of cells with diverse levels of fluorescence. Although the use of advanced techniques like imaging flow cytometry would permit a study of the same better

than conventional flow cytometry, the results of the present study do not exclude the presence of such cells.

Single-cell analytics coupled with microfluidics have enabled the elucidation of bacteria persistence, most notable being the discovery of a pre-existing population of bacteria in exponentially-growing cells that eventually formed persisters (Balaban et al, 2004; Shah et al, 2006; Orman and Brynildsen, 2013). The current study utilised bacteria immobilised within a flow-cell and coupled it to fluorescence microscopy to evaluate changes in the population of KpIMS38 on exposure to levofloxacin. The cells grew normally, dividing and increasing in number, in the absence of antibiotic treatment. On exposure to levofloxacin, cell division was halted and accompanied by cell death. Removal of the antibiotic stress by growth in drug-free medium surprisingly did not result in a resumption of bacterial growth and division, even 8 hours after discontinuation of the antibiotic-treatment. Cell elongation was observed in the population of KpIMS38; present in the culture prior to antibiotic treatment, their number increased on exposure to levofloxacin. Also distinct was the consistent fluorescence of the reporter mCherry from the cells, indicating continued cell metabolism. A study carried out to study the persistence of *E. coli* treated with ampicillin observed the presence of two kinds of cells that were physically identical (deduced through flow cytometry and microscopy) but only one group was able to grow in fresh media. Those that grew were deduced to be persisters and those that didn't were identified as viable but non-culturable (VBNC) cells; the later outnumbering the former (Power et al, 2021). The occurrence of VBNC cells in the levofloxacin-treated culture would explain the absence of cell division observed even after removal of the antibiotic. An argument against the same can be made on the basis that if persisters were present they should have grown during the revival phase, i.e., in the presence of antibiotic-free medium, though an explanation for the same can be afforded by the scarceness of

persisters compared to VBNC cells in the culture. VBNC cells outnumbered persisters by approximately 100:1 in *E. coli* (Orman and Brynildsen, 2013), were present in exponential-phase cultures along with persister cells and survived treatment with lethal concentrations of antibiotics (Ayrapetyan et al, 2015; Gonçalves and de Carvalho, 2016). The presence of VBNCs in KpIMS38 treated with levofloxacin would explain the presence of metabolically-active cells observed during microscopy as well as flow cytometry. Although the results obtained in the present study do not confirm the involvement of VBNC in the biphasic survival of KpIMS38 to levofloxacin, they merely highlight the heterogeneity present in the bacterial population and require specialised analyses to pin down a distinct mode of survival.

Overall, the observations reported in this section indicated persister-cell formation in a clinical isolate of *K. pneumoniae* on exposure to the fluoroquinolone levofloxacin. Persistence was non-heritable and conferred cross-tolerance to lethal concentrations of other antibiotics. Furthermore, KpIMS38 consisted of two subpopulations P1 and P2, the latter consisting of larger cells. Treatment with levofloxacin did not reduce cellular metabolism although cell division was stalled and did not resume even after the removal of the antibiotic.

4.2 Elucidation of the genome and transcriptome of persister cells formed by *K. pneumoniae*

4.2.1 Background of the study

The observations made and results obtained through experimentation carried out in the preceding section unambiguously indicate the formation of persister cells by the *Klebsiella pneumoniae* isolate KpIMS38. As indicated by the available literature and our results, not all isolates of a species and not all species of a genus form persister cells. In order to proceed further in our investigation of this phenomenon, it was important to acquire insights into the genetic composition of the isolate as well as differential gene-expression patterns during persistence. We therefore proceeded to sequence the genome of KpIMS38. Subsequently, we analysed the whole-cell transcriptome of KpIMS38 persisters and observed the expression profile.

The profile of transcribed genes in persister cells formed by KpIMS38 on treatment with levofloxacin was acquired through the use of Next-Gen Sequencing (NGS) technology. The workflow for the same involved sequencing and annotating the genome of KpIMS38 cells, sequencing the mRNA obtained from KpIMS38 cells treated with levofloxacin using the genome as reference, and identifying the expression profile of the annotated genes. The entire workflow was conducted at the lab-facility of M/s Thermofisher Scientific Pvt Ltd, India. The genome sequence was analysed using various web-based software to annotate the genome as well as obtain additional information about the organism. Further, differential gene expression on treatment with levofloxacin was also analysed across different functional categories in the transcriptome of KpIMS38.

4.2.2 Analysis of the genome sequence of KpIMS38, a persister-forming clinical isolate of *K. pneumoniae*

4.2.2.1 Sequencing and annotation of the genome of KpIMS38 by Next-Gen DNA

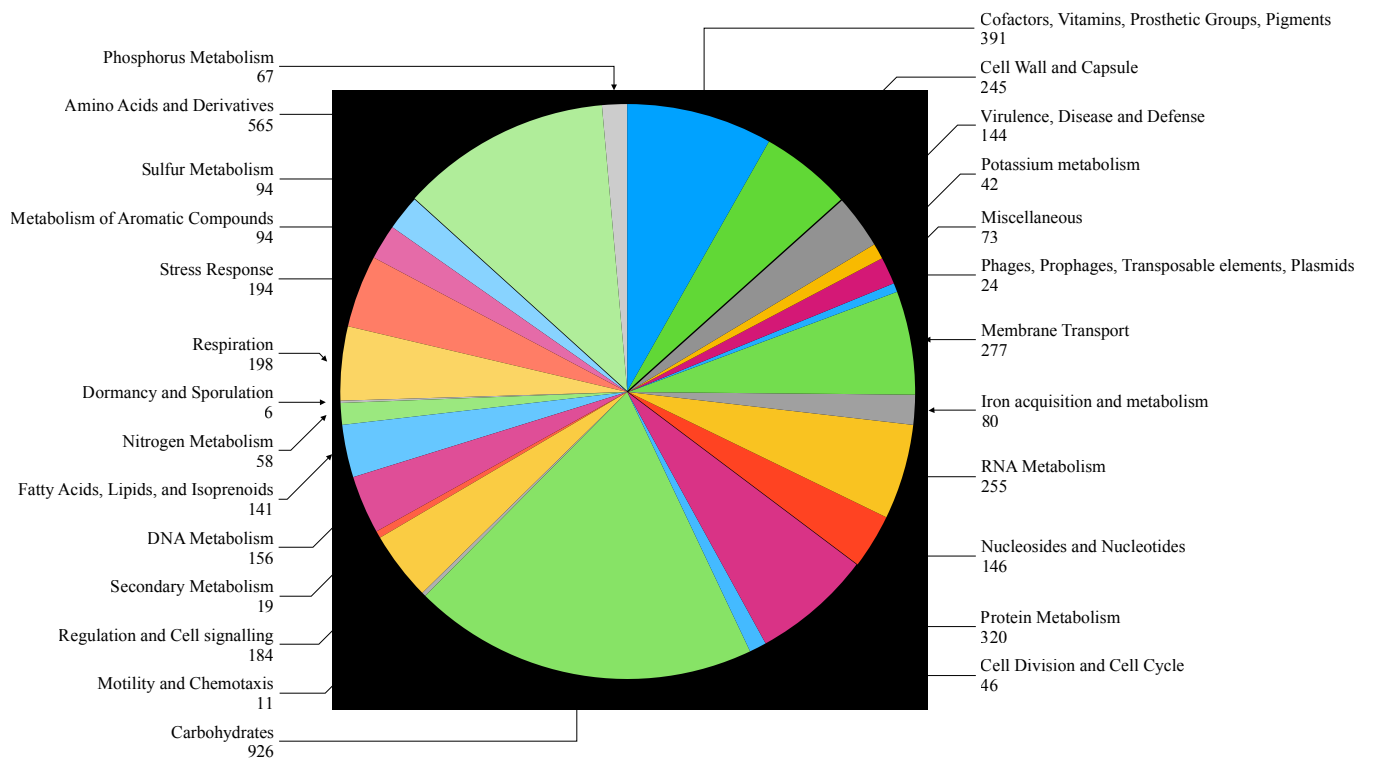
Sequencing

A total of 597006766 bases in the form of 1700049 reads were obtained with an average read length of 351 bases. The reads were assembled to yield 169 contigs, the average contig size being 72636 bases. These contigs amounted to 5308664 bases, with a G+C content of 57.3%. After annotation using the RAST server, 4284 protein-coding genes with assigned functions were identified within the genome of KpIMS38. In addition, 92 genes coding for RNAs and 902 genes coding for hypothetical proteins were also identified.

In addition, the inherent plasmid DNA within KpIMS38, named as pKpIMS38, was also sequenced. The DNA sequence was obtained as 60120 reads comprising of 18357749 bases in all, with an average read length of 305 bases. The reads were assembled into 71 contigs, amounting to a total of 21082 bp in size with 42.59% G+C and the average contig size being 398 bases. The contigs were run through the Genemark S software to predict coding genes and were annotated using the Blast2GO algorithm to yield 39 genes. However, 14 genes had neither any functional description nor gene ontology, but all were of an average size of 37 bp. Of the remaining 25 genes, 9 showed up as hypothetical proteins and 5 as uncharacterised. Blast2GO could assign functions to a total of 11 genes among which gene ontologies were obtained for only 7 genes.

The contigs representing the sequenced chromosomal genome of KpIMS38 were analysed by RAST. Genes annotated through the RAST server were categorized by the software into categories on the basis of their function (Figure 4.2.1). Categories represented large groups of genes broadly clubbed together based on functional similarity. Each category

was divided into sub-categories, which were further segregated into subsystems. Each subsystem consisted of genes with a common functional role. For example, the subsystem “DNA repair, UvrABC system” was located within the DNA repair subcategory, which itself was one of the 156 subcategories grouped under the DNA Metabolism category. The subsystem consisted of 6 features or genes grouped into 4 roles – Excinuclease ABC subunit A, Excinuclease ABC subunit B, Excinuclease ABC subunit C, Excinuclease ABC subunit A paralog of unknown function and Excinuclease cho (excinuclease ABC alternative C subunit).



Of the total number of annotated genes, 60% of the genome of KpIMS38 was grouped into subsystems, accounting for 3095 genes. Most of the genes identified belonged to the

Carbohydrates category (926 genes), followed by Amino acids and its derivatives (565 genes). The KpIMS38 genome did not contain any genes for photosynthesis.

4.2.2.2 Determination of the sequence type of KpIMS38 using Multi-Locus Sequence

Typing

The genome sequence was used to perform multi-locus sequence typing (MLST) using the MLST 2.0 tool available on the Centre for Genomic Epidemiology (CGE) website. The MLST results revealed the isolate KpIMS38 belonged to the sequence type ST-13. The details of the analysis are presented in table 4.2.1.

Table 4.2.1 Sequence type of KpIMS38 obtained through the MLST 2.0 tool.

Locus	Identity	Coverage	Alignment length	Allele length	Allele
<i>gapA</i>	100	100	450	450	gapA_2
<i>infB</i>	100	100	318	318	infB_3
<i>mdh</i>	100	100	477	477	mdh_1
<i>pgi</i>	100	100	432	432	pgi_1
<i>phoE</i>	100	100	420	420	phoE_10
<i>rpoB</i>	100	100	501	501	rpoB_1
<i>tonB</i>	100	100	414	414	tonB_19

4.2.2.3 Identification of resistance genes in the genome of KpIMS38

The ResFinder 4.1 tool, hosted on the CGE website, was used to identify the number and type of antibiotic-resistance genes present in the genome of KpIMS38. The ResFinder analysis indicated the current isolate possessed a genetic background to confer resistance to beta-lactams, aminoglycosides and fosfomycin. Loci for the genes *bla*_{SHV-101}, *bla*_{CTX-M-15}, *aac*(3)-II_d and *fosA* were identified within the genome of KpIMS38, each with 99% or greater identity to the corresponding gene sequences. The details of the analysis have been reported in table 4.2.2. Of note is the presence of the gene *bla*_{CTX-M-15}, which has been

indicated by the ResFinder tool to confer resistance to the beta-lactam drugs amoxicillin, ampicillin, aztreonam, cefepime, cefotaxime, ceftazidime, ceftriaxone, piperacillin and ticarcillin. The gene *aac(3)-IIId*, also present in the genome, was shown to possess the ability to resist the aminoglycosides apramycin, dibekacin, gentamicin, netilmicin, sisomicin and tobramycin.

Table 4.2.2 Antibiotic-resistance genes identified in the genome of KpIMS38 using ResFinder 4.1. The identified genes are listed along with the identity of the hit (%), the coverage of the query vis-à-vis the subject sequence (%), the type of drug-resistance conferred, and the accession number of the subject sequence.

Gene	Homology (%)	Coverage (%)	Resistance	Accession no. (of homologous genes from the database)
<i>bla_{SHV-101}</i>	99.88	100	Beta-lactams	EU155018
<i>bla_{CTX-M-15}</i>	100	100	Beta-lactams	AY044436
<i>aac(3)-IIId</i>	99.88	100	Aminoglycoside	EU022314
<i>fosA</i>	99.52	100	Fosfomycin	ACWO01000079

The genome sequence of KpIMS38 was also analysed using the Resistance Gene Identifier (RGI) 5.2.0 tool available on the Comprehensive Antibiotic Resistance Database (CARD) 3.1.4 (McArthur et al, 2013). The output contained a list of hits that were categorised on the basis of the identity between the test and database sequences; perfect hits had 100% identity while strict hits had a homology lower than 100%. The results were compiled in table 4.2.3, where each hit was tabulated along with the identity to its corresponding sequence in KpIMS38, the mechanism of resistance it imparts, the classes of drugs it can impart resistance to, and the gene-family to which it belongs; all the information being supplied by the output from RGI.

A total of four perfect and seventeen strict hits were obtained in the genome of KpIMS38. The gene identified as *bla_{SHV-101}* by ResFinder was identified by RGI as SHV1 with 100%

identity, while *bla*_{CTX-M-15} was correctly identified with 100% identity. The gene *aac*(3)-II_d was also identified by RGI with 100% identity, unlike the 99.88% homology observed using ResFinder. A gene *kpnF* coding for an antibiotic efflux pump was identified with 100% identity by RGI in the genome of KpIMS38 but was absent from the ResFinder analysis.

RGI identified seventeen antibiotic-resistance genes in the genome-sequence of KpIMS38 with sub-100% or "strict" homology. Eleven genes were associated with antibiotic efflux, while five of the remaining were categorised under altering the target of the antibiotic. The hits generated by RGI under the antibiotic efflux category included three members from the resistance-nodulation-cell division (RND) superfamily of efflux pumps, five belonging to the major facilitator superfamily (MFS) and a single member from the ATP-binding cassette (ABC) superfamily of efflux pumps. In addition, two hits were obtained – one belonging to the class of general bacterial porins, and the other categorised under both porins as well as RND superfamily of efflux pumps. The hits mapped to the RND superfamily were described by RGI to provide resistance to aminoglycosides, aminocoumarins, fluoroquinolones, macrolides, penam group of β -lactams and tetracycline, whereas those from the MFS imparted resistance to aminoglycosides, cephalosporins and cephamycins, fluoroquinolones, macrolides, antibiotics belonging to the penam and penem groups of β -lactams, peptide antibiotics, rifamycins and tetracycline. The hit mapped to the ABC pump was reported as inducing resistance to nitroimidazole antibiotics, while that categorised under general bacterial porins was associated with reduced permeability to carbapenems, cephalosporins, cephamycins, monobactams, and the penam and penem group of antibiotics. The hit associated with both porins and RND efflux pumps had the potential to impart resistance to a wide variety of antibiotic compounds, which included monobactam; carbapenems, cephalosporins, cephamycins,

fluoroquinolones, glycylicyclines, penams and penems, phenicol antibiotics, rifamycins, tetracycline and triclosan.

Also of significance are the categorisation of genes involved in routine cellular metabolism as contributors to antibiotic resistance. Mutations were mapped by RGI to single-nucleotide polymorphisms (SNPs) viz. R234F in Ef-Tu and E350Q in UhpT, that resulted in a propensity to cause resistance against pulvomycin, a translation inhibitor, and fosfomycin, an inhibitor of the bacterial cell-wall synthesis. The mutation in *marR* was not attributed to a SNP but was classified as protein overexpression by RGI, conferring resistance to a wide range of antimicrobial compounds viz. cephalosporins, chloramphenicol, fluoroquinolones, glycylicyclines, penams, rifamycins, tetracycline and triclosan.

The CARD database, queried by RGI to identify antibiotic-resistance genes, was formulated using the genome of *E. coli*. Due to the lack of an option to query the database for genes specifically pertaining to *K. pneumoniae*, each of the sequence-hits obtained by RGI were reassessed using the BLASTx algorithm available on the NCBI server. The comparison indicated that there was agreement on the function assigned to fourteen of the total twenty-one hits. However, the function ascribed by RGI was found to be misleading for eight hits that accounted for 38% of the total results. A common observation was the categorisation of the *kpn* genes by RGI under the MFS efflux system, whereas they actually belong to or show similarity to genes from the SMR superfamily of efflux pumps. This misclassification was identified in two of the *kpn* genes, namely, *kpnF* and *kpnE*. The other two *kpn* genes identified by RGI, i.e., *kpnG* and *kpnH* were observed to correctly map to the MFS efflux system. However, they were identified by BLASTx as *emrA* and *emrB* respectively. Another feature observed was the categorisation of transcriptional regulators by RGI as components of bacterial efflux systems. The hit "CRP", categorised

under RND superfamily, was actually found to be a DNA-binding protein that acted as a global transcriptional regulator in *K. pneumoniae*. A similar function was unearthed for the hit "H-NS", which was grouped under both MFS and RND superfamilies of efflux pumps by RGI. The hit "*emrR*" was categorised as a member of the MFS and implicated in fluoroquinolone resistance but was identified as a transcriptional repressor MprA present in various species of *Klebsiella*. Similarly, the "*marA*" and "*marR*" genes categorised under both the RND efflux system and general bacterial porins were actually identified as transcriptional regulators MarA and MarR responsible for the activity of the multidrug efflux pump AcrAB.

The seventeenth "strict" gene identified by RGI showed 99.28% homology to the fosfomycin resistance gene *fosA6*, a fosfomycin thiol transferase. The nucleotide sequence was analysed using the BLASTn algorithm, whose results identified the gene as a fosfomycin resistance glutathione transferase belonging to the FosA family in multiple strains of *K. pneumoniae* with 100% identity. The homology of the protein translated from the nucleotide sequence was assessed using the BLASTx algorithm, and the top 100 hits obtained belonged to FosA5 family fosfomycin resistance glutathione transferases. The top hit – with 100% identity – was identified in Enterobacteriaceae, while the successive 9 hits mapped to *Klebsiella pneumoniae* with 99.28% homology. The reason for the sub-100% homology was due to the presence of single amino acid changes in the protein sequence. These changes were observed at various positions within the amino acid sequence but were limited to one single change per sequence. These results indicated the wide array of genes present in KpIMS38 that could potentially confer upon the isolate the ability to resist the action of antibiotics from various classes.

Table 4.2.3 Antibiotic-resistance genes identified in the genome of KpIMS38 using RGI 5.2.0. Each of the hits are tabulated along with the homology (%), the resistance-mechanism of the gene and its functional classification. The functional classification of each hit was verified by blastx and is also presented along with its homology (%) within brackets. MFS – Major facilitator superfamily, RND – Resistance-nodulation-cell division superfamily, ABC – ATP-binding cassette superfamily, SMR – Small multidrug resistance, ESBL – Extended-spectrum β -lactamase, cAMP – cyclic Adenosine monophosphate.

Hit	Homology (%)	Mechanism	Gene Family (RGI)	Gene function (blastx) with homology (%)
<i>kpnF</i>	100	Efflux	MFS efflux system	SMR subunit KpnF (99.08)
SHV-1	100	Drug inactivation	SHV β -lactamase	SHV-1 β -lactamase (100)
CTX-M-15	100	Drug inactivation	CTX-M β -lactamase	Class A ESBL CTX-M-197 (99.66)
AAC(3)-IId	100	Drug inactivation	aac(3) aminoglycoside acetyltransferase	Aminoglycoside N-acetyltransferase AAC(3)-IId (99.65)
<i>kpnG</i>	99.74	Efflux	MFS efflux system	MFS periplasmic adaptor subunit EmrA (99.74)
<i>kpnE</i>	99.17	Efflux	MFS efflux system	SMR subunit KpnE (99.17)
CRP	99.05	Efflux	RND efflux system	cAMP-activated global transcriptional regulator CRP (99.52)
H-NS	94.07	Efflux	MFS efflux system, RND efflux system	DNA-binding transcriptional regulator H-NS (99.26)
<i>kpnH</i>	93.95	Efflux	MFS efflux system	MFS permease subunit EmrB (99.80)

Hit	Homology (%)	Mechanism	Gene Family (RGI)	Gene function (blastx) with homology (%)
<i>msbA</i>	92.78	Efflux	ABC efflux system	ABC permease MsbA (99.83%)
<i>emrR</i>	92.57	Efflux	MFS efflux system	Transcriptional repressor MprA (99.43)
<i>baeR</i>	92.05	Efflux	RND efflux system	Two-component system response regulator BaeR (99.58)
<i>adeF</i>	41.71	Efflux	RND efflux system	RND permease AcrD (99.90)
<i>marA</i>	92.74	Efflux, reduced permeability	RND efflux system, general bacterial porin	AcrAB transcriptional activator MarA (99.19)
<i>fosA6</i>	99.28	Drug inactivation	Fosfomycin thiol transferase	FosA5 family glutathione transferase (99.28)
<i>eptB</i>	99.46	Drug-target alteration	pmr phosphoethanolamine transferase	Kdo-(2)-lipid A phosphoethanolamine 7"-transferase (99.82)
<i>arnT</i>	99.09	Drug-target alteration	pmr phosphoethanolamine transferase	Lipid IV(A) 4-amino-4-deoxy-L-arabinosyltransferase (100)
<i>E.coli</i> EF-Tu mutant	97.97	Drug-target alteration	Elfamycin resistant EF-Tu	Translation elongation factor Ef-Tu (100)
<i>E.coli</i> <i>uhpT</i> mutant	95.03	Drug-target alteration	Antibiotic-resistant UhpT	Hexose-6-phosphate:phosphate antiporter UhpT (99.78)
<i>E.coli</i> <i>marR</i> mutant	84.03	Efflux, drug-target alteration	RND efflux system	Transcriptional regulator MarR (100)
OmpK37	99.47	Reduced permeability	General bacterial porin	Porin OmpK37 (99.73)

4.2.2.4 Identification of virulence genes in the genome of KpIMS38

The number and type of virulence genes in the genome sequence of KpIMS38 were analysed using the Single genome analysis tool available through BacWGSTdb (Feng et al, 2021). The results of the analysis are presented in table 4.2.4. The table contains the homology of each of the virulence genes identified as well as its functional annotation as determined through the BacWGST database. A total of 63 genes were identified by the program with a median homology of 99.19%; the lowest recorded homology being 86.75%. The list included genes commonly associated with virulence, such a genes for the synthesis of fimbriae, pili, extracellular capsule, the siderophore enterobactin and the type VI secretion system.

Table 4.2.4 Virulence genes identified in the genome of KpIMS38 using the Single genome analysis tool. Each of the genes identified is tabulated along with its homology and its functional annotation as derived using the BacWGST database. LPS – Lipopolysaccharide, T6SS – Type VI secretion system.

Gene	Homology	Functional annotation
<i>entB</i>	99.41	2,3-dihydro-2,3-dihydroxybenzoate synthetase
<i>entA</i>	98.47	2,3-dihydroxybenzoate-2,3-dehydrogenase
<i>gnd</i>	95.02	6-phosphogluconate dehydrogenase
<i>acrA</i>	99.41	Acriflavine resistance protein A
<i>acrB</i>	99.65	Acriflavine resistance protein B
<i>yagY/ecpB</i>	88.41	<i>E. coli</i> common pilus chaperone EcpB
<i>yagZ/ecpA</i>	90.24	<i>E. coli</i> common pilus structural subunit EcpA
<i>yagX/ecpC</i>	87.48	<i>E. coli</i> common pilus usher EcpC
<i>ybdA</i>	99.36	Enterobactin exporter ents
<i>entE</i>	99.38	Enterobactin synthase subunit E

Gene	Homology	Functional annotation
<i>fes</i>	99.01	Enterobactin/ferric enterobactin esterase
<i>entD</i>	97.46	Enterochelin synthetase component D
<i>mrkD</i>	99.4	Fimbrial adhesin protein precursor MrkD
<i>mrkC</i>	99.32	Fimbrial biogenesis outer membrane usher protein precursor MrkC
<i>mrkB</i>	99.86	Fimbrial chaperone protein MrkB precursor
<i>wbbM</i>	98.89	Glycosyltransferase
<i>wbbN</i>	98.66	Glycosyltransferase
<i>wbbO</i>	99.38	Glycosyltransferase family 1 protein
<i>kfoC</i>	99.34	Glycosyltransferase family 2 protein
<i>fepC</i>	99.5	Iron-enterobactin transporter ATP-binding protein
<i>fepB</i>	99.69	Iron-enterobactin transporter periplasmic binding protein
<i>fepG</i>	99.19	Iron-enterobactin transporter permease
<i>entC</i>	99.33	Isochorismate synthase
<i>wzt</i>	97.3	LPS O-antigen ABC transport system ATP-binding component
<i>wzm</i>	99.23	LPS O-antigen ABC transport system transmembrane component
<i>mrkI</i>	98.97	LuxR family regulatory protein
<i>manC</i>	97.1	Mannose-1-phosphate guanylyltransferase
<i>fepA</i>	97.36	Outer membrane receptor FepA
<i>fimD</i>	99.13	Outer membrane usher protein
<i>fimC</i>	99.59	Periplasmic chaperone
<i>cpsACP</i>	91.15	Phosphatase PAP2 family protein
<i>mrkJ</i>	100	Phosphodiesterase
<i>manB</i>	98.69	Phosphomannomutase

Gene	Homology	Functional annotation
<i>yagW/ecpD</i>	88.92	Polymerized tip adhesin of ECP fibers
<i>ykgK/ecpR</i>	86.75	Regulator protein EcpR
<i>iroE</i>	99.04	Siderophore esterase IroE
<i>wzi</i>	87.05	Surface assembly of capsule
<i>mrkH</i>	100	Transcriptional activator
<i>rcaA</i>	99.84	Transcriptional activator for ctr capsule biosynthesis
<i>fimK</i>	99.28	Transcriptional regulator
<i>rcaB</i>	100	Transcriptional regulator RcsB
<i>fimH</i>	99.01	Type 1 fimbrial adhesin precursor
<i>fimG</i>	99.4	Type 1 fimbrial minor component
<i>fimF</i>	98.87	Type 1 fimbrial minor component
<i>fimA</i>	99.82	Type 1 major fimbrial subunit precursor
<i>fimI</i>	99.37	Type 1 pilus biosynthesis fimbrial protein
<i>mrkA</i>	95.07	Type 3 fimbrial major pilin subunit mrka
<i>mrkF</i>	100	Type 3 fimbrial minor pilin subunit mrkf
<i>icmF/tssM</i>	97.6	T6SS protein TssM
<i>clpV/tssH</i>	98.83	T6SS ATPase TssH
<i>tssF</i>	99.43	T6SS baseplate subunit TssF
<i>tssG</i>	99.36	T6SS baseplate subunit TssG
<i>vasE/tssK</i>	99.33	T6SS baseplate subunit TssK
<i>vipB/tssC</i>	98.38	T6SS contractile sheath large subunit VipB
<i>vipA/tssB</i>	99.19	T6SS contractile sheath small subunit VipA
<i>sciN/tssJ</i>	100	T6SS lipoprotein TssJ

Gene	Homology	Functional annotation
<i>dotU/tssL</i>	99.28	T6SS protein TssL
<i>hcp/tssD</i>	99.39	T6SS protein belonging to Hcp family
<i>fimB</i>	99.17	Tyrosine recombinase
<i>fimE</i>	99.01	Tyrosine recombinase
<i>glf</i>	98.1	UDP-galactopyranose mutase
<i>ugd</i>	95.63	UDP-glucose 6-dehydrogenase
<i>galF</i>	99.44	UTP-glucose-1-phosphate uridylyl transferase subunit GalF

4.2.2.5 Identification of extrachromosomal elements in the genome of *KpIMS38*

The genome of *KpIMS38* was analysed to search for extrachromosomal elements. The Single genome analysis tool available on BacWGSTdb provided information on plasmids present within the genome while the online tool Phaster (Arndt et al, 2016) was used to obtain information about bacteriophages present within the sequence.

The tool discovered three replication-origins within the genome of *KpIMS38*. The replicons for the plasmids Col(pHAD28), IncFII(K) and IncR were identified with 95.5, 95.9 and 99.2 % homology respectively, all of whom have been reported in gram-negative bacteria. The program also predicted the presence of two distinct plasmids integrated within the chromosome of *KpIMS38*. A larger plasmid "pKPN-d6b" sized 26.45 kb was identified along with a smaller plasmid "punamed6" that was 7.12 kb in size. Both plasmids were identified with 99% homology and bore similarity to plasmids described in clinical strains of *K. pneumoniae* causing infection in humans. The larger plasmid was originally reported in a strain Kpn555 in USA in the year 2014, while the smaller plasmid was first described in the strain BD_DM_697 three years later in Dhaka, Bangladesh.

The details of the output obtained from Phaster are compiled in table 4.2.5 and revealed a total of five prophage regions present in the chromosome of KpIMS38. Three regions were denoted as ‘intact’ prophages while the remaining two (regions 2 and 5) were classified as ‘incomplete’. This classification was determined by a composite score calculated factoring the number of phage genes detected, the size of the prophage region detected, the number of proteins detected in the region and the proportion of phage proteins accounting for those detected (Zhou et al, 2011). A majority of the bacteriophages the five regions showed homology to were previously not known to infect *Klebsiella*. The largest of the identified phage genomes – region 1 – had a total of fifty seven protein-coding genes of which thirty two were associated with the phage SPN1S identified in *Salmonella*. Thirty one genes from region 1 exhibited sequence-similarity to phage genes belonging to the *Escherichia* phage ϕ v10. The highest number of bacteriophage genes identified in regions 2 and 4 mapped to Enterobacteria phages ϕ P27 and mEp235 and were not associated with a specific bacterial genus. *Escherichia* phages had the highest number of genes homologous to those identified in regions 3 and 5. Additionally, the Enterobacteria phage mEp235 also had the highest number of similar genes (seven) to those in region 3. Protein-coding genes with sequence-similarity to genes from phages known to infect *Klebsiella* were also identified in each of the five prophage regions by Phaster. The number of such genes, however, was very small; specifically limited to one gene per region and therefore insufficient to identify the prophages as belonging to specific *Klebsiella* phages (Table 4.2.5).

Table 4.2.5 Prophage regions located in the genome of KpMS38 by Phaster. Each of the regions identified by the program is tabulated along with its size (in kb), the total number of protein-coding genes present in the region, the bacteriophage with the most number of proteins similar to those identified (referred to here as the most common phage), the classification of the phage, and the proportion of similar proteins in the most common phage (in %). All of the bacteriophages identified as most-common phage belonged to the order Caudovirales, hence the classification contains information from the family level onwards. Additionally, any phages associated with *Klebsiella* are also listed along with the number of genes it contains that are similar to genes identified by Phaster in brackets.

Prophage region	Size (kb)	Total proteins	Most common phage	Classification of most common phage	Phage-protein similarity (%)	<i>Klebsiella</i> phages (number of proteins)
1	53.9	57	<i>Salmonella</i> phage SPN1S	Podoviridae › Uetakevirus	56.14	Phage 13 (1), Phage ST15-OXA48φ14.1 (1)
2	21	12	Enterobacteria phage φP27	Myoviridae	16.66	-
3	30.9	44	<i>Escherichia</i> phage HK75	Siphoviridae › Hendrixvirinae › Saikungvirus	15.9	Phage PKP126 (1), Phage Sin4 (1), Phage Sugarland (1), Phage Seifer (1), Phage vB_Kpn_IME260 (1)
			Enterobacteria phage mEp235	Siphoviridae › Hendrixvirinae › Nochtlivirus	15.9	
4	29.1	40	Enterobacteria phage mEp235	Siphoviridae › Hendrixvirinae › Nochtlivirus	30	Phage N137 (1), Phage TSK1 (1), Phage PKP126 (1), Phage Sin4 (1)
5	11.4	15	<i>Escherichia</i> phage 500465-1	Myoviridae › Peduovirinae › Felsduovirus	86.66	Phage ST437-OXA245φ4.1 (1), Phage ST15-OXA48φ14.1 (1)

4.2.3 Analysis of the whole-cell transcriptome of persister cells formed by KpIMS38 on treatment with levofloxacin

Persister cells represent a state that is metabolically distinct from its non-persister counterpart. The isogenic nature of persisters vis-à-vis non-persister cells further highlights the significance of elucidating the pattern of gene expression in the former. Having obtained a genome sequence of KpIMS38 (as previously indicated in section 4.2.2), we acquired the transcriptomes of untreated and levofloxacin-treated cultures of KpIMS38 and compared both to obtain the relative gene expression in KpIMS38 persisters.

4.2.3.1 Determination of the expression profile of KpIMS38 persister cells by RNA-Seq

A reference-guided analysis was utilized to analyse the transcriptome of KpIMS38 cells treated with levofloxacin. Here, the reads were aligned to the annotated genome of KpIMS38 using Tophat2 (Kim et al, 2013); any reads that didn't map to the genome were aligned using Bowtie2 (Langmead and Salzberg, 2012). The statistics from the assembly are presented in table 4.2.6, through which it is indicated that a major part of the transcripts obtained from both untreated and levofloxacin-treated cells mapped to the genome sequence of KpIMS38.

Table 4.2.6 Statistics of the assembly of the RNA transcripts from untreated as well as levofloxacin-treated KpIMS38 as performed using NGS.

Samples	Untreated	Levofloxacin-treated
Total Reads per sample	9,819,170	8,958,680
Reads mapped through Tophat2	8,485,523	7,635,819
Reads mapped through Bowtie2	1,239,596	1,061,999
Total mapped reads	9,725,119	8,697,818
% mapped reads on genome	99.04%	97.08%

4.2.3.2 Evaluation of gene expression across various categories in KpIMS38 persister cells

The gene expression in untreated and levofloxacin-treated cells was compiled and the changes in expression for genes in all twenty six categories were quantified on the basis of the $\log_2(\text{fold change})$ observed. The transcriptome thereby obtained indicated differential gene expression in a total of 2874 genes on treating KpIMS38 with 256 $\mu\text{g/mL}$ of levofloxacin. Further scrutiny indicated the presence a large cluster comprised of genes involved in basic cellular metabolism. The categories "Carbohydrates", "Amino Acids & derivatives" and "Protein Metabolism" accounted for 1000 ($\approx 35\%$) of the differentially expressed genes (Table 4.2.7). This was followed by genes categorised "Membrane Transport" and "Cofactors, Vitamins, Prosthetic groups and Pigments", accounting for 207 and 204 genes respectively. Gene-expression was observed in the categories "DNA Metabolism" and "Stress Response", both accounting for 140 genes each with differential expression. The category where treatment with levofloxacin perturbed the expression of the fewest number of genes was "Secondary Metabolism" with 3 genes. This was followed by 4 genes from "Motility & Chemotaxis" and 5 genes from "Dormancy & Sporulation". Comparing the differential expression of genes as a percentage of the total number of genes annotated in the category revealed striking differences from the previous trends. Treatment with levofloxacin affected the expression of genes belonging to "DNA Metabolism" the most; almost 90% of the genes being differentially expressed (Table 4.2.7). This was followed by genes representing the category "Virulence, Disease and Defence", with 83.33% showing differential expression. The category "Dormancy & Sporulation" was tied at second place with 83.33% of its genes being differentially expressed, while it was ranked third from the bottom when comparing the absolute number of genes. In contrast, "Carbohydrates" was ranked twentieth by the same metric owing to its 444 differentially-

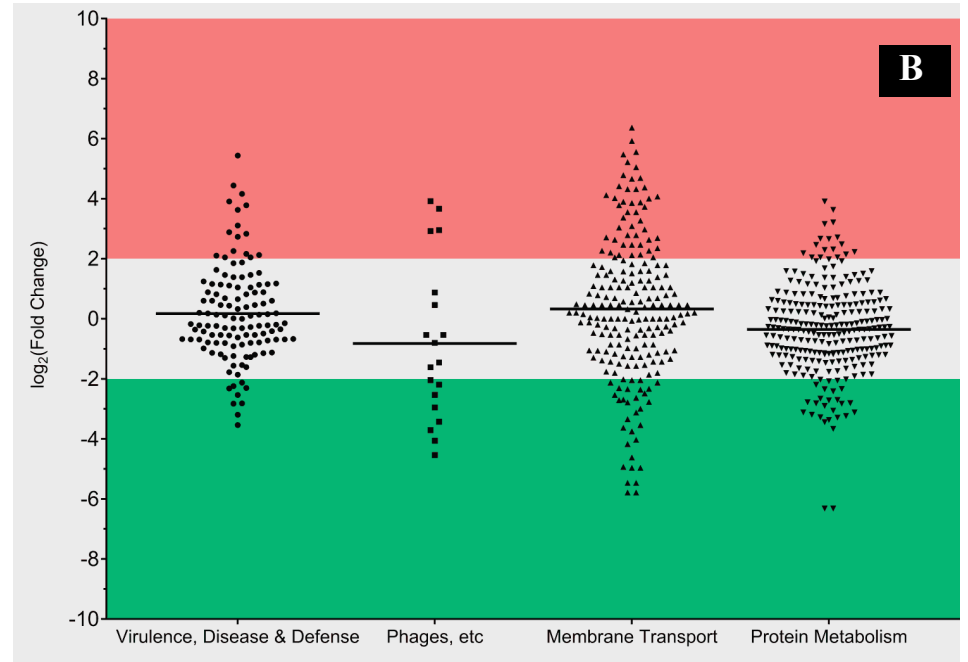
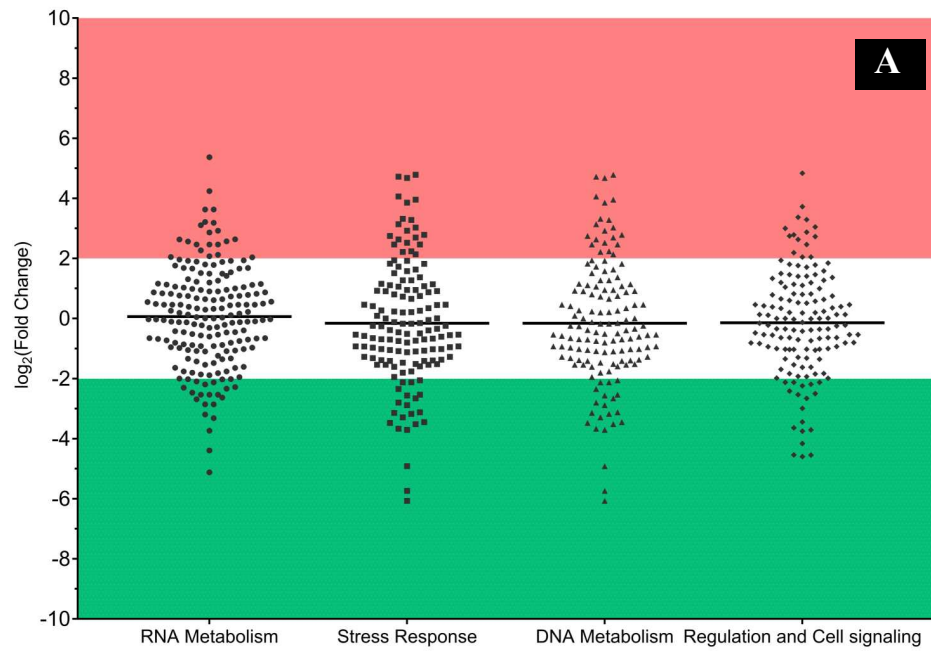
expressed genes accounting for only about 48% of the total number belonging to the category. While genes involved in the protein metabolism were also highly affected by exposure to levofloxacin (80%), what is striking is the high proportion of genes associated with "Phages, Prophages, Transposable elements and Plasmids" (79.17%) being influenced by the same.

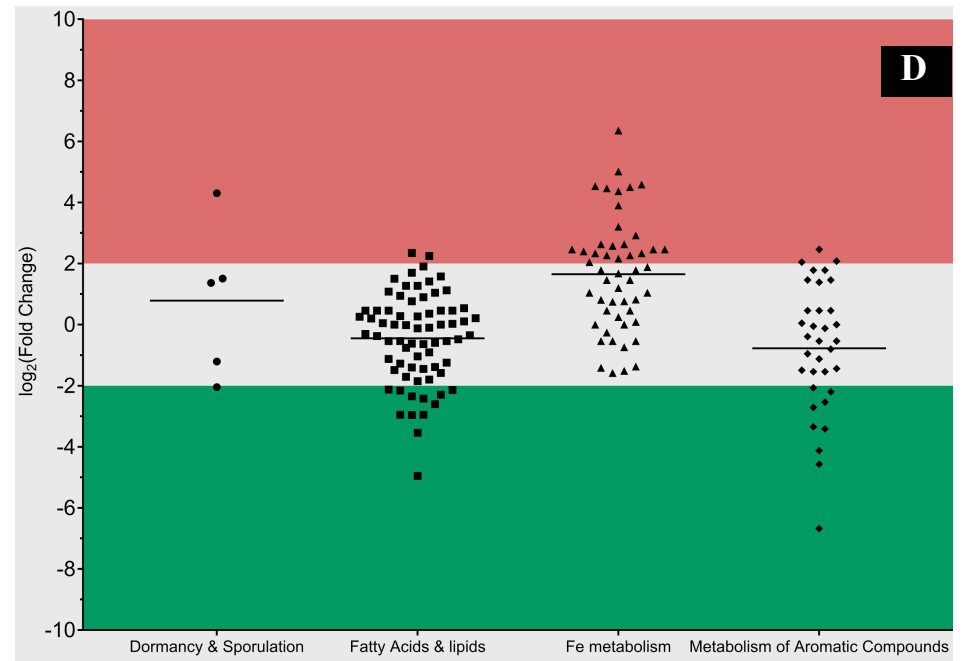
The $\log_2(\text{fold change})$ values of 2 and -2 were chosen as cut-off levels for the analysis and genes showing expression above 2 and below -2 were examined (Figure 4.2.2 A – G). The category "Carbohydrates" contained the highest number of upregulated genes. A total of 55 genes exhibited a $\log_2(\text{fold change})$ greater than 2 (Figure 4.2.2 G). These included genes involved in the central metabolism such as fructose-6-bisphosphate aldolase and pyruvate kinase genes, the transcriptional repressor of the *lac* operon *lacI*, and the glycerol-3-phosphate ABC transporter *ugpB*. The category with the second-most number of upregulated genes was "Membrane Transport" with 47 genes (Figure 4.2.2 B), including the oligopeptide transport system permease *oppC*, Acyl-CoA thioesterase associated with the *tol-pal* system, and the *tonB* receptor involved in iron transport. The category "Amino Acids and Derivatives" had the third-most number of upregulated genes with 38 genes (Figure 4.2.2 C). This included the D-serine specific permease *dsdX*, pyridoxal-phosphate dependant cysteine synthase B, and the aminodeoxychorismate synthase *pabB* involved in folate synthesis. Out of the 26 categories of annotated genes, 12 categories had more than 10 upregulated genes, whereas genes grouped in the categories "Motility and Chemotaxis" and "Secondary Metabolism" did not show upregulation on levofloxacin treatment (Figure 4.2.2 E and F respectively).

Table 4.2.7 Statistics of differential gene-expression in categories on exposure of KpIMS38 to levofloxacin. The statistics of the distribution of genes within a category based on $\log_2(\text{fold change})$ values for each gene are tabulated and include the differentially-expressed genes as an absolute number (DE genes) as well as a percentage against the total genes in the category (DE genes %), the genes with the lowest (Minimum) and highest expression (Maximum) within the category, and the median $\log_2(\text{fold change})$ value for the category (Median).

Category	DE genes	DE genes %	Minimum	Median	Maximum
Carbohydrates	444	47.95	-8.27	-0.26	5.27
Amino Acids & derivatives	300	53.10	-9.46	-0.42	7.19
Protein Metabolism	256	80.00	-6.32	-0.35	3.91
Membrane Transport	207	74.73	-5.78	0.20	6.37
Cofactors, Vitamins, Prosthetic groups and Pigments	205	52.43	-7.25	-0.54	4.05
RNA Metabolism	185	72.55	-5.12	0.05	5.37
Cell Wall & Capsule	149	60.82	-5.07	-0.67	6.29
DNA Metabolism	140	89.74	-6.07	-0.39	4.79
Stress Response	140	72.16	-6.07	-0.39	4.79
Regulation and Cell signalling	139	75.54	-4.60	-0.16	4.84
Virulence, Disease & Defence	120	83.33	-3.54	-0.16	5.44
Respiration	109	55.05	-5.00	-1.16	5.40

Category	DE genes	DE genes %	Minimum	Median	Maximum
Nucleosides & Nucleotides	95	65.07	-2.54	0.34	4.62
Fatty Acids & lipids	71	50.35	-4.95	-0.30	2.35
Iron metabolism	51	63.75	-1.58	1.79	6.36
Miscellaneous	44	60.27	-1.97	0.02	5.05
Sulphur Metabolism	37	39.36	-2.58	1.13	4.59
Metabolism of Aromatic Compounds	34	36.17	-6.68	-0.54	2.46
Nitrogen Metabolism	31	53.45	-2.12	0.00	6.24
Cell Division & cell cycle	30	65.22	-2.69	-0.44	2.69
Phosphorous Metabolism	30	44.78	-3.49	1.80	6.18
Potassium metabolism	26	61.90	-2.50	-0.24	2.98
Phages, Prophages, Transposable elements and Plasmids	19	79.17	-4.54	-1.45	3.92
Dormancy & Sporulation	5	83.33	-2.05	1.37	4.31
Motility & Chemotaxis	4	36.36	-2.56	-0.75	1.36
Secondary Metabolism	3	15.79	-2.04	0.00	1.39





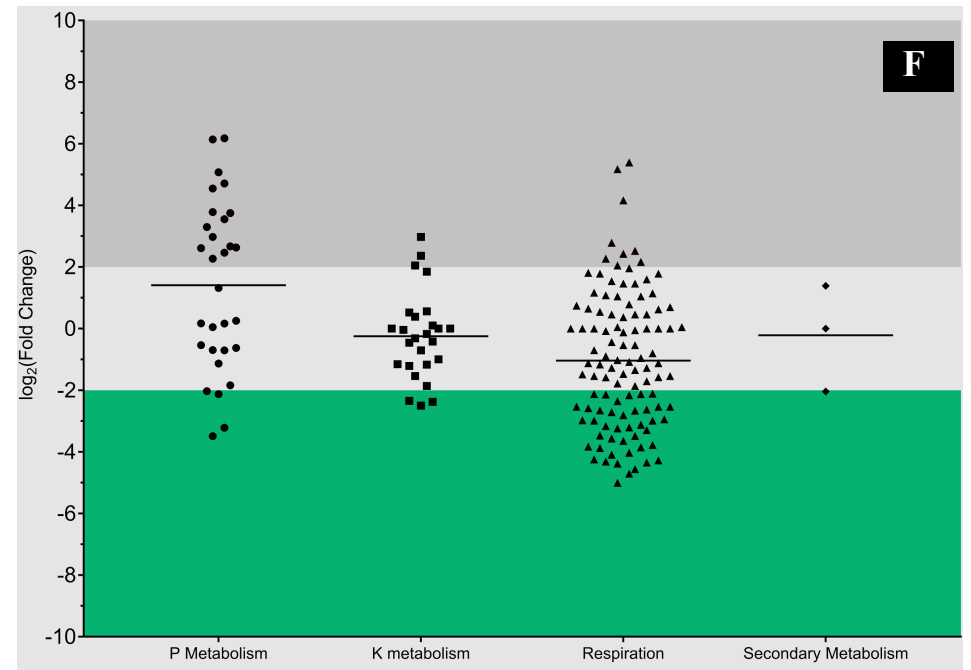
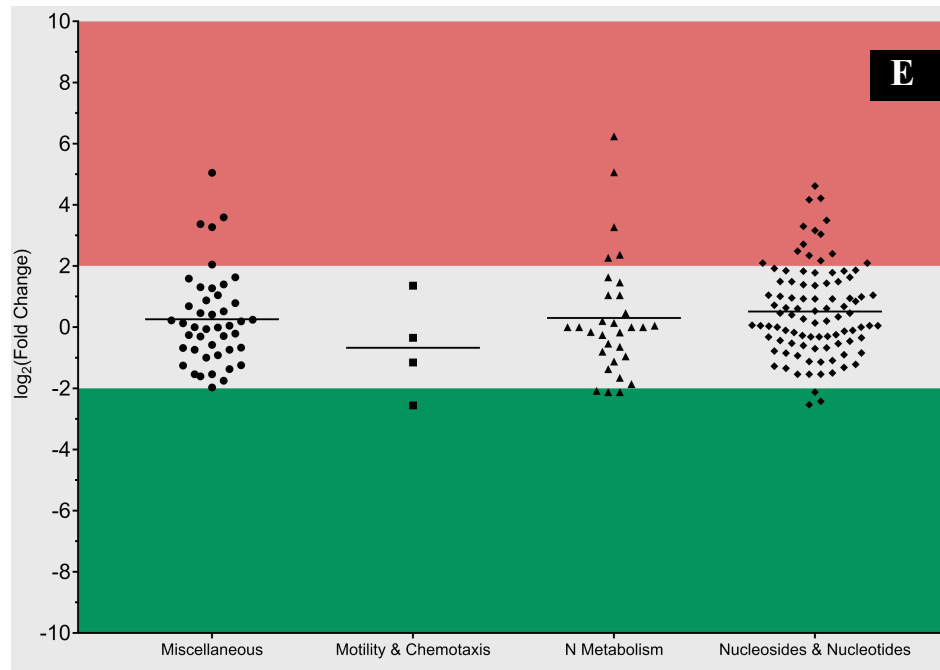




Figure 4.2.2 Expression of genes in KpIMS38 treated with levofloxacin across all categories (A-G). Expression values were represented as the log₂(fold change) for each gene, obtained from the RNA Seq analysis, and were plotted as frequency distributions for all genes within a category as defined by the annotation of the genome of KpIMS38. Cut-off values of +2 and -2 on the Y-axis were defined and the regions designated by red and green zones respectively.

The gene with the highest expression in levofloxacin-treated cells was *umuD*, with a $\log_2(\text{fold change})$ of 8.05. The gene codes for UmuD, which forms a homodimer that in turn associated with UmuC to form the bacterial DNA Polymerase V, which is involved in translesion repair of DNA during DNA damage (Henrikus et al, 2018).

The category “Amino Acids and Derivatives” contained the greatest number of genes whose expression was downregulated in KpIMS38 exposed to levofloxacin. A total of 77 genes belonging to the category exhibited a $\log_2(\text{fold change})$ lower than -2, examples of which include the *puu* genes in the gene-cluster associated with putrescine utilization such as the gamma-glutamyl-putrescine synthetase, gamma-glutamyl-GABA hydrolase and gamma-glutamyl-putrescine oxidase, and genes coding for alpha and beta subunits of tryptophan synthase that is involved in the synthesis of tryptophan. The second-most number of downregulated genes was observed in the category “Carbohydrates” (74) with the expression of genes involved in the glyoxylate cycle such as isocitrate lyase and malate synthase as well as acetyl CoA synthetase (involved in aerobic respiration via the TCA cycle), and PEP carboxykinase (involved in gluconeogenesis) expressed at a lower level in persister cells than their non-persister counterparts. It was closely followed by the “Cofactors, Vitamins, Prosthetic Groups, Pigments” category with 43 genes showing downregulation in persister cells (Figure 4.2.2 C). These included genes involved in cobalamine synthesis such as precorrin-3b C17-methyltransferase, precorrin-6x reductase and sirohydrochlorin cobaltochelate, *thiF*, *thiG* and *thiH* involved in thiamine biosynthesis. Eleven categories exhibited downregulation in more than 10 genes, while the categories “Iron Acquisition and Metabolism” (Figure 4.2.2 D) and “Miscellaneous” (Figure 4.2.2 E) did not contain any genes showing $\log_2(\text{Fold Change})$ lower than -2. The gene least expressed in levofloxacin-treated cells was the Anthranilate phosphoribosyl

transferase gene, with a $\log_2(\text{fold change})$ of -9.46 , that belonged to the category “Amino Acids and Derivatives” was involved in the synthesis of tryptophan.

Further details on expression profile of KpIMS38 treated with levofloxacin were obtained on examining gene-expression within the categories. Expression patterns were inspected within categories which had the highest proportion of differentially-expressed genes and the salient features of each are collated below.

Expression was examined in "DNA Metabolism", where almost 90% of the genes annotated were differentially-expressed, across the various subcategories contained within it. Genes related to DNA replication and CRISPR systems were downregulated. Among the *ruvABC* genes, which are involved in the Holliday junction and consequently listed under the subcategory "DNA recombination", the expression of *ruvA* and *-B* was upregulated while *ruvC* was observed to be downregulated. "DNA repair" was the subcategory with the largest number of differentially-expressed genes. Among the 82 genes, 50% of them were upregulated. The DNA repair genes *umuC* and *-D* were the most highly-expressed, followed by *recN* and *recA*. Genes involved in mismatch repair systems were downregulated, as were genes coding for RecF and RecR proteins involved in the recFOR repair system. Interestingly, the expression of *recO* was upregulated. There were a number of genes which could not be classified under any subcategory and remained as such. Among such genes, those involved in the chromosome partitioning system MukBEF as well coding for the α and β subunits of histone-like HU proteins were downregulated.

The category "Virulence, Disease & Defense" contained various genes of significant functions. Two genes associated with the Yid hyperadherence system – *yidE* and *yidR* – were downregulated while the expression of *yidP* from the same system was upregulated. Half of the total number of genes under the subcategory "Bacteriocins" were upregulated,

including the gene responsible for production of Colicin V. The expression pattern for genes associated with the Colicin E2 differed, with three of the four genes viz. *creA*, *creC* and *creD* upregulated and the singular gene *creB* downregulated. The subcategory "Antibiotic Resistance" contained the largest number of differentially-expressed genes (80) among whom 50% were upregulated. Among the most-upregulated genes were 4 associated with the RND efflux system, 4 with the homeostasis of copper, and 1 each with the MFS efflux system and the Hemolysin D family.

Genes under the category "Dormancy & Sporulation" were not classified into subcategories, and all the five differentially-expressed genes belonged to the subsystem "Persister Cells". The gene involved in inhibiting cell division *sulA* was the most upregulated, followed by *hipA* and *-B* associated with the HipBA toxin-antitoxin system.

Among genes grouped under the category "Protein Metabolism", the largest number of differentially-expressed genes were found within the subcategory "Protein Biosynthesis". Among the 145 differentially-expressed genes, 39% were upregulated. Some of the genes with the highest positive-difference in expression coded for the translation elongation factor Ef-G, ribosomal small-subunit proteins S20p and S21p, YchF from the Obg family of GTPases and cysteine-tRNA deacylase. In addition, genes coding for the translation initiation factor IF1 and the elongation factor Ef-Tu were also upregulated. The subcategory "Protein degradation" contained the second-highest number of differentially-expressed genes, but among the 40 genes only 20% were upregulated. Only 3 genes exhibited a $\log_2(\text{fold change})$ higher than 1, of whom two code for carboxypeptidases involved in peptidoglycan biosynthesis and the other specifies the proteolytic subunit ClpP of the Clp protease. Interestingly, genes that were downregulated the most also coded for components of the Clp protease in *clpA*, *clpX* and *clpB*. A high proportion (61%) of the genes associated under the subcategory "Protein Folding" were observed to

be downregulated, most of whom were involved in the biogenesis of c-type cytochromes, in periplasmic disulfide interchange, and chaperones involved in the maturation of Fe-S proteins. The upregulated genes coded for the chaperones DnaK, DnaJ, HtpG and GrpE.

An interesting observation in the expression pattern of genes grouped under the subcategory "Phages and Prophages" was while genes specifying the phage capsid and involved in phage packaging were downregulated, those upregulated the most were coactivators of phage gene expression *ibrA* and *ibrB*. In addition, genes coding for the phage tail-fibers and the small subunit of the phage terminase were also upregulated.

Genes associated with the subcategories "Programmed cell-death and Toxin-Antitoxin systems" and "Quorum Sensing and Biofilm Formation" were grouped under the category "Regulation and Cell signaling". The most-upregulated genes in the former coded for toxins associated with the toxin-antitoxin systems *phd-doc* and *relE*. The gene coding for the cognate antitoxin of *relE* – *relB* – was also upregulated, though its expression was 2 orders of magnitude lower than *relE*. Most of the genes involved in biofilm synthesis were upregulated while those involved in the transport and processing of the autoinducer 2 (AI-2) were downregulated.

Among the genes associated with "Membrane Transport", 65% of the genes categorized under the type IV secretion system were upregulated. Twenty four of those genes were involved in the conjugative transfer of IncF plasmid. Genes involved in the biogenesis of type IV pili were downregulated. Differential gene expression was also observed in genes classified under the type VII secretion system. An upregulation of the genes associated with the colonization factor antigen 1 fimbriae and a downregulation of genes involved in the synthesis of mannose-sensitive type-1 pili was observed.

4.2.3 Discussion

The intrigue of bacterial persistence can be ascribed to the manifestation of phenotypic heterogeneity in a clonal population of cells. Persister cells have been identified as isogenic with respect to their non-persister counterparts from the same bacterial population (Balaban et al, 2019). Persistence is known to be mediated by signals and mechanisms conventionally associated with the cellular response to stress, which in turn are inherent within the genome of all bacteria (Gollan et al, 2019). Therefore, it is vital to examine these stress responses in light of persistence to gain an understanding of the nexus between them that drives the formation of a subpopulation to survive lethal stress. The results of the present section detail the findings from the whole-genome sequence of KpIMS38, which include genes mediating antibiotic resistance and virulence as well as prophages and plasmids associated with the genome. Gene-expression in persisters of KpIMS38 was also analysed through comparing the transcriptomes of levofloxacin-treated KpIMS38 cultures with their untreated counterparts. Genes mediating DNA repair, protein synthesis, biofilm formation, antibiotic efflux as well as toxin-antitoxin systems were differentially expressed in KpIMS38 persisters.

MLST has been applied towards surveilling the dissemination of antibiotic resistance in bacterial pathogens, with distinct resistance mechanisms found to be associated with pathogenic isolates that cause epidemics (Castanheira et al, 2021). CTX-M have become among the most widespread extended-spectrum beta-lactamases (ESBLs) in the world, overtaking the previously-prevalent TEM and SHV enzymes. This transmission, initially believed to be random, was attributed to *E. coli* strains belonging to the sequence type ST-131 (Banerjee and Johnson, 2014). However, no epidemics have been attributed to ST-13, the type to which KpIMS38 belongs.

The genome of KpIMS38 indicated the presence of genes imparting resistance to beta-lactam, aminoglycoside and fosfomycin classes of antibiotics. CTX-M-15, one the beta-lactamases identified, is frequently encountered in the Indian subcontinent among bacterial strains that exhibit resistance to beta-lactam antibiotics (Bevan et al, 2017). SHV beta-lactamases are frequently observed in clinical isolates of *K. pneumoniae* (Castanheira et al, 2021), imparting credence to the detection of the enzyme SHV-101 in KpIMS38 – a clinical isolate of *K. pneumoniae*. Both SHV-101 and CTX-M-15 function as ESBLs and confer the bacterium with the ability to hydrolyze extended-spectrum beta-lactam antibiotics such as cefotaxime, ceftriaxone and ceftazidime (Castanheira et al, 2021).

Amino acid substitutions in genes coding for SHV and TEM beta-lactamase enzymes reportedly confer resistance to beta-lactamase inhibitors such as clavulanic acid and sulbactam. These variants however are unable to overcome inhibition caused by other inhibitors, namely, tazobactam and avibactam (Bradford et al, 2004; Dubois et al, 2004, 2008; Mendonça et al, 2009; Lahiri et al, 2016). KpIMS38 did not possess the prescribed amino-acid substitutions in either of the two beta-lactamase genes identified. Furthermore, the antibiotic sensitivity profile of KpIMS38 indicated resistance to the combinations of beta-lactam and beta-lactamase-inhibitors containing clavulanic acid and tazobactam. This could indicate the involvement of carbapenemases, enzymes that possess the ability to hydrolyse a wide range of antibiotics in addition to carbapenems, which includes penicillins, cephalosporins and aztreonam (Queenan and Bush, 2007). On the basis of their active-site architecture, carbapenemases are categorised as either serine carbapenemases, metallo-beta-lactamases or oxacillin-hydrolysing (OXA) beta-lactamases (Bush and Bradford, 2019). Clavulanic acid and tazobactam are ineffective at inhibiting serine carbapenemases as well as metallo-beta-lactamases (Bush and Bradford, 2019). OXA beta-lactamases are resistant to clavulanic acid but are inhibited by tazobactam (Ehmann et al,

2013), whereas sulbactam has no reported inhibitory activity against either of the carbapenemases (Bush and Bradford, 2019). The resistance of KpIMS38 towards all beta-lactam and beta-lactamase inhibitor combinations tested except ampicillin – sulbactam coupled with the absence of carbapenemases genes in the genome of KpIMS38 rule out the presence of carbapenemases. Additionally, this represents a mode of resistance to beta-lactams that is as of yet unexplored.

The presence of *aac(3)-IId*, coding for an aminoglycoside acetyltransferase, in the genome of KpIMS38 confers resistance to gentamycin. The gene has also been associated with enhanced resistance to kanamycin (Zhang et al, 2021), though it did not impart kanamycin resistance to KpIMS38. The plasmid vectors used to carry out expression studies (detailed in section 3.1.2) possessed a kanamycin-resistance gene as the selection marker, and was used to generate stable transformants in KpIMS38. This indicates a lack of resistance to kanamycin inherent within the isolate. The sensitivity of KpIMS38 to amikacin could be attributed to the antibiotic being introduced in antibiotic therapy much later than gentamycin (Bodendoerfer et al, 2020), resistance to which is mediated by *aac(3)-IId* (Shaw et al, 1993). Additionally, resistance to amikacin requires *aac(6)* enzymes (Mancini et al, 2019), which are absent in KpIMS38.

Utilisation of two different algorithms to predict resistance genes in the genome of KpIMS38 yielded outcomes with some overlap with regard to beta-lactamase and aminoglycosidase-encoding genes. A substantial discrepancy between outputs of the two lay in the 17 additional genes identified by RGI (as seen in section 4.2.2.3). While most of the genes were associated with efflux mechanisms, certain mutations were also identified in genes involved in routine cellular metabolism. It is worth noting, however, that the database queried by the algorithm to determine resistance genes was constructed using sequences from the genome of *E. coli*. Sequence discrepancies inherent between different

bacterial genera cannot serve as grounds to declare genes as mutational variants with the ability to confer resistance. Similarly, most of the resistance genes categorised under efflux were in truth identified as components of various metabolic pathways. CRP and H-NS, associated with the RND and MFS efflux systems by RGI, were actually identified as the cAMP-activated global transcriptional regulator CRP and a DNA-binding transcriptional regulator H-NS respectively. The *marA* gene categorised under the RND efflux system as well as a general bacterial porin was identified as a transcriptional activator of the AcrAB efflux pump. While MarA, the product of the *marA* gene, is known to positively regulate expression of the tripartite efflux pump AcrAB-TolC, overexpression of the pump is a prerequisite for antibiotic resistance through that particular mode (Weston et al, 2018).

The presence of multiple genes associated with virulence is indicative of the ability of the bacterial isolate to infect a host system and cause disease. However, the growing understanding alludes to the concerted activation of genes in response to multiple environmental cues encountered on colonising a host, thereby leading to the induction of various pathways that culminate in pathogenesis by the bacterium (Thomas and Wigneshweraraj, 2014). The association of over 60 different genes from the genome of KpIMS38 with virulence is confirmative of its status as a clinical isolate as well as indicative of its ability to cause infection and disease in a host system.

The single genome analysis tool predicted the presence of two distinct plasmids integrated in the genome of KpIMS38. This distinction was not afforded through the plasmid sequencing performed separately, where information of annotated genes present in the plasmid was limited. The intrigue, however, comes from the presence of plasmid sequences within the genomic DNA of KpIMS38. The presence of plasmid replication-origin sequences could indicate the plasmids were integrated within the genome of KpIMS38, resulting in the formation of a Hfr (high frequency recombination) strain. Although this

would offer an explanation for the acquisition of resistance genes, additional analyses are necessary to confirm the veracity of this hypothesis. A plasmid with IncFII(K) origin of replication was implicated in the spread of antibiotic resistance by Enterobacteriaceae. The resultant nosocomial infections facilitated the spread of multiple resistance genes including *bla_{CTX-M-15}* and *aac(3)-IId* (Dolejska et al, 2012). Reports have found the IncR origin-of-replication to be associated with multireplicon plasmids (Chen et al, 2006; Shen et al, 2009; Frasson et al, 2012; Drieux et al, 2013). This could point to the presence of a single large plasmid in that contains both IncFII(K) and IncR replication-origins integrated in the genome of KpIMS38.

The presence of gene clusters homologous to five distinct bacteriophage genomes was indicative of a high degree of bacteriophage infection in nature. The characterization of the five regions as belonging to phages known to principally infect bacterial genera other than *Klebsiella* is of some significance, as is the presence of single genes mapping to unique *Klebsiella* phages within each of the regions. The findings imply the possible existence of niches that facilitate horizontal gene transfer among various bacterial species in nature. A direct association of prophages with persistence is being unearthed. Sandvik et al (2015) noted treating *S. aureus* with lower concentrations of ciprofloxacin resulted in lytic activation of cryptic phages that killed the cells and resulted in fewer survivors. Higher concentrations of the same antibiotic inhibited cell metabolism and subsequently prophage activation, which resulted in biphasic killing and a greater numbers of survivors. A much more consequential finding was the discovery of the lytic activation of the prophage $\phi 80$ to be responsible for the reduced persistence of an *E. coli* $\Delta 10TA$ strain. Treatment with an intermediate concentration of quinolones was determined to bring about activation of the prophage and treated and not the deletion of 10 individual TA modules (Harms et al, 2017). Prophages become cryptic when genes essential for lytic development are inactivated,

usually through deletion or mutation in the phage genome (Campbell, 1998). The prophage-regions 2 and 5 in KpIMS38, identified as incomplete due to the regions not containing the complete set of bacteriophage genes, could represent cryptic prophages. However the incomplete regions could just as well be attributed to the lack of sequencing coverage, since the sequence obtained was a draft and not a complete genome. It is nevertheless worth reinvestigating the weak persistence of KpIMS38 with lower concentrations of levofloxacin (as reported in figure 4.1.3) to assess the involvement of bacteriophages in cell death.

Differential gene expression in KpIMS38 cultures treated with levofloxacin indicates a degree of active metabolism occurring within the persister population. Persistence has been classically associated with an attenuation of the overall metabolism of the cell (Harms et al, 2016), which would explain reduced expression of genes pertaining to vital cellular processes such as motility, protein synthesis and replication. An upregulation of gene expression would, therefore, provide an unmistakable indication of the cellular response to generate and mediate persistence. Persister cells formed by exposure to fluoroquinolones mobilise DNA repair pathways to maintain the state, harnessing the SOS response as well as repair systems involving *rec* and *ruv* genes (Murawski and Brynildsen, 2021). It was therefore unsurprising to observe differential expression in 90% of the genes associated with the category "DNA metabolism" and the most overexpressed genes – *umuD*, *umuC*, *recN* and *recA* – to be associated with DNA repair. Persistence induced by treatment with levofloxacin has been reported to generate filamentous *E. coli* cells with delayed partitioning of the chromosome and cytoplasm (Barrett et al, 2019). The appearance of long cells in KpIMS38 cultures treated with levofloxacin, detected through flow cytometry and microscopy, could therefore find explanation in the downregulation of genes involved in

chromosome partitioning and the upregulation of *sulA*, the cell division inhibitor in cell populations treated with levofloxacin.

KpIMS38 persisters exhibited an increased expression of genes coding for efflux pumps belonging to the RND superfamily, which were among the most upregulated genes from the category "Virulence, disease and defence". Persisters formed by stationary-phase *E. coli* treated with the fluoroquinolone delafloxacin was mediated through the RND efflux system AcrAB-TolC, although the same was not implicated in persistence caused by levofloxacin (Byrd et al, 2021). Although KpIMS38 persisters were formed from exponential-phase cultures and using levofloxacin, a deeper examination of the efflux-gene upregulation would aid in understanding persistence in *K. pneumoniae*.

A basal level of cellular metabolism was observed in *S. aureus* persister cells that involved the function of glycolysis, the tricarboxylic acid (TCA) cycle as well as the pentose phosphate pathways (Prax and Bertram, 2014). The upregulation of 55 genes associated with carbohydrate metabolism on treating KpIMS38 with levofloxacin appeared to be at odds with the metabolic ceasure associated with the persister state. Further examination indicated the activation metabolic networks that are generate energy through the non-glycolytic Entner-Doudoroff (ED) pathway as well as the methylglyoxal pathway (Spector, 2009). This was in opposition to the observations in *E. coli* persisters generated by rifampicin exposure, where proteins involved in central carbon metabolism viz. glycolysis, TCA cycle and the pentose phosphate pathway were downregulated (Sulaiman et al, 2018). Studies conducted previously have demonstrated persister cells to resume metabolism, also known as 'waking', when supplemented with various sugars including arabinose, glucose, fructose, mannitol, sucrose (Allison et al, 2011; Abokhalil et al, 2020; Yamasaki et al, 2020). These findings taken together with the observations from the current study of upregulated sugar-influx genes hint at the pre-conditioning of KpIMS38 persisters to

receive sugars and resuscitate to form normally-metabolising cells. The upregulation in the membrane transport genes observed in KpIMS38 persisters corroborated the outcomes of a proteomic analysis conducted on rifampin-induced *E. coli* persisters. There, persister cell formation was accompanied by a 4-fold increase in the expression of membrane proteins (Sulaiman et al, 2018).

Various studies investigating bacterial persisters have routinely identified an elevated expression of toxin-antitoxin (TA) systems (Shah et al, 2006; Keren et al, 2011). A similar examination in the transcriptome of KpIMS38 demonstrated an increase in the expression of three TA systems on treatment with levofloxacin. All three systems were belonged to Type-II TA loci; two – *relBE* and *phd-doc* – were classed into the "Regulation and Cell signaling" category whereas *hipBA* was grouped under the category "Dormancy and Sporulation". Genes for both the toxin and its cognate antitoxin were upregulated in KpIMS38 persisters, though the toxin was expressed at a higher level. All three modules have been associated with bacterial persistence in response to a variety of stress factors (Black et al, 1994; Christensen et al, 2001; Christensen and Gerdes, 2004; Keren et al, 2004; Nguyen et al, 2011; Helaine et al, 2014). Despite an increase in their expression, the true test of the influence exerted by these TA systems on KpIMS38 persistence would be an increase in persister cell formation on ectopic overexpression of the genes and/or a reduction of the same on obstruction of the activity of the genes.

The classical notions of persistence envisioned a state of metabolic ceasure within the bacterial cell that could be reversed in the absence of the stress factor (Keren et al, 2011; Maisonneuve and Gerdes, 2014). Nonetheless, a growing body of work has led credence to the dynamic nature of persistence where a certain degree of cellular metabolism does occur within the persister cells while under exposure to the stressor inducing it. Although 61% of the differentially-expressed genes pertaining to and grouped under the subcategory "Protein

biosynthesis" were downregulated in KpIMS38 persisters, genes for the translation initiation factor IF1 and translation elongation factors Ef-Tu and Ef-G were upregulated, indicating a degree of protein synthesis within the cells.

A recent study highlighted the significance of GTPases belonging to the Obg family in bacterial persistence. Obg was activated by the alarmone (p)ppGpp produced during the stringent response, and directed the transcription of the type I TA module *hokB-sokB* (Verstraeten et al, 2015). The toxin HokB forms a transmembrane channel in the inner membrane that alters the ion flux and subsequently depolarizes the membrane. The effects of depolarization extended included impairment of ATP synthesis as well as the amelioration of replication and protein synthesis, culminating in persistence (Yamaguchi et al, 2011). The gene *ychF*, that codes for a GTPase belonging to the Obg family, was expressed at a higher level in KpIMS38 cells treated with levofloxacin. The observations of Verstraeten and colleagues were in the context of ObgE, CgtA, YhbZ and not YchF GTPases. Nonetheless, a high degree of structural conservation has been observed among the various members of the Obg family of GTPases (Leipe et al, 2002). Also, the *hipBA* TA locus was expressed at a heightened level in KpIMS38 persisters, which is significant since the activity of *hipA* increases the production of (p)ppGpp (Hansen et al, 2012) that in turn activates the Obg family GTPases as described previously. Taken together, the observations could be indicative of a similar role for YchF in persistence of KpIMS38.

The Clp protease has been implicated in bacterial persistence for its role in activating toxins belonging to type II TA systems. The protease acts on the toxin-antitoxin complex, degrading the antitoxin in a (p)ppGpp-dependant manner to extricate to toxin (Wang and Wood, 2011; Hansen et al, 2012; Brzozowska and Zielenkiewicz, 2013). The Clp protease is a complex made up of the protease subunit ClpP and one of many chaperones such as ClpX, ClpA, ClpC. Substrate specificity is conferred by the chaperones, which unfold

proteins and introduce them into the degradation chamber, formed by ClpP, in an ATP-dependant manner thereby instigating targeted proteolysis (Olivares et al, 2016). Treatment of KpIMS38 with levofloxacin led to an increase in the expression of *clpP*, but surprisingly saw a downregulation of genes coding for the associated chaperones viz. *clpA*, *clpX* and *clpB*. The ability of the chaperones to function independent of ClpP coupled with their functional necessity of ATP might be suggestive of a hitherto unknown regulatory mechanism employed by stressed bacteria to reduce energy expenditure by inhibiting their expression. Nonetheless, the absence of directed proteolytic activity, essential for the activity of TA modules, stands at odds to the increased expression of *hipBA* in KpIMS38 persisters. Additionally, the absence of the Lon protease in the transcriptome analysis is also striking since studies on *E. coli* persisters have extensively documented the involvement of *lon* (Gerdes and Maisonneuve, 2012). Taken together, these observations represent a novel scenario where persistence might be effectuated by mechanisms unknown as of yet.

A similar trend was observed in the expression of phage proteins. Genes coding for the capsid and packaging of the genetic material into the capsid were downregulated while those specifying the coactivators of phage-gene expression viz. *ibrA* and *ibrB* were expressed at a higher level in KpIMS38 treated with levofloxacin. *E. coli* treated with fluoroquinolones experienced a lytic activation of prophages from the genome, which eventually resulted in cell death (Sandvik et al, 2015). The results of the present study differ from it with no expression of the phage-structural genes. Reports on *ibrA* and *-B* are sparse, with a study carried out by Sandt et al (2002) identifying both genes to be present as overlapping sequences in a genetic island in the genome of *E. coli*. Together the genes drove the expression of *eib* genes, which specify immunoglobulin-binding surface proteins that confer the bacterium with resistance to complement proteins.

Summarising the observations reported in this section, the genome of KpIMS38 was sequenced to obtain a draft genome. The genome possessed information about the various genes that imparted resistance and virulence to KpIMS38 as well as extrachromosomal elements such as prophages and plasmids integrated within it. The genome was used to acquire transcriptomes of KpIMS38 persisters, formed on treatment with levofloxacin, as well as non-persisters and both compared to observe the differential gene-expression in persisters. Persistence was seen to cause variation in the expression of genes associated with antibiotic efflux, DNA repair, biofilm synthesis, protein synthesis and TA systems.

4.3 Elucidation of the role of various genes in persister-cell formation in *K. pneumoniae*

4.3.1 Background of the study

Persister-cell formation in bacteria is mediated by various physiological pathways that involve numerous genes working in tandem to bring about and maintain the persister state. That being said, different stimuli activate different sets of pathways. Comparing the transcriptomes of KpIMS38 persisters and non-persisters revealed the presence of differentially-expressed genes, which belonged to pathways with different functions. Expression of those genes could be essential to the persistence of KpIMS38 and therefore need to be examined by carrying out expression studies that involve deletion or silencing as well as overexpression of the genes and assaying persister-cell formation.

4.3.2 Validation of an appropriate reference genes to study gene expression in KpIMS38 persisters formed by exposure to levofloxacin

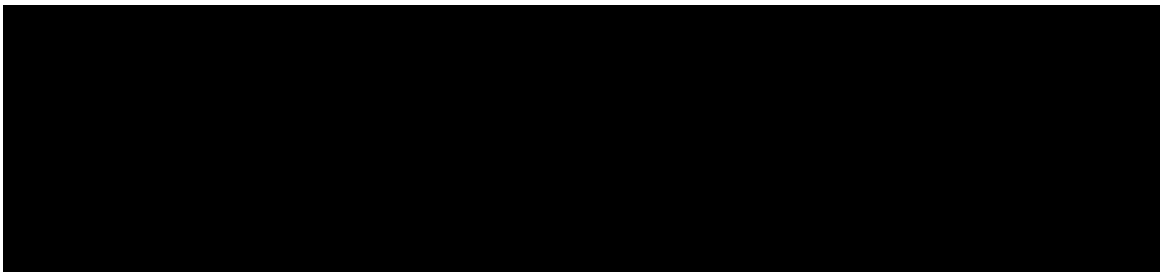
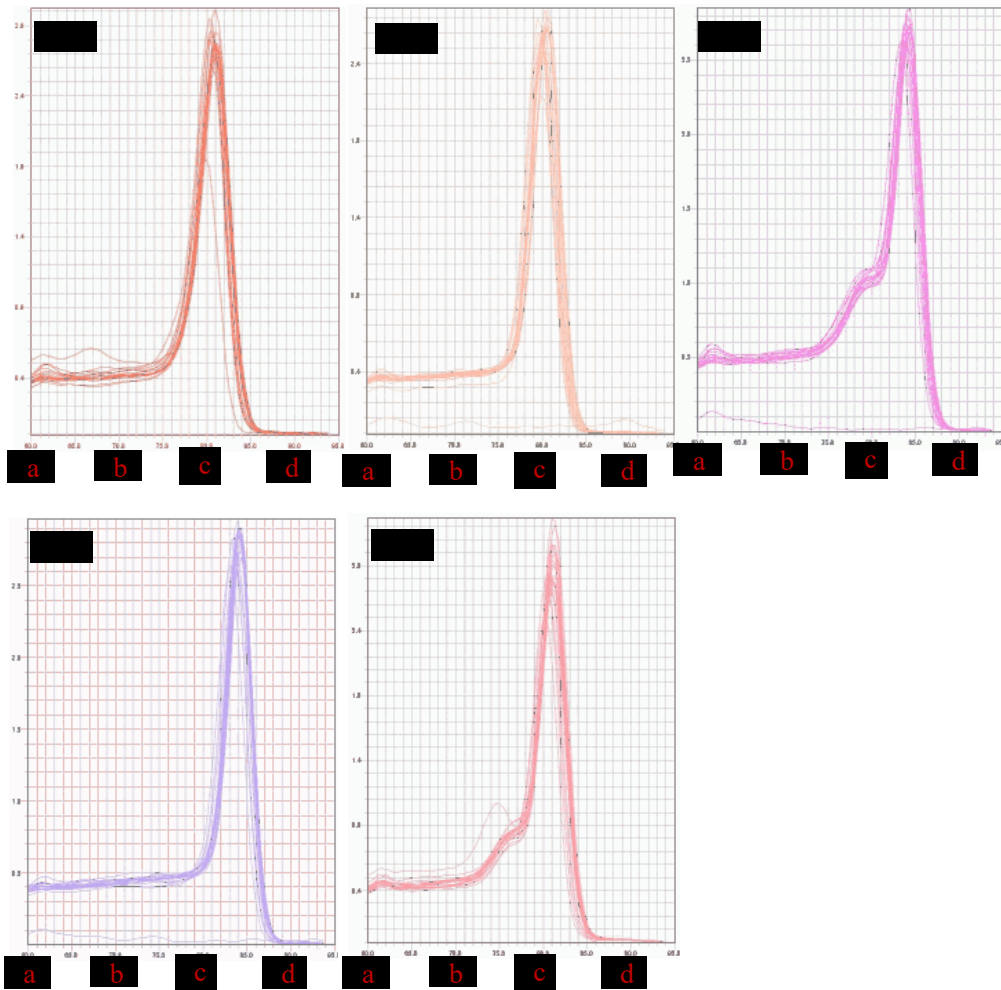
Real-time PCR, or qPCR, is a powerful tool to study the expression of genes in a particular system (Mangold et al, 2011). The threshold cycle or C_q value obtained upon the amplification of each gene in a qPCR is an indication of the amount of the gene-specific transcripts are present, which in turn represents the expression of genes. An advantage of qPCR is the ease of comparing gene expression within a particular system across multiple conditions, which is performed by comparing the gene expression in a test condition with that of the same gene in a control condition. Choosing an appropriate reference gene is the most important parameter to achieve accurate quantification of gene expression. An ideal reference gene should be stably expressed at a basal level that co-relates with the total amounts of mRNA within a cell (Bustin et al, 2009). This becomes all the more crucial in persister cells, where most of the bacterial metabolism is stalled, thereby rendering most of

the conventional reference genes unusable to study gene expression. Based on the transcriptome study performed earlier, a total of five genes viz. *dnaJ*, *groEL*, *kp4432*, *kp751* and *rpoB*, were chosen and their suitability as reference genes evaluated.

qPCR for all the five genes was performed using template cDNA from non-persister as well as levofloxacin-induced persister cells. Each primer pair designed to amplify a specific candidate gene yielded specific products without any non-specific amplification (Figure 4.3.1). All primers amplified their specific targets with an efficiency greater than 95% (Table 4.3.1). The C_q values for all the genes fell between the range of 16 to 22 (Figure 4.3.2). Among the genes assessed, the greatest variation in C_q values – measured as the difference between the lowest and highest C_q values in untreated as well as treated condition - was observed in *dnaJ* while the least variation was observed in *groEL*.

Table 4.3.1 Efficiency of amplification by qPCR for each primer pair corresponding to the candidate reference genes. Efficiency is represented as a percentage and calculated using the formula $E\% = 100 * E/2$, where E is the efficiency of amplification calculated using the formula as stated in section 3.3.9.1 of this document. Values are represented as the mean with the standard deviation (n=3) for untreated and levofloxacin-treated samples.

Gene	Function	E% untreated	E% treated
<i>dnaJ</i>	Chaperone protein	96.48 ± 2.03	99.96 ± 2.09
<i>groEL</i>	Heat Shock Protein 60 family chaperone protein	92.19 ± 0.99	94.14 ± 2.47
<i>rpoB</i>	RNA Polymerase Beta subunit	96.47 ± 0.36	98.84 ± 3.98
<i>kp751</i>	Glycerol Dehydrogenase	96.11 ± 0.63	98.11 ± 3.42
<i>kp4432</i>	Phenylacetaldehyde Dehydrogenase	97.28 ± 1.46	99.97 ± 2.93



The stability of gene expression for the five candidate genes was assessed using the BestKeeper, Delta Ct, geNorm and NormFinder algorithms, using the RefFinder tool, the results of which were compiled in table 4.3.2. Each of the genes was assigned a weight by RefFinder based on the results of the four algorithms. The weights were used to calculate the geometric mean (GM) for all the genes, based on which an order of expression-stability was obtained, and ordered in table 4.3.3. The gene *kp4432* was the most stable with a GM of 1.41, while *groEL* was the least stable (GM = 4.23) (Table 4.3.3). This was backed up by the results obtained from individual algorithms used by RefFinder, with *kp4432* being

the most stable, followed by *kp751* and *rpoB* (Table 4.3.2). geNorm and BestKeeper also ranked *kp751* along with *kp4432*. All algorithms ranked *dnaJ* as the least stable gene, followed by *groEL*; an exception to this was the Delta Ct algorithm, which ranked *kp751* as the second-most unstable.

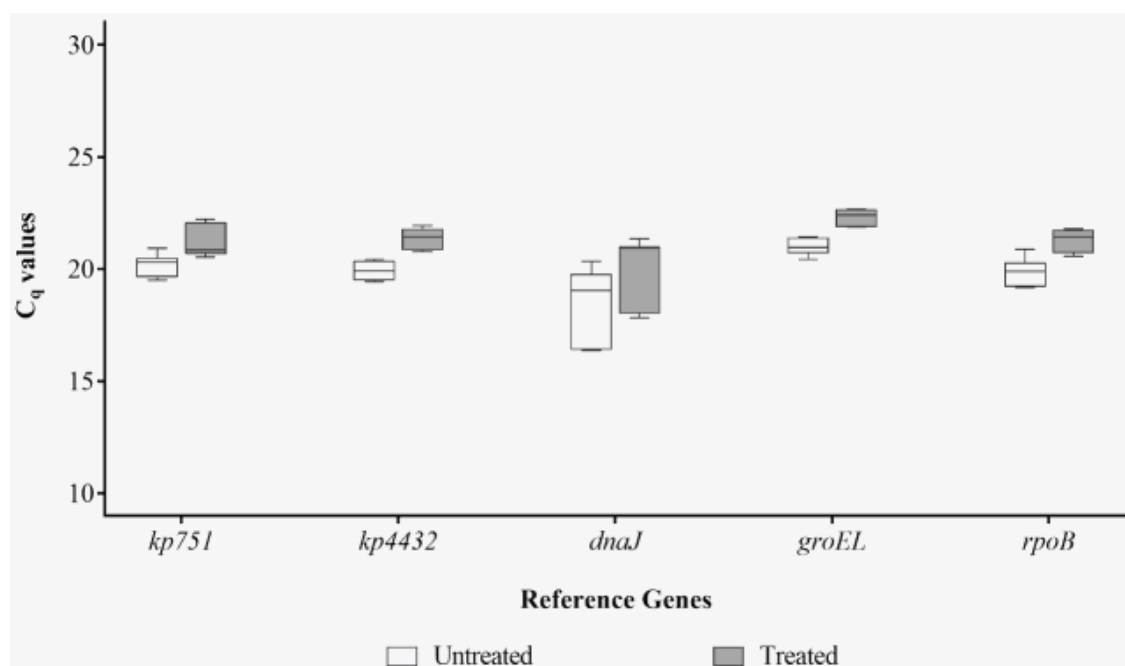


Table 4.3.2 Candidate genes ranked according to their stability as obtained from Delta-Ct, BestKeeper, NormFinder and geNorm algorithms using the RefFinder tool. 4432 = *kp4432*, 751 = *kp751*, Av. SD = Average of standard deviation, SD ± CP = Standard deviation ± Crossing points, SV = Stability value, M = M value.

Rank	Delta-Ct		BestKeeper		NormFinder		geNorm	
	Gene	Av. SD	Gene	SD±CP	Gene	SV	Gene	M
1	4432	0.67	4432	2.49	4432	0.02	4432/751	0.04
2	<i>rpoB</i>	0.70	751	2.52	751	0.05	<i>rpoB</i>	0.06
3	<i>groEL</i>	0.74	<i>rpoB</i>	2.53	<i>rpoB</i>	0.06	<i>groEL</i>	0.08
4	751	0.75	<i>groEL</i>	2.62	<i>groEL</i>	0.10	<i>dnaJ</i>	0.16
5	<i>dnaJ</i>	1.86	<i>dnaJ</i>	2.75	<i>dnaJ</i>	0.27		

Table 4.3.3 Candidate genes ranked according to their stability using the RefFinder tool. Stability was represented as the comprehensive score, which in turn was obtained from the geometric mean of the results of all four algorithms used.

Rank	Comprehensive value	
	Gene	Geometric Mean
1	<i>kp4432</i>	1.41
2	<i>kp751</i>	1.86
3	<i>rpoB</i>	2.71
4	<i>dnaJ</i>	3.34
5	<i>groEL</i>	4.29

The relative expression of specific genes was assessed using *kp751*, *kp4432* and *rpoB* as reference genes. The genes were chosen on the basis of their expression levels in KpIMS38 persisters determined from the transcriptome analysis carried out as detailed section 4.2.3 of this document. The genes chosen included the phage shock proteins *pspA*, *pspC*, *pspD*, *pspF* and *pspG*, and a coactivator *ibrA*. A majority of the genes chosen are reported to be involved in persister cell formation in bacteria (Harrison et al, 2009; Vega et al, 2012; Levin-Reisman et al, 2017; Liu et al, 2017). The gene expression was represented as the fold change, which was calculated according to the equation

$$\text{Fold-change (FC)} = 2^{-\Delta\Delta Cq}$$

$\Delta\Delta Cq$ was calculated by the equation

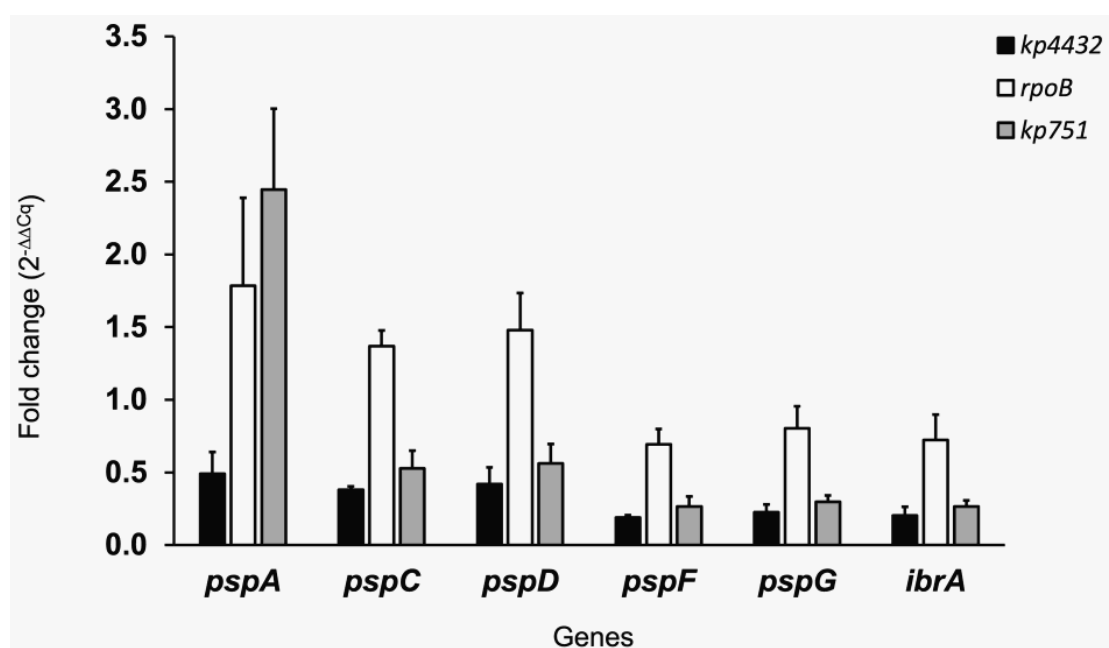
$$\Delta\Delta Cq = \left(Cq_{\text{gene-of-interest}} - Cq_{\text{reference gene}} \right)_{\text{treated}} - \left(Cq_{\text{gene-of-interest}} - Cq_{\text{reference gene}} \right)_{\text{untreated}}$$

where "treated" represents levofloxacin treatment (Livak and Schmittgen, 2001). Genes normalized using *rpoB* had the highest fold-change (Table 4.3.4), while those normalized to *kp4432* had the lowest. The fold-change observed using *rpoB* as a reference gene was approximately 3.5 times higher than that using *kp4432* as a reference gene (Figure 4.3.3).

An exception to this trend was seen in the expression of *pspA*; the fold change when normalised to *kp751* was almost 5 times that when normalised to *kp4432*, whereas the fold change when normalised to *rpoB* was about 3.5 times higher than that using *kp4432*.

Table 4.3.4 Fold-change for each of the genes obtained using *kp4432*, *rpoB*, or *kp751* as reference genes. Values for fold-change are represented as the average (Av) with the standard deviation (SD) among replicates (n = 3).

Gene	Fold change (Av ± SD) when normalised to		
	<i>kp4432</i>	<i>rpoB</i>	<i>kp751</i>
<i>pspA</i>	0.49 ± 0.15	1.79 ± 0.60	2.45 ± 0.56
<i>pspC</i>	0.38 ± 0.02	1.37 ± 0.11	0.53 ± 0.12
<i>pspD</i>	0.42 ± 0.11	1.48 ± 0.26	0.56 ± 0.13
<i>pspF</i>	0.19 ± 0.01	0.69 ± 0.11	0.27 ± 0.07
<i>pspG</i>	0.23 ± 0.05	0.80 ± 0.15	0.30 ± 0.04
<i>ibrA</i>	0.20 ± 0.06	0.72 ± 0.18	0.27 ± 0.04



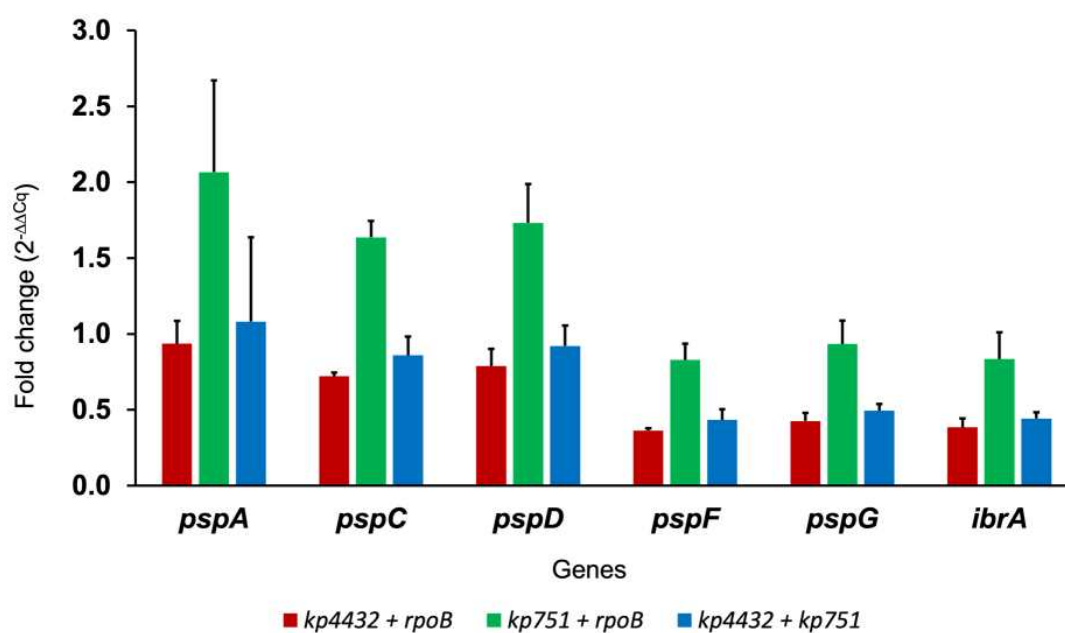
The trend with regard to the variation among replicates was not as straightforward. Gene expression normalized with *kp4432* was observed to be the least variant among the three candidate reference genes when observed for the *psp* genes tested except *pspG* (Figure 4.3.3). Expression of *pspG* and *ibrA* was least variant when normalised to *kp751*, though the same when normalised to *kp4432* was only 1.24 and 1.38 times respectively greater than the former (Table 4.3.4). Fold change obtained by normalising gene expression to *rpoB* was the most variant in five of the six genes examined. The exception was in *pspC*, with expression normalised to *kp751* having a higher standard deviation than that normalised to *rpoB*, though the difference between both was only 0.01.

Table 4.3.5 Fold-change for each of the genes obtained using combinations of *kp4432*, *rpoB*, or *kp751* as reference genes. Values for fold-change are represented as the average (Av; n = 3) with the standard deviation (SD) among replicates.

Gene	Fold change (Av ± SD) when normalised to		
	<i>kp4432</i> + <i>rpoB</i>	<i>kp751</i> + <i>rpoB</i>	<i>kp4432</i> + <i>kp751</i>
<i>pspA</i>	0.94 ± 0.30	2.07 ± 0.49	1.08 ± 0.22
<i>pspC</i>	0.72 ± 0.03	1.64 ± 0.26	0.86 ± 0.10
<i>pspD</i>	0.79 ± 0.17	1.73 ± 0.18	0.92 ± 0.15
<i>pspF</i>	0.36 ± 0.04	0.83 ± 0.18	0.43 ± 0.07
<i>pspG</i>	0.43 ± 0.09	0.93 ± 0.05	0.49 ± 0.05
<i>ibrA</i>	0.38 ± 0.10	0.83 ± 0.10	0.44 ± 0.07

The expression of the six genes was further assessed using pairs of reference genes to normalize gene expression. Gene expression calculated using a combination of *kp751* and *rpoB* as reference genes displayed the highest fold change, whereas the least fold change was observed with the combination of *kp4432* and *rpoB* (Figure 4.3.4). The difference between the both, though, was not as large as that observed using single reference genes (Table 4.3.5). Gene expression normalised to *kp751* and *rpoB* was only 2.2 times higher

than that when normalised to *kp4432* and *rpoB*. As with single reference genes, variation in the fold change among replicates did not follow a straightforward trend. While the combination of *kp751* and *rpoB* resulted in the most variant expression, this was observed in only *pspA*, *-C*, *-D*, and *-F*. The fold change observed when using *kp4432* and *kp751* together as reference genes resulted in the least variation in four genes viz. *pspA*, *-D*, *-G* and *ibrA*. Gene expression normalised to the pair of *kp4432* and *rpoB* was the least variant for *pspC* and *pspF* but was most variant for *pspG* and *ibrA*.



To summarise, the results of the investigation indicated using dual reference genes provided a reliable measure of gene expression compared to a single reference gene during gene expression-studies in bacterial persister cells. In the present study, the pair of the genes *kp4432* and *rpoB* were suited to evaluating gene-expression in KpIMS38, and all subsequent qPCR studies involved the use of the pair of the genes as internal reference controls.

4.3.2 Assessment of the expression profile of toxin-antitoxin genes found in KpIMS38 during persistence

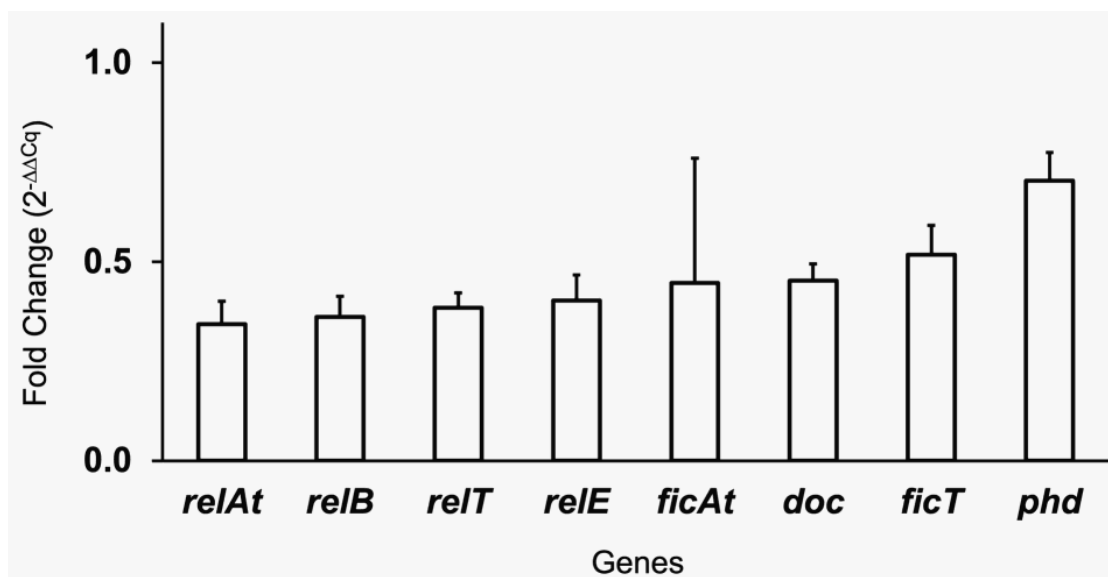
The role of toxin-antitoxin genes in persister cell formation was examined by qPCR for four cognate toxin-antitoxin gene pairs viz. *relTA*, *relBE*, *ficTA* and *phd-doc*. RNA was extracted from KpIMS38 treated with 256 µg/mL levofloxacin for 8 hours as well as from an untreated KpIMS38 culture, reverse-transcribed to cDNA and probed with gene-specific primers to measure the transcript levels of all the genes. Gene expression from the levofloxacin-treated sample was normalized to the pair of reference genes, i.e., *kp4432* and *rpoB*, and then to the untreated sample, and represented as the fold change. The fold change was calculated according to the formula mentioned in section 4.2.1.3 of this document.

The results indicated within a cognate pair, the toxin and the antitoxin were expressed at same levels on treatment of KpIMS38 with levofloxacin. The fold change for a toxin was only 1.1 times higher than its cognate antitoxin. The only notable exception was the *phd-doc* gene pair, where it was the *phd* antitoxin that was expressed 1.5 times higher than the *doc* toxin. The pattern of expression of the genes studied was found to be stable across replicates, with the exception of the *fic* antitoxin *ficAt*. The standard deviation (SD) for the fold change of *ficAt* was 0.31. This was not only 5 times the SD observed for all the other genes studied but was close to the mean fold change of 0.46 for the remaining genes.

Altogether, the observations from these experiments do not clearly indicate the involvement of the toxin-antitoxin systems studied in persister-cell formation of KpIMS38. This, however, requires to be substantiated through gene-deletion and gene-overexpression studies.

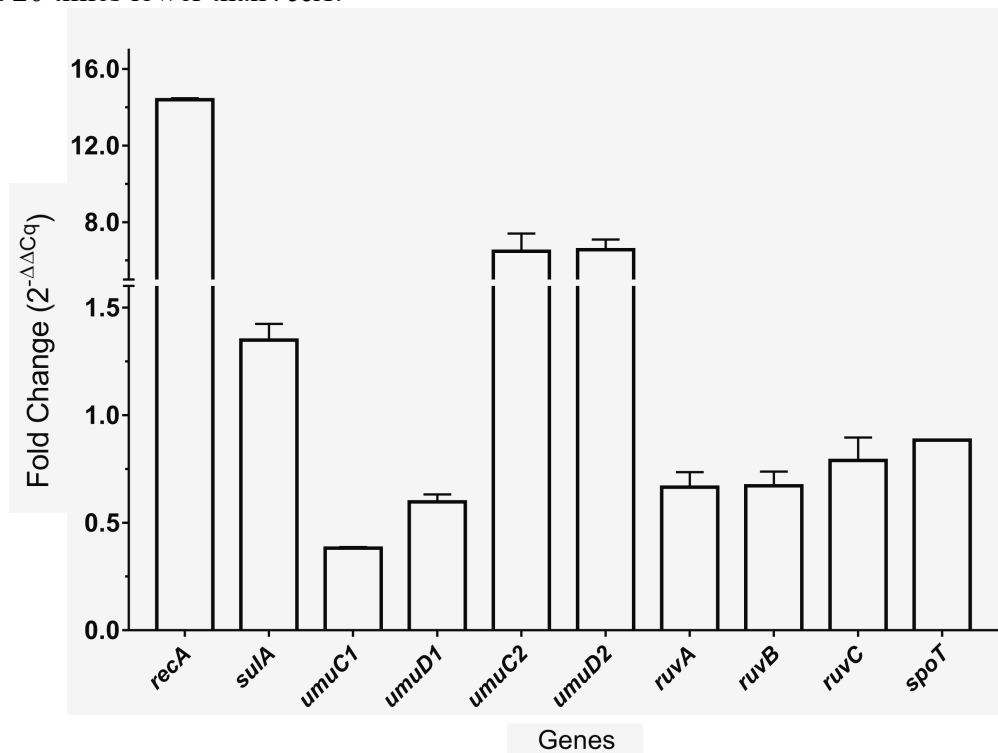
Table 4.3.6 Expression of toxin-antitoxin genes in KpIMS38 on treatment with levofloxacin. Fold-change values, calculated using both *kp4432* and *rpoB* as reference genes, were obtained for each gene and represented as the average (Av; n=3). Whiskers represent the standard deviation (SD) among replicates.

Gene	Fold change (Av ± SD)
<i>relT</i>	0.38 ± 0.04
<i>relAt</i>	0.34 ± 0.06
<i>relE</i>	0.40 ± 0.06
<i>relB</i>	0.36 ± 0.05
<i>ficT</i>	0.52 ± 0.07
<i>ficAt</i>	0.45 ± 0.31
<i>doc</i>	0.45 ± 0.04
<i>phd</i>	0.70 ± 0.07



4.3.3 Profiling the expression of stress-response genes in KpIMS38 persister cells

The expression of genes that are involved in mediating the bacterial response to stresses was assessed using qPCR. The genes chosen for this exercise included *recA*, *sulA*, *umuC*, *umuD*, *ruvA*, *ruvB*, *ruvC*, and *spoT*. The primers were used to probe cDNA obtained from bacteria treated with levofloxacin as well as untreated bacterial cultures after 8 hours of incubation. The $\Delta\Delta C_q$ values normalized to the pair of *kp4432* and *rpoB* and further to the untreated sample were used to calculate the fold change for each gene, represented in figure 4.3.6 and table 4.3.7. The greatest expression in KpIMS38 persisters was observed in *recA*. This was followed by the DNA polymerase V genes *umuD*, *umuC* and by the cell-division inhibitor *sulA*. The Holliday junction-resolvase genes *ruvA* and *-B* were the least expressed, almost 20 times lower than *recA*.



Exposing KpIMS38 to levofloxacin resulted in a biphasic reduction in the cell numbers, with the population size falling by 2 orders of magnitude within the first two hours of

antibiotic treatment. This time-period represents a phase when the bacteria alter their expression profile in response to the antibiotic, the understanding of which is crucial to elucidating the involvement of various genes in bringing about persistence. Hence, the expression of the stress-response genes was further examined at different time intervals. Therein, cellular RNA was extracted 15, 30, 45, 60, and 120 minutes post-levofloxacin treatment, converted to cDNA and used to perform qPCR. Untreated cultures were used as controls and extracted at same time points. At all the time points chosen for assessment of gene expression, *recA* was the most expressed gene among those tested, with a fold change consistently above 10 (Table 4.3.8). *ruvC* exhibited the least expressed of the genes was not consistently one single gene, with having the least expression at the time-points 15, 30 and 120 minutes while *spoT* had the least expression at 45 and 60 minutes.

Table 4.3.7 Fold-change for the stress-response genes in KpIMS38 upon treatment with levofloxacin for 8 hours. Expression values are represented as the mean fold change (Av; n = 2) with the standard deviation (SD) for each gene.

Gene	Fold Change (Av ± SD)	Gene	Fold Change (Av ± SD)
<i>recA</i>	14.40 ± 0.06	<i>sulA</i>	1.35 ± 0.05
<i>umuC1</i>	0.38 ± 0.00	<i>ruvA</i>	0.67 ± 0.05
<i>umuD1</i>	0.60 ± 0.02	<i>ruvB</i>	0.67 ± 0.05
<i>umuC2</i>	6.48 ± 0.66	<i>ruvC</i>	0.79 ± 0.08
<i>umuD2</i>	6.57 ± 0.38	<i>spoT</i>	0.88 ± 0.00

As expected, the level of expression was seen to vary across time for each gene (Figures 4.3.7 and 4.3.8). On observing the fold change values, a general pattern was identified. The expression rose, peaked at 30 or 45 minutes after levofloxacin exposure, and dropped thereafter; the least expression being observed at the 8-hour mark. This trend was observed for most of the genes, with a few exceptions. The lowest expression for *umuC2* and *umuD2*

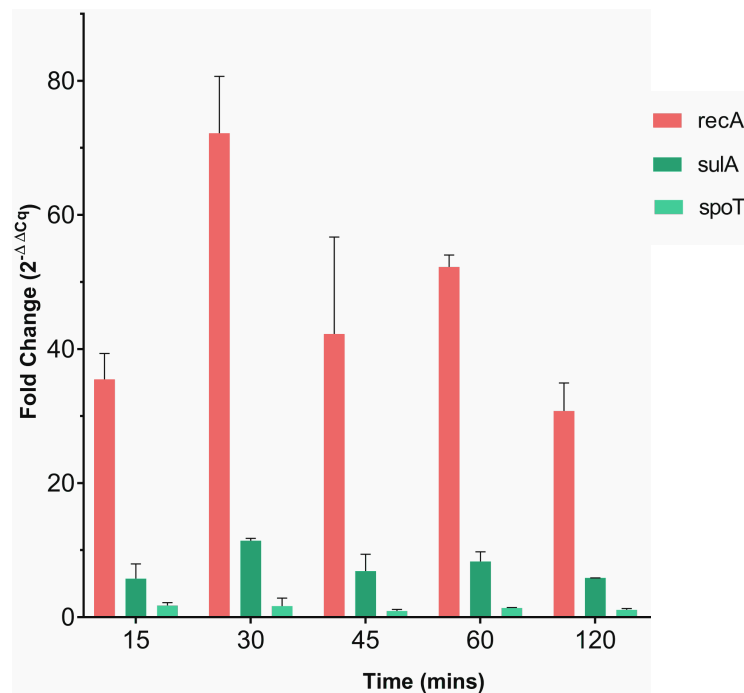
was observed 120 minutes post-antibiotic treatment, while the highest expression for *ruvA* and *ruvB* was 60 minutes after levofloxacin exposure. The profile for *spoT* contrasted with the rest of the genes, with the highest expression observed 15 minutes after exposure to levofloxacin. Aside from a strong dip at the 45-minute mark, the expression reduced gradually till it was at its lowest at the 8th hour.

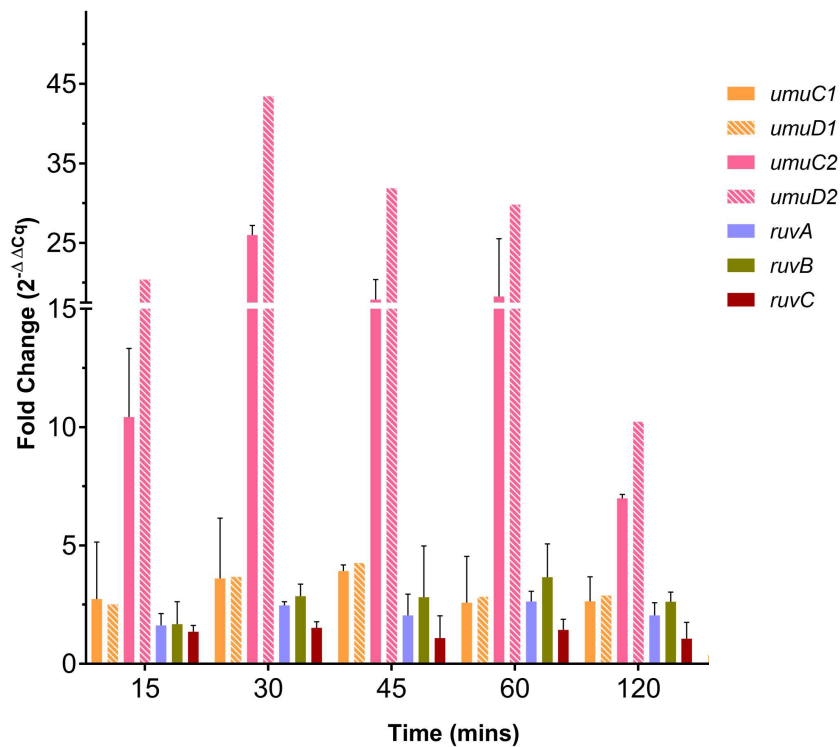
Table 4.3.8 Expression of the stress-response genes in KpIMS38 15, 30, 45, 60 and 120 minutes after treatment with levofloxacin. Expression values are represented as the mean fold change (\bar{A}_v ; $n = 2$) with the standard deviation (SD) for each gene.

Gene	Fold change ($\bar{A}_v \pm \text{SD}$) observed after (mins)				
	15	30	45	60	120
<i>recA</i>	35.49 \pm 2.73	72.20 \pm 6.01	42.24 \pm 10.23	52.26 \pm 1.25	30.78 \pm 2.95
<i>sulA</i>	5.76 \pm 1.56	11.43 \pm 0.25	6.89 \pm 1.77	8.34 \pm 1.02	5.87 \pm 0.01
<i>umuC1</i>	2.74 \pm 1.70	3.61 \pm 1.80	3.92 \pm 0.19	2.59 \pm 1.39	2.65 \pm 0.73
<i>umuD1</i>	2.51 \pm 0.94	3.68 \pm 1.63	4.26 \pm 0.53	2.83 \pm 0.62	2.89 \pm 0.36
<i>umuC2</i>	10.43 \pm 2.05	26.00 \pm 0.86	17.89 \pm 1.79	18.28 \pm 5.13	6.99 \pm 0.12
<i>umuD2</i>	20.42 \pm 5.14	43.45 \pm 3.29	31.88 \pm 1.82	29.83 \pm 1.92	10.23 \pm 0.53
<i>ruvA</i>	1.63 \pm 0.35	2.47 \pm 0.11	2.05 \pm 0.63	2.63 \pm 0.31	2.05 \pm 0.38
<i>ruvB</i>	1.68 \pm 0.67	2.86 \pm 0.37	2.82 \pm 1.53	3.67 \pm 0.99	2.63 \pm 0.29
<i>ruvC</i>	1.36 \pm 0.19	1.53 \pm 0.18	1.09 \pm 0.67	1.43 \pm 0.32	1.07 \pm 0.49
<i>spoT</i>	1.77 \pm 0.29	1.69 \pm 0.83	0.95 \pm 0.15	1.40 \pm 0.04	1.11 \pm 0.14

Considering the four DNA polymerase V genes, a distinct difference between the expression levels of the homologs was observed. The *umuC1-umuD1* pair was expressed at a much lower level than its counterpart homologs. At any given time, the fold change for either gene from the *umuC2-umuD2* pair was not less than 2.5 times that of its homolog; the greatest being observed at the 8th hour with the expression of *umuC2* being almost 19

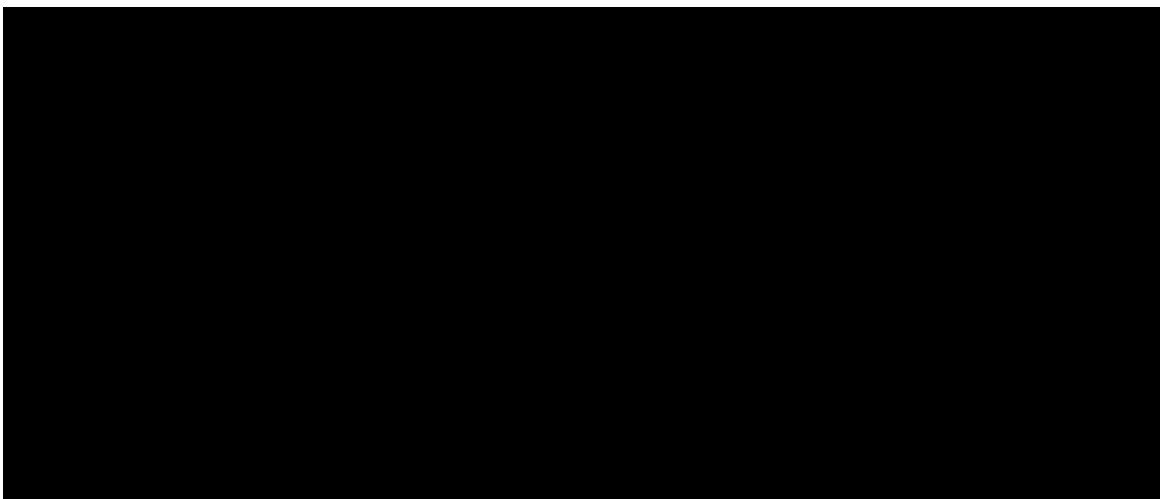
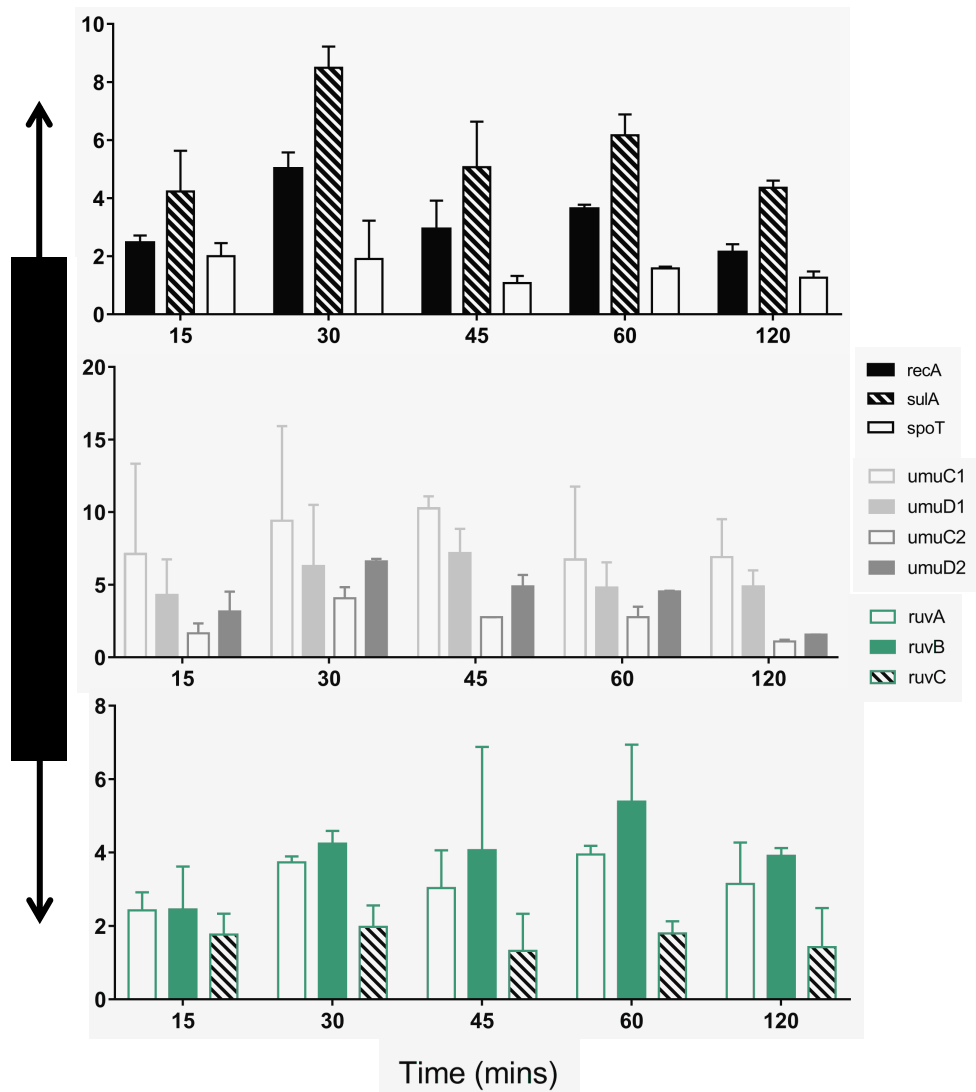
times that of *umuC1*. Within the *ruvABC* gene triplet, the pattern of expression of *ruvA* closely matched that of *ruvB*. Both genes were upregulated by about 1.5-fold 15 minutes after exposure to levofloxacin, from where they peaked at the 60 minute-mark and fell till they were at their lowest when measured 8 hours post-antibiotic treatment. At the point of their highest expression, *ruvB* was upregulated a full 1-fold more than *ruvA*. While *ruvC* followed the same pattern of expression, the level of expression was much lower than the other two. At the point of maximum expression, which was the 30th minute for *ruvC*, the gene was upregulated a complete two folds lower than *ruvA* and *ruvB* at their highest expression.





Additionally, gene expression was also normalised to the expression observed 8 hours after treatment with levofloxacin. Namely, the ratio of the fold change at a specific time point to the fold change after 8 hours was calculated for each gene at all the time points considered in the study, i.e., 15, 30, 45, 60, and 120 minutes (Figure 4.3.9). The results obtained possessed a degree of variation compared to those obtained from purely fold-change values. For instance, the fold-change of *recA* was the highest among all the genes but the ratio of the fold change was distinctly lower. The highest *recA* expression was recorded after 30 minutes in both sets of data, but while the fold change was 72, the ratio was only 5. This pattern where the fold-change ratio was markedly lower than the fold change was observed for all the time-points, although it should be noted that the trend of expression was similar for both sets of results. Another distinct observation was the fold-change ratio of *umuC1D1* being higher than that of *umuC2D2*. Also, *umuC1* had a higher ratio than *umuD1*, differing

from the other pair where the fold-change ratio of *umuD2* was higher than *umuC2*. The expression-trend for the *ruv* genes across time was similar when assessing both fold change as well as the fold-change ratio; the expression of *ruvA* and *-B* gradually increased till it



peaked at 60 minutes, whereas *ruvC* was expressed at a constant level throughout the timeframe of the assessment.

Taken together, the aforementioned observations are suggestive of the involvement of DNA repair mechanisms in the persistence of KpIMS38.

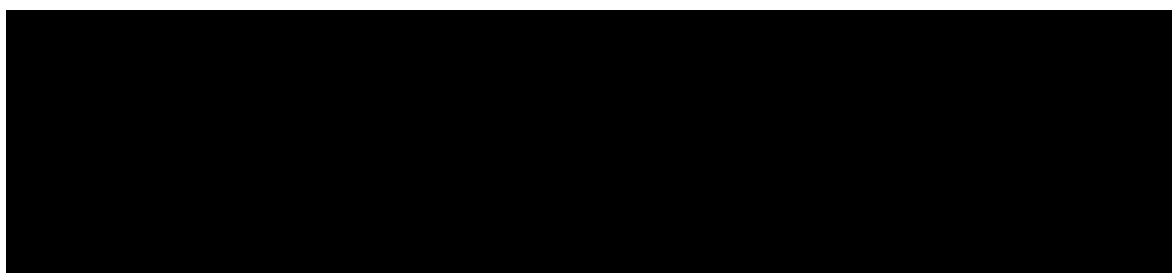
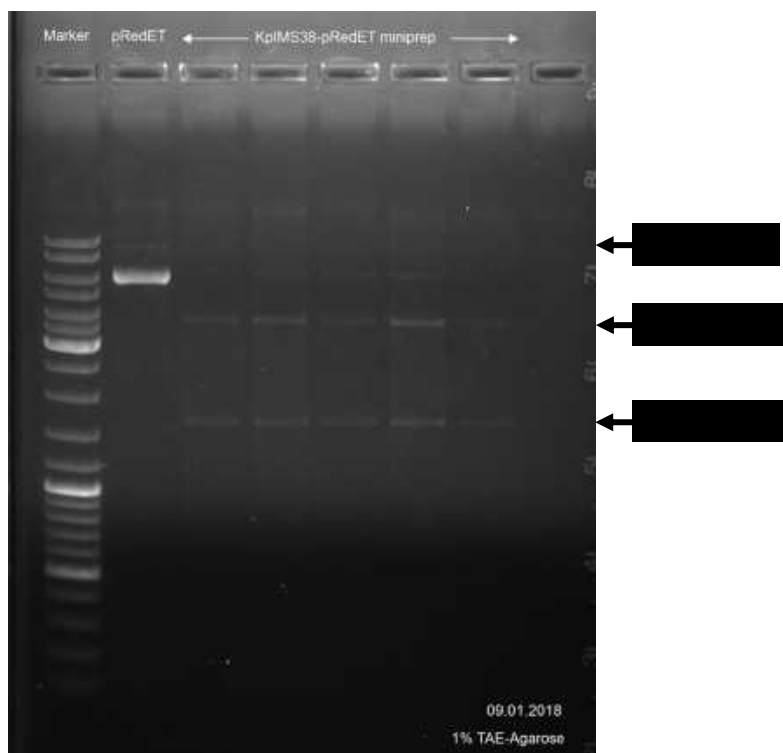
4.3.4 Assessment of the involvement of various genes in persister cell-formation in KpIMS38 by inhibiting gene expression

4.3.4.1 Generation of deletion mutants in KpIMS38 by lambda recombineering using pRedET

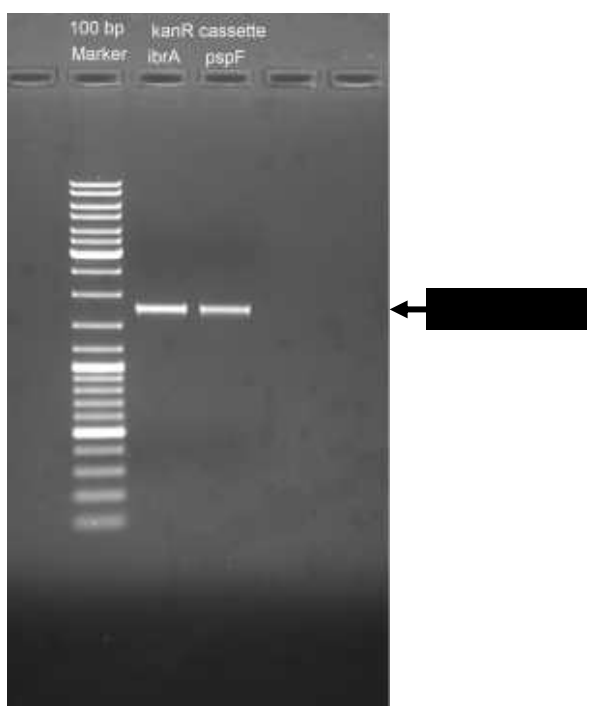
To explore the genetic basis of persister cell formation in KpIMS38, the loss-of-function approach was chosen. Herein, the ability of strains of KpIMS38 containing deletions of single genes to form persister cells in response to treatment with levofloxacin was examined. To achieve this, the Red/ET recombination approach was adopted wherein the target gene was disrupted by the insertion of a DNA cassette consisting of an antibiotic-resistance gene flanked by flippase recognition target (FRT) sites. Briefly, the strain, containing the gene targeted for deletion, was transformed with the plasmid pRedET. Then, the deletion cassette was constructed by PCR, yielding a linear DNA molecule consisting of the FRT cassette flanked by 60 bp “overhang” sequences – homologous to the target gene – at both ends of the molecule. The plasmid pRedET was induced to express the *red $\gamma\beta\alpha$* operon, the deletion cassette transformed into the strain and homologous recombination allowed to occur. Cells containing the cassette inserted within the target gene were then selected by growth in the presence of the antibiotic. Transformants with kanamycin resistance were checked for successful insertion of the deletion cassette by PCR. This schematic represents cases of successful as well as unsuccessful creation of deletion-mutants.

Genes were chosen for this exercise based on the expression pattern as inferred from the transcriptome of KpIMS38 persisters as well as qPCR studies. A total of four genes were targeted for deletion viz. *ibrA*, *pspF*, *doc* and *relE*. The latter two genes are toxins belonging to the toxin-antitoxin cognate gene-pairs *phd-doc* and *relBE* respectively. While *pspF* belongs to the *psp* operon involved in the bacterial response to unfolded

proteins, *ibrA* is a coactivator of phage gene expression. Deletion was carried out using the procedures mentioned in section 3.3.9.4 of this document.



KpIMS38 was successfully transformed with pRedET, as visualized by agarose gel electrophoresis of the plasmid DNA extracted from the plasmid transformants (Figure 4.3.10). The bands corresponding to supercoiled, linear and open-circular forms of the plasmid were visible in all the transformants examined, and corresponded to the sizes as seen against the purified pRedET plasmid DNA. Bands of the sizes of approximately 1700 bp and 3700 bp were also visible in plasmid DNA extracted from KpIMS38-pRedET transformants, and corresponded to the plasmid inherently present in KpIMS38 (Figure 4.3.10).

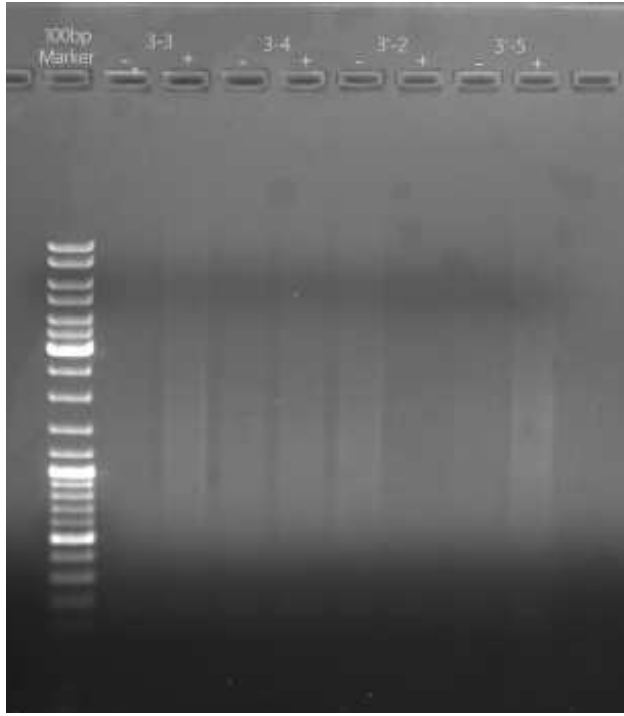
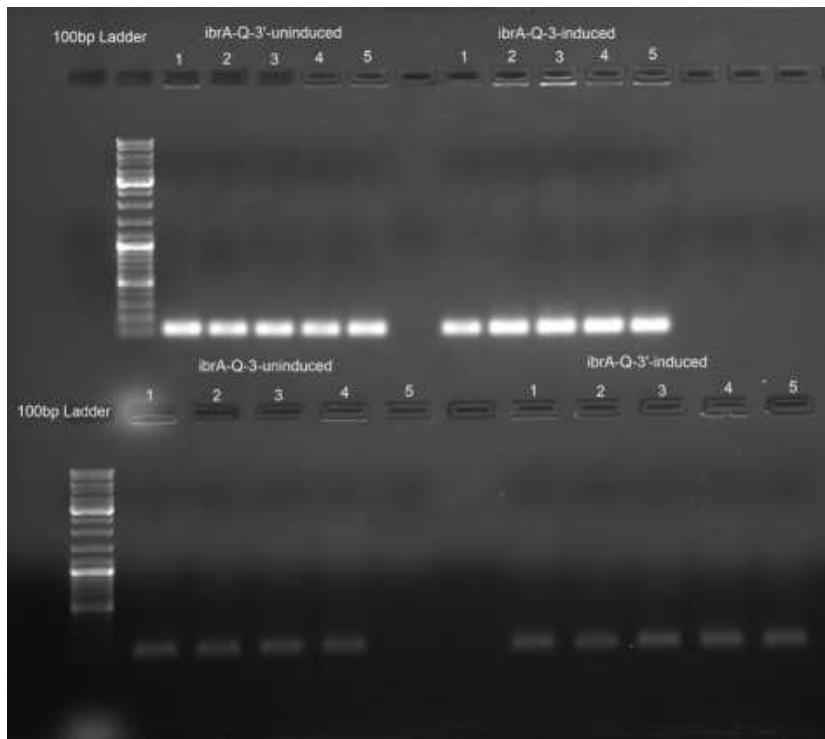


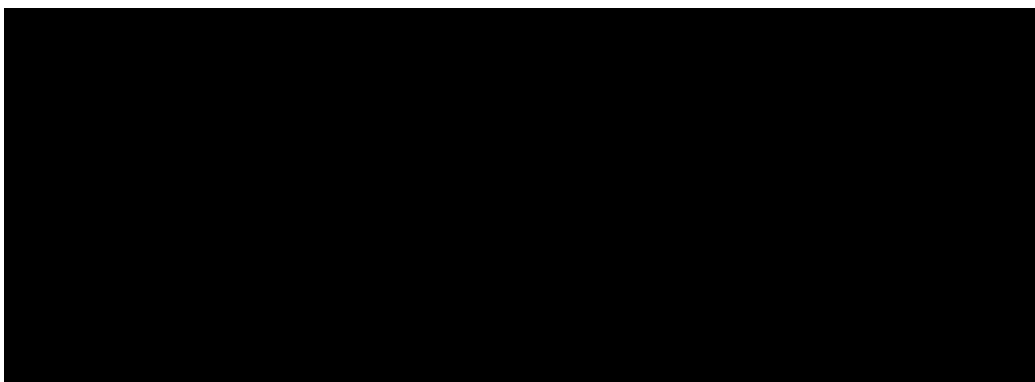
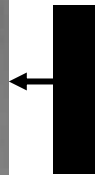
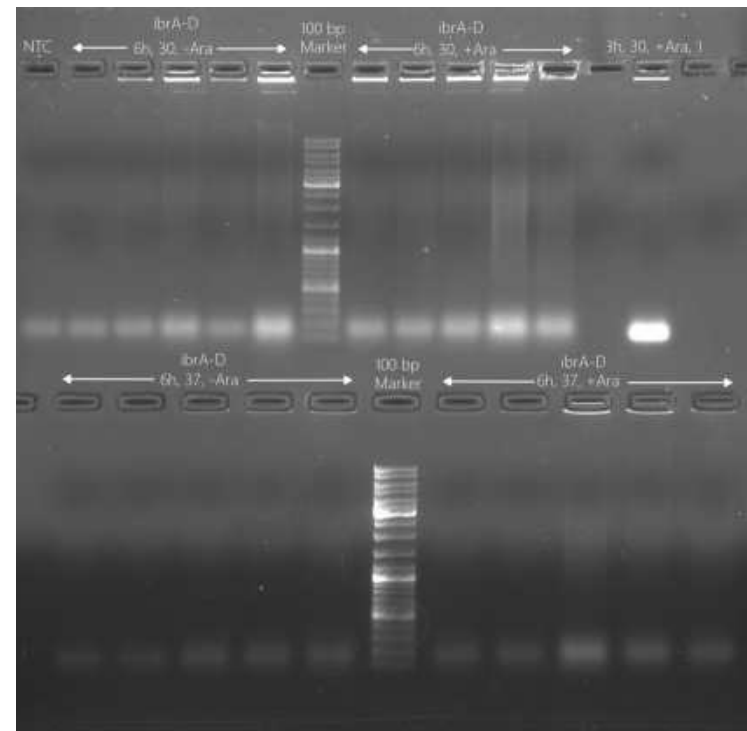
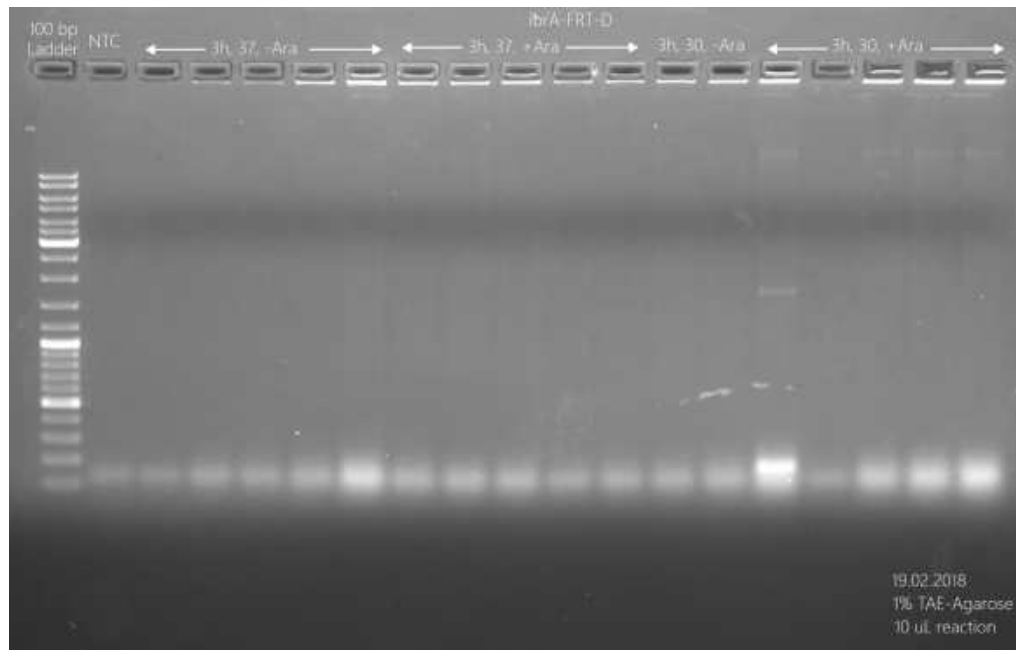
The deletion cassettes for the genes *ibrA* and *pspF* were synthesized by high-fidelity PCR, resulting in double stranded DNA cassettes containing 50 bp sequences at the 5' and 3' ends, homologous to either gene-of-interest. The resulting DNA molecules were approximately 1700 bp in size (Figure 4.3.11).

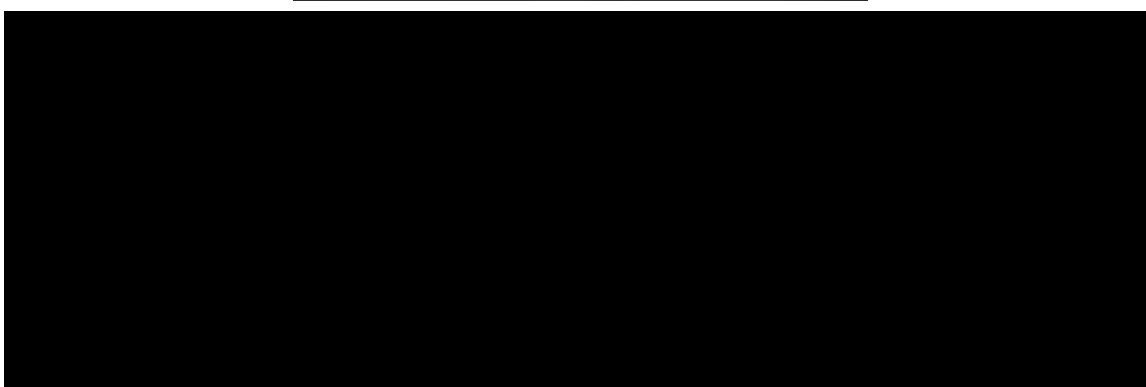
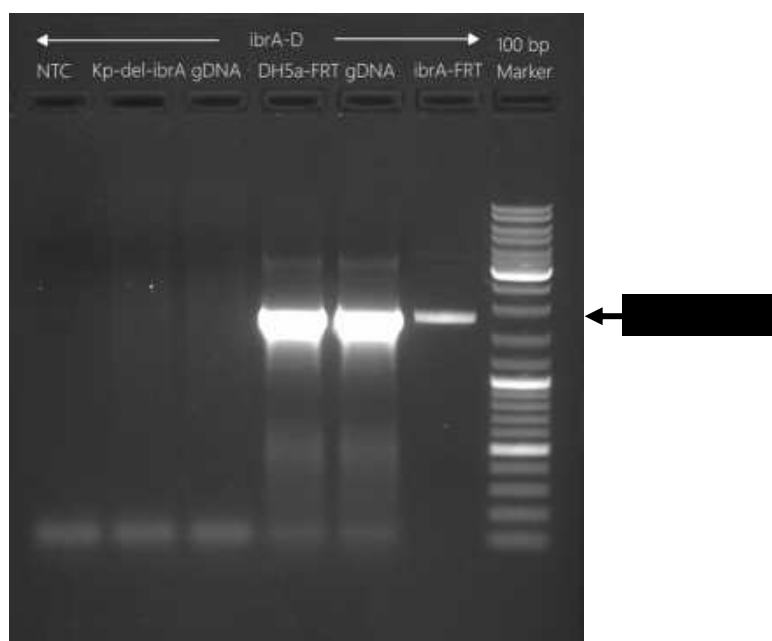
Deletion of *ibrA* was initially attempted, with the protocol of transformation stated previously in this section followed. Briefly, KpIMS38-pRedET was induced with 0.4 % of L-arabinose for 1 hour at 37°C and transformed with 75 ng of the *ibrA* cassette by electroporation using a 2 mm electroporation cuvette at 1350 V with a 5 ms time-constant protocol. After revival in LB broth at 37°C for 3 hours, the culture was plated on LBA-Kan¹⁵. Colonies obtained on both uninduced and induced plates were examined using the *ibrA*-Q-F and -Q-R primers (Table 3.3.17) through colony PCR. Amplicons corresponding to 100 bp were obtained for all the reactions, i.e., uninduced as well as

induced (Figure 4.3.12). Additionally, genomic DNA was extracted from each of the colonies assessed and was used as template to perform a PCR using the cassette-synthesis primers *ibrA-D-F* and *-D-R* (Table 3.3.20). No amplicons were visible for either the uninduced or induced colonies (Figure 4.3.13).

The deletion experiment was repeated with a few changes. KpIMS38 transformed with the deletion-cassette for *ibrA* was incubated at 30°C for 90 minutes, then supplemented with 0.4% L-arabinose to induce expression of genes on the plasmid pRedET. The culture was then incubated at 30°C as well as 37°C grown for 3 hours and 6 hours post-induction before spread-planting on LBA-Kan¹⁵. From the resultant transformants each of the four conditions employed, five colonies were selected and colony PCR performed with the cassette-synthesis primers *ibrA-D-F* and *-D-R*. A single band corresponding to 1700 bp was observed in one reaction using a colony treated with L-arabinose at 30°C for 3 hours (Figure 4.3.14). Primer-dimers were observed for the rest of the reactions, with no other amplicons seen (Figure 4.3.15). To further confirm, genomic DNA was extracted from each of the colonies assessed and used as template to perform a PCR using the cassette-synthesis primers *ibrA-D-F* and *-D-R*. No amplicon corresponding to the deletion cassette was observed in the reactions. In comparison, a 1700-bp amplicon was observed in the positive-control – that used the *EcoΔmanZYX::kan^R* genomic DNA – as well as in the lane run with purified *ibrA*-cassette DNA (Figure 4.3.16).

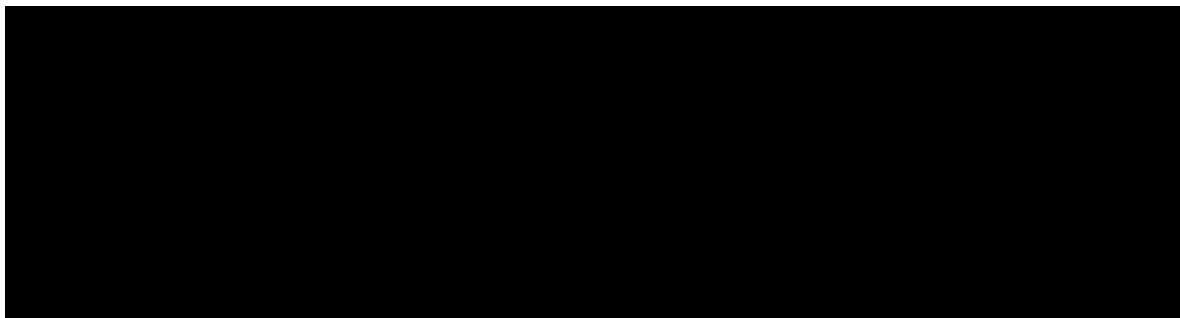
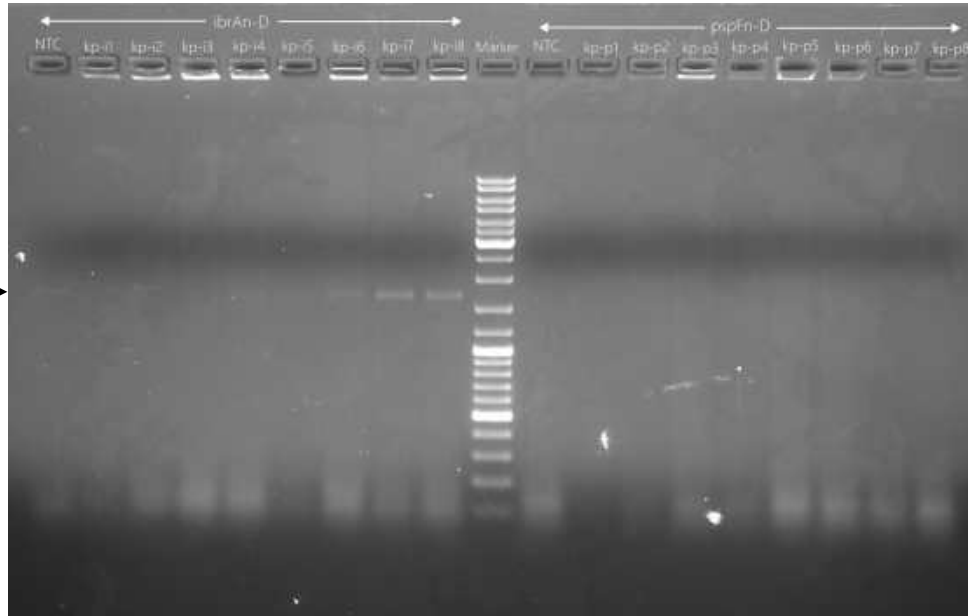






New cassette-synthesis primers were designed for the genes *ibrA*, *pspF*, *doc* and *relE*, such that each primer had 60-bp homology regions and the regions were separated by a minimum distance of 100 bp in the genome of KpIMS38. Deletion cassettes for each of the genes were synthesized using the new primers (Table 3.3.20) and were used to carry out deletion. KpIMS38-pRedET cells were treated with 0.4% L-arabinose at 37°C for 1 hour, and transformed using 600 ng of the deletion cassettes for *ibrA* and *pspF* individually. Transformation was carried out in 2 mm electroporation cuvettes at 2500 V using a 5 ms time-constant protocol, and the cultures were revived in LB broth at 37°C for 3 hours. Colonies obtained on LBA-Kan¹⁵ plates were assessed using the new cassette-synthesis primers for both the genes viz. *ibrAn-D-F* and *-D-R*, and *pspFn-D-F* and *-D-R* (Table 3.3.20) through colony PCR. Amplicons corresponding to approximately 1700 bp

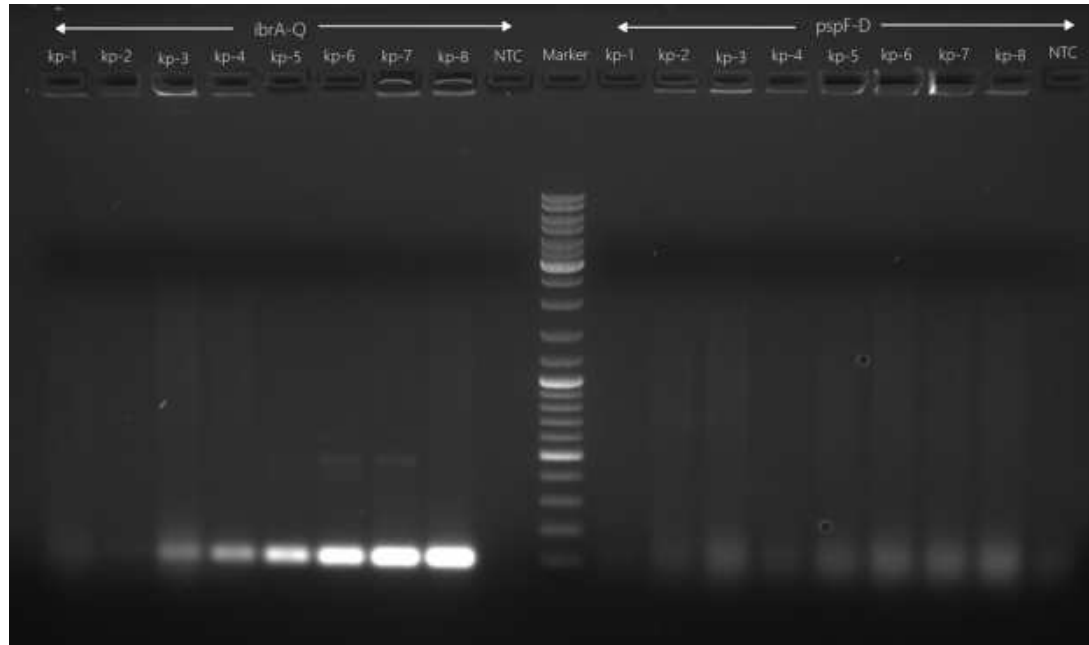
were clearly visible in two (kp-i7 and -i8) of the eight reactions obtained from putative $\Delta i brA$ colonies (Figure 4.3.17). Amplicons of the same size were faintly visible in three (kp-i4, -i5 and -i6) of the eight total reactions performed. In contrast, there were no



amplicons visible in the reactions performed using colonies from putative $\Delta pspF$ colonies, even after repeating the PCR (Figure 4.3.17). When the PCR was repeated for the putative $\Delta i brA$ colonies using the *ibrA*-Q primers, amplicons corresponding to the qPCR product of *ibrA*, i.e, 103 bp were visible in reactions for six (kp-i3 to -i8) colonies (Figure 4.3.18).

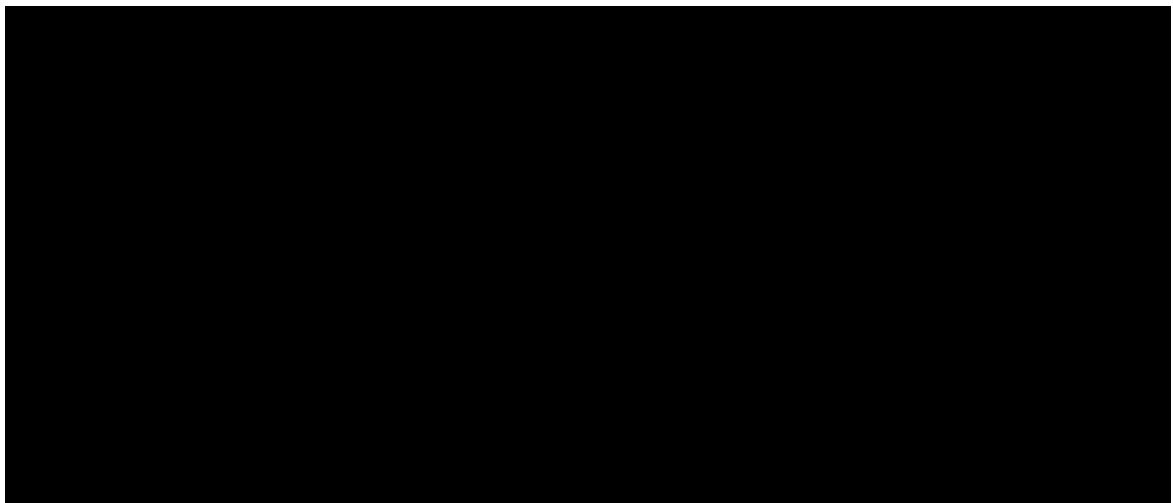
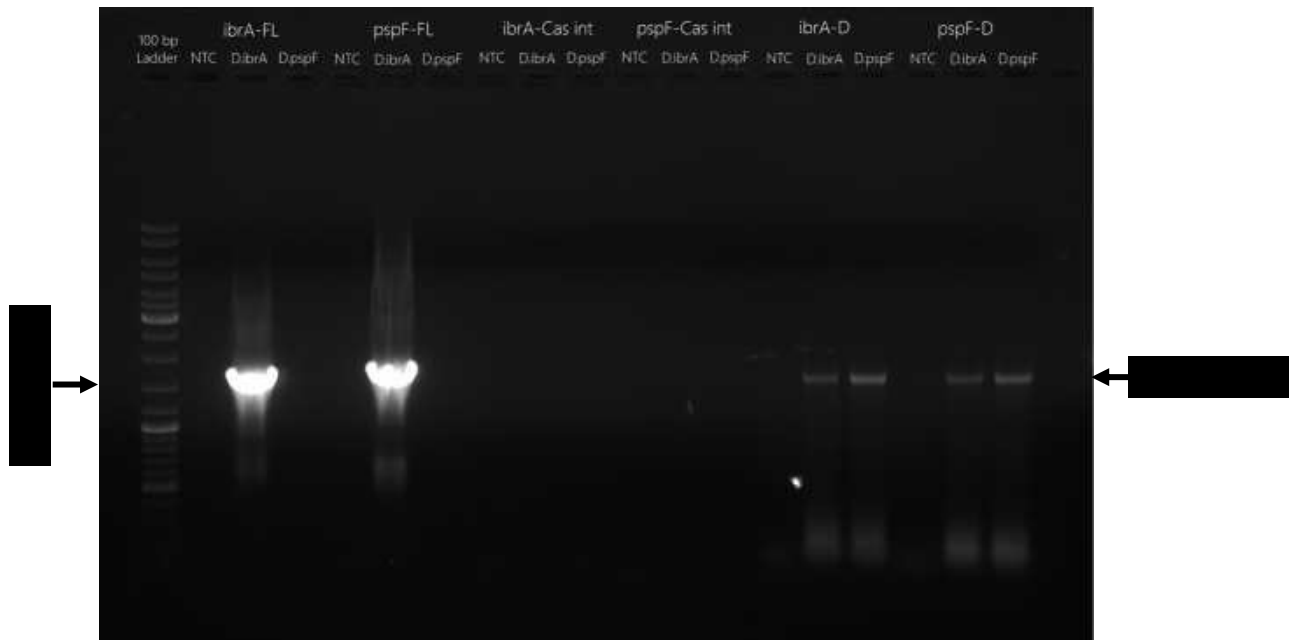
Genomic DNA was extracted from the putative deletion mutants (for both genes) and used to perform a PCR using full-length primers, which amplify the entire reading frame of the genes *ibrA* (*ibrA*-FL-F and -FL-R) and *pspF* (*pspF*-FL-F and -FL-R). In addition, reactions were also set up using an internal primer FRTcas-Int-F, which binds within the

FRT-pgk-gb2-neo-FRT region, along with the reverse primer for the corresponding gene (Table 3.3.21). This was performed to verify the insertion of the FRT deletion-cassette in and thereby ascertain deletion of the genes. PCR with full-length primers should ideally

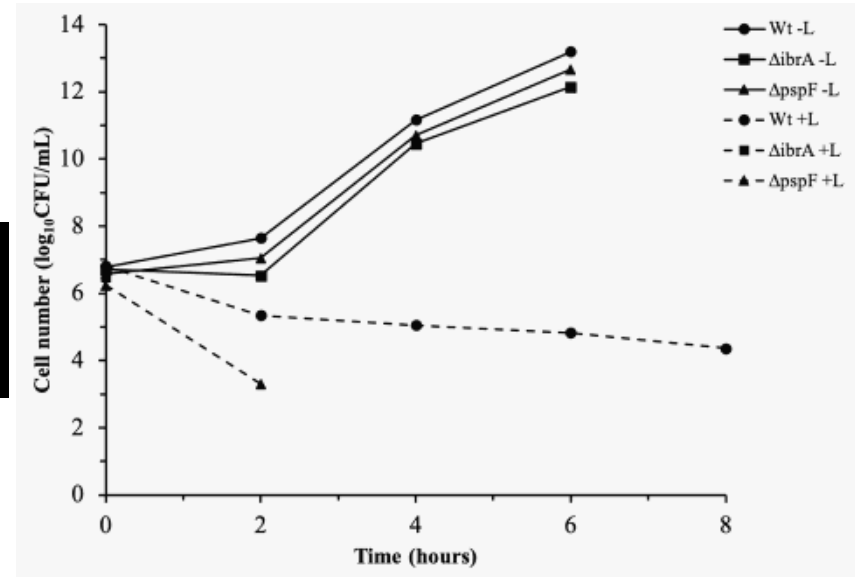
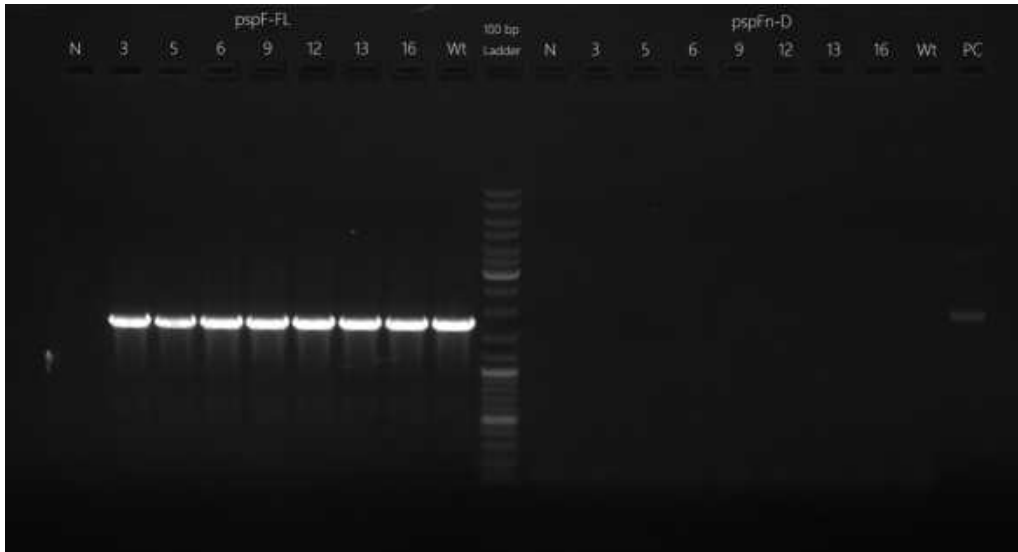


yield amplicons about 2000 bp long in deletion-positive strains compared to 1700 bp amplicons in wild-type KpIMS38, due to the insertion of the deletion-cassette. Similarly, PCR using the reverse full-length primer along with FRTcas-Int-F should generate an amplicon in deletion-positive strains and no amplification in the wild-type. Amplicons approximately 1700 bp in size were observed in reactions using full-length primers for both genes in the $\Delta ibrA$ strain (Figure 4.3.19). No amplicons were observed for the same in the $\Delta pspF$ strain. Reactions using the internal primer along with the reverse primer to verify the insertion of the cassette within the specific gene did not yield any amplicons for either of the putative deletion mutants. These results indicated the absence of the deletion cassette inserted in the genome and lack of deletion of *ibrA* and *pspF*.

Genomic DNA from multiple putative Δ *pspF* isolates was extracted and PCR repeated using the full-length as well as cassette-synthesis primers for *pspF*. Genomic DNA from wild-type KpIMS38 and *Eco* Δ *manZYX::kanR* were used as positive controls for the



respective reactions. Amplicons approximately 1700 bp in size were observed for the putative mutants as well as in the positive control reaction using the *pspFnD* primers (Figure 4.3.20). While a band of the size range between 1500 bp and 2000 bp was observed in the positive-control reaction for the *pspF-FL* primers, no amplicons were observed for the Δ *pspF* reactions.



Taken together, the above results indicate:

- a) the deletion-cassettes were present in the genome
- b) no change in the size of the full-length gene sequence, and
- c) no amplification in reactions using the internal primer along with a full-length primer

in the putative mutants. This is suggestive of the deletion cassette being inserted within the genome of KpIMS38 but not at the intended site.

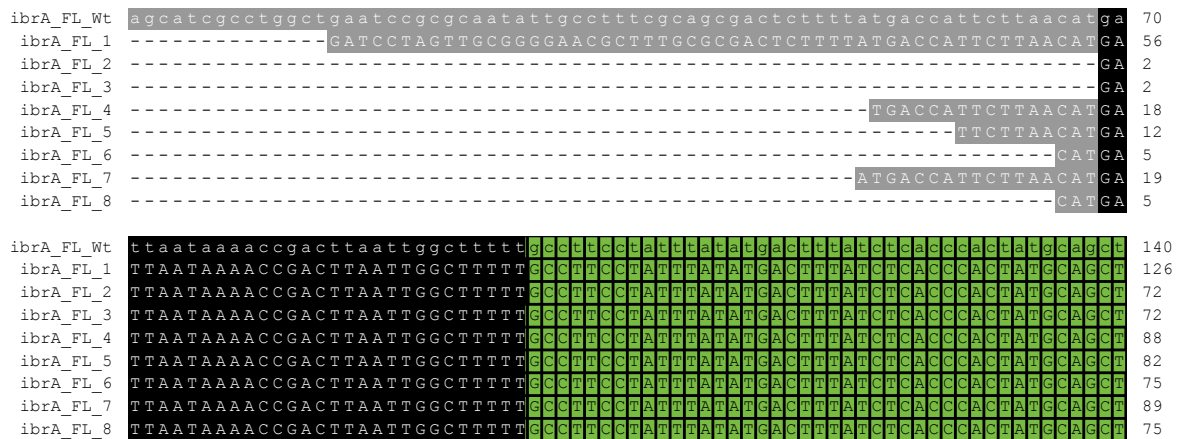
Table 4.3.9 Survival of putative \DeltaibrA and \DeltapspF strains of KpIMS38 in levofloxacin compared to the wild type (Wt). Cell numbers of untreated cultures (-L) as well as those treated with 256 $\mu\text{g}/\text{mL}$ levofloxacin (+L) were reported as $\log_{10}\text{CFU}/\text{mL}$, with averages (Av) of biological replicates (n=2) and the standard deviation (SD) represented here.

Time (hours)	Cell Number ($\log_{10}\text{CFU}/\text{mL}$; Av \pm SD)					
	Wt -L	\DeltaibrA -L	\DeltapspF -L	Wt +L	\DeltaibrA +L	\DeltapspF +L
0	6.78	6.71	6.57	6.80 \pm 0.04	6.48 \pm 0.00	6.24 \pm 0.00
2	7.64	6.53	7.04	5.35 \pm 0.02		3.30 \pm 0.00
4	11.16	10.45	10.70	5.05 \pm 0.00		
6	13.19	12.15	12.66	4.83 \pm 0.02		
8				4.36 \pm 0.23		

The response of the putative deletion mutants to levofloxacin was assessed using the time-kill assay, as a means of identifying whether the insertion of the deletion-cassette within the genome had perturbed the persistence of KpIMS38 in any manner. The survival of one putative \DeltaibrA and one putative \DeltapspF isolates in 256 $\mu\text{g}/\text{mL}$ levofloxacin was observed and compared to that of the type KpIMS38. Experiments were carried out in LB or LB-Kan¹⁵ broth media, according to the protocol mentioned in section 3.3.6.1 of this document. The putative mutant-strains of KpIMS38 exhibited a pattern of growth similar

to the wild-type when grown in the absence of levofloxacin (Figure 4.3.21). Neither the *ΔibrA* nor the *ΔpspF* (putative) strains grew in levofloxacin, unlike the wild-type KpIMS38 that exhibited conventional biphasic killing (Table 4.3.9).

To determine whether the *ΔibrA* isolates obtained truly contain the deletion cassette inserted within the *ibrA* gene, a PCR was performed using the *ibrA*-FL primers with genomic DNA isolated putative *ΔibrA* isolates. The amplicons observed were acquired from the gel and the individual oligonucleotides subjected to Sanger's sequencing, according to the protocols described in sections 3.2.3 and 3.2.4 respectively of this document. The sequences obtained were compared by performing a multiple-sequence alignment with the MAFFT algorithm using T-Coffee (Notredame et al, 2000). The sequence of *ibrA* from wild-type KpIMS38 as the reference sequence. Among the eight sequences obtained from the putative *ibrA* mutants, *ibrA_FL_1* was the only one obtained as a complete sequence from DNA sequencing whereas the remaining seven sequences were obtained with gaps. Nevertheless, all eight sequences were identical to wild-type *ibrA* (Figure 4.3.22). The region contained within both the 60-bp overhangs, that was expected to contain the FRT deletion cassette in *ΔibrA* mutants, did not exhibit any sequence dissimilarity between the reference and the eight sequences. This indicated a lack of deletion of *ibrA*.



```

ibrA_FL_Wt      tcacgcccatacaacatagataatctttttccggatatacagatctacattaattaccaccatgcatcttcg 210
ibrA_FL_1      TCACGCCCATCAACATAGA TAATCTTTTTCCGGATATCAGCATCTACATTAATTACCACCATGCATCTTTCG 196
ibrA_FL_2      TCACGCCCATCAACATAGA TAATCTTTTTCCGGATATCAGCATCTACATTAATTACCACCATGCATCTTTCG 142
ibrA_FL_3      TCACGCCCATCAACATAGA TAATCTTTTTCCGGATATCAGCATCTACATTAATTACCACCATGCATCTTTCG 142
ibrA_FL_4      TCACGCCCATCAACATAGA TAATCTTTTTCCGGATATCAGCATCTACATTAATTACCACCATGCATCTTTCG 158
ibrA_FL_5      TCACGCCCATCAACATAGA TAATCTTTTTCCGGATATCAGCATCTACATTAATTACCACCATGCATCTTTCG 152
ibrA_FL_6      TCACGCCCATCAACATAGA TAATCTTTTTCCGGATATCAGCATCTACATTAATTACCACCATGCATCTTTCG 145
ibrA_FL_7      TCACGCCCATCAACATAGA TAATCTTTTTCCGGATATCAGCATCTACATTAATTACCACCATGCATCTTTCG 159
ibrA_FL_8      TCACGCCCATCAACATAGA TAATCTTTTTCCGGATATCAGCATCTACATTAATTACCACCATGCATCTTTCG 145

ibrA_FL_Wt      caaaatcattttttaactgaattaatcaccatattaatgaatgatcgagaggcatcacggcccaattta 280
ibrA_FL_1      CAAAATCATTTTTTAACTGAATTAATCACCATATTAATGAATGATCGAGAGGCATCACGGCCCAAATTTA 266
ibrA_FL_2      CAAAATCATTTTTTAACTGAATTAATCACCATATTAATGAATGATCGAGAGGCATCACGGCCCAAATTTA 212
ibrA_FL_3      CAAAATCATTTTTTAACTGAATTAATCACCATATTAATGAATGATCGAGAGGCATCACGGCCCAAATTTA 212
ibrA_FL_4      CAAAATCATTTTTTAACTGAATTAATCACCATATTAATGAATGATCGAGAGGCATCACGGCCCAAATTTA 228
ibrA_FL_5      CAAAATCATTTTTTAACTGAATTAATCACCATATTAATGAATGATCGAGAGGCATCACGGCCCAAATTTA 222
ibrA_FL_6      CAAAATCATTTTTTAACTGAATTAATCACCATATTAATGAATGATCGAGAGGCATCACGGCCCAAATTTA 215
ibrA_FL_7      CAAAATCATTTTTTAACTGAATTAATCACCATATTAATGAATGATCGAGAGGCATCACGGCCCAAATTTA 229
ibrA_FL_8      CAAAATCATTTTTTAACTGAATTAATCACCATATTAATGAATGATCGAGAGGCATCACGGCCCAAATTTA 215

ibrA_FL_Wt      atcacagcgaataacgccccttctggttcccccgctgccagaaacaataatcgaccattaatttcctacccc 350
ibrA_FL_1      ATCACAGCGAATAACGCCCTTCTGTTCCCCGCTGCCAGAAACAATAATCGACCATTAATTTCTTACCCC 336
ibrA_FL_2      ATCACAGCGAATAACGCCCTTCTGTTCCCCGCTGCCAGAAACAATAATCGACCATTAATTTCTTACCCC 282
ibrA_FL_3      ATCACAGCGAATAACGCCCTTCTGTTCCCCGCTGCCAGAAACAATAATCGACCATTAATTTCTTACCCC 282
ibrA_FL_4      ATCACAGCGAATAACGCCCTTCTGTTCCCCGCTGCCAGAAACAATAATCGACCATTAATTTCTTACCCC 298
ibrA_FL_5      ATCACAGCGAATAACGCCCTTCTGTTCCCCGCTGCCAGAAACAATAATCGACCATTAATTTCTTACCCC 292
ibrA_FL_6      ATCACAGCGAATAACGCCCTTCTGTTCCCCGCTGCCAGAAACAATAATCGACCATTAATTTCTTACCCC 285
ibrA_FL_7      ATCACAGCGAATAACGCCCTTCTGTTCCCCGCTGCCAGAAACAATAATCGACCATTAATTTCTTACCCC 299
ibrA_FL_8      ATCACAGCGAATAACGCCCTTCTGTTCCCCGCTGCCAGAAACAATAATCGACCATTAATTTCTTACCCC 285

ibrA_FL_Wt      tcatcgttttatactgagetaacgggaattttctactattaaaggattaatggtcATGTCGTTTATTAAT 420
ibrA_FL_1      TCATCGTTTTACTGAGCTAACGGGAATTTTCTACTATTTAAAGGATTAATGGTCATGTCGTTTATTAAT 406
ibrA_FL_2      TCATCGTTTTACTGAGCTAACGGGAATTTTCTACTATTTAAAGGATTAATGGTCATGTCGTTTATTAAT 352
ibrA_FL_3      TCATCGTTTTACTGAGCTAACGGGAATTTTCTACTATTTAAAGGATTAATGGTCATGTCGTTTATTAAT 352
ibrA_FL_4      TCATCGTTTTACTGAGCTAACGGGAATTTTCTACTATTTAAAGGATTAATGGTCATGTCGTTTATTAAT 368
ibrA_FL_5      TCATCGTTTTACTGAGCTAACGGGAATTTTCTACTATTTAAAGGATTAATGGTCATGTCGTTTATTAAT 362
ibrA_FL_6      TCATCGTTTTACTGAGCTAACGGGAATTTTCTACTATTTAAAGGATTAATGGTCATGTCGTTTATTAAT 355
ibrA_FL_7      TCATCGTTTTACTGAGCTAACGGGAATTTTCTACTATTTAAAGGATTAATGGTCATGTCGTTTATTAAT 369
ibrA_FL_8      TCATCGTTTTACTGAGCTAACGGGAATTTTCTACTATTTAAAGGATTAATGGTCATGTCGTTTATTAAT 355

ibrA_FL_Wt      ATCCCTTACCGGAATCGGTGCTGCAGGCAACTGAGCAGCGGATCCAGTGGGTCATCGATAATTTTTTCGGG 490
ibrA_FL_1      ATCCCTTACCGGAATCGGTGCTGCAGGCAACTGAGCAGCGGATCCAGTGGGTCATCGATAATTTTTTCGGG 476
ibrA_FL_2      ATCCCTTACCGGAATCGGTGCTGCAGGCAACTGAGCAGCGGATCCAGTGGGTCATCGATAATTTTTTCGGG 422
ibrA_FL_3      ATCCCTTACCGGAATCGGTGCTGCAGGCAACTGAGCAGCGGATCCAGTGGGTCATCGATAATTTTTTCGGG 422
ibrA_FL_4      ATCCCTTACCGGAATCGGTGCTGCAGGCAACTGAGCAGCGGATCCAGTGGGTCATCGATAATTTTTTCGGG 438
ibrA_FL_5      ATCCCTTACCGGAATCGGTGCTGCAGGCAACTGAGCAGCGGATCCAGTGGGTCATCGATAATTTTTTCGGG 432
ibrA_FL_6      ATCCCTTACCGGAATCGGTGCTGCAGGCAACTGAGCAGCGGATCCAGTGGGTCATCGATAATTTTTTCGGG 425
ibrA_FL_7      ATCCCTTACCGGAATCGGTGCTGCAGGCAACTGAGCAGCGGATCCAGTGGGTCATCGATAATTTTTTCGGG 439
ibrA_FL_8      ATCCCTTACCGGAATCGGTGCTGCAGGCAACTGAGCAGCGGATCCAGTGGGTCATCGATAATTTTTTCGGG 425

ibrA_FL_Wt      CATCTGTGTCTCTTTTTCCGGGGGAAAAGACTCCACCGTTATGCTGCATTTAAACCGCCAGGCGGCGCGG 560
ibrA_FL_1      CATCTGTGTCTCTTTTTCCGGGGGAAAAGACTCCACCGTTATGCTGCATTTAAACCGCCAGGCGGCGCGG 546
ibrA_FL_2      CATCTGTGTCTCTTTTTCCGGGGGAAAAGACTCCACCGTTATGCTGCATTTAAACCGCCAGGCGGCGCGG 492
ibrA_FL_3      CATCTGTGTCTCTTTTTCCGGGGGAAAAGACTCCACCGTTATGCTGCATTTAAACCGCCAGGCGGCGCGG 492
ibrA_FL_4      CATCTGTGTCTCTTTTTCCGGGGGAAAAGACTCCACCGTTATGCTGCATTTAAACCGCCAGGCGGCGCGG 508
ibrA_FL_5      CATCTGTGTCTCTTTTTCCGGGGGAAAAGACTCCACCGTTATGCTGCATTTAAACCGCCAGGCGGCGCGG 502
ibrA_FL_6      CATCTGTGTCTCTTTTTCCGGGGGAAAAGACTCCACCGTTATGCTGCATTTAAACCGCCAGGCGGCGCGG 495
ibrA_FL_7      CATCTGTGTCTCTTTTTCCGGGGGAAAAGACTCCACCGTTATGCTGCATTTAAACCGCCAGGCGGCGCGG 509
ibrA_FL_8      CATCTGTGTCTCTTTTTCCGGGGGAAAAGACTCCACCGTTATGCTGCATTTAAACCGCCAGGCGGCGCGG 495

ibrA_FL_Wt      TTACAGGGGAAAAAATCTGCGTGTGTGTTTATTGACTGGGAGGGCAGTTCCTGACCATCGCCCACT 630
ibrA_FL_1      TTACAGGGGAAAAAATCTGCGTGTGTGTTTATTGACTGGGAGGGCAGTTCCTGACCATCGCCCACT 616
ibrA_FL_2      TTACAGGGGAAAAAATCTGCGTGTGTGTTTATTGACTGGGAGGGCAGTTCCTGACCATCGCCCACT 562
ibrA_FL_3      TTACAGGGGAAAAAATCTGCGTGTGTGTTTATTGACTGGGAGGGCAGTTCCTGACCATCGCCCACT 562
ibrA_FL_4      TTACAGGGGAAAAAATCTGCGTGTGTGTTTATTGACTGGGAGGGCAGTTCCTGACCATCGCCCACT 578
ibrA_FL_5      TTACAGGGGAAAAAATCTGCGTGTGTGTTTATTGACTGGGAGGGCAGTTCCTGACCATCGCCCACT 572
ibrA_FL_6      TTACAGGGGAAAAAATCTGCGTGTGTGTTTATTGACTGGGAGGGCAGTTCCTGACCATCGCCCACT 565
ibrA_FL_7      TTACAGGGGAAAAAATCTGCGTGTGTGTTTATTGACTGGGAGGGCAGTTCCTGACCATCGCCCACT 553
ibrA_FL_8      TTACAGGGGAAAAAATCTGCGTGTGTGTTTATTGACTGGGAGGGCAGTTCCTGACCATCGCCCACT 565

ibrA_FL_Wt      GTGAAAAACTGCGTGCGCTGTATGCGGATGTCATCGAAACCTTTTACTGGGTCGCCCTGCCGCTCACCAC 700
ibrA_FL_1      GTGAAAAACTGCGTGCGCTGTATGCGGATGTCATCGAAACCTTTTACTGGGTCGCCCTGCCGCTCACCAC 686
ibrA_FL_2      GTGAAAAACTGCGTGCGCTGTATGCGGATGTCATCGAAACCTTTTACTGGGTCGCCCTGCCGCTCACCAC 632
ibrA_FL_3      GTGAAAAACTGCGTGCGCTGTATGCGGATGTCATCGAAACCTTTTACTGGGTCGCCCTGCCGCTCACCAC 632
ibrA_FL_4      GTGAAAAACTGCGTGCGCTGTATGCGGATGTCATCGAAACCTTTTACTGGGTCGCCCTGCCGCTCACCAC 648
ibrA_FL_5      GTGAAAAACTGCGTGCGCTGTATGCGGATGTCATCGAAACCTTTTACTGGGTCGCCCTGCCGCTCACCAC 642
ibrA_FL_6      GTGAAAAACTGCGTGCGCTGTATGCGGATGTCATCGAAACCTTTTACTGGGTCGCCCTGCCGCTCACCAC 635
ibrA_FL_7      ----- 553
ibrA_FL_8      GTGAAAAACTGCGTGCGCTGTATGCGGATGTCATCGAAACCTTTTACTGGGTCGCCCTGCCGCTCACCAC 635

```



```

ibrA_FL_Wt CCAAAATGCCCTGACGCAGTATAAAGCCGCAATGGCAATGCTGGGAGCCCGGAACCGAGTGGGTACGCCAG 770
ibrA_FL_1 CCAAAATGCCCTGACGCAGTATAAAGCCGCAATGGCAATGCTGGGAGCCCGGAACCGAGTGGGTACGCCAG 756
ibrA_FL_2 CCAAAAT----- 639
ibrA_FL_3 CCAAAAT----- 639
ibrA_FL_4 CCAAAATGCCCTGACGCAGTATAAAGCCGCAATGGCAATGCTGGGAGCCCGGAACCGAGTGGGTACGCCAG 718
ibrA_FL_5 CCAAAATG----- 650
ibrA_FL_6 CCAAAATGCCCTGACG----- 651
ibrA_FL_7 ----- 553
ibrA_FL_8 CCAAAATGCCCTGACGCAGTATAAAGCCGCAATGGCAATGCTGGGAGCCCGGAACCGAGTGGGTACGCCAG 705

ibrA_FL_Wt CCGCCGCCTTGGGCCATTACCCACCCGGGCTATTTTTTCATTTTATCAACCCGGAATGAGCTTTGAAGCCT 840
ibrA_FL_1 CCGCCGCCTTGGGCCATTACCCACCCGGGCTATTTTTTCATTTTATCAACCCGGAATGAGCTTTGAAGCCT 826
ibrA_FL_2 ----- 639
ibrA_FL_3 ----- 639
ibrA_FL_4 CCGCCGCCTTGGGCCATTACCCACCCGGGCTAC----- 751
ibrA_FL_5 ----- 650
ibrA_FL_6 ----- 651
ibrA_FL_7 ----- 553
ibrA_FL_8 CCGC----- 709

ibrA_FL_Wt TCGTCAGCCATTTTCGCCGAGTGGTTTTTTCGACGCGTCGTCGCCGCCGCGCTGCTGGTGGGCATTCGCGCCGA 910
ibrA_FL_1 TCGTCAGCCATTTTCGCCGAGTGGTTTTTTCGACGCGTCGTCGCCGCCGCGCTGCTGGTGGGCATTCGCGCCGA 896
ibrA_FL_2 ----- 639
ibrA_FL_3 ----- 639
ibrA_FL_4 ----- 751
ibrA_FL_5 ----- 650
ibrA_FL_6 ----- 651
ibrA_FL_7 -----GTGGTTTTTCGACGCGTCGTCGCCGCCGCGCTGCTGGTGGGCATTCGCGCCGA 604
ibrA_FL_8 -----AGCGTCGTCGCCGCCGCGCTGCTGGTGGGCATTCGCGCCGA 749

ibrA_FL_Wt CGAATCGCTAAATCGCTTTATGACGATTTCTTTCACAGCGTAAACAGCGCTCGCCGACGATAAAACCATGG 980
ibrA_FL_1 CGAATCGCTAAATCGCTTTATGACGATTTCTTTCACAGCGTAAACAGCGCTCGCCGACGATAAAACCATGG 966
ibrA_FL_2 -----GCGCCGACGATAAAACCATGG 659
ibrA_FL_3 -----GCGCCGACGATAAAACCATGG 659
ibrA_FL_4 -----TTTCACAGCGTAAACAGCGCTCGCCGACGATAAAACCATGG 791
ibrA_FL_5 -----CTTCACAGCGTAAACAGCGCTCGCCGACGATAAAACCATGG 691
ibrA_FL_6 -----CAACAGCGTAAACAGCGCTCGCCGACGATAAAACCATGG 690
ibrA_FL_7 CGAATCGCTAAATCGCTTTATGACGATTTCTTTCACAGCGTAAACAGCGCTCGCCGACGATAAAACCATGG 674
ibrA_FL_8 CGAATCGCTAAATCGCTTTATGACGATTTCTTTCACAGCGTAAACAGCGCTCGCCGACGATAAAACCATGG 819

ibrA_FL_Wt ACCACTTCAGCGCCGGGGCGGCCACGCTGGTACATCTACCCGCTCTATGACTGGAAAACCGCCGATATCT 1050
ibrA_FL_1 ACCACTTCAGCGCCGGGGCGGCCACGCTGGTACATCTACCCGCTCTATGACTGGAAAACCGCCGATATCT 1036
ibrA_FL_2 ACCACTTCAGCGCCGGGGCGGCCACGCTGGTACATCTACCCGCTCTATGACTGGAAAACCGCCGATATCT 729
ibrA_FL_3 ACCACTTCAGCGCCGGGGCGGCCACGCTGGTACATCTACCCGCTCTATGACTGGAAAACCGCCGATATCT 729
ibrA_FL_4 ACCACTTCAGCGCCGGGGCGGCCACGCTGGTACATCTACCCGCTCTATGACTGGAAAACCGCCGATATCT 861
ibrA_FL_5 ACCACTTCAGCGCCGGGGCGGCCACGCTGGTACATCTACCCGCTCTATGACTGGAAAACCGCCGATATCT 761
ibrA_FL_6 ACCACTTCAGCGCCGGGGCGGCCACGCTGGTACATCTACCCGCTCTATGACTGGAAAACCGCCGATATCT 760
ibrA_FL_7 ACCACTTCAGCGCCGGGGCGGCCACGCTGGTACATCTACCCGCTCTATGACTGGAAAACCGCCGATATCT 744
ibrA_FL_8 ACCACTTCAGCGCCGGGGCGGCCACGCTGGTACATCTACCCGCTCTATGACTGGAAAACCGCCGATATCT 889

ibrA_FL_Wt GGACTTGGTTTGCCAAAAGCGGCGAGCCCTATAAACCCTGTGACGATCTGATGTATCAGGCCGGGGTGC 1120
ibrA_FL_1 GGACTTGGTTTGCCAAAAGCGGCGAGCCCTATAAACCCTGTGACGATCTGATGTATCAGGCCGGGGTGC 1106
ibrA_FL_2 GGACTTGGTTTGCCAAAAGCGGCGAGCCCTATAAACCCTGTGACGATCTGATGTATCAGGCCGGGGTGC 799
ibrA_FL_3 GGACTTGGTTTGCCAAAAGCGGCGAGCCCTATAAACCCTGTGACGATCTGATGTATCAGGCCGGGGTGC 799
ibrA_FL_4 GGACTTGGTTTGCCAAAAGCGGCGAGCCCTATAAACCCTGTGACGATCTGATGTATCAGGCCGGGGTGC 931
ibrA_FL_5 GGACTTGGTTTGCCAAAAGCGGCGAGCCCTATAAACCCTGTGACGATCTGATGTATCAGGCCGGGGTGC 831
ibrA_FL_6 GGACTTGGTTTGCCAAAAGCGGCGAGCCCTATAAACCCTGTGACGATCTGATGTATCAGGCCGGGGTGC 830
ibrA_FL_7 GGACTTGGTTTGCCAAAAGCGGCGAGCCCTATAAACCCTGTGACGATCTGATGTATCAGGCCGGGGTGC 814
ibrA_FL_8 GGACTTGGTTTGCCAAAAGCGGCGAGCCCTATAAACCCTGTGACGATCTGATGTATCAGGCCGGGGTGC 959

ibrA_FL_Wt GCTGCGCTATATGCGCATTTGCGAACCGTTTGGTCCCAGCAGCGCCAGGGGCTGTGGCTGTATCACGTG 1190
ibrA_FL_1 GCTGCGCTATATGCGCATTTGCGAACCGTTTGGTCCCAGCAGCGCCAGGGGCTGTGGCTGTATCACGTG 1176
ibrA_FL_2 GCTGCGCTATATGCGCATTTGCGAACCGTTTGGTCCCAGCAGCGCCAGGGGCTGTGGCTGTATCACGTG 869
ibrA_FL_3 GCTGCGCTATATGCGCATTTGCGAACCGTTTGGTCCCAGCAGCGCCAGGGGCTGTGGCTGTATCACGTG 869
ibrA_FL_4 GCTGCGCTATATGCGCATTTGCGAACCGTTTGGTCCCAGCAGCGCCAGGGGCTGTGGCTGTATCACGTG 1001
ibrA_FL_5 GCTGCGCTATATGCGCATTTGCGAACCGTTTGGTCCCAGCAGCGCCAGGGGCTGTGGCTGTATCACGTG 901
ibrA_FL_6 GCTGCGCTATATGCGCATTTGCGAACCGTTTGGTCCCAGCAGCGCCAGGGGCTGTGGCTGTATCACGTG 900
ibrA_FL_7 GCTGCGCTATATGCGCATTTGCGAACCGTTTGGTCCCAGCAGCGCCAGGGGCTGTGGCTGTATCACGTG 884
ibrA_FL_8 GCTGCGCTATATGCGCATTTGCGAACCGTTTGGTCCCAGCAGCGCCAGGGGCTGTGGCTGTATCACGTG 1029

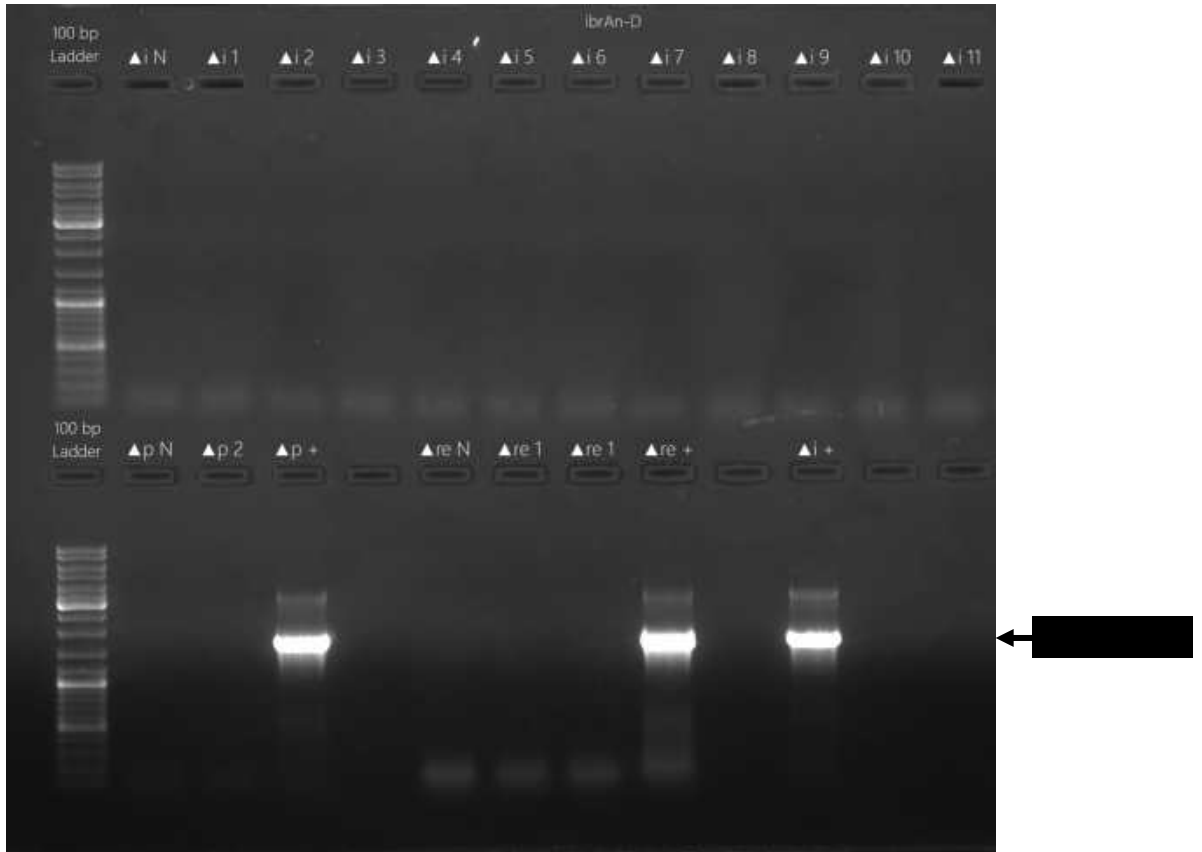
ibrA_FL_Wt CTGGAACCTGAGCGCTGGGCGCGCATGTGCCAGCGAGTGAGCGGCGCGCACAGCGGCGGGGTCTATGCCG 1260
ibrA_FL_1 CTGGAACCTGAGCGCTGGGCGCGCATGTGCCAGCGAGTGAGCGGCGCGCACAGCGGCGGGGTCTATGCCG 1246
ibrA_FL_2 CTGGAACCTGAGCGCTGGGCGCGCATGTGCCAGCGAGTGAGCGGCGCGCACAGCGGCGGGGTCTATGCCG 939
ibrA_FL_3 CTGGAACCTGAGCGCTGGGCGCGCATGTGCCAGCGAGTGAGCGGCGCGCACAGCGGCGGGGTCTATGCCG 939
ibrA_FL_4 CTGGAACCTGAGCGCTGGGCGCGCATGTGCCAGCGAGTGAGCGGCGCGCACAGCGGCGGGGTCTATGCCG 1071
ibrA_FL_5 CTGGAACCTGAGCGCTGGGCGCGCATGTGCCAGCGAGTGAGCGGCGCGCACAGCGGCGGGGTCTATGCCG 971
ibrA_FL_6 CTGGAACCTGAGCGCTGGGCGCGCATGTGCCAGCGAGTGAGCGGCGCGCACAGCGGCGGGGTCTATGCCG 970
ibrA_FL_7 CTGGAACCTGAGCGCTGGGCGCGCATGTGCCAGCGAGTGAGCGGCGCGCACAGCGGCGGGGTCTATGCCG 954
ibrA_FL_8 CTGGAACCTGAGCGCTGGGCGCGCATGTGCCAGCGAGTGAGCGGCGCGCACAGCGGCGGGGTCTATGCCG 1099

```

ibrA_FL_Wt	GGCATGATAATCAGTTCACGGTCATCGGAAAATCGACAAGCCCGACCACCTGACGTGGAAAAGCTACGC	1330
ibrA_FL_1	GGCATGATAATCAGTTCACGGTCATCGGAAAATCGACAAGCCCGACCACCTGACGTGGAAAAGCTACGC	1316
ibrA_FL_2	GGCATGATAATCAGTTCACGGTCATCGGAAAATCGACAAGCCCGACCACCTGACGTGGAAAAGCTACGC	1009
ibrA_FL_3	GGCATGATAATCAGTTCACGGTCATCGGAAAATCGACAAGCCCGACCACCTGACGTGGAAAAGCTACGC	1009
ibrA_FL_4	GGCATGATAATCAGTTCACGGTCATCGGAAAATCGACAAGCCCGACCACCTGACGTGGAAAAGCTACGC	1141
ibrA_FL_5	GGCATGATAATCAGTTCACGGTCATCGGAAAATCGACAAGCCCGACCACCTGACGTGGAAAAGCTACGC	1041
ibrA_FL_6	GGCATGATAATCAGTTCACGGTCATCGGAAAATCGACAAGCCCGACCACCTGACGTGGAAAAGCTACGC	1040
ibrA_FL_7	GGCATGATAATCAGTTCACGGTCATCGGAAAATCGACAAGCCCGACCACCTGACGTGGAAAAGCTACGC	1024
ibrA_FL_8	GGCATGATAATCAGTTCACGGTCATCGGAAAATCGACAAGCCCGACCACCTGACGTGGAAAAGCTACGC	1169
ibrA_FL_Wt	CCTGTTCTCTGCTCGACAGCATGCCGGA AACCCGCGGAGCACTACCGCAATAAAAATCGCCGTCTACCTG	1400
ibrA_FL_1	CCTGTTCTCTGCTCGACAGCATGCCGGA AACCCGCGGAGCACTACCGCAATAAAAATCGCCGTCTACCTG	1386
ibrA_FL_2	CCTGTTCTCTGCTCGACAGCATGCCGGA AACCCGCGGAGCACTACCGCAATAAAAATCGCCGTCTACCTG	1079
ibrA_FL_3	CCTGTTCTCTGCTCGACAGCATGCCGGA AACCCGCGGAGCACTACCGCAATAAAAATCGCCGTCTACCTG	1079
ibrA_FL_4	CCTGTTCTCTGCTCGACAGCATGCCGGA AACCCGCGGAGCACTACCGCAATAAAAATCGCCGTCTACCTG	1211
ibrA_FL_5	CCTGTTCTCTGCTCGACAGCATGCCGGA AACCCGCGGAGCACTACCGCAATAAAAATCGCCGTCTACCTG	1111
ibrA_FL_6	CCTGTTCTCTGCTCGACAGCATGCCGGA AACCCGCGGAGCACTACCGCAATAAAAATCGCCGTCTACCTG	1110
ibrA_FL_7	CCTGTTCTCTGCTCGACAGCATGCCGGA AACCCGCGGAGCACTACCGCAATAAAAATCGCCGTCTACCTG	1094
ibrA_FL_8	CCTGTTCTCTGCTCGACAGCATGCCGGA AACCCGCGGAGCACTACCGCAATAAAAATCGCCGTCTACCTG	1239
ibrA_FL_Wt	CGCTGGTACCAGAAAAAAGGTATGGAGGATATTCCGGATACCCAACCTGCGGACATTGGCACCAAAGATA	1470
ibrA_FL_1	CGCTGGTACCAGAAAAAAGGTATGGAGGATATTCCGGATACCCAACCTGCGGACATTGGCACCAAAGATA	1456
ibrA_FL_2	CGCTGGTACCAGAAAAAAGGTATGGAGGATATTCCGGATACCCAACCTGCGGACATTGGCACCAAAGATA	1149
ibrA_FL_3	CGCTGGTACCAGAAAAAAGGTATGGAGGATATTCCGGATACCCAACCTGCGGACATTGGCACCAAAGATA	1149
ibrA_FL_4	CGCTGGTACCAGAAAAAAGGTATGGAGGATATTCCGGATACCCAACCTGCGGACATTGGCACCAAAGATA	1281
ibrA_FL_5	CGCTGGTACCAGAAAAAAGGTATGGAGGATATTCCGGATACCCAACCTGCGGACATTGGCACCAAAGATA	1181
ibrA_FL_6	CGCTGGTACCAGAAAAAAGGTATGGAGGATATTCCGGATACCCAACCTGCGGACATTGGCACCAAAGATA	1180
ibrA_FL_7	CGCTGGTACCAGAAAAAAGGTATGGAGGATATTCCGGATACCCAACCTGCGGACATTGGCACCAAAGATA	1164
ibrA_FL_8	CGCTGGTACCAGAAAAAAGGTATGGAGGATATTCCGGATACCCAACCTGCGGACATTGGCACCAAAGATA	1309
ibrA_FL_Wt	TCCCATCCTGGCGGCGAGTCTGCAAAGTACTGCTCAAT	1540
ibrA_FL_1	TCCCATCCTGGCGGCGAGTCTGCAAAGTACTGCTCAAT	1526
ibrA_FL_2	TCCCATCCTGGCGGCGAGTCTGCAAAGTACTGCTCAAT	1219
ibrA_FL_3	TCCCATCCTGGCGGCGAGTCTGCAAAGTACTGCTCAAT	1219
ibrA_FL_4	TCCCATCCTGGCGGCGAGTCTGCAAAGTACTGCTCAAT	1351
ibrA_FL_5	TCCCATCCTGGCGGCGAGTCTGCAAAGTACTGCTCAAT	1251
ibrA_FL_6	TCCCATCCTGGCGGCGAGTCTGCAAAGTACTGCTCAAT	1250
ibrA_FL_7	TCCCATCCTGGCGGCGAGTCTGCAAAGTACTGCTCAAT	1234
ibrA_FL_8	TCCCATCCTGGCGGCGAGTCTGCAAAGTACTGCTCAAT	1379
ibrA_FL_Wt	CCCAACCAAAAAGCAGCCACT	1610
ibrA_FL_1	CCCAACCAAAAAGCAGCCACT	1596
ibrA_FL_2	CCCAACCAAAAAGCAGCCACT	1289
ibrA_FL_3	CCCAACCAAAAAGCAGCCACT	1289
ibrA_FL_4	CCCAACCAAAAAGCAGCCACT	1421
ibrA_FL_5	CCCAACCAAAAAGCAGCCACT	1321
ibrA_FL_6	CCCAACCAAAAAGCAGCCACT	1320
ibrA_FL_7	CCCAACCAAAAAGCAGCCACT	1304
ibrA_FL_8	CCCAACCAAAAAGCAGCCACT	1440
ibrA_FL_Wt	TTATGCAACAACAACCTGAgcaggcgctggaagcttacctgcaaaagctggatgacgagggc	1671
ibrA_FL_1	TTATGCAACAACAACGACGAGGGCC	1622
ibrA_FL_2	-----	1289
ibrA_FL_3	-----	1289
ibrA_FL_4	TTATGCAACAAC	1433
ibrA_FL_5	TTATGC	1327
ibrA_FL_6	-----	1320
ibrA_FL_7	TTATGC	1310
ibrA_FL_8	-----	1440

Figure 4.3.22 Comparison of the *ibrA* sequences obtained from putative Δ *ibrA* strains by multiple sequence alignment. The sequences from eight strains (*ibrA_FL_1* to -8), obtained using the *ibrA*-FL primers, are compared with the *ibrA* sequence from wild-type KpIMS38 (*ibrA_FL_Wt*) using T-Coffee. Base-matches are highlighted as black, mismatches as grey and gaps depicted by "-". Additionally, regions corresponding to the 60 bp overhangs chosen to construct the deletion cassette for *ibrA* are highlighted (green and red shading) in the sequence, with green boxes representing the 5' overhang and red boxes the 3' overhang regions.

The deletion-procedure was repeated where deletion cassettes for *ibrA*, *pspF*, *doc* and *relE* were synthesized. Prior to their transformation into KpIMS38 containing pRedET, the transformants were induced with 0.4% L-arabinose at 37°C for 90 minutes. Five

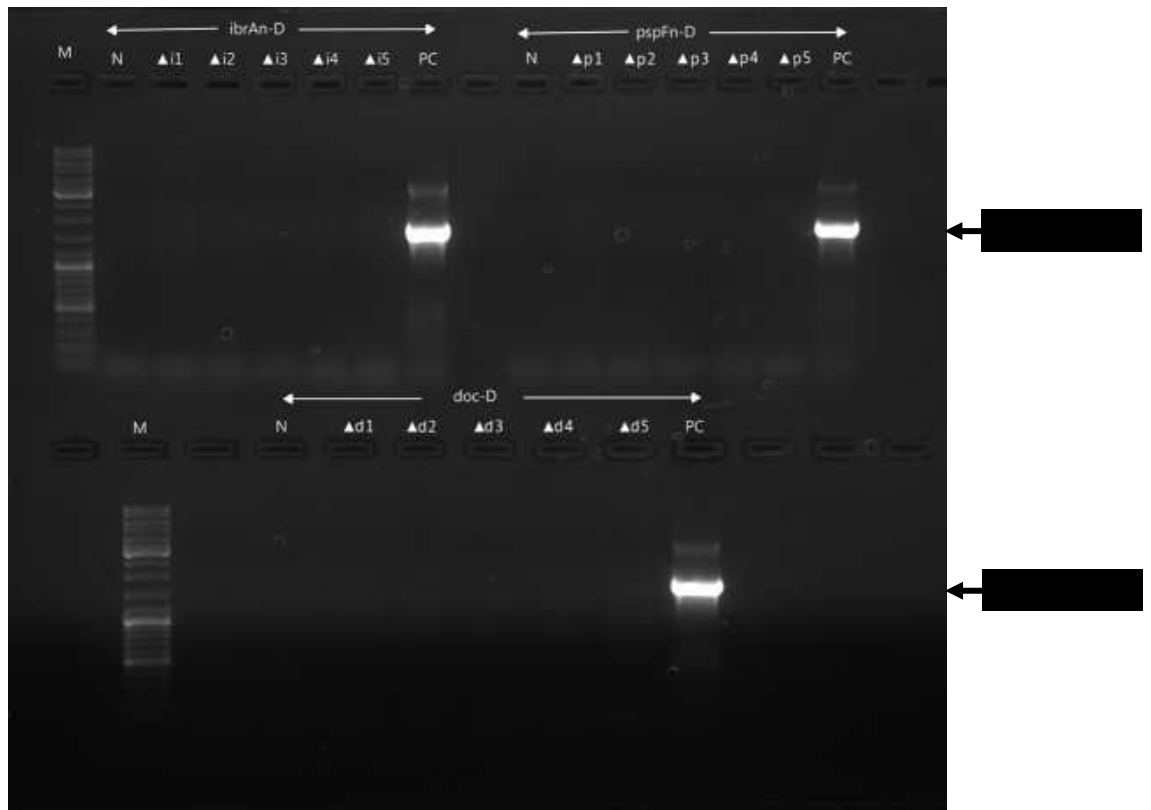


hundred nanograms of each cassette were used to transform KpIMS38-pRedET in 2 mm electroporation cuvettes at 2500 V using a 5 ms time-constant protocol. The cultures were revived in LB broth for 3.5 hours and plated on LBA-Kan¹⁵. Transformants were obtained for all the genes except *doc*. Genomic DNA was extracted from putative mutants for each

of the three genes and used to perform PCR using the cassette-synthesis primers for the respective genes (Table 3.3.20). Positive reactions were expected to yield 1700 bp amplicons, identical to the outcome from the positive-control reactions that were also set up with each primer pair using the genomic DNA from *EcoΔmanZYX::kanR*. Reactions were also set up with the *ibrAn-D* primers using the genomic DNA from the putative *ΔibrA* isolate previously obtained. No amplicons were obtained in reactions for transformants of all the three genes, i.e., for putative *ΔibrA*, *ΔpspF* and *ΔrelE* isolates (Figure 4.3.23). An amplicon approximately 1700 bp in size was observed for the positive control reactions of all the three genes, as well as for the putative *ΔibrA* mutant analyzed here.

A repetition of the deletion-procedure was performed once more, with a few modifications. *KpIMS38* was transformed with 75 ng of pRedET through electroporation, carried out at 2500 V with a 5 ms time-constant protocol in 2 mm electroporation cuvettes. The culture was revived, spread-plated on selective medium and plasmid DNA analyzed from the transformants for the presence of pRedET. *KpIMS38-pRedET* cultures were induced with 0.4% L-arabinose prior to transformation at 37°C for 70 minutes. Six hundred nanograms the deletion cassettes for *ibrA*, *pspF*, *doc* and *relE* were used to transform the cells in 2 mm electroporation cuvettes at 1350 V using a 5 ms time-constant protocol. After revival of the cultures in LB broth for 3.5 hours and plating on LBA-Kan¹⁵, transformants were obtained for all the genes except for *relE*. Genomic DNA was extracted from putative mutants for each of the three genes and used to perform PCR using the cassette-synthesis primers for the respective genes (Table 3.3.20). Reactions were also set up with each primer pair using the genomic DNA from *EcoΔmanZYX::kanR* as a positive control. No amplicons were obtained in reactions with transformants for all the three genes, i.e., for putative *ΔibrA*, *ΔpspF* and *Δdoc* isolates (Figure 4.3.24). An

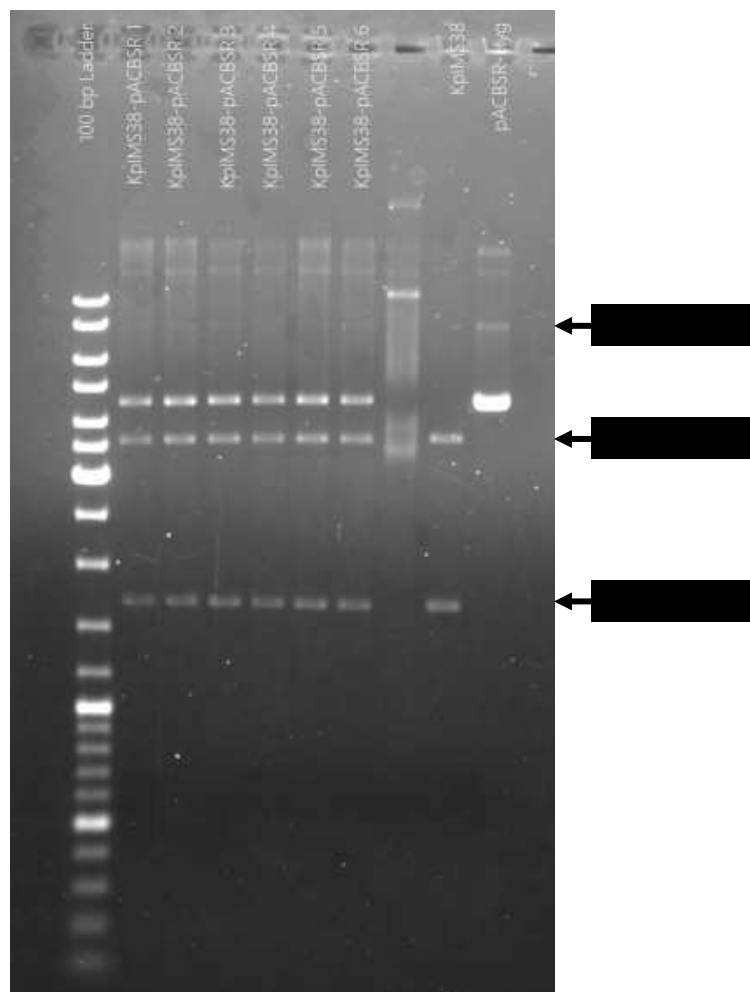
amplicon approximately 1700 bp in size was observed for the positive-control reactions of all the three genes.



Taken together, these results indicated the system of generating gene-deletions, i.e., lambda recombineering using pRedET, was not suited to KpIMS38. Owing to the lack of cassette-insertion as well as insertion of the cassette at non-specific sites, we were compelled to seek out alternative methods to accomplish our goal of creating gene-deletions in KpIMS38.

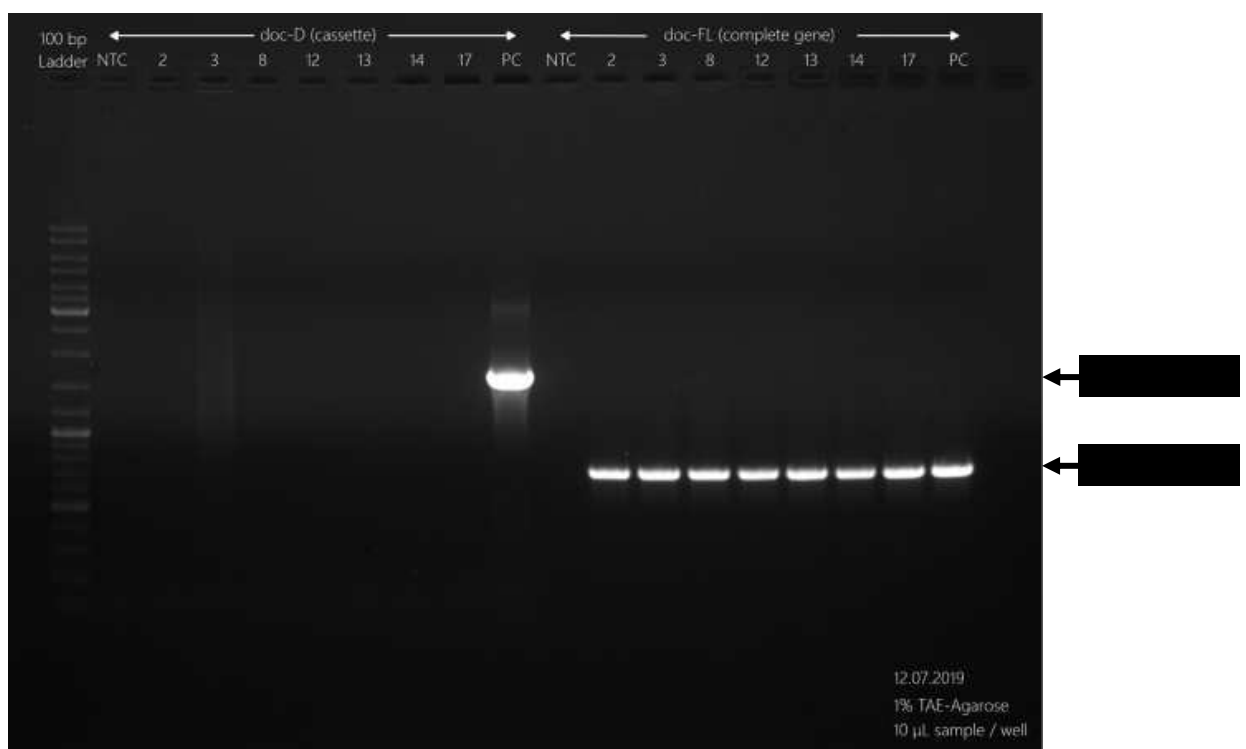
4.3.4.2 Use of *pACBSR-hyg* to generate deletion-mutants in *KpIMS38*

A new technique was chosen to perform gene deletions in *KpIMS38* to overcome the shortcomings of the aforementioned attempts at creating deletion-mutants. This technique made use of the plasmid *pACBSR-hyg*, a 7660 bp plasmid contained a hygromycin resistance gene and expressed the Red recombinase genes under control of an arabinose-inducible promoter. The minimum inhibitory concentration (MIC) of hygromycin for *KpIMS38* was examined to ensure viability of the technique, and a two-fold dilution



series of hygromycin in Muller-Hinton (MH) broth was used to determine the same according to the protocol mentioned in section 3.3.4.1 of this document. The MIC of hygromycin for KpIMS38 was 50 $\mu\text{g}/\text{mL}$ and was sufficient to allow for selection of pACBSR-hyg transformants at 100 $\mu\text{g}/\text{mL}$.

KpIMS38 cells were transformed with pACBSR-hyg according to the protocol outlined in section 3.2.7.3 of this document, and plasmid DNA from the transformants analysed to confirm the presence of the plasmid in the cells. The transformants were seen to possess

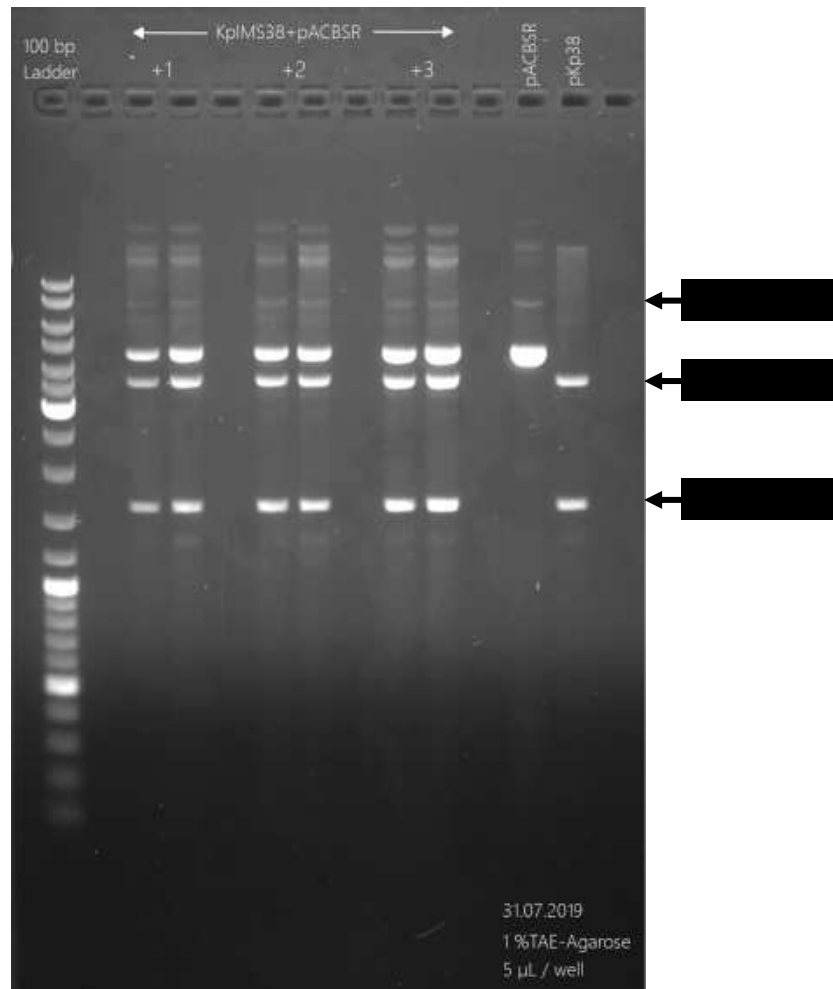


the plasmid pACBSR-hyg, in addition to the native plasmid contained within KpIMS38 (Figure 4.3.25).

KpIMS38-pACBSR-hyg was transformed with the FRT-deletion cassette for the gene *doc* according to the protocol outlined in section 3.2.8.5 of this document. Transformation of 1050 ng of the deletion cassette was carried out using uninduced as well as L-arabinose-induced cultures, the transformants revived in SOC broth at 37°C for 3 hours and cultured on LBA-Kan¹⁵. Transformants were obtained in the induced setup alone, and individual colonies analysed using colony PCR with the deletion and full-length primers for *doc* (Table 3.3.20 and 3.3.21 respectively). Genomic DNA from *EcoΔmanZYX::kanR* and from wild-type KpIMS38 were used to set up positive control-reactions. While a 1700 bp amplicon was obtained in the control reaction for the deletion cassette, no amplicons were observed in reactions for any of the transformants (Figure 4.3.26). For reactions assessing the full-length *doc* gene, a single amplicon of the size 752 bp was observed in the positive-control as well as in all the transformants tested. This indicated the *doc* deletion-cassette had not inserted within the genome of KpIMS38.

A successive experiment was performed with a few changes to the protocol previously used. KpIMS38-pACBSR-hyg was induced with L-arabinose for 2 hours at 30°C and transformed with 750 ng of the deletion cassette for *doc* at 1350 V through a 5 ms time-constant protocol in a 1 mm electroporation cuvette. After revival of the cultures for 2 hours as well as 3 hours, no colonies were obtained after being plated on LBA-Kan¹⁵ plates.

To verify the stability of pACBSR-hyg in KpIMS38, transformants of KpIMS38 containing pACBSR-hyg were subcultured on agar made from Luria broth with low-salt (Lennox, 1955) and containing 100 $\mu\text{g}/\text{mL}$ of hygromycin (LBA-Lx-Hyg¹⁰⁰) for three successive generations. Plasmid DNA was extracted from all three cultures, using the protocol outlines in section 3.2.2 of this document, and compared by agarose-gel electrophoresis. Bands corresponding to pACBSR-hyg were visible in plasmid DNA



from cultures across all three generations (Figure 4.3.27) indicating no loss of the plasmid in transformed cultures.

The deletion-procedure was repeated further with modifications to the initial protocol used. L-arabinose-induced cultures of KpIMS38-pACBSR-hyg were transformed with 1000 ng of the deletion cassette for *ibrA*, *pspF* and *doc* at 1350V, with a 5 ms time-constant protocol in 1mm electroporation cuvettes, but no transformants were obtained when plated on LBA-Kan¹⁵. Furthermore, transformation of the deletion cassette for *pspF* was carried out using two different electroporation conditions. One batch of KpIMS38-pACBSR-hyg was added 1500 ng of the cassette and pulsed with a time-constant protocol at 1350 V twice, with a 5-second interval separating both pulses. Another batch was added 1500 ng of the cassette and pulsed with a time-constant protocol at 2000 V once. Both cultures were revived at 37°C for 2 hours. However, neither culture yielded transformants on the LBA-Kan¹⁵ plates. This procedure was replicated, the only difference being the cultures were revived post-electroporation at 37°C for 90 minutes. However, the result was the same, with no colonies observed either of the transformation conditions. The procedure was then replicated a third time, with the duration for post-electroporation revival increased to 3 hours. After plating the cultures on LBA-Kan¹⁵ and incubation at 37°C, fewer than 10 colonies were obtained for the single-pulsed and double-pulsed transformant-conditions. The colony diameter was ≤ 1 mm, but upon inoculation into LB broth, did not show any growth.

The process of transformation was performed directly using the protocol specified by Huang et al (2014). Briefly, a single colony of KpIMS38-pACBSR-Hyg was inoculated into 2.5 mL LB-Lx-Hyg¹⁰⁰ and incubated overnight at 30°C. Of the resultant culture, 1 mL was inoculated into 99 mL LB-Lx-Hyg¹⁰⁰ containing 0.1M L-Arabinose and the culture incubated for 2.5 hours at 30°C. The culture was halved, each cell pellet washed

with 20 mL 10% glycerol thrice, and resuspended in a minimal volume of the supernatant. Cell suspensions were individually added 1500 ng of deletion cassettes for either *doc* or *relE* and the suspensions transferred to 1 mm electroporation cuvettes. The cells were pulsed once at 1350 V with a 5 ms time-constant protocol, revived with 500 μ L SOC broth, incubated at 37°C for 120 mins and plated on LBA-Kan¹⁵. After 48 hours of incubation, no colonies were obtained for cultures transformed with either of the deletion cassettes.

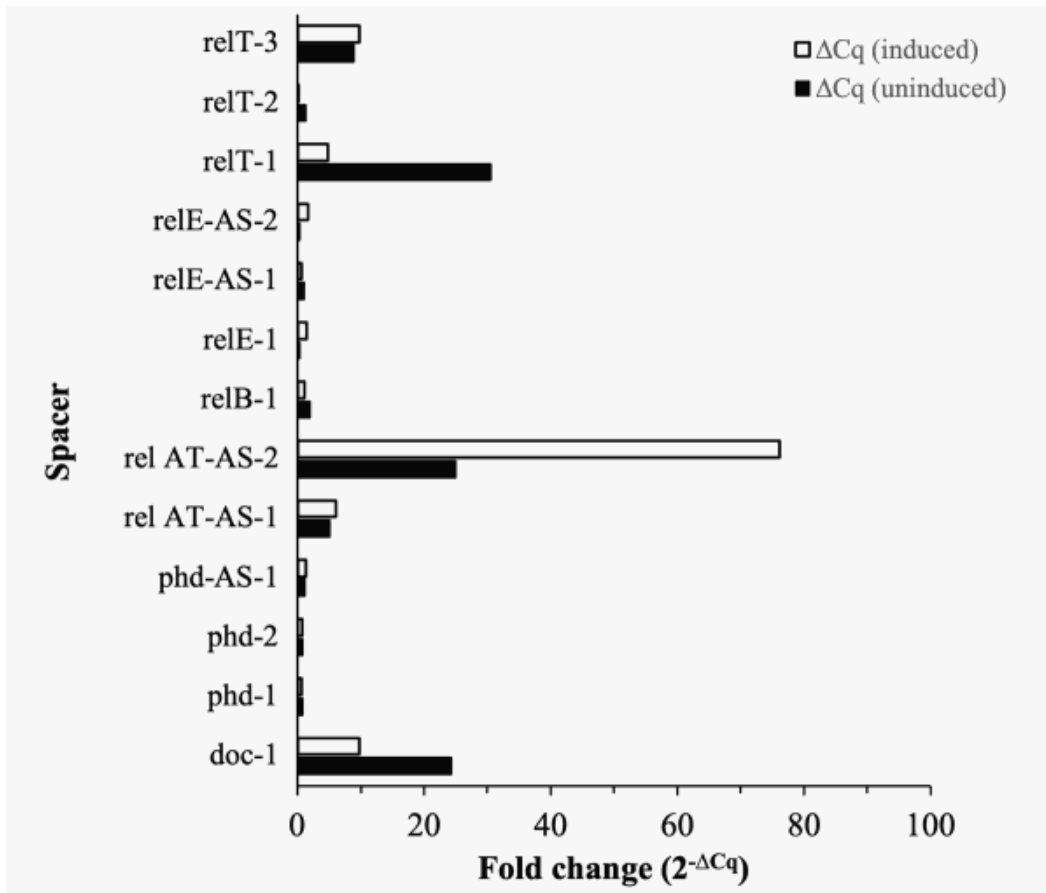
The aforementioned results, therefore, indicated the inability of lambda recombineering mediated by pACBSR-hyg to successfully generate deletion mutants in KpIMS38. They also highlighted the need to adopt an alternative strategy to perturb the expression of single genes to study their functional relevance to persistence in KpIMS38.

4.3.4.3 Gene silencing in KpIMS38

Multiple constructs, each containing spacer DNA sequences specific to a gene-of-interest, were created using the plasmid 148cr. Each spacer was inserted into the backbone through cloning, and the resultant constructs were transformed into KpIMS38 by electroporation, growth on LBA-Kan⁵⁰ considered positive for transformation.

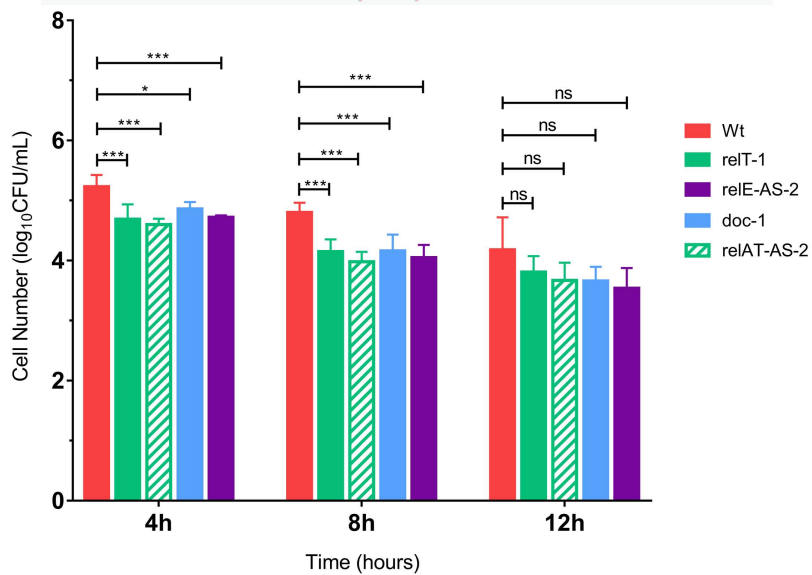
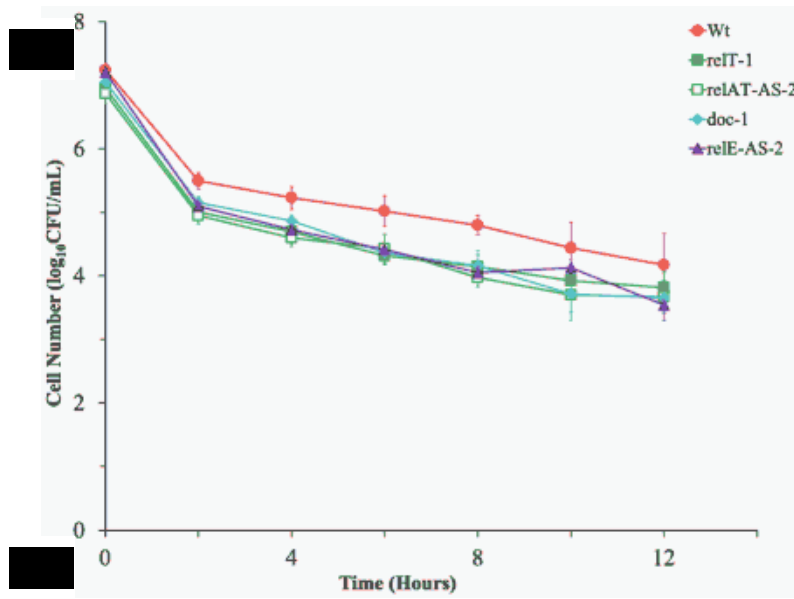
The expression of the gene, putatively silenced by transformation with a corresponding spacer, was assessed by measuring the level of transcription of the gene through qPCR. The C_q values were obtained for each gene in uninduced conditions as well as upon induction with 0.05 μ g/mL of tetracycline, and compared between the putative silenced strain and its wild-type counterpart for that particular gene. The resultant fold-change ($2^{-\Delta C_q}$) values were obtained for each of the genes in their corresponding silenced condition for uninduced as well tetracycline-induced conditions. A reduction in the expression of the genes was observed in certain silencing screens (Figure 4.3.28). The greatest difference in expression was observed for *relAT*, which had a fold-change of 76.11 in the

strain containing the *rel* AT-AS-2 silencer in the induced condition. In comparison, the fold-change for the same was 24.93 in the uninduced condition. A fold change greater



than 10 was also observed for the genes *doc*, *relE* and *relT* in strains containing the silencers *doc-1*, *relE-AS-2* and *relT-1* respectively. Consequently, these strains including the strain with the *rel* AT-AS-2 silencer were chosen to examine their response to levofloxacin.

The strains were incubated in MH broth containing 256 $\mu\text{g/mL}$ of levofloxacin, and their survival measured by performing viable counts on MH agar at bihourly intervals. The wild type KpIMS38 was also subjected to the same treatment and its survival measured.



The cell number was calculated based on the \log_{10} (CFU/mL) and represented as a

function of time (Figure 4.3.29A). The KpIMS38 cultures – wild-type as well as strains with single genes silenced – exhibited biphasic killing as a function of time when treated with 256 µg/mL of levofloxacin. The number of cells were reduced by almost 2 orders of magnitude 2 hours after exposure to levofloxacin, with the reduction much more gradual over the successive period for all the cultures assessed (Table 4.3.10). The number of persister cells formed on treating the strains containing a silenced gene with levofloxacin were lower than that observed in the wild-type strain.

Table 4.3.10 Survival of KpIMS38 strains putatively silenced for *relT*, *relAt*, *doc* and *relE*. Silencing was achieved using the RNA spacers *relT*-1, *relAT*-AS-2, *doc*-1 and *relE*-AS-2 for the respective genes in individual strains. Cell numbers of the silenced strains, as well as the wild type (Wt), obtained on treatment with 256 µg/mL levofloxacin were represented as the $\log_{10}(\text{CFU/mL})$ with averages of biological replicates (*Av*) (*n*=2) and the standard deviation (*SD*) represented here.

Time (hours)	Cell Number ($\log_{10}\text{CFU/mL}$; <i>Av</i> ± <i>SD</i>)				
	Wt	<i>relT</i> -1	<i>relE</i> -AS-2	<i>doc</i> -1	<i>relAT</i> -AS-2
0	7.24 ± 0.10	6.95 ± 0.11	7.21 ± 0.03	7.05 ± 0.23	6.87 ± 0.16
2	5.49 ± 0.13	5.01 ± 0.07	5.09 ± 0.05	5.15 ± 0.09	4.95 ± 0.12
4	5.23 ± 0.18	4.69 ± 0.23	4.72 ± 0.02	4.86 ± 0.10	4.60 ± 0.09
6	5.02 ± 0.24	4.32 ± 0.14	4.41 ± 0.03	4.36 ± 0.02	4.43 ± 0.23
8	4.80 ± 0.15	4.15 ± 0.19	4.05 ± 0.15	4.16 ± 0.24	3.98 ± 0.14
10	4.44 ± 0.40	3.92 ± 0.18	4.13 ± 0.13	3.71 ± 0.42	3.70 ± 0.27
12	4.18 ± 0.49	3.81 ± 0.24	3.54 ± 0.24	3.66 ± 0.21	3.67 ± 0.26

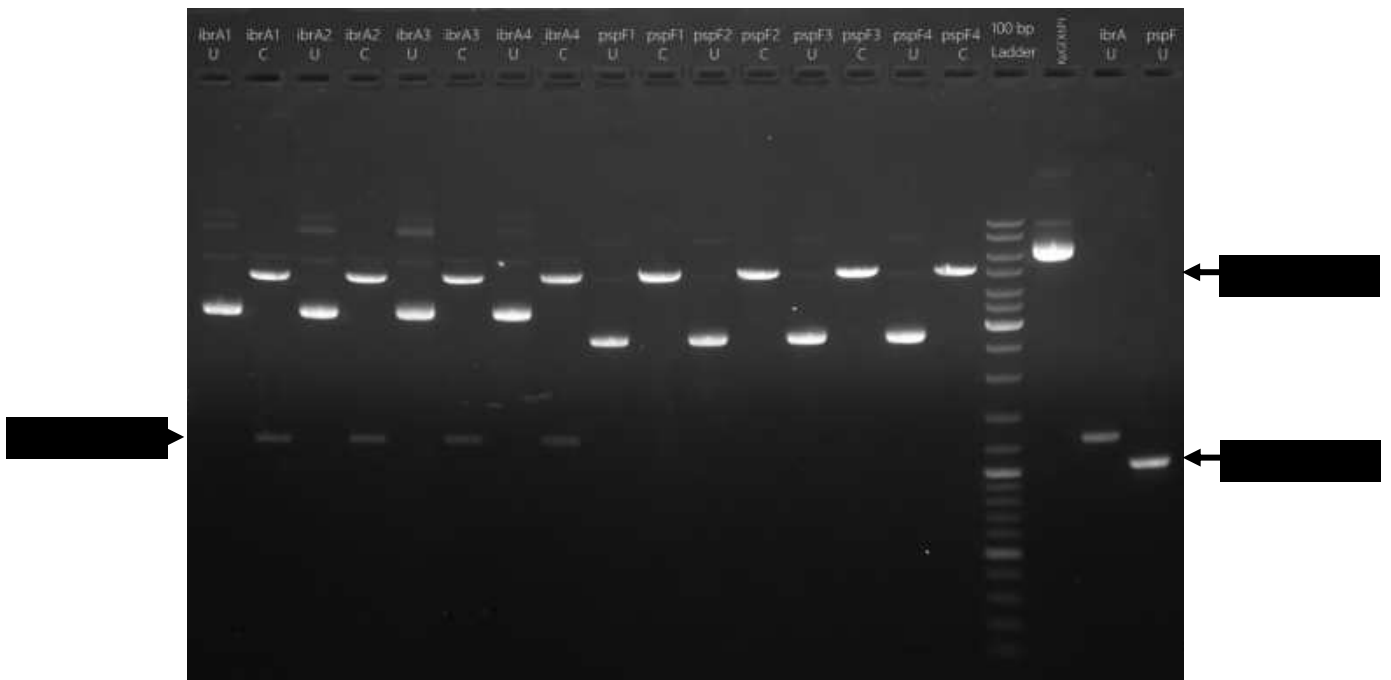
To examine whether the reduction was significant, cell numbers were considered at specific time-points viz. 4, 8 and 12 hours after antibiotic-exposure, and compared with that obtained in wild-type KpIMS38. To carry out the same, a Student's T-test was performed comparing the $\log_{10}\text{CFU/mL}$ for each silenced screen against the wild type for

each time point. A two-sample T-test was performed considering equal variance, which in turn was determined by conducting an F-test. The p -values for each of the T-tests were obtained, and it was observed that the reduction in cell numbers in all the strains containing a silenced gene was significant when measured 4 hours and 8 hours after exposure to levofloxacin (Figure 4.3.29B). A deviation to this trend was observed in 12 hour-cultures, with the reduction in cell numbers of the silencing screen non-significant compared to the wild-type.

Taken together, these results indicated that silencing specific toxin and antitoxins significantly hindered persister-cell formation in KpIMS38.

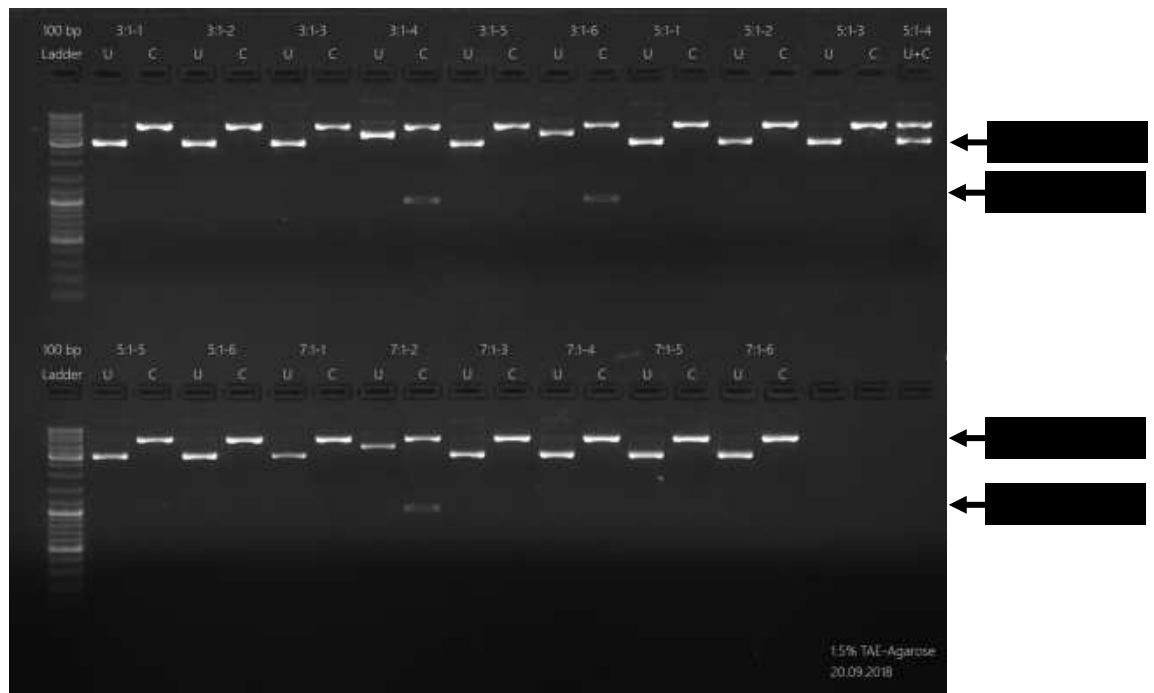
4.3.5 Assessment of the involvement of genes in persister cell-formation by overexpression screens

To study the involvement of specific genes in persister-cell formation in KpIMS38 treated with levofloxacin, episomal copies of the genes were introduced into the isolate to create strains overexpressing the gene. The genes studied in the previous section by loss-of-function experiments viz. *ibrA*, *pspF*, *doc* and *relE* as well as the antitoxin genes *phd* and *relB* were introduced into plasmid vectors. The genes were then transformed into wild type KpIMS38 and their ability to form persister cells assessed.



The effect of the genes *ibrA* and *pspF* on persister cell formation in KpIMS38 were first studied. Episomal copies of the genes were introduced into wild type KpIMS38 for the

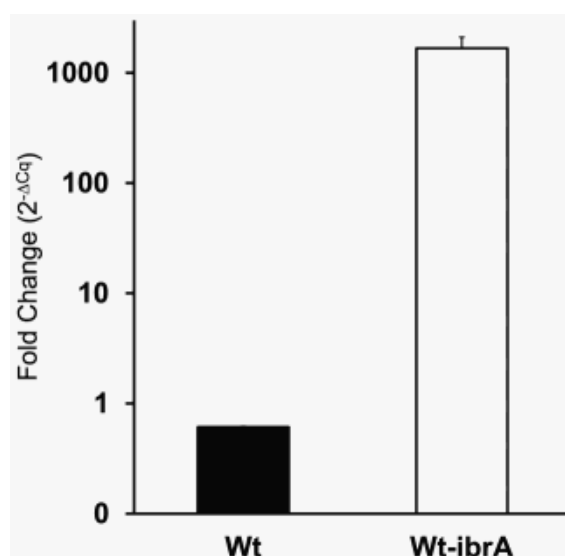
respective genes, i.e., $\Delta ibrA$ and $\Delta pspF$. The entire process of molecular cloning and transformation was carried out according to the protocol specified in section 3.3.9.6 of this document. After transformation of the ligation-products of both genes into individual batches of chemically-competent DH5 α cells and plating on LBA-Kan¹⁵, plasmid DNA



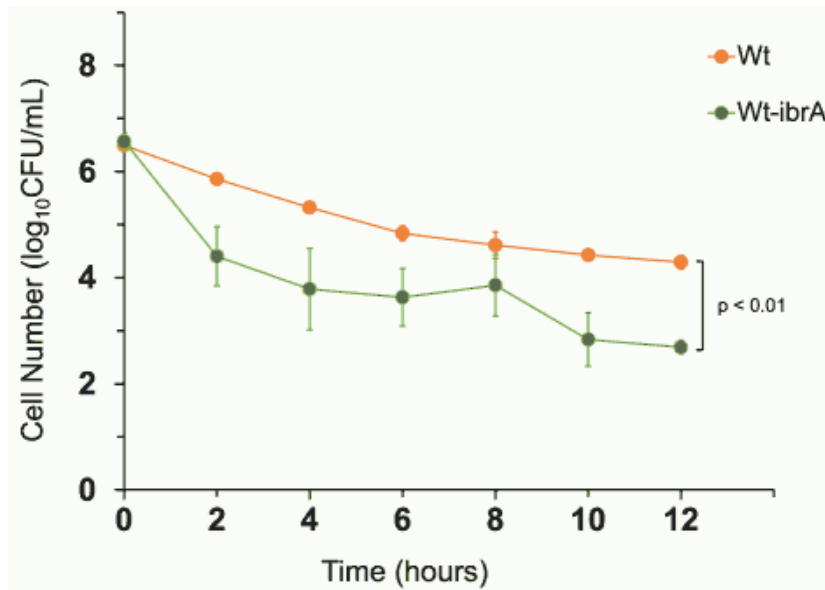
was extracted from both sets of colonies according to the protocol described in section 3.2.2 of this document. The plasmid DNA was subjected to restriction digestion according to the protocol outlined in table 3.3.28 of this document, using the corresponding enzymes described in table 3.3.25, and the products visualised by agarose-gel electrophoresis. DNA bands of the sizes 1249 bp (Figure 4.3.30) and 1011 bp (Figure 4.3.31) were obtained for each of the reactions, in addition to the 5000 bp linear plasmid DNA.

The plasmid pGEX-6P-1^K-*ibrA* was transformed into KpIMS38 to examine the effect of overexpression of *ibrA* on persister cell-formation. Transformation was carried out, RNA

extracted from individual isolates and converted to cDNA. The cDNA was used to perform qPCR to examine the expression of *ibrA*, normalized to the reference genes *kp4432* and *rpoB*, according to the procedures outlined in section 3.3.9.6 of this document. A much higher expression of *ibrA* – with a fold change of over 1500 – was observed in the overexpression strain compared to that in wild-type KpIMS38, which exhibited a fold-change of 0.61 (Figure 4.3.32).



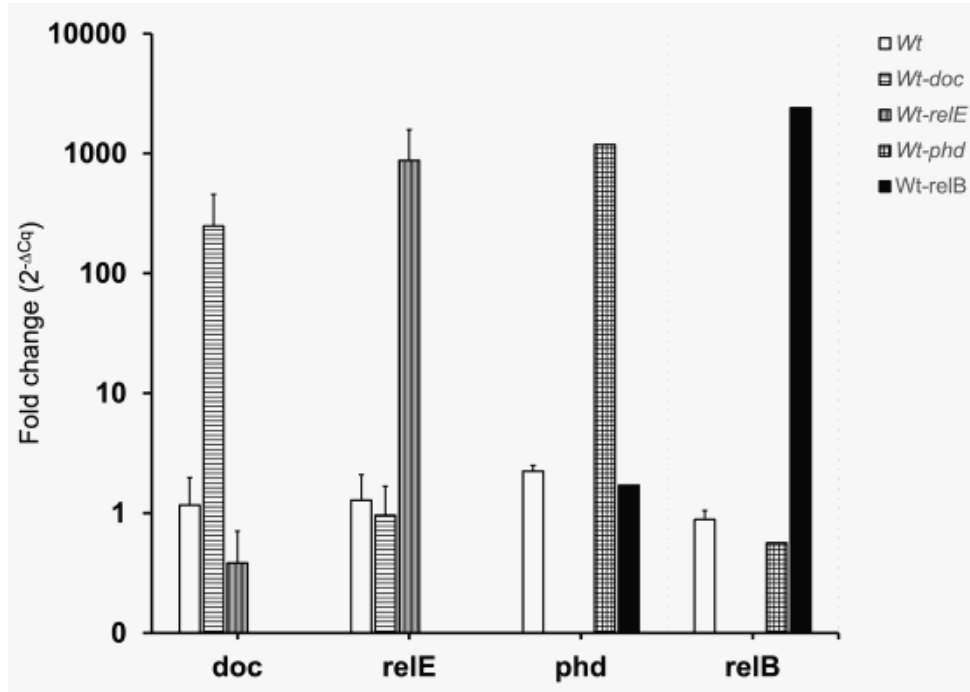
The effect of overexpression of *ibrA* was assessed by studying the survival of the overexpression strains in levofloxacin as a function of time. The cultures were exposed to levofloxacin and the number of surviving bacteria (log₁₀CFU/mL) enumerated according to the procedures outlined in section 3.3.9.6. The KpIMS38 strain containing *ibrA* on the plasmid, i.e., the overexpression strain, exhibited biphasic killing on treatment with levofloxacin. The number of survivors, though, was significantly lower than that observed for the wild-type (Figure 4.3.33).



The effect of overexpression of individual genes from toxin-antitoxin modules on persister cell formation in KpIMS38 were studied using two toxin-antitoxin modules viz. *phd-doc* and *relBE*. Coding sequences for each of the four genes were inserted into individual pGEX-6P-1^K plasmids, and each of the constructs introduced into KpIMS38 according to the procedures outline in section 3.3.9.6 of this document. Expression of the genes from corresponding plasmids in KpIMS38 was assayed by qPCR as described in section 3.3.9.6 of this document, and represented as the fold-change. Strains overexpressing *doc* and *relE* showed much higher levels of expression for the respective genes compared to the wild-type KpIMS38 strain. The same was observed for *phd* and *relB* in strains where they were overexpressed (Figure 4.3.34).

The effect of overexpression of each of the toxin and antitoxin genes on the survival of KpIMS38 in levofloxacin was assessed by studying the killing of overexpression screens

for each gene in the antibiotic as a function of time. The strains were treated with levofloxacin and viable count of the survivors carried out according to the protocols outlined in section 3.3.9.6 of this document. All the strains overexpressing either of the



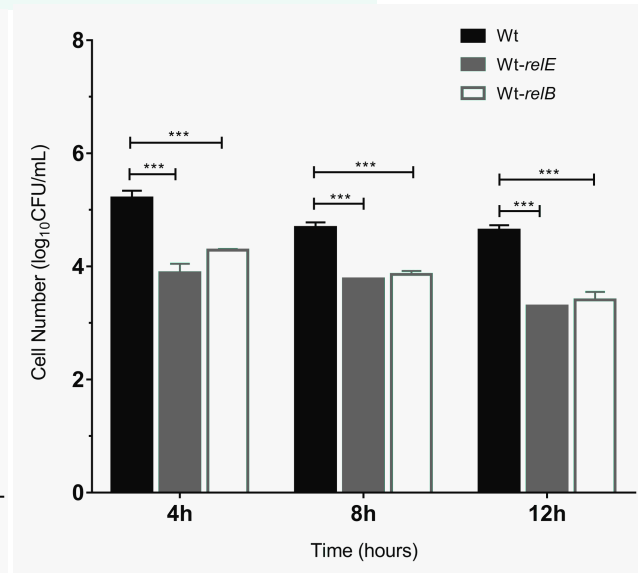
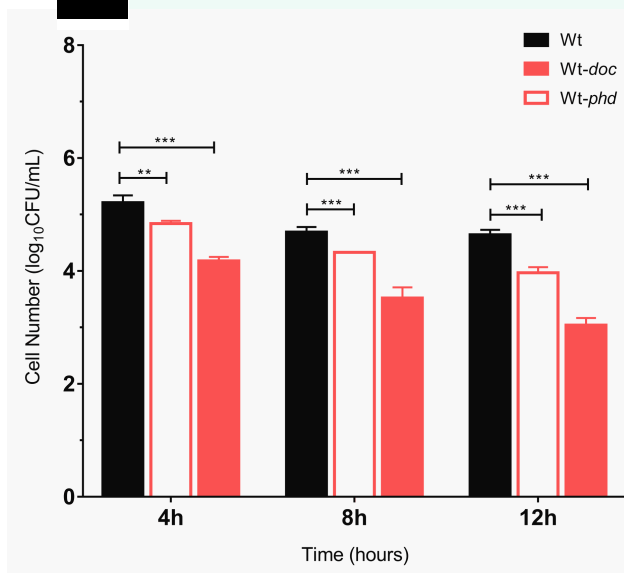
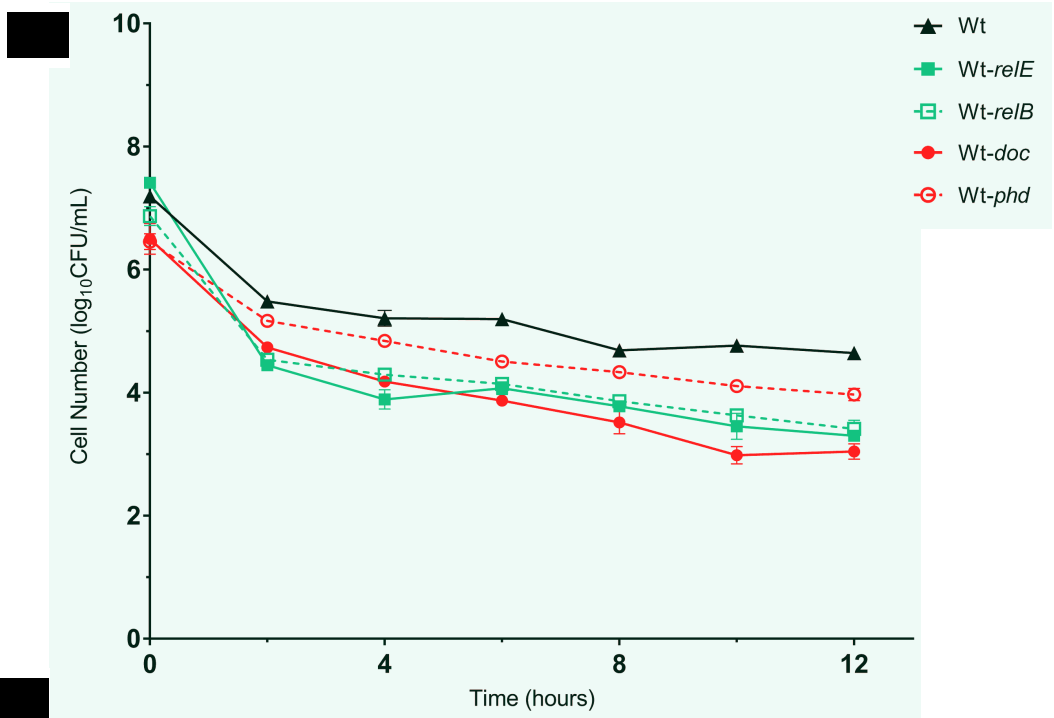
genes exhibited biphasic killing (Table 4.3.11). The strains overexpressing the antitoxins had a higher cell number on exposure to levofloxacin than those overexpressing the antitoxins (Figure 4.3.35 A). The number of persister cells, when measured 12 hours after treatment with levofloxacin, was the lowest in the strain overexpressing the *doc* toxin, and the highest in that overexpressing the *phd* antitoxin, though it was still lower than that obtained for the wild type strain. To determine whether the reduction in the number of survivors was significant, the cell numbers for each overexpression strain at 4, 8, and 12

hours were compared with those at the same time points for wild-type KpIMS38 using the Student's T-test. A two-sample T-test was performed and the p-values for each of the comparisons indicated overexpressing either of a toxin/antitoxin gene significantly reduced the number of cells surviving exposure to levofloxacin (Figure 4.3.35 B).

Table 4.3.11 Effect of the overexpression of toxin-antitoxin genes on persister-cell formation in KpIMS38. Survival of KpIMS38 strains overexpressing *doc* (Wt-*doc*), *relE* (WT-*relE*), *phd* (Wt-*phd*) and *relB* (Wt-*relB*) treated with 256 µg/mL levofloxacin was assessed along with that for the wild type (Wt). Cell numbers of the strains were represented as the log₁₀(CFU/mL) with averages of biological replicates (Av; n=2) and the standard deviation (SD) represented.

Time (hours)	Cell Number (log ₁₀ CFU/mL; Av ± SD)				
	Wt	Wt- <i>doc</i>	Wt- <i>relE</i>	Wt- <i>phd</i>	Wt- <i>relB</i>
0	7.19 ± 0.05	6.50 ± 0.25	7.41 ± 0.09	6.45 ± 0.13	6.87 ± 0.16
2	5.48 ± 0.06	4.74 ± 0.05	4.45 ± 0.04	5.17 ± 0.04	4.53 ± 0.03
4	5.21 ± 0.13	4.18 ± 0.07	3.89 ± 0.16	4.84 ± 0.05	4.29 ± 0.02
6	5.20 ± 0.10	3.87 ± 0.09	4.07 ± 0.10	4.51 ± 0.05	4.14 ± 0.09
8	4.69 ± 0.09	3.52 ± 0.19	3.78 ± 0.00	4.33 ± 0.01	3.86 ± 0.06
10	4.77 ± 0.10	2.98 ± 0.14	3.45 ± 0.21	4.11 ± 0.02	3.63 ± 0.07
12	4.64 ± 0.09	3.04 ± 0.13	3.30 ± 0.00	3.97 ± 0.10	3.41 ± 0.14

Taken together, the results obtained in this section manage to shed some light on the cellular mechanisms involved in the persistence of KpIMS38. While there is some indication of the role of certain toxin-antitoxin-systems in mediating persister-cell formation, the involvement of mechanisms associated with DNA repair is much more straightforward. The aforementioned results also indicate the importance of validating reference genes to study gene expression, and state the suitability of *kp4432* and *rpoB* to be used as paired reference genes to study persistence in KpIMS38.



4.3.6 Discussion

The phenomenon of persistence is effectuated by mechanisms conventionally employed by bacteria to mitigate stress. Various genes act on cellular processes at various times to bring about a state of tolerance to the stress encountered. Although there exists a degree of similitude in the mechanisms of persister-formation brought on by certain stresses, as seen in (p)ppGpp-mediated persistence, other stresses induce persistence for the same organism through widely varying pathways. An example of the same is observed when analysing persistence in *E. coli* K-12; (p)ppGpp signalling controls persistence through Lon/Clp proteases and type-II TA systems coding for mRNA interferases as well as through the Obg and *hok-sok* TA locus that reduces membrane potential, while *tisB-istR* bring about persistence in response to activation of the SOS repair pathway (Harms et al, 2016). This underscores the necessity of investigating the mechanistic aspects of KpIMS38 persisters formed by treatment to levofloxacin.

Examining mRNA transcripts affords a visualization of the changes in gene-expression that promulgate a phenotype (Bustin et al, 2009). Quantitative real time PCR (qPCR) is widely used to quantify relative gene expression owing to the ease of investigating gene expression across multiple conditions (VanGuilder et al, 2008). The credibility of the technique is heavily contingent on the reference genes used to normalise expression; an ideal reference necessitating stable expression correlating to the total mRNA present in the cell (Bustin et al, 2009). This feature requires special consideration when dealing with bacterial persisters since a large number of genes that are conventionally used to normalise expression become unsuitable due to the ceasure of cellular metabolism during persistence (Gollan et al, 2019). Therefore, an appropriate reference gene to carry out expression studies in KpIMS38 persisters was sought out. Five genes were chosen as candidates based on the transcriptome of KpIMS38 persisters, namely *dnaJ*, *groEL*, *kp4432*, *kp751* and *rpoB*. DnaJ and GroEL

act as a chaperone proteins while RpoB is a component of the DNA-dependant RNA polymerase beta subunit. The genes *kp4432* and *kp751* specified a NAD-dependant phenylacetaldehyde dehydrogenase and a glycerol dehydrogenase respectively. Expression studies conducted in bacteria have conventionally used genes associated with transcription, translation, and RNA metabolism as controls, such as the genes coding 16S rRNA (Reniere et al, 2015; Sun et al, 2017) and *rpoB* (Stenico et al, 2014; Reniere et al, 2015). Other commonly used reference genes include *recA* (Florindo et al, 2012; Kaluzna et al, 2017), *gyrA* (Liu et al, 2013; Wen et al, 2016) and *ftsZ* (Brudal et al, 2013; Sumbly et al, 2012), chiefly since they are stably expressed under conditions of varying physiology and nutritional substrates. This is, however, belied by reports of significant variation in the transcription of conventionally-used reference genes across various bacteria (Theis et al, 2007), in diverse microenvironments (Jacob et al, 2011) and upon exposure to certain compounds (Stenico et al, 2014).

Using non-validated reference genes can lead to misinterpretation of expression-patterns (Dheda et al, 2004). The levels of ribosomal RNA (rRNA), which make up a considerable fraction of the RNA extracted from bacteria cells, have been reported to vary with changes in experimental conditions (Tang et al, 2007). The paucity of mRNA transcribed from genes compared to the transcribed rRNA in persister cells coupled with the small number of cells acquired further compound its use to study expression in persisters. Additionally, exposure of bacterial cells to fluoroquinolones influences the expression of genes involved in DNA repair, including *gyrA*, *gyrB* and *recA* (Dörr et al, 2009). Therefore, it was essential to validate gene expression in KpIMS38 persisters using a completely different set of genes as candidate reference genes. *rpoB* is a frequent candidate used to normalise gene expression despite reports attributing a high degree of variation in its expression under certain experimental conditions (Sumbly et al, 2012; Stenico et al, 2014). Studies have

validated *gapA* which specifies glyceraldehyde-3-phosphate dehydrogenase, a key component of the glycolytic pathway, to be a competent reference gene (Løvdal and Saha, 2014). Studies have employed genes specifying other dehydrogenases such as D-Lactate dehydrogenase (Zhao et al, 2011; Sumby et al, 2012), glutamate dehydrogenase (Kirk et al, 2014), NADH dehydrogenase (Jacob et al, 2011) as reference genes, despite not all of them actually being validated as suitable reference genes under the experimental conditions.

The RefFinder tool functions by collating the outcomes obtained by BestKeeper (Rasmussen, 2001), Delta Ct (Silver et al, 2006), geNorm (Vandesompele et al, 2002) and Normfinder (Andersen et al, 2004) to obtain a cumulative score according to which individual genes are ranked according to descending order of stability. A considerable degree of variation among replicates was observed when using *kp751* alone as a reference genes, rendering it unacceptable to normalise gene expression in KpIMS38 persisters. The low variation among replicates observed when using *kp4432* as the reference gene was compounded by the lowest fold-change across all three candidate reference genes, potentially under-representing gene expression in persisters formed by levofloxacin treatment. Using the pair of *kp4432* and *rpoB* produced expression less variant than other combinations of genes tested, a phenomenon observed in studies conducted along similar lines (Savli et al, 2003; Zhao et al, 2011; Gomes et al, 2018; García-Laviña et al, 2019) with some going so far as to employ three reference genes to normalise gene expression in bacteria (Brudal et al, 2013)].

The expression of select genes in persister cells was examined using the pair of validated reference genes, focusing on four TA systems and the phage-shock response operon based on observations from the transcriptome of KpIMS38 cells treated with levofloxacin. All the genes tested were upregulated in KpIMS38 persisters generated on treatment with

levofloxacin. A variety of studies examining persistence in bacteria have uncovered the involvement of TA systems in propagating the condition (Harrison et al, 2009; Norton and Mulvey, 2012; Tripathi et al, 2014; Shan et al, 2017; Levin-Reisman et al, 2017). The interplay between free toxin and its antitoxin-bound form within the cell influences cellular processes, culminating in metabolic dormancy and/or an enhanced ability to withstand lethal stress through persistence (Harms et al, 2016). Among the TA loci examined in the present study, the antitoxin was expressed at a higher level than its cognate toxin. Although the gene coding for the toxin *ficT* was expressed at a higher level than its antitoxin counterpart *ficA*, the high standard deviation observed for the antitoxin could interfere with reliably assessing the expression of the gene in KpIMS38 persisters. Taken together, these findings are indicative of four TA modules not contributing to persister cell formation in KpIMS38. Despite a considerable body of implicating toxin-antitoxin modules in mediating bacterial persistence, a growing body of knowledge exists providing evidence that states while toxin-antitoxin modules are expressed during persistence, not all of them lead to persister cell formation. Shan et al (2017) observed certain TA systems to be upregulated during conditions of abiotic stress without themselves increasing the persistence, and while Harms et al (2017) showed that TA modules that encode mRNA endonucleases did not actually interact with the Lon protease in a (p)ppGpp- dependent manner and lead to persister cell formation in *E. coli strains* in unstressed conditions as was previously thought. This would explain the lack of upregulation of TA modules in persister cells of KpIMS38.

Under conditions of envelope stress, protein mislocalisation in the inner membrane, osmotic or ethanol shock (Yamaguchi and Darwin, 2012), a transcriptional activator PspF dissociates from PspA and activates expression of the *psp* genes – *pspA*, *-B*, *-C*, *-D*, *-E* located downstream in an operon, and *pspG* located distally. This helps the cell tide over

the stress condition by performing roles which include maintaining the permeability-barrier of the inner membrane (through PspB and -C) as well as the proton-motive force (Flores-Kim and Darwin, 2016). The *psp* system has been implicated in the formation of persister cells, where stationary-phase as well as exponential-phase cultures of *E. coli* K-12 treated with indole exhibited an increased expression of *pspA*, followed by either of *pspB*, -C or -D. The level of expression for all *psp* genes was, however, markedly lower in exponential-phase cultures as against stationary-phase cultures (Vega et al, 2012). The *psp* system also has the ability to augment persister formation induced by other response pathways (Liu et al, 2017). *pspD* followed by *pspA* were among the most highly expressed *psp* genes identified in KpIMS38 persisters. While the role of PspA in the unfolded protein response is well known, functioning as an inhibitor of the operon, there is a lack of information regarding the function of PspD. Additionally, the expression of *ibrA* in KpIMS38 persisters was also assessed. The gene, which was showed up as the most upregulated in the transcriptome, was expressed only 1-fold higher when assessed by qPCR.

The study of bacterial persistence has implicated specific pathways that conventionally mediate the bacterial stress responses (Gollan et al, 2019). The role of the SOS response in facilitating the formation of persister cells on exposure to DNA-damaging agents has been highlighted (Dörr et al, 2009). The association of genes involved in the cellular response to DNA damage, namely *recA*, *umuC*, *umuD* and *ruvABC*, with persister cell formation in KpIMS38 was examined in the current study through assessing their expression. Among the eight genes chosen, seven were associated with the DNA-damage response while *spoT* was chosen to examine the role of the stringent response – mediated through the (p)ppGpp signalling pathway – in KpIMS38 persisters. RecA is involved in DNA break-repair via homologous recombination as well as in translesion DNA synthesis and induction of the SOS response (Galletto and Kowalczykowski, 2007). *sulA* is a component of the SOS

system and is involved in inhibiting bacterial cell division by binding to and sequestering FtsZ (Masuda et al, 2012). The UmuD protein undergoes post-translational modification to form UmuD'. Two subunits of UmuD' associate with UmuC to form the heterotrimeric UmuD'₂C that functions as DNA Polymerase V to catalyze DNA synthesis opposite to lesions such as cyclobutyl dimers in the DNA strand (Lovett, 2011). Two homologs each of *umuC* and *umuD* were identified in the genome of KpIMS38 during annotation. They were named *umuC1*, *umuC2*, *umuD1*, and *umuD2* on the basis of their proximity to each other, and all four genes were considered for the current analysis. The proteins RuvA, RuvB and RuvC form a tripartite complex to resolve a Holliday junction, the four-way DNA intermediate formed between the DNA strands on either side of a double strand break. RuvA binds to DNA in the presence of ATP, and with RuvB results in the formation of a DNA heteroduplex. RuvC then associates with the pair and makes incisions in two strands of the heteroduplex, thereby resolving it (Hoff et al, 2017). The enzyme SpoT is involved in the turnover of the alarmone Guanosine tetra/pentaphosphate ((p)ppGpp) in Gram-negative bacteria. In response to the presence of uncharged tRNA at the aminoacyl site (A site) of the bacterial ribosome, SpoT catalyzes the conversion of Adenosine triphosphate (ATP) and Guanosine triphosphate (GTP) to form Guanosine tetraphosphate (ppGpp) and Guanosine pentaphosphate (pppGpp). Additionally, the enzyme also catalyzes the hydrolysis of ppGpp to GTP and of pppGpp to Guanosine diphosphate (GDP), with the release of pyrophosphate (P_i) in both situations (Dalebroux and Swanson, 2012), while SpoT is known to generally display weak synthetase and strong hydrolase activities (Kim et al, 2018). The expression of the given genes was examined after 8 hours of levofloxacin treatment. Subsequently, gene expression was also measured at various time intervals within 2 hours of exposure to levofloxacin to observe the immediate changes that occurred on antibiotic treatment.

The trend of a sharp increase in the expression level to peak at 30 minutes followed by a steady reduction to a minimum at the 8th hour was observed for all DNA-repair associated-genes viz. *recA*, *umuC* and *umuD*. At all the time points chosen for analysis, the expression of *recA* was consistently the highest among the eight genes tested. Along with *umuC* and *umuD*, *recA* continued to be expressed at a high level after treatment with levofloxacin for 8 hours. These results could be indicative of KpIMS38 persisters constantly requiring the activity of DNA repair – through SOS repair mechanisms – to maintain the state of persistence. The observation also highlights the continued metabolism in KpIMS38 persisters and is in line with the results obtained from flow cytometry and microscopy that indicated metabolic activity within the surviving population of cells. Another feature observed was a greater degree of expression of certain genes during the initial stages of encountering levofloxacin. The *ruv* genes exhibited peak expression 30 to 60 minutes after levofloxacin exposure, but were reduced almost 4 times when assessed 8 hours after treatment. A similar trend was observed in the expression of *sulA*. On the other hand, the highest level of *spoT* expression was recorded 15 minutes after antibiotic-exposure, with a gradual reduction after 8 hours of levofloxacin treatment. These results could imply the involvement of two kinds of genes in KpIMS38 persistence: genes that are expressed at a high level on encountering levofloxacin but gradually reduce with time, and genes that are continually expressed at a high level after the initial antibiotic-exposure. Genes like *recA*, *sulA* and *umuCD* fall in the latter category and could indicate their necessity to KpIMS38 maintaining persistence. Genes in the other category include *ruvABC* i.e., whose expression declines after initially increasing on levofloxacin exposure. This could be indicative of the requirement of the latter to initiate persistence and the former to maintain cells in the state of persistence.

On exposure to levofloxacin, the cell number within a KpIMS38 culture falls swiftly within the first two hours. This period is expected to represent a stage when the patterns of gene expression within the cell are altered to convert normally metabolising cells into persister cells. In comparison, KpIMS38 cultures treated with levofloxacin for 8 hours are expected to consist of cells wherein the pattern of gene expression is stable. Therefore, normalising gene expression from the early time-points to expression after 8 hours affords a deeper insight into changing expression patterns leading up to persistence. For instance, *recA* and *umuC2D2* were expressed at a high level throughout persistence, including after 8 hours of treatment with levofloxacin. In comparison, the fold-change ratio for the genes was not as elevated with the ratio of only *umuD2* at 30 minutes exceeding 5. This indicated the constantly high level of expression of the genes upon immediate as well as prolonged exposure to levofloxacin. The fold-change ratio also highlighted the role of *spoT* in the persistence of KpIMS38; expression immediately peaked 15 minutes after encountering levofloxacin, stayed so for another 15 minutes and gradually fell. This could be indicative of a greater necessity of *spoT* activity to initiate persistence but not so much to maintain it. Assessing the fold-change ratio brought out the differences between the two copies of *umuCD*. The heightened expression of the pair of *umuC1* and *umuD1* during the initial phase of persistence was clearly visible, compared to their counterparts, i.e., *umuC2* and *umuD2* that were expressed at a high level throughout levofloxacin treatment. Furthermore, *umuC1* was expressed at a higher level than *umuD1*, while the converse was true for *umuC2* and *-D2*. These findings both copies of *umuCD*, despite being operational at different stages, are relevant to the persistence of KpIMS38. No alteration in gene-expression patterns were observed with the fold-change ratio of *ruvABC* genes; the expression of *ruvA* and *-B* gradually increased to its peak at 60 minutes and eventually fell while *ruvC* was expressed at a low but constant level throughout treatment with levofloxacin.

The concept of genes influencing persistence at different time points was demonstrated by Wu et al (2015), with the possibility of a cooperation between the early- and late-persister genes facilitating a transition of persisters from shallow to deep persistence. The same study also observed the importance of *recA* in maintaining persistence beyond 4 hours and *umuD* beyond 24 hours of exposure to antibiotics. While the study was performed on stationary-phase *E. coli* cells, the results from the current study indicate a degree of conformity between the roles of certain genes in response to stress caused by treatment with fluoroquinolone antibiotics.

Lambda recombineering was employed in an attempt to create mutants for the genes *ibrA*, *pspF*, *doc* and *relE* in KpIMS38 and study their role in its persistence. The lambda recombineering system, modified from the Red system of recombination inherent in the bacteriophage lambda, provides a means to modify bacterial chromosomes and replace genes in a highly efficient manner (Murphy, 2016). The technique has been applied to carry out recombination in a variety of organisms including *E. coli*, *Salmonella*, *Vibrio cholerae* and *Pseudomonas aeruginosa* (Wei et al, 2012). When applied in KpIMS38, the endeavour was met with a degree of success, namely, in the deletion of *ibrA*. This was first identified by the presence of a DNA fragment of approximately 1700 bp corresponding to the FRT deletion cassette. The putative Δ *ibrA* strain lost the ability to survive in 256 μ g/mL levofloxacin. However, PCRs set up to amplify a region internal to the deletion cassette did not yield any amplification products. In addition, amplification of the full-length sequence of *ibrA* produced a DNA molecule of a size comparable to the wild-type version of the gene instead a larger molecule expected from insertion of the FRT cassette within the gene sequence. The sum total of observations demonstrated the putative mutant of *ibrA* to be, in reality, not a mutant at all. All further endeavours at creating deletions in *ibrA* using the lambda recombineering system yielded the same outcomes as obtained when attempting

deletion in *pspF*, *doc* and *relE*, where no insertion of the deletion-cassette into the gene-of-interest was obtained. A study by Wei et al (2012) attempting to create gene-deletions in the chromosomal DNA of *K. pneumoniae* using the lambda recombineering system observed that although the strains were successfully transformed with the plasmid carrying the recombinase genes, the recombinase was non-functional, and no activity was detected. This was hypothesized to be due to the inability of the plasmids to replicate within *K. pneumoniae*.

A novel plasmid was synthesized by Huang et al (2014) to carry out lambda recombineering in *K. pneumoniae* cells. The plasmid, pACBSR-Hyg, expressed the lambda recombinase genes under control of an arabinose promoter and could be selected for by resistance to hygromycin. Transformation of the plasmid into KpIMS38 was stable, and attempts were made to carry out the deletion of the toxin genes *doc* and *relE*. However, all attempts were futile as evidenced from the absence of the deletion cassette and the presence of corresponding genes in intact condition in the genome of the transformants. Taken together, these observations indicate the intractability of creating gene mutations in KpIMS38 through lambda recombineering. Both the methods of lambda recombineering, i.e., using pRedET and pACBSR-hyg, have been successfully used to create gene deletions in *K. pneumoniae* (Seo et al., 2009; Wei et al, 2012, 2013; Farzand et al., 2019). The ineffectiveness of the technique in the present study could, therefore, be attributed to its use in a non-standard isolate *K. pneumoniae* that is uncharacterised relative to standard strains of the same.

RNA interference emerged as a promising avenue to study gene function while circumventing deletion-associated lethality (Zhang et al, 2021). The same is accomplished in bacteria by repurposing the CRISPR-Cas system of genome editing. Conventionally, the Cas9 protein is directed by a single-stranded "guide" RNA to a specific DNA sequence in

the chromosome to instigate a double-stranded break at the site (Deltcheva et al, 2011), which can then be repaired using a template DNA thereby resulting in the insertion of the template at the site (Zhang et al, 2021). Mutations in Cas9 to disable its nuclease activity generate an inactive form called dCas9, which retains the ability to bind to guide RNA (Jinek et al, 2012). The complex retains the ability to associate with the target DNA in the chromosome, and when targeted to the coding or promotor sequence has been demonstrated to impede the RNA polymerase thereby inhibiting transcription and expression of the gene (Zhang et al, 2021). To perform the same in KpIMS38, the CRISPR-based gene silencing system developed by Dr. D Rath at BARC, India was employed (Rath et al, 2015). Silencing was verified through qPCR for the TA gene-pairs viz. *rel*, *relBE*, and *phd-doc* targeted, and a difference in the expression between uninduced and tetracycline-induced strains was considered as evidence toward silencing of a gene. While four genes exhibited differences in expression, discrepancies were observed. While the toxins *relT* and *doc* appeared to be silenced, as evidenced by a lowering of their expression upon induction with tetracycline, the same induction had a converse effect on *relAt* and *relB*. Both the genes, incidentally cognate antitoxins to *relT* and *relE* respectively, were expressed at a higher level in the induced condition. Notwithstanding the disparate results from silencing the individual genes, each of them resulted in a significant reduction in the number of persisters formed.

Overexpression of TA genes in KpIMS38 diminished its persistence in response to levofloxacin. Strains overexpressing one of the four genes from the *relBE* and *phd-doc* TA systems exhibited biphasic killing, implying overexpression did not abrogate persister-cell formation. However, persisters were formed in each of the four overexpression-screens were significantly fewer than the wild-type. These outcomes, taken with those acquired from deletion or silencing of genes, suggest the association between TA systems and

persistence in KpIMS38 is incongruous. The pasTI TA system was determined to be essential for persistence in a uropathogenic isolate of *E. coli* but did not influence persister-cell formation in the laboratory strain K-12, indicating the genetic context to be an important factor in the activity of TA systems (Norton and Mulvey, 2012). Persister-cell formation by *E. coli* in response to abiotic stresses was associated an increase in the expression of certain TA modules, including *relBE*, which incidentally did not influence persistence even though their mediation of the same had been reported elsewhere. An explanation for this difference was afforded by the lack of detectable activity from the toxins expressed thereby implying insufficient activation of the TA systems to affect persistence (Shan et al, 2017). Furthermore, overexpressing toxin genes on high-copy number plasmid vectors – to delineate the mechanisms through which they affect cellular processes and thereby effectuate persistence – is liable to generate artifacts. This makes it vital to identify the precise conditions which activate TA modules, so that the comparison between persister and non-persister cells can be drawn with authenticity (Ronneau and Helaine, 2019). Hence, the outcomes of this study suggest the link between persistence in KpIMS38 and TA systems could not be clearly defined, and deeper analyses are required to clearly define their contribution to persister-cell formation.

Conclusion

This chapter summarizes the principal findings obtained in the present study and propounds their significance. It also delineates prospective directions for future work in the field.

Section 4.1 Detection and characterization of persister cells in *K. pneumoniae*

- Persister cells were formed in response to a specific antibiotic, levofloxacin.
- Persister formation increased with an increase in the concentration of the antibiotic as well as with the age of the inoculum.
- Persistence was non-heritable, conferred cross-tolerance to other antibiotics, and did not involve mutations that increased resistance to the antibiotic.
- Persister cells consisted of two sub-populations P1 and P2, which remained metabolically active despite treatment with levofloxacin.
- Treatment with levofloxacin halted cell division and led to accumulation of long cells. The cells did not resume division and growth on the removal of levofloxacin in the time frame they were observed.

Section 4.2 Elucidation of the genome and transcriptome of persister cells formed by *K. pneumoniae*

- A draft genome sequence of KpIMS38 was obtained, with the genome possessing genes that contribute to resistance and virulence, as well as containing bacteriophages.
- The transcriptome of KpIMS38 persisters formed on levofloxacin-treatment indicated differential gene expression in genes associated with DNA repair, antibiotic efflux, protein synthesis, biofilm synthesis and TA systems.

Section 4.3 Investigation of the role of various genes in persister-cell formation in *K. pneumoniae*

- The gene-pair of *kp4432* and *rpoB* were best suited as reference genes to study gene expression of KpIMS38 persisters.

- DNA damage response plays a role in persistence in KpIMS38 and not the stringent response. Cell division is inhibited, promoting the elongation of the cell.
- Gene deletion using lambda recombineering was unsuccessful in KpIMS38.
- CRISPR-based silencing of certain toxin and antitoxins reduced the number of persister cells formed, whereas overexpression of toxin and antitoxin genes also reduced persister cell formation in KpIMS38.

Overall, the current study confirms levofloxacin induced persister cell formation in exponential growing culture of *Klebsiella pneumoniae*. Further, results indicate that levofloxacin induced persistence is driven by the SOS response pathway characterized by upregulation of *recA* and *umuCD*.

Significance of the thesis

The present study highlights the ability of a clinical isolate of *Klebsiella pneumoniae*, which exhibits an extremely-drug resistant (XDR) phenotype, to form persisters in response to levofloxacin at concentrations much higher than its inhibitory concentrations. Observations from flow cytometry and live-cell microscopy inferred the possible role of a viable but not culturable (VBNC) state in the survival of KpIMS38 persisters to levofloxacin. This, coupled the ability of persisters to tolerate suprainhibitory concentrations other antibiotics, spotlights the public-health risk inherent in strains. Infections caused by persister-forming organisms could result in the failure of treatment options and the development of chronic infections.

The outcomes of the present study highlighted the variation of gene-expression with time during persistence – some genes being continually expressed while others expressed only upon encountering stress – thus depicting expression to be of a multidimensional nature.

Additionally, the present study underscores the importance of validating reference genes when examining gene-expression to ensure the reliability of the study.

Future directions

The present study examined persister-cell formation in a clinical isolate of *Klebsiella pneumoniae* on exposure to levofloxacin, phenotypically characterising the persisters formed and examining specific genes for their involvement in persistence. The results obtained herein afford some degree of insight into the understanding of infectious diseases, which could further be enhanced through in vivo studies observing KpIMS38 infections in suitable cell lines and/or animal models as to whether persistence is perceived in those systems. Establishing a genetic screen would be invaluable in ascertaining the functional association of the various genes highlighted in this study to levofloxacin-mediated persistence in KpIMS38.

References

- Aakre CD, Phung TN, Huang D, Laub MT. A Bacterial Toxin Inhibits DNA Replication Elongation through a Direct Interaction with the β Sliding Clamp. *Molecular Cell* 2013; 52:617–28.
<https://doi.org/10.1016/j.molcel.2013.10.014>.
- Adams KN, Takaki K, Connolly LE, Wiedenhoft H, Winglee K, Humbert O, et al. Drug Tolerance in Replicating Mycobacteria Mediated by a Macrophage-Induced Efflux Mechanism. *Cell* 2011; 145:39–53.
<https://doi.org/10.1016/j.cell.2011.02.022>.
- Aldred KJ, Kerns RJ, Osheroff N. Mechanism of Quinolone Action and Resistance. *Biochemistry* 2014; 53:1565–74. <https://doi.org/10.1021/bi5000564>.
- Alkasir R, Ma Y, Liu F, Li J, Lv N, Xue Y, et al. Characterization and transcriptome analysis of *Acinetobacter baumannii* persister cells. *Microbial Drug Resistance* 2018; 24:1466–74. <https://doi.org/10.1089/MDR.2017.0341>.
- Allison KR, Brynildsen MP, Collins JJ. Metabolite-enabled eradication of bacterial persisters by aminoglycosides. *Nature* 2011; 473:216–20.
<https://doi.org/10.1038/nature10069>.
- Amato SMM, Orman MA a, Brynildsen MPP. Metabolic Control of Persister Formation in *Escherichia coli*. *Molecular Cell* 2013; 50:475–87.
<https://doi.org/10.1016/j.molcel.2013.04.002>.
- Amsler K, Santoro C, Foleno B, Bush K, Flamm R. Comparison of Broth Microdilution, Agar Dilution, and Etest for Susceptibility Testing of Doripenem against Gram-Negative and Gram-Positive Pathogens. *Journal of Clinical Microbiology* 2010; 48:3353–7. <https://doi.org/10.1128/JCM.00494-10>.
- Andersen CL, Jensen JL, Ørntoft TF. Normalization of real-time quantitative reverse transcription-PCR data: A model-based variance estimation approach to identify

- genes suited for normalization, applied to bladder and colon cancer data sets. *Cancer Research* 2004; 64:5245–50. <https://doi.org/10.1158/0008-5472.CAN-04-0496>.
- Andrews JM. Determination of minimum inhibitory concentrations. *Journal of Antimicrobial Chemotherapy* 2001; 48:5–16. https://doi.org/10.1093/jac/48.suppl_1.5.
 - Arndt D, Grant JR, Marcu A, Sajed T, Pon A, Liang Y, et al. PHASTER: a better, faster version of the PHAST phage search tool. *Nucleic Acids Research* 2016; 44:W16–21. <https://doi.org/10.1093/NAR/GKW387>.
 - Ayrapetyan M, Williams TC, Baxter R, Oliver JD. Viable but nonculturable and persister cells coexist stochastically and are induced by human serum. *Infection and Immunity* 2015; 83:4194–203. <https://doi.org/10.1128/IAI.00404-15>.
 - Aziz RK, Bartels D, Best AA, DeJongh M, Disz T, Edwards RA, et al. The RAST Server: Rapid Annotations using Subsystems Technology. *BMC Genomics* 2008; 9:75. <https://doi.org/10.1186/1471-2164-9-75>.
 - Baharoglu Z, Mazel D. SOS, the formidable strategy of bacteria against aggressions. *FEMS Microbiology Reviews* 2014; 38:1126–45. <https://doi.org/10.1111/1574-6976.12077>.
 - Bakkeren E, Diard M, Hardt W-D. Evolutionary causes and consequences of bacterial antibiotic persistence. *Nature Reviews Microbiology* 2020; 18:479–90. <https://doi.org/10.1038/s41579-020-0378-z>.
 - Bakkeren E, Huisman JS, Fattinger SA, Hausmann A, Furter M, Egli A, et al. *Salmonella* persisters promote the spread of antibiotic resistance plasmids in the gut. *Nature* 2019; 573:276–80. <https://doi.org/10.1038/s41586-019-1521-8>.

- Balaban NQ, Helaine S, Lewis K, Ackermann M, Aldridge B, Andersson DI, et al. Definitions and guidelines for research on antibiotic persistence. *Nature Reviews Microbiology* 2019; 17:441–8. <https://doi.org/10.1038/s41579-019-0196-3>.
- Balaban NQ, Merrin J, Chait R, Kowalik L, Leibler S. Bacterial Persistence as a Phenotypic Switch. *Science* (1979) 2004; 305:1622–5. <https://doi.org/10.1126/science.1099390>.
- Banerjee R, Johnson JR. A new clone sweeps clean: the enigmatic emergence of *Escherichia coli* sequence type 131. *Antimicrob Agents Chemother* 2014; 58:4997–5004. <https://doi.org/10.1128/AAC.02824-14>.
- Bankevich A, Nurk S, Antipov D, Gurevich AA, Dvorkin M, Kulikov AS, et al. SPAdes: A New Genome Assembly Algorithm and Its Applications to Single-Cell Sequencing. *Journal of Computational Biology* 2012; 19:455–77. <https://doi.org/10.1089/cmb.2012.0021>.
- Bankevich A, Nurk S, Antipov D, Gurevich AA, Dvorkin M, Kulikov AS, et al. SPAdes: A New Genome Assembly Algorithm and Its Applications to Single-Cell Sequencing. *Journal of Computational Biology* 2012; 19:455–77. <https://doi.org/10.1089/cmb.2012.0021>.
- Barrett TC, Mok WWK, Murawski AM, Brynildsen MP. Enhanced antibiotic resistance development from fluoroquinolone persisters after a single exposure to antibiotic. *Nature Communications* 2019 10:1 2019; 10:1–11. <https://doi.org/10.1038/s41467-019-09058-4>.
- Bauer AW, Kirby WM, Sherris JC, Turck M. Antibiotic susceptibility testing by a standardized single disk method. *Am J Clin Pathol* 1966; 45:493–6.
- Bauer AW, Kirby WM, Sherris JC, Turck M. Antibiotic susceptibility testing by a standardized single disk method. *Am J Clin Pathol* 1966; 45:493–6.

- Bertram R, Schuster CF. Post-transcriptional regulation of gene expression in bacterial pathogens by toxin-antitoxin systems. *Frontiers in Cellular and Infection Microbiology* 2014; 4:6. <https://doi.org/10.3389/FCIMB.2014.00006/BIBTEX>.
- Besemer J, Borodovsky M. Heuristic approach to deriving models for gene finding. *Nucleic Acids Research* 1999; 27:3911–20. <https://doi.org/10.1093/nar/27.19.3911>.
- Bevan ER, Jones AM, Hawkey PM. Global epidemiology of CTX-M β -lactamases: temporal and geographical shifts in genotype. *Journal of Antimicrobial Chemotherapy* 2017; 72:2145–55. <https://doi.org/10.1093/JAC/DKX146>.
- Bhargava N, Sharma P, Capalash N. Pyocyanin stimulates quorum sensing-mediated tolerance to oxidative stress and increases persister cell populations in *Acinetobacter baumannii*. *Infect Immun* 2014; 82:3417–25. <https://doi.org/10.1128/IAI.01600-14>.
- Bigger JW. Treatment of Staphylococcal Infections With Penicillin By Intermittent Sterilisation. *The Lancet* 1944; 244:497–500. [https://doi.org/10.1016/S0140-6736\(00\)74210-3](https://doi.org/10.1016/S0140-6736(00)74210-3).
- Black DS, Irwin B, Moyed HS. Autoregulation of hip, an operon that affects lethality due to inhibition of peptidoglycan or DNA synthesis. *Journal of Bacteriology* 1994; 176:4081–91. <https://doi.org/10.1128/JB.176.13.4081-4091.1994>.
- Blango MG, Mulvey MA. Persistence of Uropathogenic *Escherichia coli* in the Face of Multiple Antibiotics. *Antimicrobial Agents and Chemotherapy* 2010; 54:1855–63. <https://doi.org/10.1128/AAC.00014-10>.
- Blower TR, Salmond GPC, Luisi BF. Balancing at survival's edge: the structure and adaptive benefits of prokaryotic toxin–antitoxin partners. *Current Opinion in Structural Biology* 2011; 21:109–18. <https://doi.org/10.1016/J.SBI.2010.10.009>.
- Bodendoerfer E, Marchesi M, Imkamp F, Courvalin P, Böttger EC, Mancini S. Co-occurrence of aminoglycoside and β -lactam resistance mechanisms in

aminoglycoside- non-susceptible *Escherichia coli* isolated in the Zurich area, Switzerland. *International Journal of Antimicrobial Agents* 2020; 56:106019. <https://doi.org/10.1016/j.ijantimicag.2020.106019>.

- Boggild A, Sofos N, Andersen KR, Feddersen A, Easter AD, Passmore LA, et al. The Crystal Structure of the Intact *E. coli* RelBE Toxin-Antitoxin Complex Provides the Structural Basis for Conditional Cooperativity. *Structure* 2012; 20:1641–8. <https://doi.org/10.1016/J.STR.2012.08.017>.
- Bojsen R, Regenberg B, Gresham D, Folkesson A. A common mechanism involving the TORC1 pathway can lead to amphotericin B-persistence in biofilm and planktonic *Saccharomyces cerevisiae* populations. *Sci Rep* 2016; 6:21874. <https://doi.org/10.1038/srep21874>.
- Booth VH, Green DE. A wet-crushing mill for micro-organisms. *Biochemical Journal* 1938; 32:855–61. <https://doi.org/10.1042/bj0320855>.
- Bortolaia V, Kaas RS, Ruppe E, Roberts MC, Schwarz S, Cattoir V, et al. ResFinder 4.0 for predictions of phenotypes from genotypes. *Journal of Antimicrobial Chemotherapy* 2020; 75:3491–500. <https://doi.org/10.1093/jac/dkaa345>.
- Bradford PA, Bratu S, Urban C, Visalli M, Mariano N, Landman D, et al. Emergence of carbapenem-resistant *Klebsiella* species possessing the class A carbapenem-hydrolyzing KPC-2 and inhibitor-resistant TEM-30 beta-lactamases in New York City. *Clin Infect Dis* 2004; 39:55–60. <https://doi.org/10.1086/421495>.
- Brooun A, Liu S, Lewis K. A dose-response study of antibiotic resistance in *Pseudomonas aeruginosa* biofilms. *Antimicrobial Agents and Chemotherapy* 2000; 44:640–6.
- Brown DR. Nitrogen Starvation Induces Persister Cell Formation in *Escherichia coli*. *J Bacteriol* 2019; 201:e00622-18. <https://doi.org/10.1128/JB.00622-18>.

- Brudal E, Winther-Larsen HC, Colquhoun DJ, Duodu S. Evaluation of reference genes for reverse transcription quantitative PCR analyses of fish-pathogenic *Francisella* strains exposed to different growth conditions. BMC Res Notes 2013; 6:76. <https://doi.org/10.1186/1756-0500-6-76>.
- Brzozowska I, Zielenkiewicz U. Regulation of toxin-antitoxin systems by proteolysis. Plasmid 2013; 70:33–41. <https://doi.org/10.1016/J.PLASMID.2013.01.007>.
- Bush K, Bradford PA. Interplay between β -lactamases and new β -lactamase inhibitors. Nat Rev Microbiol 2019; 17:295–306. <https://doi.org/10.1038/S41579-019-0159-8>.
- Bushmanova E, Antipov D, Lapidus A, Suvorov V, Prjibelski AD. RnaQUAST: A quality assessment tool for de novo transcriptome assemblies. Bioinformatics 2016; 32:2210–2. <https://doi.org/10.1093/bioinformatics/btw218>.
- Bustin SA, Benes V, Garson JA, Hellemans J, Huggett J, Kubista M, et al. The MIQE Guidelines: Minimum Information for Publication of Quantitative Real-Time PCR Experiments. Clinical Chemistry 2009; 55:611–22. <https://doi.org/10.1373/clinchem.2008.112797>.
- Byrd BA, Zenick B, Rocha-Granados MC, Englander HE, Hare PJ, LaGree TJ, et al. The AcrAB-TolC efflux pump impacts persistence and resistance development in stationary-phase *Escherichia coli* following delafloxacin treatment. Antimicrobial Agents and Chemotherapy 2021; 65. <https://doi.org/10.1128/AAC.00281-21>.
- Campbell AM. Prophages and Cryptic Prophages. Bacterial Genomes, Springer, Boston, MA; 1998, p. 23–9. https://doi.org/10.1007/978-1-4615-6369-3_3.

- Carneiro S, Lourenço A, Ferreira EC, Rocha I. Stringent response of *Escherichia coli*: revisiting the bibliome using literature mining. *Microbial Informatics and Experimentation* 2011; 1:14. <https://doi.org/10.1186/2042-5783-1-14>.
- Carret G, Flandrois JP, Lobry JR. Biphasic kinetics of bacterial killing by quinolones. *J Antimicrob Chemother* 1991; 27:319–27. <https://doi.org/10.1093/JAC/27.3.319>.
- Castanheira M, Simner PJ, Bradford PA. Extended-spectrum β -lactamases: an update on their characteristics, epidemiology and detection. *JAC-Antimicrobial Resistance* 2021; 3. <https://doi.org/10.1093/jacamr/dlab092>.
- Chan WT, Espinosa M, Yeo CC. Keeping the Wolves at Bay: Antitoxins of Prokaryotic Type II Toxin-Antitoxin Systems. *Frontiers in Molecular Biosciences* 2016; 3:9. <https://doi.org/10.3389/fmolb.2016.00009>.
- Chang HC, Chang JJ, Huang AH, Chang TC. Evaluation of a capacitance method for direct antifungal susceptibility testing of yeasts in positive blood cultures. *Journal of Clinical Microbiology* 2000; 38:971–6. <https://doi.org/10.1128/jcm.38.3.971-976.2000>.
- Chatnaparat T, Li Z, Korban SS, Zhao Y. The Stringent Response Mediated by (p)ppGpp Is Required for Virulence of *Pseudomonas syringae* pv. *tomato* and Its Survival on Tomato. *Molecular Plant-Microbe Interactions* 2015; 28:776–89. <https://doi.org/10.1094/MPMI-11-14-0378-R>.
- Chen CR, Malik M, Snyder M, Drlica K. DNA gyrase and topoisomerase IV on the bacterial chromosome: quinolone-induced DNA cleavage. *J Mol Biol* 1996; 258:627–37. <https://doi.org/10.1006/JMBI.1996.0274>.
- Chen YT, Shu HY, Li LH, Liao TL, Wu KM, Shiau YR, et al. Complete nucleotide sequence of pK245, a 98-kilobase plasmid conferring quinolone resistance and

extended-spectrum-beta-lactamase activity in a clinical *Klebsiella pneumoniae* isolate. *Antimicrob Agents Chemother* 2006; 50:3861–6.

<https://doi.org/10.1128/AAC.00456-06>.

- Cherny I, Gazit E. The YefM antitoxin defines a family of natively unfolded proteins: Implications as a novel antibacterial target. *Journal of Biological Chemistry* 2004; 279:8252–61. <https://doi.org/10.1074/jbc.M308263200>.
- Cheverton AM, Gollan B, Przydacz M, Wong CT, Mylona A, Hare SA, et al. A *Salmonella* Toxin Promotes Persister Formation through Acetylation of tRNA. *Molecular Cell* 2016; 63:86–96. <https://doi.org/10.1016/j.molcel.2016.05.002>.
- Choi JS, Kim W, Suk S, Park H, Bak G, Yoon J, et al. The small RNA, SdsR, acts as a novel type of toxin in *Escherichia coli*. *RNA Biology* 2018; 15:1319–35. <https://doi.org/10.1080/15476286.2018.1532252>.
- Christensen SK, Gerdes K. Delayed-relaxed response explained by hyperactivation of RelE. *Molecular Microbiology* 2004; 53:587–97. <https://doi.org/10.1111/J.1365-2958.2004.04127.X>.
- Christensen SK, Mikkelsen M, Pedersen K, Gerdes K. RelE, a global inhibitor of translation, is activated during nutritional stress. *Proceedings of the National Academy of Sciences* 2001; 98:14328–33. <https://doi.org/10.1073/PNAS.251327898>.
- Clark WM, Lubs HA. The Differentiation of Bacteria of the Colonaerogenes Family by the Use of Indicators. *The Journal of Infectious Diseases* 1915; 17:160–73. <https://doi.org/10.1093/INFDIS/17.1.160>.
- CLSI. Performance Standards for Antimicrobial Susceptibility Testing. vol. CLSI supplement M100. 30th ed. Wayne, Pennsylvania: Clinical and Laboratory Standards Institute; 2020.

- Conesa A, Götz S, García-Gómez JM, Terol J, Talón M, Robles M. Blast2GO: A universal tool for annotation, visualization and analysis in functional genomics research. *Bioinformatics* 2005; 21:3674–6.
<https://doi.org/10.1093/bioinformatics/bti610>.
- Conesa A, Götz S, García-Gómez JM, Terol J, Talón M, Robles M. Blast2GO: A universal tool for annotation, visualization and analysis in functional genomics research. *Bioinformatics* 2005; 21:3674–6.
<https://doi.org/10.1093/bioinformatics/bti610>.
- Conlon BP, Rowe SE, Gandt AB, Nuxoll AS, Donegan NP, Zalis EA, et al. Persister formation in *Staphylococcus aureus* is associated with ATP depletion. *Nature Microbiology* 2016; 1:16051. <https://doi.org/10.1038/nmicrobiol.2016.51>.
- Correia S, Poeta P, Hébraud M, Capelo JL, Igrejas G. Mechanisms of quinolone action and resistance: where do we stand? *Journal of Medical Microbiology* 2017; 66:551–9. <https://doi.org/10.1099/jmm.0.000475>.
- Cossart P. Antibiotic Resistance. *The New Microbiology* 2018:29–38.
<https://doi.org/https://doi.org/10.1128/9781683670117.ch5>.
- Crumplin GC, Smith JT. Nalidixic Acid: an Antibacterial Paradox. *Antimicrobial Agents and Chemotherapy* 1975; 8:251. <https://doi.org/10.1128/AAC.8.3.251>.
- D'Costa VM, King CE, Kalan L, Morar M, Sung WWL, Schwarz C, et al. Antibiotic resistance is ancient. *Nature* 2011; 477:457–61. <https://doi.org/10.1038/nature10388>.
- Dalebroux ZD, Swanson MS. PpGpp: Magic beyond RNA polymerase. *Nature Reviews Microbiology* 2012; 10:203–12. <https://doi.org/10.1038/nrmicro2720>.
- Day T. Interpreting phenotypic antibiotic tolerance and persister cells as evolution via epigenetic inheritance. *Molecular Ecology* 2016; 25:1869–82.
<https://doi.org/10.1111/mec.13603>.

- de Groote VN, Verstraeten N, Fauvart M, Kint CI, Verbeeck AM, Beullens S, et al. Novel persistence genes in *Pseudomonas aeruginosa* identified by high-throughput screening. *FEMS Microbiology Letters* 2009; 297:73–9.
<https://doi.org/10.1111/j.1574-6968.2009.01657.x>.
- de Jong IG, Haccou P, Kuipers OP. Bet hedging or not? A guide to proper classification of microbial survival strategies. *Bioessays* 2011; 33:215–23.
<https://doi.org/10.1002/bies.201000127>.
- de Oliveira DMP, Forde BM, Kidd TJ, Harris PNA, Schembri MA, Beatson SA, et al. Antimicrobial Resistance in ESKAPE Pathogens. *Clinical Microbiology Reviews* 2020; 33. <https://doi.org/10.1128/CMR.00181-19>.
- Debbia EA, Roveta S, Schito AM, Gualco L, Marchese A. Antibiotic Persistence: The Role of Spontaneous DNA Repair Response. *Microbial Drug Resistance* 2001; 7:335–42. <https://doi.org/10.1089/10766290152773347>.
- Deltcheva E, Chylinski K, Sharma CM, Gonzales K, Chao Y, Pirzada ZA, et al. CRISPR RNA maturation by trans-encoded small RNA and host factor RNase III. *Nature* 2011; 471:602–7. <https://doi.org/10.1038/NATURE09886>.
- Dheda K, Huggett JF, Bustin SA, Johnson MA, Rook G, Zumla A. Validation of housekeeping genes for normalizing RNA expression in real-time PCR. *Biotechniques* 2004; 37:112 to 119.
- Dolejska M, Brhelova E, Dobiasova H, Krivdova J, Jurankova J, Sevcikova A, et al. Dissemination of IncFII(K)-type plasmids in multiresistant CTX-M-15-producing Enterobacteriaceae isolates from children in hospital paediatric oncology wards. *Int J Antimicrob Agents* 2012; 40:510–5.
<https://doi.org/10.1016/J.IJANTIMICAG.2012.07.016>.

- Dörr T, Lewis K, Vulić M. SOS Response Induces Persistence to Fluoroquinolones in *Escherichia coli*. PLoS Genetics 2009; 5:e1000760.
<https://doi.org/10.1371/journal.pgen.1000760>.
- Dörr T, Vulić M, Lewis K. Ciprofloxacin causes persister formation by inducing the TisB toxin in *Escherichia coli*. PLoS Biol 2010; 8:e1000317.
<https://doi.org/10.1371/journal.pbio.1000317>.
- Downes FP, Ito K. Compendium of methods for the microbiological examination of foods. 4th ed. Washington (D.C.): American public health association; 2001.
- Drieux L, Decré D, Frangeul L, Arlet G, Jarlier V, Sougakoff W. Complete nucleotide sequence of the large conjugative pTC2 multireplicon plasmid encoding the VIM-1 metallo- β -lactamase. J Antimicrob Chemother 2013; 68:97–100.
<https://doi.org/10.1093/JAC/DKS367>.
- Drlica K, Xu C, Wang JY, Burger RM, Malik M. Fluoroquinolone action in mycobacteria: similarity with effects in *Escherichia coli* and detection by cell lysate viscosity. Antimicrob Agents Chemother 1996; 40:1594–9.
<https://doi.org/10.1128/AAC.40.7.1594>.
- Dubois V, Poirel L, Arpin C, Coulange L, Bebear C, Nordmann P, et al. SHV-49, a Novel Inhibitor-Resistant β -Lactamase in a Clinical Isolate of *Klebsiella pneumoniae*. Antimicrobial Agents and Chemotherapy 2004; 48:4466.
<https://doi.org/10.1128/AAC.48.11.4466-4469.2004>.
- Dubois V, Poirel L, Demarthe F, Arpin C, Coulange L, Minarini LAR, et al. Molecular and biochemical characterization of SHV-56, a novel inhibitor-resistant beta-lactamase from *Klebsiella pneumoniae*. Antimicrob Agents Chemother 2008; 52:3792–4. <https://doi.org/10.1128/AAC.00387-08>.

- Duvaud S, Gabella C, Lisacek F, Stockinger H, Ioannidis V, Durinx C. Expasy, the Swiss Bioinformatics Resource Portal, as designed by its users. *Nucleic Acids Research* 2021. <https://doi.org/10.1093/nar/gkab225>.
- Ehmann DE, Jahić H, Ross PL, Gu R-F, Hu J, Durand-Réville TF, et al. Kinetics of Avibactam Inhibition against Class A, C, and D β -Lactamases. *Journal of Biological Chemistry* 2013; 288:27960–71. <https://doi.org/10.1074/jbc.M113.485979>.
- Eldar A, Elowitz MB. Functional roles for noise in genetic circuits. *Nature* 2010; 467:167–73. <https://doi.org/10.1038/nature09326>.
- Elowitz MB, Levine AJ, Siggia ED, Swain PS. Stochastic gene expression in a single cell. *Science* 2002; 297:1183–6. <https://doi.org/10.1126/science.1070919>.
- Ewing WH. Edwards and Ewing’s identification of Enterobacteriaceae. *Edwards and Ewing’s Identification of Enterobacteriaceae* 1986.
- Farzand R, Rajakumar K, Zamudio R, Oggioni MR, Barer MR, O’Hare HM. ICEKp2: description of an integrative and conjugative element in *Klebsiella pneumoniae*, co-occurring and interacting with ICEKp1. *Scientific Reports* 2019 9:1 2019; 9:1–11. <https://doi.org/10.1038/s41598-019-50456-x>.
- Feng Y, Zou S, Chen H, Yu Y, Ruan Z. BacWGSTdb 2.0: a one-stop repository for bacterial whole-genome sequence typing and source tracking. *Nucleic Acids Research* 2021; 49:D644–50. <https://doi.org/10.1093/NAR/GKAA821>.
- Fineran PC, Blower TR, Foulds IJ, Humphreys DP, Lilley KS, Salmond GPC. The phage abortive infection system, ToxIN, functions as a protein–RNA toxin–antitoxin pair. *Proceedings of the National Academy of Sciences* 2009; 106:894 LP – 899. <https://doi.org/10.1073/pnas.0808832106>.

- Fleming A. On the Antibacterial Action of Cultures of a *Penicillium*, with Special Reference to their Use in the Isolation of *B. influenzae*. *Br J Exp Pathol* 1929; 10:226–36.
- Flores-Kim J, Darwin AJ. The Phage Shock Protein Response. *Annual Review of Microbiology* 2016; 70:83–101. <https://doi.org/10.1146/annurev-micro-102215-095359>.
- Florindo C, Ferreira R, Borges V, Spellerberg B, Gomes JP, Borrego MJ. Selection of reference genes for real-time expression studies in *Streptococcus agalactiae*. *J Microbiol Methods* 2012; 90:220–7. <https://doi.org/10.1016/j.mimet.2012.05.011>.
- Frasson I, Lavezzo E, Franchin E, Toppo S, Barzon L, Cavallaro A, et al. Antimicrobial treatment and containment measures for an extremely drug-resistant *Klebsiella pneumoniae* ST101 isolate carrying pKPN101-IT, a novel fully sequenced bla(KPC-2) plasmid. *J Clin Microbiol* 2012; 50:3768–72. <https://doi.org/10.1128/JCM.01892-12>.
- Fridman O, Goldberg A, Ronin I, Shoresh N, Balaban NQ. Optimization of lag time underlies antibiotic tolerance in evolved bacterial populations. *Nature* 2014; 513:418–21. <https://doi.org/10.1038/nature13469>.
- Fung DKC, Chan EWC, Chin ML, Chan RCY. Delineation of a bacterial starvation stress response network which can mediate antibiotic tolerance development. *Antimicrob Agents Chemother* 2010; 54:1082–93. <https://doi.org/10.1128/AAC.01218-09>.
- Galletto R, Kowalczykowski SC. RecA. *Current Biology* 2007; 17:R395–7. <https://doi.org/https://doi.org/10.1016/j.cub.2007.03.009>.
- García-Laviña CX, Castro-Sowinski S, Ramón A. Reference genes for real-time RT-PCR expression studies in an Antarctic *Pseudomonas* exposed to different

- temperature conditions. *Extremophiles* 2019. <https://doi.org/10.1007/s00792-019-01109-4>.
- Gefen O, Chekol B, Strahilevitz J, Balaban NQ. TDtest: Easy detection of bacterial tolerance and persistence in clinical isolates by a modified disk-diffusion assay. *Scientific Reports* 2017; 7:1–9. <https://doi.org/10.1038/srep41284>.
 - Gerdes K, Maisonneuve E. Bacterial Persistence and Toxin-Antitoxin Loci. *Annual Review of Microbiology* 2012; 66:103–23. <https://doi.org/10.1146/annurev-micro-092611-150159>.
 - Gerdes K, Rasmussen PB, Molin S. Unique type of plasmid maintenance function: postsegregational killing of plasmid-free cells. *Proceedings of the National Academy of Sciences* 1986; 83:3116 LP – 3120. <https://doi.org/10.1073/pnas.83.10.3116>.
 - Germain E, Roghanian M, Gerdes K, Maisonneuve E. Stochastic induction of persister cells by HipA through (p)ppGpp-mediated activation of mRNA endonucleases. *Proc Natl Acad Sci U S A* 2015; 112:5171–6. <https://doi.org/10.1073/pnas.1423536112>.
 - Gibson RL, Burns JL, Ramsey BW. Pathophysiology and management of pulmonary infections in cystic fibrosis. *Am J Respir Crit Care Med* 2003; 168:918–51. <https://doi.org/10.1164/rccm.200304-505SO>.
 - Gollan B, Grabe G, Michaux C, Helaine S. Bacterial persisters and infection: Past, present, and progressing. *Annual Review of Microbiology* 2019; 73:359–85. <https://doi.org/10.1146/annurev-micro-020518-115650>.
 - Gomes AÉI, Stuchi LP, Siqueira NMG, Henrique JB, Vicentini R, Ribeiro ML, et al. Selection and validation of reference genes for gene expression studies in *Klebsiella pneumoniae* using Reverse Transcription Quantitative real-time PCR. *Scientific Reports* 2018; 8:1–14. <https://doi.org/10.1038/s41598-018-27420-2>.

- Gomez JE, McKinney JD. M. tuberculosis persistence, latency, and drug tolerance. *Tuberculosis (Edinb)* 2004; 84:29–44. <https://doi.org/10.1016/j.tube.2003.08.003>.
- Gonçalves FDA, de Carvalho CCCR. Phenotypic modifications in *Staphylococcus aureus* cells exposed to high concentrations of vancomycin and teicoplanin. *Frontiers in Microbiology* 2016; 7:13. <https://doi.org/10.3389/FMICB.2016.00013/BIBTEX>.
- Goneau LW, Yeoh NS, MacDonald KW, Cadieux PA, Burton JP, Razvi H, et al. Selective Target Inactivation Rather than Global Metabolic Dormancy Causes Antibiotic Tolerance in Uropathogens. *Antimicrobial Agents and Chemotherapy* 2014; 58:2089 LP – 2097. <https://doi.org/10.1128/AAC.02552-13>.
- Grant SS, Kaufmann BB, Chand NS, Haseley N, Hung DT. Eradication of bacterial persisters with antibiotic-generated hydroxyl radicals. *Proceedings of the National Academy of Sciences* 2012; 109:12147–52. <https://doi.org/10.1073/pnas.1203735109>.
- Greenwood D. Mucopeptide hydrolases and bacterial " persisters ". *The Lancet* 1972; 300:465–6. [https://doi.org/https://doi.org/10.1016/S0140-6736\(72\)91858-2](https://doi.org/https://doi.org/10.1016/S0140-6736(72)91858-2).
- Gupta P, Sharma R, Vyas A, Tak A, Gupta P, Sharma R, et al. Comparative evaluation of broth microdilution with E-test, Vitek 2, and disk diffusion for susceptibility testing of colistin on Gram-negative bacteria. *Indian Journal of Medical Sciences* 2021; 73:93–8. https://doi.org/10.25259/IJMS_15_2020.
- Gurevich A, Saveliev V, Vyahhi N, Tesler G. QUASt: Quality assessment tool for genome assemblies. *Bioinformatics* 2013; 29:1072–5. <https://doi.org/10.1093/bioinformatics/btt086>.

- Gurnev PA, Ortenberg R, Dörr T, Lewis K, Bezrukov SM. Persister-promoting bacterial toxin TisB produces anion-selective pores in planar lipid bilayers. *FEBS Letters* 2012; 586:2529–34. <https://doi.org/10.1016/j.febslet.2012.06.021>.
- Hahn J, Tanner AW, Carabetta VJ, Cristea IM, Dubnau D. ComGA-RelA interaction and persistence in the *Bacillus subtilis* K-state. *Mol Microbiol* 2015; 97:454–71. <https://doi.org/10.1111/mmi.13040>.
- Hansen S, Lewis K, Vulić M. Role of global regulators and nucleotide metabolism in antibiotic tolerance in *Escherichia coli*. *Antimicrob Agents Chemother* 2008; 52:2718–26. <https://doi.org/10.1128/AAC.00144-08>.
- Hansen S, Vulić M, Min J, Yen T-J, Schumacher MA, Brennan RG, et al. Correction: Regulation of the *Escherichia coli* HipBA Toxin-Antitoxin System by Proteolysis. *PLOS ONE* 2012; 7:10.1371/annotation/e608601c-eadd-4c11-adb2-7b605ab.
- Hansen S, Vulić M, Min J, Yen T-J, Schumacher MA, Brennan RG, et al. Regulation of the *Escherichia coli* HipBA Toxin-Antitoxin System by Proteolysis. *PLoS ONE* 2012; 7:e39185. <https://doi.org/10.1371/journal.pone.0039185>.
- Harms A, Fino C, Sørensen MA, Semsey S, Gerdes K. Prophages and growth dynamics confound experimental results with antibiotic-tolerant persister cells. *MBio* 2017; 8:1–18. <https://doi.org/10.1128/mBio.01964-17>.
- Harms A, Fino C, Sørensen MA, Semsey S, Gerdes K. Prophages and growth dynamics confound experimental results with antibiotic-tolerant persister cells. *MBio* 2017; 8:1–18. <https://doi.org/10.1128/mBio.01964-17>.
- Harms A, Maisonneuve E, Gerdes K. Mechanisms of bacterial persistence during stress and antibiotic exposure. *Science (1979)* 2016; 354:aaf4268. <https://doi.org/10.1126/science.aaf4268>.

- Harrison JJ, Wade WD, Akierman S, Vacchi-Suzzi C, Stremick CA, Turner RJ, et al. The Chromosomal Toxin Gene *yafQ* Is a Determinant of Multidrug Tolerance for *Escherichia coli* Growing in a Biofilm. *Antimicrobial Agents and Chemotherapy* 2009; 53:2253 LP – 2258. <https://doi.org/10.1128/AAC.00043-09>.
- Hauryliuk V, Atkinson GC, Murakami KS, Tenson T, Gerdes K. Recent functional insights into the role of (p)ppGpp in bacterial physiology. *Nature Reviews Microbiology* 2015; 13:298–309. <https://doi.org/10.1038/nrmicro3448>.
- Hayes F, Kedzierska B. Regulating Toxin-Antitoxin Expression: Controlled Detonation of Intracellular Molecular Timebombs. *Toxins* 2014, Vol 6, Pages 337-358 2014; 6:337–58. <https://doi.org/10.3390/TOXINS6010337>.
- Helaine S, Cheverton AM, Watson KG, Faure LM, Matthews S a, Holden DW. Internalization of *Salmonella* by macrophages induces formation of nonreplicating persisters. *Science (1979)* 2014; 343:204–8. <https://doi.org/10.1126/science.1244705>.
- Hengge R. The General Stress Response in Gram-Negative Bacteria. *Bacterial Stress Responses*, John Wiley & Sons, Ltd; 2010, p. 251–89. <https://doi.org/https://doi.org/10.1128/9781555816841.ch15>.
- Henrikus SS, van Oijen AM, Robinson A. Specialised DNA polymerases in *Escherichia coli*: roles within multiple pathways. *Current Genetics* 2018; 64:1189–96. <https://doi.org/10.1007/s00294-018-0840-x>.
- Hingley-Wilson SM, Ma N, Hu Y, Casey R, Bramming A, Curry RJ, et al. Loss of phenotypic inheritance associated with *ydcI* mutation leads to increased frequency of small, slow persisters in *Escherichia coli*. *Proceedings of the National Academy of Sciences* 2020; 117:4152 LP – 4157. <https://doi.org/10.1073/pnas.1914741117>.

- Hobby GL, Meyer K, Chaffee E. Activity of Penicillin in vitro. Proceedings of the Society for Experimental Biology and Medicine 1942a; 50:277–80.
<https://doi.org/10.3181/00379727-50-13772>.
- Hobby GL, Meyer K, Chaffee E. Observations on the Mechanism of Action of Penicillin. Proceedings of the Society for Experimental Biology and Medicine 1942b; 50:281–5. <https://doi.org/10.3181/00379727-50-13773>.
- Hoff G, Bertrand C, Piotrowski E, Thibessard A, Leblond P. Implication of RuvABC and RecG in homologous recombination in *Streptomyces ambofaciens*. Research in Microbiology 2017; 168:26–35.
<https://doi.org/10.1016/j.resmic.2016.07.003>.
- Hong SH, Wang X, O'Connor HF, Benedik MJ, Wood TK. Bacterial persistence increases as environmental fitness decreases. Microbial Biotechnology 2012; 5:509–22. <https://doi.org/10.1111/j.1751-7915.2011.00327.x>.
- Hossain T, Deter HS, Peters EJ, Butzin NC. Antibiotic tolerance, persistence, and resistance of the evolved minimal cell, *Mycoplasma mycoides* JCVI-Syn3B. IScience 2021; 24:102391. <https://doi.org/https://doi.org/10.1016/j.isci.2021.102391>.
- Hovingh ES, van den Broek B, Jongerius I. Hijacking complement regulatory proteins for bacterial immune evasion. Frontiers in Microbiology 2016; 7:2004.
<https://doi.org/10.3389/FMICB.2016.02004/BIBTEX>.
- Hu Y, Kwan BW, Osbourne DO, Benedik MJ, Wood TK. Toxin YafQ increases persister cell formation by reducing indole signalling. Environmental Microbiology 2015; 17:1275–85. <https://doi.org/10.1111/1462-2920.12567>.
- Huang T-W, Lam I, Chang H-Y, Tsai S-F, Palsson BØ, Charusanti P. Capsule deletion via a λ -Red knockout system perturbs biofilm formation and fimbriae

expression in *Klebsiella pneumoniae* MGH 78578. BMC Res Notes 2014; 7:13.
<https://doi.org/10.1186/1756-0500-7-13>.

- Hyatt D, Chen GL, LoCascio PF, Land ML, Larimer FW, Hauser LJ. Prodigal: Prokaryotic gene recognition and translation initiation site identification. BMC Bioinformatics 2010; 11. <https://doi.org/10.1186/1471-2105-11-119>.
- Inoue H, Nojima H, Okayama H. High efficiency transformation of *Escherichia coli* with plasmids. Gene 1990; 96:23–8. [https://doi.org/10.1016/0378-1119\(90\)90336-P](https://doi.org/10.1016/0378-1119(90)90336-P).
- Jacob TR, Laia ML, Ferro JA, Ferro MIT. Selection and validation of reference genes for gene expression studies by reverse transcription quantitative PCR in *Xanthomonas citri* subsp. *citri* during infection of *Citrus sinensis*. Biotechnology Letters 2011; 33:1177–84. <https://doi.org/10.1007/s10529-011-0552-5>.
- Jagnow J, Clegg S. *Klebsiella pneumoniae* MrkD-mediated biofilm formation on extracellular matrix- and collagen-coated surfaces. Microbiology (N Y) 2003; 149:2397–405. <https://doi.org/10.1099/MIC.0.26434-0>.
- Jesaitis AJ, Franklin MJ, Berglund D, Sasaki M, Lord CI, Bleazard JB, et al. Compromised Host Defense on *Pseudomonas aeruginosa* Biofilms: Characterization of Neutrophil and Biofilm Interactions. The Journal of Immunology 2003; 171:4329 LP – 4339. <https://doi.org/10.4049/jimmunol.171.8.4329>.
- Jinek M, Chylinski K, Fonfara I, Hauer M, Doudna JA, Charpentier E. A programmable dual-RNA-guided DNA endonuclease in adaptive bacterial immunity. Science 2012; 337:816–21. <https://doi.org/10.1126/SCIENCE.1225829>.
- Johnson PJT, Levin BR. Pharmacodynamics, population dynamics, and the evolution of persistence in *Staphylococcus aureus*. PLoS Genet 2013; 9:e1003123. <https://doi.org/10.1371/journal.pgen.1003123>.

- Jubair M, Morris JGJ, Ali A. Survival of *Vibrio cholerae* in nutrient-poor environments is associated with a novel “persister” phenotype. PLoS One 2012; 7:e45187. <https://doi.org/10.1371/journal.pone.0045187>.
- Kaiser P, Regoes RR, Dolowschiak T, Wotzka SY, Lengefeld J, Slack E, et al. Cecum Lymph Node Dendritic Cells Harbor Slow-Growing Bacteria Phenotypically Tolerant to Antibiotic Treatment. PLOS Biology 2014; 12:e1001793.
- Kaluzna M, Kuras A, Pulawska J. Validation of reference genes for the normalization of the RT-qPCR gene expression of virulence genes of *Erwinia amylovora* in apple shoots. Scientific Reports 2017; 7:96–100. <https://doi.org/10.1038/s41598-017-02078-4>.
- Kato T, Yoshida H, Miyata T, Maki Y, Wada A, Namba K. Structure of the 100S Ribosome in the Hibernation Stage Revealed by Electron Cryomicroscopy. Structure 2010; 18:719–24. <https://doi.org/https://doi.org/10.1016/j.str.2010.02.017>.
- Keren I, Kaldalu N, Spoering A, Wang Y, Lewis K. Persister cells and tolerance to antimicrobials. FEMS Microbiology Letters 2004a; 230:13–8. [https://doi.org/10.1016/S0378-1097\(03\)00856-5](https://doi.org/10.1016/S0378-1097(03)00856-5).
- Keren I, Minami S, Rubin E, Lewis KC-3119538. Characterization and transcriptome analysis of *Mycobacterium tuberculosis* persisters. MBio 2011; 2:e00100-11 ST-Characterization and transcriptome. <https://doi.org/10.1128/mBio.00100-11.Editor>.
- Keren I, Shah D, Spoering A, Kaldalu N, Lewis K. Specialized Persister Cells and the Mechanism of Multidrug Tolerance in *Escherichia coli*. Journal of Bacteriology 2004b; 186:8172–80. <https://doi.org/10.1128/JB.186.24.8172-8180.2004>.
- Kim D, Pertea G, Trapnell C, Pimentel H, Kelley R, Salzberg SL. TopHat2: Accurate alignment of transcriptomes in the presence of insertions, deletions and

gene fusions. *Genome Biology* 2013; 14:1–13. <https://doi.org/10.1186/gb-2013-14-4-r36>.

- Kim HY, Go J, Lee KM, Oh YT, Yoon SS. Guanosine tetra- and pentaphosphate increase antibiotic tolerance by reducing reactive oxygen species production in *Vibrio cholerae*. *Journal of Biological Chemistry* 2018; 293:5679–94. <https://doi.org/10.1074/jbc.RA117.000383>.
- Kim Y, Wood TK. Toxins Hha and CspD and small RNA regulator Hfq are involved in persister cell formation through MqsR in *Escherichia coli*. *Biochemical and Biophysical Research Communications* 2010; 391:209–13. <https://doi.org/10.1016/j.bbrc.2009.11.033>.
- Kirk DG, Palonen E, Korkeala H, Lindström M. Evaluation of normalization reference genes for RT-qPCR analysis of *spo0A* and four sporulation sigma factor genes in *Clostridium botulinum* Group I strain ATCC 3502. *Anaerobe* 2014; 26:14–9. <https://doi.org/10.1016/j.anaerobe.2013.12.003>.
- Knudsen GM, Ng Y, Gram L. Survival of Bactericidal Antibiotic Treatment by a Persister Subpopulation of *Listeria monocytogenes*. *Applied and Environmental Microbiology* 2013; 79:7390–7. <https://doi.org/10.1128/AEM.02184-13>.
- Kohanski MA, Dwyer DJ, Collins JJ. How antibiotics kill bacteria: from targets to networks. *Nature Reviews Microbiology* 2010; 8:423–35. <https://doi.org/10.1038/nrmicro2333>.
- Kotte O, Volkmer B, Radzikowski JL, Heinemann M. Phenotypic bistability in *Escherichia coli*'s central carbon metabolism. *Mol Syst Biol* 2014; 10:736. <https://doi.org/10.15252/msb.20135022>.

- Krumperman PH. Multiple antibiotic resistance indexing of *Escherichia coli* to identify high-risk sources of fecal contamination of foods. *Appl Environ Microbiol* 1983; 46:165–70. <https://doi.org/10.1128/AEM.46.1.165-170.1983>.
- Kubistova L, Dvoracek L, Tkadlec J, Melter O, Licha I. Environmental Stress Affects the Formation of *Staphylococcus aureus* Persisters Tolerant to Antibiotics. *Microbial Drug Resistance* 2017; 24:547–55. <https://doi.org/10.1089/mdr.2017.0064>.
- Kulengowski B, Ribes JA, Burgess DS. Polymyxin B Etest®; compared with gold-standard broth microdilution in carbapenem-resistant Enterobacteriaceae exhibiting a wide range of polymyxin B MICs. *Clinical Microbiology and Infection* 2019; 25:92–5. <https://doi.org/10.1016/j.cmi.2018.04.008>.
- Kumar S, Stecher G, Tamura K. MEGA7: Molecular Evolutionary Genetics Analysis Version 7.0 for Bigger Datasets. *Mol Biol Evol* 2016; 33:1870–4. <https://doi.org/10.1093/molbev/msw054>.
- Kwan BW, Valenta JA, Benedik MJ, Wood TK. Arrested Protein Synthesis Increases Persister-Like Cell Formation. *Antimicrobial Agents and Chemotherapy* 2013; 57:1468–73. <https://doi.org/10.1128/AAC.02135-12>.
- Lafleur MD, Qi Q, Lewis K. Patients with Long-Term Oral Carriage Harbor High-Persister Mutants of *Candida albicans*. *Antimicrob Agents Chemother* 2010; 54:39–44. <https://doi.org/10.1128/AAC.00860-09>.
- Lahiri SD, Bradford PA, Nichols WW, Alm RA. Structural and sequence analysis of class A β -lactamases with respect to avibactam inhibition: impact of Ω -loop variations. *J Antimicrob Chemother* 2016; 71:2848–55. <https://doi.org/10.1093/JAC/DKW248>.

- Langmead B, Salzberg SL. Fast gapped-read alignment with Bowtie 2. *Nature Methods* 2012; 9:357–9. <https://doi.org/10.1038/nmeth.1923>.
- Larsen M V., Cosentino S, Rasmussen S, Friis C, Hasman H, Marvig RL, et al. Multilocus sequence typing of total-genome-sequenced bacteria. *Journal of Clinical Microbiology* 2012; 50:1355–61. <https://doi.org/10.1128/JCM.06094-11>.
- Lawn SD, Butera ST, Shinnick TM. Tuberculosis unleashed: the impact of human immunodeficiency virus infection on the host granulomatous response to *Mycobacterium tuberculosis*. *Microbes and Infection* 2002; 4:635–46. [https://doi.org/https://doi.org/10.1016/S1286-4579\(02\)01582-4](https://doi.org/https://doi.org/10.1016/S1286-4579(02)01582-4).
- Lechner S, Lewis K, Bertram R. *Staphylococcus aureus* persists tolerant to bactericidal antibiotics. *Journal of Molecular Microbiology and Biotechnology* 2012; 22:235–44. <https://doi.org/10.1159/000342449>.
- Leipe DD, Wolf YI, Koonin E v., Aravind L. Classification and evolution of P-loop GTPases and related ATPases. *Journal of Molecular Biology* 2002; 317:41–72. <https://doi.org/10.1006/JMBI.2001.5378>.
- Lennox ES. Transduction of linked genetic characters of the host by bacteriophage P1. *Virology* 1955; 1:190–206. [https://doi.org/10.1016/0042-6822\(55\)90016-7](https://doi.org/10.1016/0042-6822(55)90016-7).
- Leplae R, Geeraerts D, Hallez R, Guglielmini J, Drèze P, van Melderen L. Diversity of bacterial type II toxin–antitoxin systems: a comprehensive search and functional analysis of novel families. *Nucleic Acids Research* 2011; 39:5513–25. <https://doi.org/10.1093/nar/gkr131>.
- Leung V, Lévesque CM. A stress-inducible quorum-sensing peptide mediates the formation of persister cells with noninherited multidrug tolerance. *Journal of Bacteriology* 2012; 194:2265–74. <https://doi.org/10.1128/JB.06707-11>.

- Levin BR, Concepción-Acevedo J, Udekwu KI. Persistence: a copacetic and parsimonious hypothesis for the existence of non-inherited resistance to antibiotics. *Curr Opin Microbiol* 2014; 21:18–21. <https://doi.org/10.1016/j.mib.2014.06.016>.
- Levin-Reisman I, Ronin I, Gefen O, Braniss I, Shores N, Balaban NQ. Antibiotic tolerance facilitates the evolution of resistance. *Science* 2017; 355:826–30. <https://doi.org/10.1126/science.aaj2191>.
- Levine M. Differentiation of *B. coli* and *B. aerogenes* on a Simplified Eosin-Methylene Blue Agar. *The Journal of Infectious Diseases* 1918; 23:43–7. <https://doi.org/10.1086/infdis/23.1.43>.
- Lewin CS, Howard BMA, Ratcliffe NT, Smith JT. 4-quinolones and the SOS response. *J Med Microbiol* 1989; 29:139–44. <https://doi.org/10.1099/00222615-29-2-139>.
- Lewin CS, Morrissey I, Smith JT. The mode of action of quinolones: The paradox in activity of low and high concentrations and activity in the anaerobic environment. *European Journal of Clinical Microbiology & Infectious Diseases* 1991; 10:240–8. <https://doi.org/10.1007/BF01966996>.
- Lewis K. Persister cells, dormancy and infectious disease. *Nature Reviews Microbiology* 2007; 5:48–56. <https://doi.org/10.1038/nrmicro1557>.
- Lewis K. Persister cells. *Annu Rev Microbiol* 2010; 64:357–72. <https://doi.org/10.1146/annurev.micro.112408.134306>.
- Li B, Dewey CN. RSEM: accurate transcript quantification from RNA-Seq data with or without a reference genome. *BMC Bioinformatics* 2011; 12:323. <https://doi.org/10.1186/1471-2105-12-323>.

- Li B, Zhao Y, Liu C, Chen Z, Zhou D. Molecular pathogenesis of *Klebsiella pneumoniae*. *Future Microbiology* 2014; 9:1071–81.
<https://doi.org/10.2217/fmb.14.48>.
- Li H, Handsaker B, Wysoker A, Fennell T, Ruan J, Homer N, et al. The Sequence Alignment/Map format and SAMtools. *Bioinformatics* 2009; 25:2078–9.
<https://doi.org/10.1093/bioinformatics/btp352>.
- Li P, Seneviratne CJ, Alpi E, Vizcaino JA, Jin L. Delicate Metabolic Control and Coordinated Stress Response Critically Determine Antifungal Tolerance of *Candida albicans* Biofilm Persisters. *Antimicrobial Agents and Chemotherapy* 2015; 59:6101–12. <https://doi.org/10.1128/AAC.00543-15>.
- Li Y, Zhang L, Zhou Y, Zhang Z, Zhang X. Survival of bactericidal antibiotic treatment by tolerant persister cells of *Klebsiella pneumoniae*. *Journal of Medical Microbiology* 2018; 67:273–81. <https://doi.org/10.1099/jmm.0.000680>.
- Liebens V, Defraigne V, van der Leyden A, de Groote VN, Fierro C, Beullens S, et al. A putative de-N-acetylase of the PIG-L superfamily affects fluoroquinolone tolerance in *Pseudomonas aeruginosa*. *Pathog Dis* 2014; 71:39–54.
<https://doi.org/10.1111/2049-632X.12174>.
- Liu J, Tan Y, Yang X, Chen X, Li F. Evaluation of *Clostridium ljungdahlii* DSM 13528 reference genes in gene expression studies by qRT-PCR. *J Biosci Bioeng* 2013; 116:460–4. <https://doi.org/10.1016/j.jbiosc.2013.04.011>.
- Liu S, Wu N, Zhang S, Yuan Y, Zhang W, Zhang Y. Variable persister gene interactions with (p)ppGpp for persister formation in *Escherichia coli*. *Frontiers in Microbiology* 2017; 8:1–14. <https://doi.org/10.3389/fmicb.2017.01795>.

- Liu S, Wu N, Zhang S, Yuan Y, Zhang W, Zhang Y. Variable persister gene interactions with (p)ppGpp for persister formation in *Escherichia coli*. *Frontiers in Microbiology* 2017; 8:1–14. <https://doi.org/10.3389/fmicb.2017.01795>.
- Livak KJ, Schmittgen TD. Analysis of relative gene expression data using real-time quantitative PCR and. *Methods* 2001; 25:402–8. <https://doi.org/10.1006/meth.2001.1262>.
- Løvdal T, Saha A. Reference Gene Selection in *Carnobacterium maltaromaticum*, *Lactobacillus curvatus*, and *Listeria innocua* Subjected to Temperature and Salt Stress. *Mol Biotechnol* 2014; 56:210–22. <https://doi.org/10.1007/s12033-013-9697-x>.
- Lovett ST. The DNA Damage Response. *Bacterial Stress Responses*, Second Edition, American Society of Microbiology; 2011, p. 205–28.
- MacConkey A. Lactose-Fermenting Bacteria in Faeces. *Journal of Hygiene* 1905; 5:333–79. <https://doi.org/10.1017/S002217240000259X>.
- Magiorakos AP, Srinivasan A, Carey RB, Carmeli Y, Falagas ME, Giske CG, et al. Multidrug-resistant, extensively drug-resistant and pandrug-resistant bacteria: An international expert proposal for interim standard definitions for acquired resistance. *Clinical Microbiology and Infection* 2012; 18:268–81. <https://doi.org/10.1111/j.1469-0691.2011.03570.x>.
- Maisonneuve E, Castro-camargo M, Gerdes K. (p)ppGpp Controls Bacterial Persistence by Stochastic Induction of Toxin-Antitoxin Activity. *Cell* 2013; 154:1140–50. <https://doi.org/10.1016/j.cell.2013.07.048>.
- Maisonneuve E, Gerdes K. Molecular Mechanisms Underlying Bacterial Persisters. *Cell* 2014; 157:539–48. <https://doi.org/10.1016/J.CELL.2014.02.050>.

- Malik M, Capecchi J, Drlica K. Lon Protease Is Essential for Paradoxical Survival of *Escherichia coli* Exposed to High Concentrations of Quinolone. *Antimicrobial Agents and Chemotherapy* 2009; 53:3103. <https://doi.org/10.1128/AAC.00019-09>.
- Mancini S, Marchesi M, Imkamp F, Wagner K, Keller PM, Quiblier C, et al. Population-based inference of aminoglycoside resistance mechanisms in *Escherichia coli*. *EBioMedicine* 2019; 46:184–92. <https://doi.org/10.1016/J.EBIOM.2019.07.020>.
- Mangold S, Valdés J, Holmes D, Dopson M. Sulfur Metabolism in the Extreme Acidophile *Acidithiobacillus caldus*. *Frontiers in Microbiology* 2011; 2:17. <https://doi.org/10.3389/fmicb.2011.00017>.
- Marimon O, Teixeira JMC, Cordeiro TN, Soo VWC, Wood TL, Mayzel M, et al. An oxygen-sensitive toxin–antitoxin system. *Nature Communications* 2016; 7:13634. <https://doi.org/10.1038/ncomms13634>.
- Martínez-Martínez L, Pascual A, Jacoby GA. Quinolone resistance from a transferable plasmid. *The Lancet* 1998; 351:797–9. [https://doi.org/https://doi.org/10.1016/S0140-6736\(97\)07322-4](https://doi.org/https://doi.org/10.1016/S0140-6736(97)07322-4).
- Martins PMM, Wood TK, de Souza AA. Persister cells form in the plant pathogen *Xanthomonas citri* subsp. *citri* under different stress conditions. *Microorganisms* 2021; 9:1–15. <https://doi.org/10.3390/microorganisms9020384>.
- Masuda H, Tan Q, Awano N, Wu K-P, Inouye M. YeeU enhances the bundling of cytoskeletal polymers of MreB and FtsZ, antagonizing the CbtA (YeeV) toxicity in *Escherichia coli*. *Molecular Microbiology* 2012; 84:979–89. <https://doi.org/10.1111/j.1365-2958.2012.08068.x>.
- Mayrhofer S, Domig KJ, Mair C, Zitz U, Huys G, Kneifel W. Comparison of broth microdilution, Etest, and agar disk diffusion methods for antimicrobial susceptibility

- testing of *Lactobacillus acidophilus* group members. *Applied and Environmental Microbiology* 2008; 74:3745–8. <https://doi.org/10.1128/AEM.02849-07/ASSET/5A10CCE3-9966-4CE5-92C6-2F6120034205/ASSETS/GRAPHIC/ZAM0120889270001.JPEG>.
- McArthur AG, Waglechner N, Nizam F, Yan A, Azad MA, Baylay AJ, et al. The comprehensive antibiotic resistance database. *Antimicrob Agents Chemother* 2013; 57:3348–57. <https://doi.org/10.1128/AAC.00419-13>.
 - McCombie WR, McPherson JD, Mardis ER. Next-Generation Sequencing Technologies. *Cold Spring Harbor Perspectives in Medicine* 2019; 9:a036798. <https://doi.org/10.1101/CSHPERSPECT.A036798>.
 - McDermott W. Microbial persistence. *Yale J Biol Med* 1958; 30:257–91.
 - McKay SL, Portnoy DA. Ribosome hibernation facilitates tolerance of stationary-phase bacteria to aminoglycosides. *Antimicrob Agents Chemother* 2015; 59:6992–9. <https://doi.org/10.1128/AAC.01532-15>.
 - McNamara PJ, Proctor RA. *Staphylococcus aureus* small colony variants, electron transport and persistent infections. *Int J Antimicrob Agents* 2000; 14:117–22. [https://doi.org/10.1016/s0924-8579\(99\)00170-3](https://doi.org/10.1016/s0924-8579(99)00170-3).
 - Mechold U, Potrykus K, Murphy H, Murakami KS, Cashel M. Differential regulation by ppGpp versus pppGpp in *Escherichia coli*. *Nucleic Acids Res* 2013; 41:6175–89. <https://doi.org/10.1093/nar/gkt302>.
 - Megaw J, Gilmore BF. Archaeal persisters: Persister cell formation as a stress response in *Haloflexax volcanii*. *Frontiers in Microbiology* 2017; 8:1–10. <https://doi.org/10.3389/fmicb.2017.01589>.
 - Mendonça N, Ferreira E, Louro D, Caniça M. Molecular epidemiology and antimicrobial susceptibility of extended- and broad-spectrum beta-lactamase-

producing *Klebsiella pneumoniae* isolated in Portugal. *Int J Antimicrob Agents* 2009; 34:29–37. <https://doi.org/10.1016/J.IJANTIMICAG.2008.11.014>.

- Michiels JE, van den Bergh B, Verstraeten N, Fauvart M, Michiels J. In vitro emergence of high persistence upon periodic aminoglycoside challenge in the ESKAPE pathogens. *Antimicrobial Agents and Chemotherapy* 2016a; 60:4630–7. <https://doi.org/10.1128/AAC.00757-16>.
- Michiels JE, van den Bergh B, Verstraeten N, Michiels J. Molecular mechanisms and clinical implications of bacterial persistence. *Drug Resistance Updates* 2016b; 29:76–89. <https://doi.org/10.1016/j.drug.2016.10.002>.
- Miller JH. *Experiments in Molecular Genetics*. The University of Chicago Press; 1972. <https://doi.org/10.1086/408025>.
- Minarini LAR, Darini ALC. Mutations in the quinolone resistance-determining regions of *gyrA* and *parC* in Enterobacteriaceae isolates from Brazil. *Brazilian Journal of Microbiology* 2012; 43:1309–14.
- Mitchell G, Chen C, Portnoy DA. Strategies Used by Bacteria to Grow in Macrophages. *Microbiology Spectrum* 2016; 4. <https://doi.org/10.1128/microbiolspec.MCHD-0012-2015>.
- Möker N, Dean CR, Tao J. *Pseudomonas aeruginosa* increases formation of multidrug-tolerant persister cells in response to quorum-sensing signaling molecules. *Journal of Bacteriology* 2010; 192:1946–55. <https://doi.org/10.1128/JB.01231-09>.
- Monack DM, Mueller A, Falkow S. Persistent bacterial infections: the interface of the pathogen and the host immune system. *Nature Reviews Microbiology* 2004; 2:747–65. <https://doi.org/10.1038/nrmicro955>.

- Morrison L, Zembower TR. Antimicrobial Resistance. *Gastrointestinal Endoscopy Clinics of North America* 2020; 30:619–35.
<https://doi.org/10.1016/j.giec.2020.06.004>.
- Mouton JM, Helaine S, Holden DW, Sampson SL. Elucidating population-wide mycobacterial replication dynamics at the single-cell level. *Microbiology (Reading)* 2016; 162:966–78. <https://doi.org/10.1099/mic.0.000288>.
- Moyed HS, Bertrand KP. *hipA*, a newly recognized gene of *Escherichia coli* K-12 that affects frequency of persistence after inhibition of murein synthesis. *Journal of Bacteriology* 1983; 155:768–75. <https://doi.org/https://doi.org/10.1128/jb.155.2.768-775.1983>.
- Mueller JH, Hinton J. A Protein-Free Medium for Primary Isolation of the Gonococcus and Meningococcus. *Proceedings of the Society for Experimental Biology and Medicine* 1941; 48:330–3. <https://doi.org/10.3181/00379727-48-13311>.
- Mukherjee D, Zou H, Liu S, Beuerman R, Dick T. Membrane-targeting AM-0016 kills mycobacterial persisters and shows low propensity for resistance development. *Future Microbiol* 2016; 11:643–50. <https://doi.org/10.2217/fmb-2015-0015>.
- Mulcahy LR, Burns JL, Lory S, Lewis K. Emergence of *Pseudomonas aeruginosa* strains producing high levels of persister cells in patients with cystic fibrosis. *J Bacteriol* 2010; 192:6191–9. <https://doi.org/JB.01651-09> [pii]r10.1128/JB.01651-09.
- Munoz-Price LS, Poirel L, Bonomo RA, Schwaber MJ, Daikos GL, Cormican M, et al. Clinical epidemiology of the global expansion of *Klebsiella pneumoniae* carbapenemases. *The Lancet Infectious Diseases* 2013; 13:785–96.
[https://doi.org/10.1016/S1473-3099\(13\)70190-7](https://doi.org/10.1016/S1473-3099(13)70190-7).

- Murakami K, Ono T, Viducic D, Kayama S, Mori M, Hirota K, et al. Role for *rpoS* gene of *Pseudomonas aeruginosa* in antibiotic tolerance. *FEMS Microbiology Letters* 2005; 242:161–7. <https://doi.org/10.1016/j.femsle.2004.11.005>.
- Murawski AM, Brynildsen MP. Ploidy is an important determinant of fluoroquinolone persister survival. *Current Biology* 2021; 31:2039-2050.e7. <https://doi.org/10.1016/j.cub.2021.02.040>.
- Murphy KC. λ Recombination and Recombineering. *EcoSal Plus* 2016; 7. <https://doi.org/10.1128/ECOSALPLUS.ESP-0011-2015>.
- Nachnani S, Scuteri A, Newman MG, Avanesian AB, Lomeli SL. E-Test: A New Technique for Antimicrobial Susceptibility Testing for Periodontal Microorganisms. *Journal of Periodontology* 1992; 63:576–83. <https://doi.org/10.1902/jop.1992.63.7.576>.
- Nguyen D, Joshi-Datar A, Lepine F, Bauerle E, Olakanmi O, Beer K, et al. Active Starvation Responses Mediate Antibiotic Tolerance in Biofilms and Nutrient-Limited Bacteria. *Science* (1979) 2011; 334:982 LP – 986. [https://doi.org/10.1016/0024-4937\(90\)90045-3](https://doi.org/10.1016/0024-4937(90)90045-3).
- Nguyen D, Joshi-Datar A, Lepine F, Bauerle E, Olakanmi O, Beer K, et al. Active starvation responses mediate antibiotic tolerance in biofilms and nutrient-limited bacteria. *Science* 2011; 334:982–6. <https://doi.org/10.1126/SCIENCE.1211037>.
- Norris SJ. Antigenic variation with a twist – the *Borrelia* story. *Molecular Microbiology* 2006; 60:1319–22. <https://doi.org/https://doi.org/10.1111/j.1365-2958.2006.05204.x>.
- Norton JP, Mulvey MA. Toxin-Antitoxin Systems Are Important for Niche-Specific Colonization and Stress Resistance of Uropathogenic *Escherichia coli*. *PLOS Pathogens* 2012; 8:e1002954.

- Notredame C, Higgins DG, Heringa J. T-Coffee: A novel method for fast and accurate multiple sequence alignment. *J Mol Biol* 2000; 302:205–17. <https://doi.org/10.1006/jmbi.2000.4042>.
- Nurk S, Bankevich A, Antipov D, Gurevich A, Korobeynikov A, Lapidus A, et al. Assembling Genomes and Mini-metagenomes from Highly Chimeric Reads. In: Deng M, Jiang R, Sun F, Zhang X, editors. *Research in Computational Molecular Biology*, Berlin, Heidelberg: Springer Berlin Heidelberg; 2013, p. 158–70.
- Olivares AO, Baker TA, Sauer RT. Mechanistic insights into bacterial AAA+ proteases and protein-remodelling machines. *Nat Rev Microbiol* 2016; 14:33–44. <https://doi.org/10.1038/NRMICRO.2015.4>.
- Orman MA, Brynildsen MP. Dormancy is not necessary or sufficient for bacterial persistence. *Antimicrobial Agents and Chemotherapy* 2013; 57:3230–9. <https://doi.org/10.1128/AAC.00243-13>.
- Orman Mehmet A, Brynildsen MP. Establishment of a method to rapidly assay bacterial persister metabolism. *Antimicrob Agents Chemother* 2013; 57:4398–409. <https://doi.org/10.1128/AAC.00372-13>.
- Overbeek R, Olson R, Pusch GD, Olsen GJ, Davis JJ, Disz T, et al. The SEED and the Rapid Annotation of microbial genomes using Subsystems Technology (RAST). *Nucleic Acids Research* 2014; 42:D206–14.
- Overgaard M, Borch J, Jørgensen MG, Gerdes K. Messenger RNA interferase RelE controls *relBE* transcription by conditional cooperativity. *Mol Microbiol* 2008; 69:841–57. <https://doi.org/10.1111/j.1365-2958.2008.06313.x>.
- Page R, Peti W. Toxin-antitoxin systems in bacterial growth arrest and persistence. *Nature Chemical Biology* 2016; 12:208–14. <https://doi.org/10.1038/nchembio.2044>.

- Parascandola J. The History of antibiotics : a symposium, Madison, Wis.: American Institute of the History of Pharmacy; 1980.
- Paterson DL, Bonomo RA. Extended-spectrum β -lactamases: A clinical update. *Clinical Microbiology Reviews* 2005; 18:657–86.
<https://doi.org/10.1128/CMR.18.4.657-686.2005/ASSET/4492FF7A-9BA1-4099-B6C4-3ECFC546F9F1/ASSETS/GRAPHIC/ZCM0040521480001.JPEG>.
- Patole S, Rout M, Mohapatra H. Identification and validation of reference genes for reliable analysis of differential gene expression during antibiotic induced persister formation in *Klebsiella pneumoniae* using qPCR. *Journal of Microbiological Methods* 2021; 182:106165. <https://doi.org/10.1016/j.mimet.2021.106165>.
- Pedersen K, Gerdes K. Multiple *hok* genes on the chromosome of *Escherichia coli*. *Molecular Microbiology* 1999; 32:1090–102.
<https://doi.org/https://doi.org/10.1046/j.1365-2958.1999.01431.x>.
- Pfaffl MW, Tichopad A, Prgomet C, Neuvians TP. Determination of stable housekeeping genes, differentially regulated target genes and sample integrity: BestKeeper – Excel-based tool using pair-wise correlations. *Biotechnology Letters* 2004; 26:509–15. <https://doi.org/10.1023/B:BILE.0000019559.84305.47>.
- Pham TDM, Ziora ZM, Blaskovich MAT. Quinolone antibiotics. *Medchemcomm* 2019; 10:1719–39. <https://doi.org/10.1039/c9md00120d>.
- Pohlhaus JR, Kreuzer KN. Norfloxacin-induced DNA gyrase cleavage complexes block *Escherichia coli* replication forks, causing double-stranded breaks in vivo. *Molecular Microbiology* 2005; 56:1416–29. <https://doi.org/10.1111/J.1365-2958.2005.04638.X>.
- Pontes MH, Groisman EA. A Physiological Basis for Nonheritable Antibiotic Resistance. *MBio* 2020; 11:e00817-20. <https://doi.org/10.1128/mBio.00817-20>.

- Pontes MH, Yeom J, Groisman EA. Reducing Ribosome Biosynthesis Promotes Translation during Low Mg²⁺ Stress. *Molecular Cell* 2016; 64:480–92. <https://doi.org/https://doi.org/10.1016/j.molcel.2016.05.008>.
- Power AL, Barber DG, Groenhof SRM, Wagley S, Liu P, Parker DA, et al. The Application of Imaging Flow Cytometry for Characterisation and Quantification of Bacterial Phenotypes. *Frontiers in Cellular and Infection Microbiology* 2021; 11. <https://doi.org/10.3389/fcimb.2021.716592>.
- Prossliner T, Skovbo Winther K, Sørensen MA, Gerdes K. Ribosome hibernation. *Annual Review of Genetics* 2018; 52:321–48. <https://doi.org/10.1146/ANNUREV-GENET-120215-035130>.
- Pu Y, Zhao Z, Li Y, Zou J, Ma Q, Zhao Y, et al. Enhanced Efflux Activity Facilitates Drug Tolerance in Dormant Bacterial Cells. *Molecular Cell* 2016; 62:284–94. <https://doi.org/10.1016/j.molcel.2016.03.035>.
- Puspita M, Wasito EB, Alimsardjono L. Association of blood isolate’s multi antibiotic resistance-index on laboratory-confirmed bloodstream infection: A cross-sectional study. *Annals of Medicine and Surgery* 2021; 72:103086. <https://doi.org/10.1016/J.AMSU.2021.103086>.
- Que Y-A, Hazan R, Strobel B, Maura D, He J, Kesarwani M, et al. A quorum sensing small volatile molecule promotes antibiotic tolerance in bacteria. *PLoS One* 2013; 8:e80140–e80140. <https://doi.org/10.1371/journal.pone.0080140>.
- Que Y-A, Hazan R, Strobel B, Maura D, He J, Kesarwani M, et al. A quorum sensing small volatile molecule promotes antibiotic tolerance in bacteria. *PLoS One* 2013; 8:e80140–e80140. <https://doi.org/10.1371/journal.pone.0080140>.
- Queenan AM, Bush K. Carbapenemases: the Versatile β -Lactamases. *Clinical Microbiology Reviews* 2007; 20:440–58. <https://doi.org/10.1128/CMR.00001-07>.

- Radzikowski JL, Vedelaar S, Siegel D, Ortega ÁD, Schmidt A, Heinemann M. Bacterial persistence is an active σ^S stress response to metabolic flux limitation. *Mol Syst Biol* 2016; 12:882. <https://doi.org/10.15252/msb.20166998>.
- Ramakers C, Ruijter JM, Lekanne Deprez RH, Moorman AFM. Assumption-free analysis of quantitative real-time polymerase chain reaction (PCR) data. *Neuroscience Letters* 2003; 339:62–6. [https://doi.org/10.1016/S0304-3940\(02\)01423-4](https://doi.org/10.1016/S0304-3940(02)01423-4).
- Rasmussen R. Quantification on the LightCycler. In: Meuer S, Wittwer C, Nakagawara K-I, editors. *Rapid Cycle Real-Time PCR: Methods and Applications*, Berlin, Heidelberg: Springer Berlin Heidelberg; 2001, p. 21–34. https://doi.org/10.1007/978-3-642-59524-0_3.
- Rath D, Amlinger L, Hoekzema M, Devulapally PR, Lundgren M. Efficient programmable gene silencing by Cascade. *Nucleic Acids Research* 2015; 43:237–46. <https://doi.org/10.1093/nar/gku1257>.
- Redpath S, Ghazal P, Gascoigne NR. Hijacking and exploitation of IL-10 by intracellular pathogens. *Trends Microbiol* 2001; 9:86–92. [https://doi.org/10.1016/s0966-842x\(00\)01919-3](https://doi.org/10.1016/s0966-842x(00)01919-3).
- Ren H, He X, Zou X, Wang G, Li S, Wu Y. Gradual increase in antibiotic concentration affects persistence of *Klebsiella pneumoniae*. *Journal of Antimicrobial Chemotherapy* 2015; 70:dkv251. <https://doi.org/10.1093/jac/dkv251>.
- Reniere ML, Whiteley AT, Hamilton KL, John SM, Lauer P, Brennan RG, et al. Glutathione activates virulence gene expression of an intracellular pathogen. *Nature* 2015; 517:170–3. <https://doi.org/10.1038/nature14029>.

- Rice LB. Federal Funding for the Study of Antimicrobial Resistance in Nosocomial Pathogens: No ESKAPE. *The Journal of Infectious Diseases* 2008; 197:1079–81. <https://doi.org/10.1086/533452>.
- Ronneau S, Helaine S. Clarifying the Link between Toxin–Antitoxin Modules and Bacterial Persistence. *Journal of Molecular Biology* 2019; 431:3462–71. <https://doi.org/10.1016/j.jmb.2019.03.019>.
- Rosenberg A, Ene I V, Bibi M, Zakin S, Segal ES, Ziv N, et al. Antifungal tolerance is a subpopulation effect distinct from resistance and is associated with persistent candidemia. *Nature Communications* 2018; 9:2470. <https://doi.org/10.1038/s41467-018-04926-x>.
- Sambrook J, Fritsch EF, Maniatis T. *Molecular Cloning: A Laboratory Manual*. Cold Spring Harbor, NY: Cold Spring Harbor Laboratory Press; 1989.
- Sanchez-Vazquez P, Dewey CN, Kitten N, Ross W, Gourse RL. Genome-wide effects on *Escherichia coli* transcription from ppGpp binding to its two sites on RNA polymerase. *Proceedings of the National Academy of Sciences* 2019; 116:8310. <https://doi.org/10.1073/pnas.1819682116>.
- Sandt CH, Hopper JE, Hill CW. Activation of Prophage eib Genes for Immunoglobulin-Binding Proteins by Genes from the IbrAB Genetic Island of *Escherichia coli* ECOR-9. *Journal of Bacteriology* 2002; 184:3640. <https://doi.org/10.1128/JB.184.13.3640-3648.2002>.
- Sandvik EL, Fazen CH, Henry TC, Mok WWK, Brynildsen MP. Non-Monotonic Survival of *Staphylococcus aureus* with Respect to Ciprofloxacin Concentration Arises from Prophage-Dependent Killing of Persisters. *Pharmaceuticals* 2015, Vol 8, Pages 778-792 2015; 8:778–92. <https://doi.org/10.3390/PH8040778>.

- Savli H, Karadenizli A, Kolayli F, Gundes S, Ozbek U, Vahaboglu H. Expression stability of six housekeeping genes: A proposal for resistance gene quantification studies of *Pseudomonas aeruginosa* by real-time quantitative RT-PCR. *Journal of Medical Microbiology* 2003; 52:403–8. <https://doi.org/10.1099/jmm.0.05132-0>.
- Schmittgen TD, Livak KJ. Analyzing real-time PCR data by the comparative CT method. *Nature Protocols* 2008; 3:1101–8. <https://doi.org/10.1038/nprot.2008.73>.
- Schumacher MA, Balani P, Min J, Chinnam NB, Hansen S, Vulić M, et al. HipBA–promoter structures reveal the basis of heritable multidrug tolerance. *Nature* 2015; 524:59–64. <https://doi.org/10.1038/nature14662>.
- Schureck MA, Maehigashi T, Miles SJ, Marquez J, Cho SE, Erdman R, et al. Structure of the *Proteus vulgaris* HigB-(HigA)₂-HigB Toxin-Antitoxin Complex. *Journal of Biological Chemistry* 2014; 289:1060–70. <https://doi.org/10.1074/JBC.M113.512095>.
- Scott CC, Botelho RJ, Grinstein S. Phagosome Maturation: A Few Bugs in the System. *The Journal of Membrane Biology* 2003; 193:137–52. <https://doi.org/10.1007/s00232-002-2008-2>.
- Sengupta S, Siliciano RF. Targeting the Latent Reservoir for HIV-1. *Immunity* 2018; 48:872–95. <https://doi.org/10.1016/j.immuni.2018.04.030>.
- Seo MY, Seo JW, Heo SY, Baek JO, Rairakhwada D, Oh BR, et al. Elimination of by-product formation during production of 1,3-propanediol in *Klebsiella pneumoniae* by inactivation of glycerol oxidative pathway. *Appl Microbiol Biotechnol* 2009; 84:527–34. <https://doi.org/10.1007/S00253-009-1980-1>.
- Shah D, Zhang Z, Khodursky AB, Kaldalu N, Kurg K, Lewis K. Persisters: a distinct physiological state of *E. coli*. *BMC Microbiol* 2006; 6:53. <https://doi.org/10.1186/1471-2180-6-53>.

- Shan Y, Brown Gandt A, Rowe SE, Deisinger JP, Conlon BP, Lewis K. ATP-Dependent Persister Formation in *Escherichia coli*. *MBio* 2017; 8:e02267-16. <https://doi.org/10.1128/mBio.02267-16>.
- Shan Y, Lazinski D, Rowe S, Camilli A, Lewis K. Genetic basis of persister tolerance to aminoglycosides in *Escherichia coli*. *MBio* 2015; 6:e00078-15. <https://doi.org/10.1128/mBio.00078-15>.
- Shapiro J a., Nguyen VL, Chamberlain NR. Evidence for persisters in *Staphylococcus epidermidis* RP62a planktonic cultures and biofilms. *Journal of Medical Microbiology* 2011; 60:950–60. <https://doi.org/10.1099/jmm.0.026013-0>.
- Shatalin K, Shatalina E, Mironov A, Nudler E. H₂S: A Universal Defense Against Antibiotics in Bacteria. *Science (1979)* 2011; 334:986–90. <https://doi.org/10.1126/science.1209855>.
- Shaw KJ, Rather PN, Hare RS, Miller GH. Molecular genetics of aminoglycoside resistance genes and familial relationships of the aminoglycoside-modifying enzymes. *Microbiological Reviews* 1993; 57:138–63. <https://doi.org/10.1128/MR.57.1.138-163.1993>.
- Shen P, Wei Z, Jiang Y, Du X, Ji S, Yu N, et al. Novel genetic environment of the carbapenem-hydrolyzing beta-lactamase KPC-2 among Enterobacteriaceae in China. *Antimicrob Agents Chemother* 2009; 53:4333–8. <https://doi.org/10.1128/AAC.00260-09>.
- Silver N, Best S, Jiang J, Thein SL. Selection of housekeeping genes for gene expression studies in human reticulocytes using real-time PCR. *BMC Molecular Biology* 2006; 7:33. <https://doi.org/10.1186/1471-2199-7-33>.
- Simmons JS. A Culture Medium for Differentiating Organisms of Typhoid-Colon Aerogenes Groups and for Isolation of Certain Fungi With Colored Plate. *The*

Journal of Infectious Diseases 1926; 39:209–14.

<https://doi.org/10.1093/INFDIS/39.3.209>.

- Singh SK, Mishra M, Sahoo M, Patole S, Sahu S, Misra SR, et al. Antibiotic resistance determinants and clonal relationships among multidrug-resistant isolates of *Klebsiella pneumoniae*. *Microbial Pathogenesis* 2017; 110:31–6.
<https://doi.org/10.1016/j.micpath.2017.06.013>.
- Slattery A, Victorsen AH, Brown A, Hillman K, Phillips GJ. Isolation of highly persistent mutants of *Salmonella enterica* serovar Typhimurium reveals a new toxin-antitoxin module. *J Bacteriol* 2013; 195:647–57.
<https://doi.org/10.1128/JB.01397-12>.
- Smith LM, May RC. Mechanisms of microbial escape from phagocyte killing. *Biochemical Society Transactions* 2013; 41:475–90.
<https://doi.org/10.1042/BST20130014>.
- Speck SH, Ganem D. Viral latency and its regulation: lessons from the gamma-herpesviruses. *Cell Host Microbe* 2010; 8:100–15.
<https://doi.org/10.1016/j.chom.2010.06.014>.
- Spoering AL, Lewis K. Biofilms and Planktonic Cells of *Pseudomonas aeruginosa* Have Similar Resistance to Killing by Antimicrobials. *Journal of Bacteriology* 2001; 183:6746–51. <https://doi.org/10.1128/JB.183.23.6746>.
- Stapels DAC, Hill PWS, Westermann AJ, Fisher RA, Thurston TL, Saliba A-E, et al. *Salmonella* persists undermine host immune defenses during antibiotic treatment. *Science* (1979) 2018; 362:1156–60. <https://doi.org/10.1126/science.aat7148>.
- Steinbrecher T, Prock S, Reichert J, Wadhvani P, Zimpfer B, Bürck J, et al. Peptide-Lipid Interactions of the Stress-Response Peptide TisB That Induces Bacterial

Persistence. *Biophysical Journal* 2012; 103:1460–9.

<https://doi.org/10.1016/j.bpj.2012.07.060>.

- Stenico V, Baffoni L, Gaggia F, Biavati B. Validation of candidate reference genes in *Bifidobacterium adolescentis* for gene expression normalization. *Anaerobe* 2014; 27:34–9. <https://doi.org/10.1016/j.anaerobe.2014.03.004>.
- Stepanyan K, Wenseleers T, Duéñez-Guzmán EA, Muratori F, Van den Bergh B, Verstraeten N, et al. Fitness trade-offs explain low levels of persister cells in the opportunistic pathogen *Pseudomonas aeruginosa*. *Molecular Ecology* 2015; 24:1572–83. <https://doi.org/https://doi.org/10.1111/mec.13127>.
- Sulaiman JE, Lam H. Proteomic Study of the Survival and Resuscitation Mechanisms of Filamentous Persisters in an Evolved *Escherichia coli* Population from Cyclic Ampicillin Treatment. *MSystems* 2020; 5. https://doi.org/10.1128/MSYSTEMS.00462-20/SUPPL_FILE/MSYSTEMS.00462-20-ST007.DOCX.
- Sumbly KM, Grbin PR, Jiranek V. Validation of the use of multiple internal control genes, and the application of real-time quantitative PCR, to study esterase gene expression in *Oenococcus oeni*. *Applied Microbiology and Biotechnology* 2012; 96:1039–47. <https://doi.org/10.1007/s00253-012-4409-1>.
- Sun Z, Deng J, Wu H, Wang Q, Yuanxing Zhang. Selection of Stable Reference Genes for Real-Time Quantitative PCR Analysis in *Edwardsiella tarda*. *J Microbiol Biotechnol* 2017; 27:112–21.
- Swayden M, Chhouri H, Anouar Y, Grumolato L. Tolerant/Persister Cancer Cells and the Path to Resistance to Targeted Therapy. *Cells* 2020; 9. <https://doi.org/10.3390/cells9122601>.

- Tan Q, Awano N, Inouye M. YeeV is an *Escherichia coli* toxin that inhibits cell division by targeting the cytoskeleton proteins, FtsZ and MreB. *Molecular Microbiology* 2011; 79:109–18. <https://doi.org/10.1111/j.1365-2958.2010.07433.x>.
- Tang R, Dodd A, Lai D, McNabb WC, Love DR. Validation of zebrafish (*Danio rerio*) reference genes for quantitative real-time RT-PCR normalization. *Acta Biochim Biophys Sin (Shanghai)* 2007; 39:384–90.
- Theis T, Skurray RA, Brown MH. Identification of suitable internal controls to study expression of a *Staphylococcus aureus* multidrug resistance system by quantitative real-time PCR. *Journal of Microbiological Methods* 2007; 70:355–62. <https://doi.org/10.1016/j.mimet.2007.05.011>.
- Theodore A, Lewis K, Vulić M. Tolerance of *Escherichia coli* to Fluoroquinolone Antibiotics Depends on Specific Components of the SOS Response Pathway. *Genetics* 2013; 195:1265–76. <https://doi.org/10.1534/genetics.113.152306>.
- Thomas MS, Wigneshweraraj S. Regulation of virulence gene expression. *Virulence* 2014; 5:832–4. <https://doi.org/10.1080/21505594.2014.995573>.
- Tobar JA, González PA, Kalergis AM. Salmonella Escape from Antigen Presentation Can Be Overcome by Targeting Bacteria to Fcγ Receptors on Dendritic Cells. *The Journal of Immunology* 2004; 173:4058–65. <https://doi.org/10.4049/JIMMUNOL.173.6.4058>.
- Torrey HL, Keren I, Via LE, Lee JS, Lewis K. High Persister Mutants in *Mycobacterium tuberculosis*. *PLoS One* 2016; 11:e0155127–e0155127. <https://doi.org/10.1371/journal.pone.0155127>.

- Tran JH, Jacoby GA, Hooper DC. Interaction of the plasmid-encoded quinolone resistance protein Qnr with *Escherichia coli* DNA gyrase. *Antimicrob Agents Chemother* 2005; 49:118–25. <https://doi.org/10.1128/AAC.49.1.118-125.2005>.
- Tran JH, Jacoby GA. Mechanism of plasmid-mediated quinolone resistance. *Proceedings of the National Academy of Sciences* 2002; 99:5638–42. <https://doi.org/10.1073/pnas.082092899>.
- Trapnell C, Williams BA, Pertea G, Mortazavi A, Kwan G, Van Baren MJ, et al. Transcript assembly and quantification by RNA-Seq reveals unannotated transcripts and isoform switching during cell differentiation. *Nature Biotechnology* 2010; 28:511–5. <https://doi.org/10.1038/nbt.1621>.
- Trastoy R, Manso T, Fernández-García L, Blasco L, Ambroa A, Pérez del Molino M, et al. Mechanisms of Bacterial Tolerance and Persistence in the Gastrointestinal and Respiratory Environments. *Clinical Microbiology Reviews* 2021; 31:e00023-18. <https://doi.org/10.1128/CMR.00023-18>.
- Tripathi A, Dewan PC, Siddique S a., Varadarajan R. MazF-induced growth inhibition and persister generation in *Escherichia coli*. *Journal of Biological Chemistry* 2014; 289:4191–205. <https://doi.org/10.1074/jbc.M113.510511>.
- Unoson C, Wagner EGH. A small SOS-induced toxin is targeted against the inner membrane in *Escherichia coli*. *Molecular Microbiology* 2008; 70:258–70. <https://doi.org/https://doi.org/10.1111/j.1365-2958.2008.06416.x>.
- Uppal S, Shetty DM, Jawali N. Cyclic AMP receptor protein regulates *cspd*, a bacterial toxin gene, in *Escherichia coli*. *Journal of Bacteriology* 2014; 196:1569–77. <https://doi.org/10.1128/JB.01476-13>.
- Uzoechi SC, Abu-Lail NI. Variations in the Morphology, Mechanics and Adhesion of Persister and Resister *E. coli* Cells in Response to Ampicillin: AFM Study.

Antibiotics 2020, Vol 9, Page 235 2020; 9:235.

<https://doi.org/10.3390/ANTIBIOTICS9050235>.

- van den Bergh B, Michiels JE, Wenseleers T, Windels EM, Boer P vanden, Kestemont D, et al. Frequency of antibiotic application drives rapid evolutionary adaptation of *Escherichia coli* persistence. Nature Microbiology 2016; 1:16020. <https://doi.org/10.1038/nmicrobiol.2016.20>.
- Vandesompele J, De Preter K, Pattyn F, Poppe B, Van Roy N, De Paepe A, et al. Accurate normalization of real-time quantitative RT-PCR data by geometric averaging of multiple internal control genes. Genome Biology 2002; 3:research0034.1. <https://doi.org/10.1186/gb-2002-3-7-research0034>.
- VanGuilder HD, Vrana KE, Freeman WM. Twenty-five years of quantitative PCR for gene expression analysis. Biotechniques 2008; 44:619–26. <https://doi.org/10.2144/000112776>.
- Vega NM, Allison KR, Khalil AS, Collins JJ. Signaling-mediated bacterial persister formation. Nature Chemical Biology 2012; 8:431–3. <https://doi.org/10.1038/nchembio.915>.
- Vega NM, Allison KR, Samuels AN, Klempner MS, Collins JJ. *Salmonella typhimurium* intercepts *Escherichia coli* signaling to enhance antibiotic tolerance. Proc Natl Acad Sci U S A 2013; 110:14420–5. <https://doi.org/10.1073/pnas.1308085110>.
- Verstraeten N, Knapen WJ, Kint CI, Liebens V, van den Bergh B, Dewachter L, et al. O₂ and Membrane Depolarization Are Part of a Microbial Bet-Hedging Strategy that Leads to Antibiotic Tolerance. Molecular Cell 2015; 59:9–21. <https://doi.org/10.1016/j.molcel.2015.05.011>.

- Vetting MW, Hegde SS, Wang M, Jacoby GA, Hooper DC, Blanchard JS. Structure of QnrB1, a plasmid-mediated fluoroquinolone resistance factor. *Journal of Biological Chemistry* 2011; 286:25265–73.
<https://doi.org/10.1074/jbc.M111.226936>.
- Völzing KG, Brynildsen MP. Stationary-phase persisters to ofloxacin sustain DNA damage and require repair systems only during recovery. *MBio* 2015; 6:1–11.
<https://doi.org/10.1128/mBio.00731-15>.
- Wada A, Igarashi K, Yoshimura S, Aimoto S, Ishihama A. Ribosome Modulation Factor: Stationary Growth Phase-Specific Inhibitor of Ribosome Functions from *Escherichia coli*. *Biochemical and Biophysical Research Communications* 1995; 214:410–7. <https://doi.org/https://doi.org/10.1006/bbrc.1995.2302>.
- Wada A, Yamazaki Y, Fujita N, Ishihama A. Structure and probable genetic location of a “ribosome modulation factor” associated with 100S ribosomes in stationary-phase *Escherichia coli* cells. *Proc Natl Acad Sci U S A* 1990; 87:2657–61.
<https://doi.org/10.1073/pnas.87.7.2657>.
- Wada A. Growth phase coupled modulation of *Escherichia coli* ribosomes. *Genes to Cells* 1998; 3:203–8. <https://doi.org/10.1046/j.1365-2443.1998.00187.x>.
- Wainwright J, Hobbs G, Nakouti I. Persister cells: formation, resuscitation and combative therapies. *Archives of Microbiology* 2021; 203:5899–906.
<https://doi.org/10.1007/s00203-021-02585-z>.
- Wainwright M, Swan HT. C.G. Paine and the earliest surviving clinical records of penicillin therapy. *Medical History* 1986; 30:42–56. <https://doi.org/DOI:10.1017/S0025727300045026>.

- Wakamoto Y, Dhar N, Chait R, Schneider K, Signorino-Gelo F, Leibler S, et al. Dynamic Persistence of Antibiotic-Stressed Mycobacteria. *Science* (1979) 2013; 339:91–5. <https://doi.org/10.1126/science.1229858>.
- Wang JD, Sanders GM, Grossman AD. Nutritional Control of Elongation of DNA Replication by (p)ppGpp. *Cell* 2007; 128:865. <https://doi.org/10.1016/J.CELL.2006.12.043>.
- Wang T, el Meouche I, Dunlop MJ. Bacterial persistence induced by salicylate via reactive oxygen species. *Sci Rep* 2017; 7:43839. <https://doi.org/10.1038/srep43839>.
- Wang X, Lord DM, Cheng H-Y, Osbourne DO, Hong SH, Sanchez-Torres V, et al. A new type V toxin-antitoxin system where mRNA for toxin GhoT is cleaved by antitoxin GhoS. *Nature Chemical Biology* 2012; 8:855–61. <https://doi.org/10.1038/nchembio.1062>.
- Wang X, Wood TK. Toxin-Antitoxin Systems Influence Biofilm and Persister Cell Formation and the General Stress Response. *Appl Environ Microbiol* 2011; 77(16):5577–83 <https://doi.org/10.1128/AEM.05068-11>.
- Wang Z, Gerstein M, Snyder M. RNA-Seq: a revolutionary tool for transcriptomics. *Nat Rev Genet* 2009; 10:57. <https://doi.org/10.1038/NRG2484>.
- Wei D, Sun J, Shi J, Liu P, Hao J. New strategy to improve efficiency for gene replacement in *Klebsiella pneumoniae*. *Journal of Industrial Microbiology and Biotechnology* 2013; 40:523–7. <https://doi.org/10.1007/S10295-013-1250-1>.
- Wei D, Wang M, Shi J, Hao J. Red recombinase assisted gene replacement in *Klebsiella pneumoniae*. *Journal of Industrial Microbiology and Biotechnology* 2012; 39:1219–26. <https://doi.org/10.1007/s10295-012-1117-x>.

- Weigel LM, Steward CD, Tenover FC. *gyrA* mutations associated with fluoroquinolone resistance in eight species of Enterobacteriaceae. *Antimicrob Agents Chemother* 1998; 42:2661–7. <https://doi.org/10.1128/AAC.42.10.2661>.
- Wen S, Chen X, Xu F, Sun H. Validation of reference genes for real-time quantitative PCR (qPCR) Analysis of *Avibacterium paragallinarum*. *PLoS ONE* 2016; 11:1–14. <https://doi.org/10.1371/journal.pone.0167736>.
- Weston N, Sharma P, Ricci V, Piddock LJV. Regulation of the AcrAB-TolC efflux pump in Enterobacteriaceae. *Research in Microbiology* 2018; 169:425–31. <https://doi.org/10.1016/J.RESMIC.2017.10.005>.
- Willey JM, Sherwood LM, Woolverton CJ. *Prescott's Microbiology*. 2017.
- Windels EM, Michiels JE, Fauvart M, Wenseleers T, van den Bergh B, Michiels J. Bacterial persistence promotes the evolution of antibiotic resistance by increasing survival and mutation rates. *The ISME Journal* 2019; 13:1239–51. <https://doi.org/10.1038/s41396-019-0344-9>.
- Winther KS, Gerdes K. Regulation of enteric *vapBC* transcription: induction by VapC toxin dimer-breaking. *Nucleic Acids Res* 2012; 40:4347–57. <https://doi.org/10.1093/nar/gks029>.
- Woodford N, Ellington MJ. The emergence of antibiotic resistance by mutation. *Clinical Microbiology and Infection* 2007; 13:5–18. <https://doi.org/10.1111/J.1469-0691.2006.01492.X>.
- Wu N, He L, Cui P, Wang W, Yuan Y, Liu S, et al. Ranking of persister genes in the same *Escherichia coli* genetic background demonstrates varying importance of individual persister genes in tolerance to different antibiotics. *Front Microbiol* 2015; 6:1003. <https://doi.org/10.3389/fmicb.2015.01003>.

- Wu Y, Vulić M, Keren I, Lewis K. Role of Oxidative Stress in Persister Tolerance. *Antimicrobial Agents and Chemotherapy* 2012; 56:4922–6. <https://doi.org/10.1128/AAC.00921-12>.
- Xie F, Xiao P, Chen D, Xu L, Zhang B. miRDeepFinder: a miRNA analysis tool for deep sequencing of plant small RNAs. *Plant Molecular Biology* 2012; 80:75–84. <https://doi.org/10.1007/s11103-012-9885-2>.
- Xiong X, Bromley EHC, Oelschlaeger P, Woolfson DN, Spencer J. Structural insights into quinolone antibiotic resistance mediated by pentapeptide repeat proteins: conserved surface loops direct the activity of a Qnr protein from a gram-negative bacterium. *Nucleic Acids Res* 2011; 39:3917–27. <https://doi.org/10.1093/NAR/GKQ1296>.
- Xu Y, Liu S, Zhang Y, Zhang W. DNA adenine methylation is involved in persister formation in *E. coli*. *Microbiological Research* 2021; 246:126709. <https://doi.org/10.1016/J.MICRES.2021.126709>.
- Yamaguchi S, Darwin AJ. Recent findings about the *Yersinia enterocolitica* phage shock protein response. *The Journal of Microbiology* 2012; 50:1–7. <https://doi.org/10.1007/s12275-012-1578-7>.
- Yamaguchi Y, Park J, Inouye M. Toxin-Antitoxin Systems in Bacteria and Archaea. *Annual Review of Genetics* 2011; 45:61–79. <https://doi.org/10.1146/annurev-genet-110410-132412>.
- Yan D, Wang X, Luo L, Cao X, Ge B. Inhibition of TLR signaling by a bacterial protein containing immunoreceptor tyrosine-based inhibitory motifs. *Nature Immunology* 2012; 13:1063–71. <https://doi.org/10.1038/ni.2417>.

- Zhang R, Xu W, Shao S, Wang Q. Gene Silencing Through CRISPR Interference in Bacteria: Current Advances and Future Prospects. *Frontiers in Microbiology* 2021; 12:567. <https://doi.org/10.3389/FMICB.2021.635227/BIBTEX>.
- Zhang X, Li Q, Lin H, Zhou W, Qian C, Sun Z, et al. High-Level Aminoglycoside Resistance in Human Clinical *Klebsiella pneumoniae* Complex Isolates and Characteristics of *armA*-Carrying IncHI5 Plasmids. *Frontiers in Microbiology* 2021; 12:617. <https://doi.org/10.3389/FMICB.2021.636396/BIBTEX>.
- Zhao S, Fung-Leung W-P, Bittner A, Ngo K, Liu X. Comparison of RNA-Seq and Microarray in Transcriptome Profiling of Activated T Cells. *PLOS ONE* 2014; 9:e78644. <https://doi.org/10.1371/JOURNAL.PONE.0078644>.
- Zhao W, Li Y, Gao P, Sun Z, Sun T, Zhang H. Validation of reference genes for real-time quantitative PCR studies in gene expression levels of *Lactobacillus casei* Zhang. *J Ind Microbiol Biotechnol* 2011; 38:1279–86. <https://doi.org/10.1007/s10295-010-0906-3>.
- Zhao X, Drlica K. Reactive oxygen species and the bacterial response to lethal stress. *Current Opinion in Microbiology* 2014; 21:1–6. <https://doi.org/https://doi.org/10.1016/j.mib.2014.06.008>.
- Zhou Y, Liang Y, Lynch KH, Dennis JJ, Wishart DS. PHAST: A Fast Phage Search Tool. *Nucleic Acids Research* 2011; 39:W347–52. <https://doi.org/10.1093/nar/gkr485>.

Appendices

A1 Media and reagents used in the present study

A1.1 Bacterial culture media

Table A1.1.1 Bacteriological growth media used in the study and their composition. HMB – HM peptone B.

Sr. No.	Medium	Application	Component	Amount (gram/ litre)	Reference
1	Nutrient Broth, pH 7.4 ± 0.2 (HiMedia, India) (M002-500G)	Routine growth and maintenance of cultures	Peptone	5.0	(Downes and Ito, 2001)
			Sodium chloride	5.0	
			HMB	1.5	
			Yeast Extract	1.5	
2	Nutrient Agar, pH 7.4 ± 0.2 (HiMedia, India) (M001-500G)	Routine growth and maintenance of cultures	Peptone	5.0	(Downes and Ito, 2001)
			Sodium chloride	5.0	
			HMB	1.5	
			Yeast Extract	1.5	
			Agar-Agar	15.0	

Sr. No.	Medium	Application	Component	Amount (gram/ litre)	Reference
3	Luria-Bertani Broth, Miller, pH 7.5±0.2 (HiMedia, India) (M1245-500G)	Growth and maintenance of transformed strains and untransformed cultures	Casein enzymic hydrolysate	10.0	(Miller, 1972)
			Yeast Extract	5.0	
			Sodium chloride	10.0	
4	Luria-Bertani Agar, Miller, pH 7.5±0.2 (HiMedia, India) (M1151-500G)	Growth and maintenance of transformed strains as well as untransformed cultures	Casein enzymic hydrolysate	10.0	(Miller, 1972)
			Yeast Extract	5.0	
			Sodium chloride	10.0	
			Agar-Agar	15.0	
5	Luria Broth, pH 7.0±0.2 (HiMedia, India) (M575-500G)	Growth and maintenance of transformed strains	Casein enzymic hydrolysate	10.0	(Lennox, 1955)
			Yeast Extract	5.0	
			Sodium chloride	5.0	
7	Mueller-Hinton Broth, pH 7.3±0.1 (HiMedia, India) (M391-500G)	Antimicrobial compound-response assays	Infusion from HM B	300.0	(Mueller and Hinton, 1941)
			Acicase™	17.5	
			Starch	1.5	

Sr. No.	Medium	Application	Component	Amount (gram/ litre)	Reference
8	Mueller-Hinton Agar, pH 7.3±0.1 (HiMedia, India) (M173-500G)	Antimicrobial compound-response assays	Infusion from HM B	300.0	(Mueller and Hinton, 1941)
			Acicase™	17.5	
			Starch	1.5	
			Agar-Agar	15.0	
9	SOB Broth, 7.0±0.2 (HiMedia, India) (M1379-500G)	Selection of plasmid transformants	Casein enzymic hydrolysate	20.0	(Sambrook et al, 1989)
			Yeast Extract	5.0	
			Sodium chloride	0.5	
			Magnesium sulphate	2.4	
			Potassium chloride	0.186	
10	Eosin-Methylene Blue Agar, pH 7.2±0.2 (HiMedia, India) (M317-500G)	Identification of bacterial species	Peptic digest of animal tissue	10.0	(Levine, 1918)
			Dipotassium phosphate	2.0	
			Lactose	5.0	
			Sucrose	5.0	

Sr. No.	Medium	Application	Component	Amount (gram/ litre)	Reference
11	MacConkey Agar, pH 7.1±0.2 (BD Difco™, USA) (212123)	Identification of bacterial species	Eosin-Y	0.4	(MacConkey, 1905)
			Methylene Blue	0.065	
			Agar-Agar	13.5	
			Pancreatic digest of gelatine	17.0	
			Peptones (meat and casein)	3.0	
			Lactose	10.0	
			Bile Salts No. 3	1.5	
			Sodium chloride	5.0	
			Neutral Red	0.03	
			Crystal Violet	0.001	
	Agar-Agar	13.5			
12	SIM Medium, pH 7.3±0.2 (HiMedia, India) (M181-100G)	Identification of indole production	HMB	3.0	(Ewing, 1986)
			Peptone	30.0	

Sr. No.	Medium	Application	Component	Amount (gram/ litre)	Reference
			Peptonized iron	0.2	
			Sodium thiosulphate	0.025	
			Agar	3.0	
13	MR-VP Medium, pH 6.9±0.2 (HiMedia, India) (M070-100G)	Identification of the end products of carbohydrate fermentation	Buffered peptone	7.0	(Clark and Lubs, 1915)
			Dextrose	5.0	
			Dipotassium phosphate	5.0	
14	Simmon's Citrate Agar, pH 6.8±0.2 (HiMedia, India) (M099-100G)	Identification of citrate- utilization	Magnesium sulphate	0.2	(Simmons, 1926)
			Ammonium dihydrogen phosphate	1.0	
			Dipotassium phosphate	1.0	
			Sodium citrate	2.0	
			Sodium chloride	5.0	
			Bromothymol blue	0.08	
			Agar	15.0	

A1.2 Chemicals and reagents used

Table A1.2.1 Chemicals used in the present study.

Sr. No.	Chemical compound	Make (Catalogue No.)
1	Acetic acid, Glacial	Fisher Scientific, USA (11007)
2	Agar-Agar	HiMedia, India (GRM666-500G)
3	Agarose	MP Biomedicals, USA (26790)
4	Bovine Serum Albumen	MP Biomedicals, USA (BSAG100)
5	5-Carboxyfluorescein diacetate (CFDA)	Sigma-Aldrich, USA (C4196-25MG)
6	Crystal Violet	Fisher Scientific, USA (C581-25G)
7	Dimethyl Sulfoxide (DMSO)	MP Biomedicals, USA (219605590)
8	Ethanol, absolute	Merck, Germany (1.00983.0511)
9	Ethidium bromide	Sigma-Aldrich, USA (E7637-5G)
10	Ethylene diamine tetraacetic acid (EDTA)	MP Biomedicals, USA (215252290)
11	Glycerol, Ultra Pure™	Invitrogen, USA (15514011)
12	HiDi Formamide	Applied Biosystems, USA (4311320)
13	Isopropyl β -D-1-thiogalactopyranoside (IPTG)	USB, USA (38220090)
14	Lysozyme	USB, USA (18645 25G)
15	β -Mercaptoethanol	Sigma-Aldrich, USA (M9250-10ML)
16	POP7 Polymer	Applied Biosystems, USA (4363785)
17	Isopropanol	HiMedia, India (MB063)
18	L-Arabinose	Sigma-Aldrich, USA (A3256-25G)
19	Propidium Iodide	HiMedia, India (TC252)
20	Proteinase-K	USB, USA (76230Z)
21	Sodium azide	Sigma-Aldrich, USA (71289-50G)
21	Tris Base	Affymetrix, USA (J75825-A7)
22	Trizma hydrochloride	Sigma-Aldrich, USA (T3253-250G)

Table A1.2.2 Reagents used in the present study.

Sr. No.	Application	Reagents	Make (catalogue No.)
1		5X Green GoTaq® Flexi Buffer	Promega, USA (M891A)
2		25mM Magnesium Chloride Solution	Promega, USA (A351B)
3		0.1 M dATP	Promega, USA (U120B)
4	PCR	0.1 M dGTP	Promega, USA (U121B)
5		0.1 M dCTP	Promega, USA (U122B)
6		0.1 M dTTP	Promega, USA (U123B)
7		GoTaq® Flexi DNA Polymerase	Promega, USA (M8295)
8	Agarose Gel Electrophoresis	GeneRuler DNA Ladder Mix	Fermentas, USA (SM0331)
9		DNA Gel Loading Dye (6X)	ThermoFisher Scientific, USA (R0611)
10	DNA Sequencing	Buffer (10X) with EDTA	Applied Biosystems, USA (402824)
11		CutSmart® Buffer, 10X	NEB, USA (B7204S)
12	Molecular Cloning	BamHI-HF restriction enzyme, 10,000 units	NEB, USA (R3136S)
13		XhoI restriction enzyme, 10,000 units	NEB, USA (R0146S)
14		Quick Ligation™ Kit	NEB, USA (M2200S)
15	RNA Extraction	RNAProtect Bacteria Reagent	QIAGEN, Germany (76506)
16	Real-Time PCR	FastStart Universal SYBR Green Master Mix with ROX 2X	Roché Diagnostics, Switzerland (04 913 914 001)
17		iTaq™ Universal SYBR® Green Supermix	Bio-Rad, USA (1725121)
18	High-Fidelity PCR	Q5 High-Fidelity 2X Master Mix	NEB, USA (M0492L)

Sr. No.	Application	Reagents	Make (catalogue No.)
19		Kovac's Indole Reagent	HiMedia, India (R008)
20	IMViC test	Methyl Red Indicator	HiMedia, India (I007)
21		Barritt Reagent A	HiMedia, India (R029)
22		Barritt Reagent B	HiMedia, India (R030)

A2 Commercial kits used in the present study

- i. Genra Puregene Yeast/Bact Kit B (QIAGEN, Germany; 158567)
- ii. QIAprep Spin Miniprep Kit (QIAGEN, Germany; 27106)
- iii. QIAquick Gel Extraction Kit (QIAGEN, Germany; 28706)
- iv. BigDye™ Terminator v3.1 Cycle Sequencing Kit (Applied Biosystems, USA; 4337455)
- v. RNeasy Mini Kit (QIAGEN, Germany; 74106)
- vi. SuperScript™ IV First-Strand Synthesis System (Invitrogen, USA; 18091050)
- vii. Quick & Easy *E. coli* Gene Deletion Kit (Gene Bridges, Germany; K006)
- viii. Ion Xpress™ Plus Fragment Library Kit (Thermo Fisher Scientific, USA; 4471269)
- ix. MICROBExpress™ Bacterial mRNA Enrichment Kit (Invitrogen, USA; AM1905)
- x. iScript™ Reverse Transcription Supermix for RT-qPCR (Bio-Rad, USA; 1708841)

A3 Instruments used in the present study

- i. Elix® Essential Water Purification System (Merck, USA; C1051530)

- ii. Milli-Q® Reference Water Purification System (Merck, USA; C79625)
- iii. Class II A2 Biosafety Cabinet, 1300 Series (Thermo Scientific™, USA; 1367)
- iv. New Brunswick™ Innova® 42R Incubator Shaker (Eppendorf, Germany; M1335-0016)
- v. SL 8R Small Benchtop Centrifuge (Thermo Scientific™, USA; 75007224)
- vi. Centrifuge 5420 (Eppendorf, Germany; 5420000113)
- vii. C1000 Touch Thermal Cycler with Dual 48/48 Fast Reaction Module (Bio-Rad, USA; 185-1148)
- viii. Wide Mini-Sub® Cell GT Complete System (Bio-Rad, USA; 170-448)
- ix. Mini-Sub® Cell GT Complete Systems (Bio-Rad, USA; 170-4486)
- x. AccuBlock™ Digital Dry Bath (Labnet International, USA; D1301-230V)
- xi. Oakton pH 700 Benchtop Meter (Cole-Parmer, USA; UE-35419-10)
- xii. Chemidoc MP Imaging System (Bio-Rad, USA; 17001402)
- xiii. Quintix® Precision Balance (Sartorius, Germany; QUINTIX213-1SAR)
- xiv. F12-ED Refrigerated / Heating Circulator (Julabo, Germany; 9116612)
- xv. Gene Pulser Xcell™ Total System (Bio-Rad, USA; 1652660)
- xvi. 3130xl Genetic Analyzer (Applied Biosystems, USA; 3130XLR)
- xvii. 7500 Fast Real-Time PCR System (Applied Biosystems, USA; 4351106)
- xviii. LSRFortessa™ cell analyzer (BD Biosciences, USA; 649225)
- xix. TCS SP8 confocal microscope (Leica Microsystems, Germany)
- xx. NanoDrop OneC (Thermo Scientific™, USA; ND-ONEC-W)
- xxi. Thermomixer C (Eppendorf, Germany; 5382000015)
- xxii. LSR Fortessa Flow Cytometer (BD Biosciences, USA)
- xxiii. Ion OneTouch™ 2 Instrument (Thermo Fisher Scientific, USA; 4474778)
- xxiv. Ion S5™ System (Thermo Fisher Scientific, USA; A27212)

- xxv. 90 mm Glass Filter Holder Kit (Millipore, USA; XX10 090 20)
- xxvi. Vacuum Pressure Pump, 220V (Millipore, USA; XX55 220 50)

A4 Software used in the present study

- i. MEGA7 (Kumar et al, 2016)
- ii. FACSDiva (BD Biosciences, USA)
- iii. FlowJo 10.7.1 (BD Biosciences, USA)
- iv. Clustal Omega (www.ebi.ac.uk/Tools/msa/clustalo/)
- v. T-Coffee (tcoffee.crg.eu/apps/tcoffee/index.html)
- vi. BLAST (blast.ncbi.nlm.nih.gov/Blast.cgi)
- vii. Genome Compiler (Genome Compiler Corporation, USA)
- viii. SPAdes (Bankevich et al, 2012)
- ix. QUAST (Gurevich et al, 2013)
- x. Prodigal (Hyatt et al, 2010)
- xi. Genemark (Besemer and Borodovsky, 1999)
- xii. Blast2GO (Conesa et al, 2005)
- xiii. RAST (rast.nmpdr.org) (Aziz et al, 2008; Overbeek et al, 2014)
- xiv. 3130xl Data Collection Software 4 (Applied Biosystems, USA)
- xv. MLST 2.0 (Multi-Locus Sequence Typing) (Larsen et al, 2012)
- xvi. ResFinder 4.1 (cge.cbs.dtu.dk/services/ResFinder/) (Bortolaia et al, 2020)
- xvii. Resistance Gene Identifier (RGI) 5.2.0 (McArthur et al, 2013)
- xviii. Single genome analysis (Feng et al, 2021)
- xix. RefFinder (Xie et al, 2012)
- xx. Phaster (Arndt et al, 2016)
- xxi. NEBioCalculator® v1.12.0 (NEB, USA)

A5 PCA of KpIMS38 cultures treated with levofloxacin.

Culture-aliquots of KpIMS38, untreated (1-, 3-, 5-, 7-, 9-, 11- and 13A) as well as treated with 256 µg/mL levofloxacin (2-, 4-, 6-, 8-, 10-, 12-, 14A), were sampled at bihourly intervals, stained with the dye CFDA and analysed by flow cytometry. Each cell population was gated into two subpopulations P3 and P4. They were further gated (B and C) to determine the stained cell-population (CFDA⁺ for P4 and Q2 for P3). They were used to calculate the mean fluorescence intensity (FITC-A) of untreated (15) and levofloxacin-treated (16) cultures in P3 (15- and 16 B) as well as P4 (15- and 16A) subpopulations.

